

**STRUCTURE AND REACTIVITY OF THE  
1,3-DIOXOLAN-2-YLIUM ION SYSTEM**

**By**

**JOHN PAUL BELLAVIA, B. Sc.**

**A Thesis**

**Submitted to the School of Graduate Studies**

**in Partial Fulfilment of the Requirements**

**for the Degree**

**Doctor of Philosophy**

**McMaster University**

**(c) Copyright by John Paul Bellavia, September 1994.**

**STRUCTURE AND REACTIVITY OF THE  
1,3-DIOXOLAN-2-YLIUM ION SYSTEM**

DOCTOR OF PHILOSOPHY (1994)  
(Chemistry)

McMASTER UNIVERSITY  
Hamilton, Ontario

TITLE:                      Structure and Reactivity of the 1,3-Dioxolan-2-ylum  
Ion System

AUTHOR:                  John Paul Bellavia, B. Sc. (McMaster University)

SUPERVISOR:            Dr. R.F. Childs

NUMBER OF PAGES:    xiv, 209

## Abstract

The 1,3-dioxolan-2-ylum ion is an important intermediate occurring in many carbohydrate transformations. The system has been widely studied, yet conflicting views on the effect of substituents on the ground state structure of 1,3-dioxolan-2-ylum ions have been presented. This thesis embodies the results of a series of investigations, utilizing a number of complementary techniques, to examine the effect of substitution on the structure and reactivity of a homologous series of 1,3-dioxolan-2-ylum ions.

The possible use of the 1,3-dioxolan-2-ylum system as a model for the transition state structures of nucleophilic displacement reactions has been explored. The intramolecular nucleophilic attack of an acetate group on a 1,3-dioxolan-2-ylum ion has been investigated for a series of C(4)-aryl substituted cations. A Hammett study revealed that this isomerization reaction proceeds via a step-wise mechanism involving a carbenium ion intermediate. In contrast, when the C(4) substituent is hydrogen or methyl, a concerted isomerization mechanism is operative, as revealed by semi-empirical calculations. It is suggested that when the C(4) substituent is sufficiently electron donating, the system may adopt a trigonal bipyramidal geometry and hence may serve as a model for the S<sub>N</sub>2 transition state.

Dual substituent parameter (DSP) correlations were used to establish the dependence of the <sup>13</sup>C chemical shifts of the 1,3-dioxolan-2-ylum ion system on the

electron donating power of the C(4)-aryl substituent. These correlations support the inclusion of an ionic resonance contributor to the ground state description of the system. The weight given to the ionic resonance contributor increases with better electron donating C(4)-substituents.

X-ray crystallography has been used to determine the solid state structures of two 1,3-dioxolan-2-ylum ion salts with different C(4) substituents. The changes in bond lengths observed in going from a hydrogen to a phenyl substituent at C(4) are partly attributed to the increased importance of the ionic resonance structure in the aryl system.

Semi-empirical calculations at the AM1 level revealed the effects of differential C(4)-substitution. Better electron donating substituents lowered the isomerization barrier and increased the relative importance of the ionic resonance contributor in the ground state, in accord with the experimentally determined results. The ability of a CF<sub>3</sub> substituent at C(2) to achieve similar changes in structure and reactivity was also established.

## **Acknowledgements**

I wish to thank my research supervisor, Dr. R. F. Childs, for his guidance, support and patience throughout the course of this work. I would also like to thank the members of my supervisory committee, Dr. P. Harrison and Dr. J. Warkentin for their helpful comments and suggestions.

I am grateful for the technical assistance provided by: Dr. D. Hughes, Mr. B. Sayer, Mr. I. Thompson and Dr. A. Bain of the NMR facility; Dr. R. Smith and Mr. F. Ramelan of the mass spectroscopy facility; Dr. J. Britten, Dr. C. Frampton, and Dr. T. Wark of the x-ray crystallography facility.

For providing an enjoyable atmosphere in which to work, I wish to thank my lab mates in ABB 359, past and present. Special thanks goes to Brad, George and Teresa for their friendship inside and outside of the lab. I would also to thank Fred, Dave, and Tex for their valued insights into the human condition.

Finally, I wish to thank my family for their constant support and encouragement.

## Table of Contents

	Page
Descriptive Note	ii
Abstract	iii
Acknowledgements	v
List of Tables	ix
List of Figures	xii
Chapter 1: Introduction	1
1.1 Oxonium Ion Stability	2
1.2 Preparation of 1,3-dioxolan-2-ylum Ions	6
1.3 Role of the Anion	10
1.4 Reaction with Nucleophiles	12
1.5 Dioxolanylium Ions as Intermediates in Carbohydrate Rearrangements	17
1.6 Synthetic Utility	20
1.7 X-ray Crystallographic Studies	22
1.8 $^{13}\text{C}$ NMR Investigations	32
1.9 Semi-Empirical Calculations	35
1.10 Objectives	37
Chapter 2: NMR Study	40
<u>Part A: Synthesis</u>	
2.1 Routes Toward Dioxolanylium Ion Precursors	41
2.2 Generation of the Dioxolanylium Ion	43
<u>Part B: Dynamic NMR Studies</u>	
2.3 $^1\text{H}$ NMR of Dioxolanylium Ions	44

<b>Table of Contents (cont.)</b>	<b>Page</b>
2.4 Measurement of Isomerization Rate Constants by Total Bandsiape Analysis	50
2.5 Mechanism of Isomerization for Aryl Dioxolanylium Ions	54
2.6 Isomerization of Non-aryl Dioxolanylium Salts	64
2.7 Lewis Acid Adducts	70
 <b>Part C: <sup>13</sup>C NMR Correlation Analysis</b>	
2.8 <sup>13</sup> C NMR of Aryl Dioxolanylium Salts	75
2.9 NMR Correlation Analysis	77
2.10 Summary	86
 <b>Chapter 3: Crystallographic Study of Dioxolanylium Ion Structure</b>	 88
3.1 X-ray Structure Determinations	88
3.2 Conformation of the Dioxolanylium Cation	100
3.3 C-O Bond Lengths in 36 and 39	103
3.4 Summary	106
 <b>Chapter 4: Semi-Empirical Investigation of Dioxolanylium Ion Structure and Reactivity</b>	 107
4.1 Structure of the Aryl Substituted Dioxolanylium Ions	107
4.2 Charge Distribution	122
4.3 Modelling the Isomerization Reaction of the Aryl System	125
4.4 Modelling the Isomerization Reaction of the Non-aryl System	136
4.5 Effect of the Trifluoroacetate Group	140
4.6 Comparison of X-ray Crystal Structures with AM1 optimized Geometries	147
4.7 Summary	147
 <b>General Summary</b>	 148b
 <b>Chapter 5: Experimental</b>	 149
5.1 Materials	149
5.2 Instrumentation	149
5.3 Syntheses	159
5.4 AM1 Calculations	167



<b>Table of Contents (cont.)</b>	<b>Page</b>
<b>Appendix</b>	<b>169</b>
<b>References</b>	<b>199</b>

## List of Tables

	Page
1.1 Stabilization energies of substituted methyl cations in the gas phase.	3
1.2 Gas phase heats of formation of selected cations.	3
1.3 Relative heats of protonation in FSO <sub>3</sub> H at 25 °C.	5
1.4 Leaving groups and acceptors for the preparation of 1,3-dioxolan-2-ylum ions via Route 2.	9
1.5 C-O bond lengths in ethers and esters.	23
1.6 Selected bond lengths for 1,3-dioxolan-2-ylum salts.	26
1.7 Mean O-C(alkyl) bond lengths.	30
1.8 <sup>13</sup> C chemical shift differences in 1,3-dioxolan-2-ylum ions and 1,3-dioxolanes in CH <sub>3</sub> CN.	33
1.9 Charge densities calculated from <sup>13</sup> C chemical shifts.	35
2.1 NMR data for 36 and 37 in CD <sub>3</sub> NO <sub>2</sub> .	45
2.2 <sup>1</sup> H chemical shifts of 38-42.	46
2.2 Rates of isomerization of 33-37 in CD <sub>3</sub> NO <sub>2</sub> .	
2.3 <sup>13</sup> C chemical shifts of 38-42.	47
2.4 NMR data for Lewis acid complexes 43 and 44.	48
2.5 Rate of isomerization of 38-42 in CD <sub>3</sub> NO <sub>2</sub> .	52
2.6 Activation parameters for the isomerization of 38-42.	61

<b>List of Tables (cont.)</b>	<b>Page</b>
2.7 Rate of isomerization of <b>36</b> and <b>37</b> in $\text{CD}_3\text{NO}_2$ .	69
2.8 Rate of isomerization of <b>43</b> in $\text{CD}_2\text{Cl}_2$ .	73
2.9 Evaluation of the single (SSP) and dual (DSP) substituent parameter correlation models.	80
2.10 Dual substituent parameter correlations.	82
3.1 Selected bond lengths for <b>36</b> .	89
3.2 Selected bond angles for <b>36</b> .	89
3.3 Selected bond lengths for <b>39</b> .	90
3.4 Selected bond angles for <b>39</b> .	90
3.5 Selected least-squares plane data for <b>36</b> and <b>39</b> .	91
4.1 Selected AM1 optimized bond lengths for <b>38-42</b> and <b>45</b> .	109
4.2 Selected AM1 optimized bond angles for <b>38-42</b> and <b>45</b> .	110
4.3 Selected AM1 optimized bond lengths for <b>51a-f</b> .	114
4.4 Selected AM1 calculated charge densities for <b>38-42</b> and <b>45</b> .	123
4.5 Selected AM1 optimized bond lengths and bond angles for <b>52a-f</b> .	129
4.6 Calculated charge densities for <b>52a-f</b> .	130
4.7 Calculated isomerization barriers.	131
4.8 Selected AM1 optimized bond angles for <b>53</b> and <b>54</b> .	137
4.9 Selected AM1 optimized bond lengths for <b>55-56</b> and <b>61-62</b> .	139
4.10 Selected AM1 optimized bond lengths for <b>36-37</b> and <b>57-58</b> .	142

<b>List of Tables (cont.)</b>	<b>Page</b>
4.11 Selected AM1 optimized bond angles for 59 and 60.	143
5.1 Structure determination summary for 36.	153
5.2 Structure determination summary for 39.	156
A1 Atomic co-ordinates ( $\times 10^4$ ) and equivalent isotropic displacement parameters ( $\text{\AA}^2 \times 10^3$ ) for 36.	169
A2 Anisotropic displacement parameters ( $\text{\AA}^2 \times 10^3$ ) for 36.	170
A3 Hydrogen atom co-ordinates ( $\times 10^4$ ) and isotropic displacement parameters ( $\text{\AA}^2 \times 10^3$ ) for 36.	171
A4 Atomic co-ordinates ( $\times 10^4$ ) and equivalent isotropic displacement parameters ( $\text{\AA}^2 \times 10^3$ ) for 39.	172
A5 Anisotropic displacement parameters ( $\text{\AA}^2 \times 10^3$ ) for 39.	173
A6 Hydrogen atom co-ordinates ( $\times 10^4$ ) and isotropic displacement parameters ( $\text{\AA}^2 \times 10^3$ ) for 39.	174
A7 Observed and calculated structure factors for 36.	175
A8 Observed and calculated structure factors for 39.	187

## List of Figures

	Page
1.1 Reaction of ambident cations with nucleophiles.	14
1.2 Effect of cation stability on nucleophilic addition.	16
2.1 Variable temperature <sup>1</sup> H NMR spectra of <b>42</b> in CD <sub>3</sub> NO <sub>2</sub> : coalescence of acetate and acetoxonium methyl resonances.	53
2.2 Hammett plot for C(4)-aryl substituted dioxolanylium ion isomerization.	55
2.3 Isomerization mechanisms.	57
2.4 Plot of isomerization barrier vs $\sigma^+$ for aryl dioxolanylium ions.	63
2.5 Selective inversion experiment: response of C(2) resonance for <b>36</b> .	67
2.6 Selective inversion experiment: response of C(9) resonance for <b>36</b> .	68
3.1 Conformation of <b>36</b> .	92
3.2 Unit cell packing in <b>36</b> (viewed along z-axis).	93
3.3 Stereoscopic view of unit cell contents for <b>36</b> (viewed along z-axis).	94
3.4 Conformation of <b>39</b> .	95
3.5 Unit cell packing in <b>39</b> (viewed along x-axis).	96
3.6 Unit cell packing in <b>39</b> (viewed along z-axis).	97
3.7 Stereoscopic view of unit cell contents for <b>39</b> (viewed along z-axis).	98
3.8 Intermolecular interaction in <b>39</b> .	99
4.1 AM1 optimized conformation of <b>39</b> .	110

<b>List of Figures (cont.)</b>	<b>Page</b>
4.2 Plot of C(2)-O(3) bond lengths in 38-42 and 45 vs $\sigma'$ .	113
4.3 Plot of C(4)-O(3) bond lengths in 38-42 and 45 vs $\sigma'$ .	115
4.4 Dihedral angle $\phi$ in aryl dioxolanylium ions.	119
4.5 Plot of O(3)-C(4)-C(1')-C(2') dihedral angles in 38-42 and 45 vs $\sigma^+$ .	121
4.6 Plot of calculated charge density vs. C(4) chemical shift for aryl dioxolanylium ions.	124
4.7 Reaction co-ordinate diagram for step-wise isomerization.	126
4.8 AM1 optimized conformation of 52b.	128
4.9 Plot of calculated vs. experimental reaction barriers for aryl dioxolanylium ion isomerization	133
4.10 Reaction co-ordinate diagram for concerted isomerization.	134
4.11 AM1 optimized conformation of 53.	137
4.12 AM1 optimized conformation of 55.	138

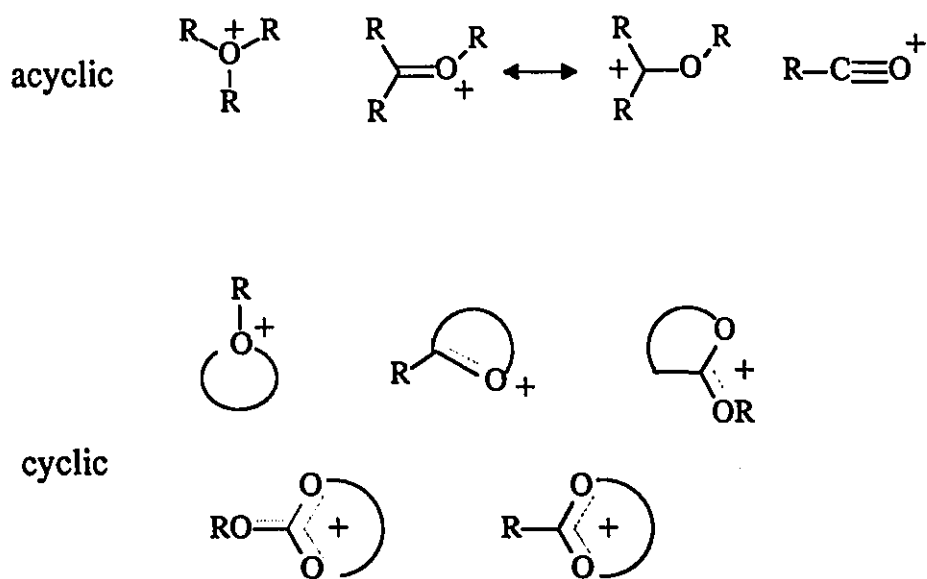
*"Nature is a language - can't you read?"*

**Morrissey**

## Chapter 1

### Introduction

Oxonium ions are of fundamental importance to organic chemistry, occurring in a wide range of reactions and transformations. They are among the best studied of all organic intermediates and have been extensively reviewed.<sup>1-3</sup> The term oxonium ion is applied to a species containing a positively charged trivalent oxygen atom with an electron octet. The ions may be classified as *saturated* (containing 3 C-O single bonds) or *unsaturated* (containing a C-O double bond). A further distinction may be made between cyclic and acyclic oxonium ions. The general structures of the various oxonium ion types are shown in Scheme 1.1.

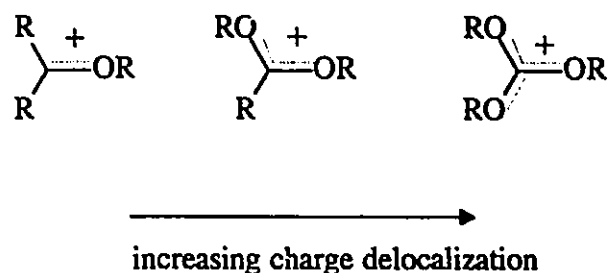


Scheme 1.1



### 1.1 Oxonium Ion Stability

One reason for the vast amount of attention paid to oxonium ions is their ease of study resulting from their greater stability over their carbenium ion counterparts. Oxonium ions can be regarded as carbenium ions with a stabilizing heteroatom substituent. Increased charge delocalization is expected to decrease the relative energy of the ion as shown in the following series (Scheme 1.2)<sup>2</sup>:



Scheme 1.2

This stability sequence has been found to be valid in the gas phase.<sup>4,5</sup> The stabilization energies of a series of differentially substituted ions were calculated from the difference in appearance potentials of  $\text{CH}_3^+$  and the corresponding ion (Table 1.1). As the number of oxygen atoms adjacent to the positive center is increased, a progressive increase in ion stability is observed.

Table 1.1: Stabilization energies of substituted methyl cations in the gas phase.

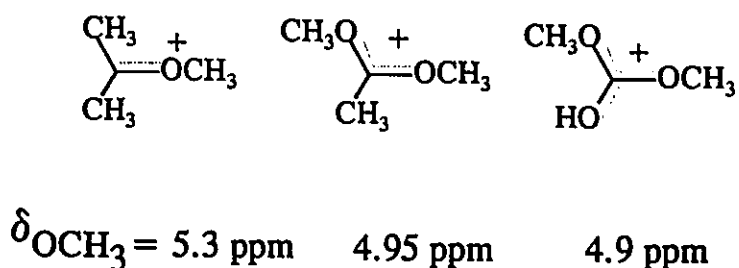
Cation	S.E. (kcal/mol)
$\text{CH}_3^+$	0
$\text{CH}_3\text{CH}_2^+$	$37 \pm 3$
$(\text{CH}_3\text{O})\text{CH}_2^+$	$66 \pm 3$
$(\text{CH}_3\text{O})_2\text{CH}^+$	$85 \pm 3$
$(\text{CH}_3\text{O})_3\text{C}^+$	$90 \pm 3$

The stabilizing ability of an oxygen atom can be further illustrated by comparing the gas phase heats of formation of oxonium ions with those of cations substituted by an adjacent halogen, alkyl group, or sulfur atom (Table 1.2).<sup>46</sup> The oxygen atom is by far the most efficient stabilizer of an adjacent positive charge and is comparable to the stabilizing ability of a nitrogen atom, as evidenced by the lower heats of formation for these ions.

Table 1.2: Gas phase heats of formation of selected cations.

Cation	$\Delta H_f$ (kcal/mol)
$\text{CH}_3^+$	258
$\text{CH}_3\text{CH}_2^+$	224
$\text{HOCH}_2^+$	174
$\text{CH}_3\text{OCH}_2^+$	158, 167-173
$(\text{CH}_3\text{O})_2\text{C}^+\text{CH}_3$	131
$(\text{CH}_3\text{O})_3\text{C}^+$	66-74
$\text{H}_2\text{NCH}_2^+$	176
$\text{HSCH}_2^+$	212
$\text{CH}_3\text{SCH}_2^+$	199
$\text{FCH}_2^+$	233, 197
$\text{ClCH}_2^+$	228, 296
$\text{BrCH}_2^+$	220, 217
$\text{ICH}_2^+$	232, 221

The stability of oxonium ions in solution cannot be directly inferred from the order established for the gas phase. However, the effect of increased oxygen substitution on charge delocalization within oxonium ions has been investigated by  $^1\text{H}$  NMR.<sup>7</sup> The proton chemical shift of the  $\text{OCH}_3$  group in a series of structurally related ions was found to move progressively to higher field with increased oxygen substitution (Scheme 1.3). The order is consistent with that established for the gas phase and with the notion that charge delocalization (and hence stability) increases with increased oxygen substitution.

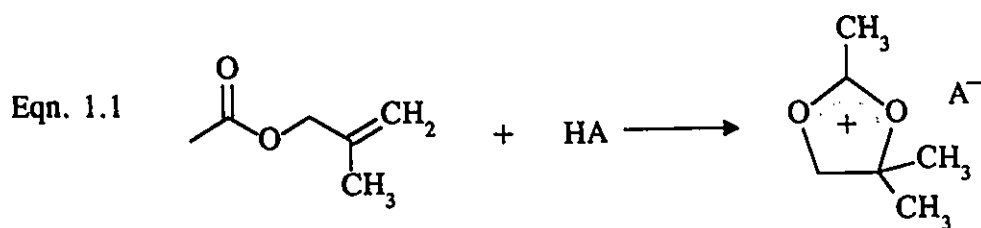


Scheme 1.3

The heats of protonation for a variety of oxygen-containing compounds have been determined in  $\text{FSO}_3\text{H}$  (Table 1.3)<sup>1</sup>. Particularly striking are the low heats of protonation measured for the olefin-containing esters. This is a result of the protonation-cyclization reaction which gives the stable 1,3-dioxolan-2-ylum ion (Eqn. 1.1).

Table 1.3: Relative Heats of Protonation in Fluorosulfonic Acid at 25 °C.

Compound	$\Delta H_{R+}$ , FSO <sub>3</sub> H (kcal/mol)
Ph <sub>2</sub> C=CH <sub>2</sub>	-14.7 ± 0.2
H <sub>3</sub> C-COCH <sub>3</sub>	-19.1 ± 0.1
CH <sub>3</sub> COOEt	-17.4 ± 0.1
PhCOCl	-6.0 ± 0.5
Et <sub>2</sub> O	-19.1 ± 0.7
EtOH	-19.1
H <sub>2</sub> O	-16.4
Et <sub>3</sub> N	-49.2 ± 0.3
CH <sub>3</sub> COOCH <sub>2</sub> C(CH <sub>3</sub> )=CH <sub>2</sub>	-31.5 ± 0.4
C <sub>6</sub> H <sub>5</sub> COOCH <sub>2</sub> C(CH <sub>3</sub> )=CH <sub>2</sub>	-28.6 ± 0.2
<i>p</i> -MeOC <sub>6</sub> H <sub>4</sub> COOCH <sub>2</sub> C(CH <sub>3</sub> )=CH <sub>2</sub>	-32.6 ± 0.8



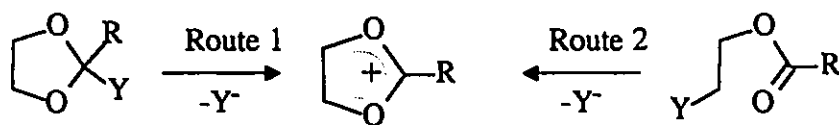
Inspection of the values in Table 1.3 reveals that the heat of formation of the 1,3-dioxolanylium ion is nearly twice that observed for the protonation of ethyl acetate and more than twice that of the protonation of 1,1-diphenylethylene. Also of interest are the relative heats of protonation obtained for the 2-phenyl- versus the 2-methyl-1,3-dioxolanylium ion. The lower  $\Delta H_{R+}$  for the latter was attributed to the greater resonance interaction of the phenyl ring with the ester function in the ground state than in the corresponding atoms in the cation.

Since the focus of this thesis is the 1,3-dioxolan-2-ylum ion, the remaining

discussion of oxonium ion chemistry will concentrate on this system.

## 1.2 Preparation of 1,3-dioxolan-2-ylum Ions

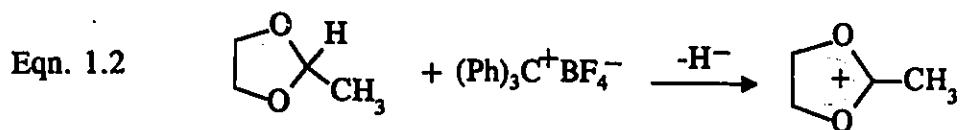
Most routes towards the 1,3-dioxolan-2-ylum ion can be classified into one of two categories.<sup>1,3</sup> Route 1 represents the splitting off of a suitable leaving group from the preformed heterocycle. Route 2 involves an intramolecular alkylation (Scheme 1.4).



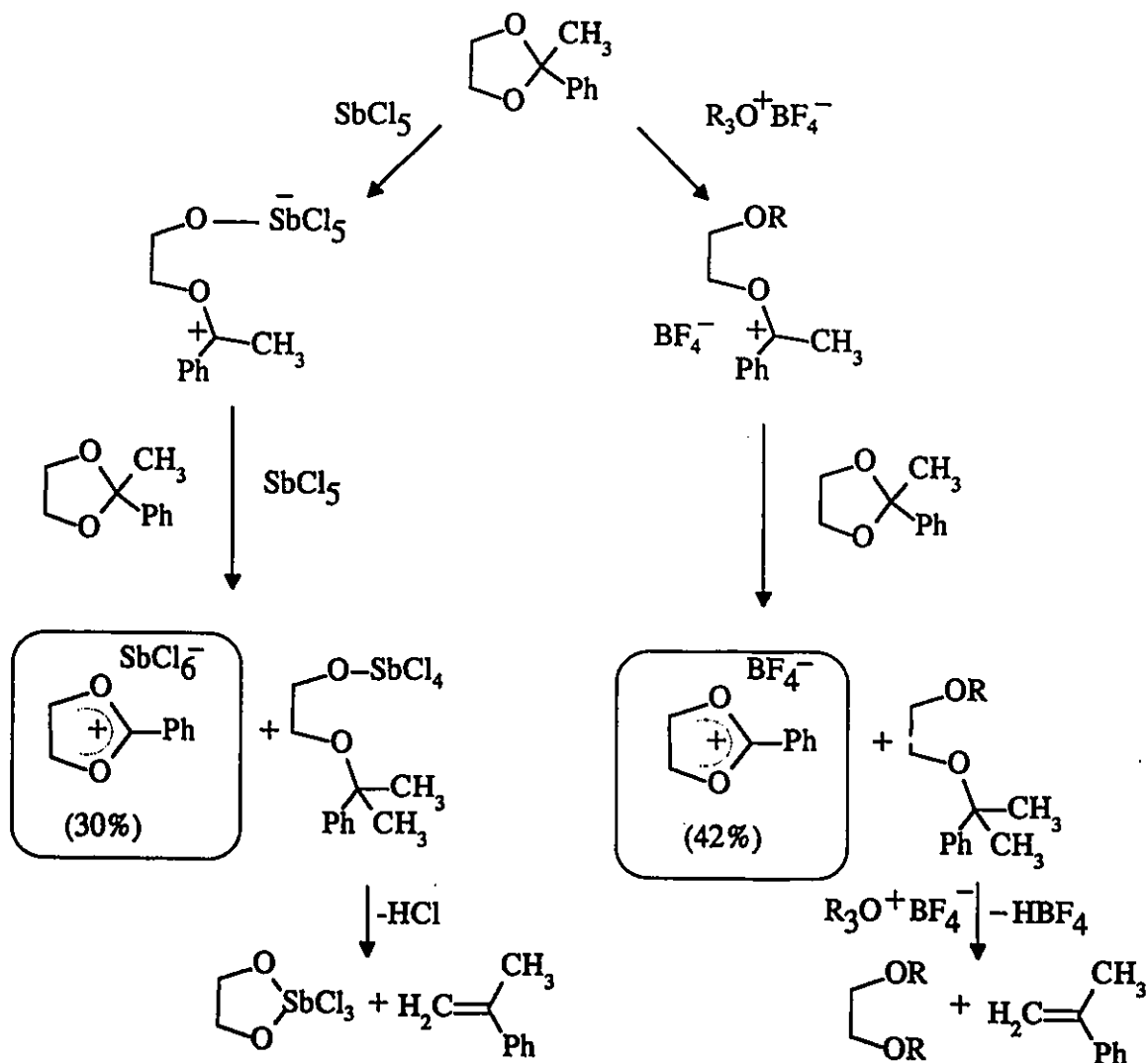
Scheme 1.4

### (i) Route 1

Hydride abstraction from 1,3-dioxolan derivatives may be accomplished with the use of a suitable acceptor such as: trialkyloxonium, triphenyl carbenium, alkoxy-carbenium, dialkoxy-carbenium, aryl diazonium salts or with alkyl halide/AgBF<sub>4</sub> (Eqn. 1.2).<sup>2,8</sup>

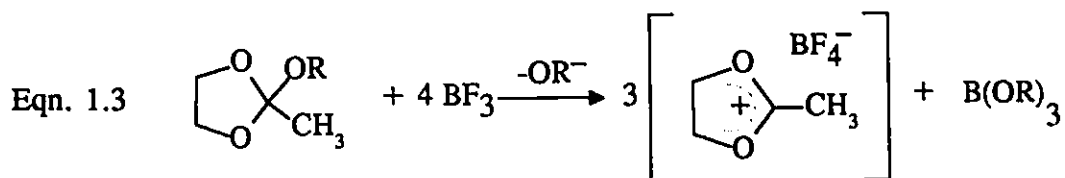


Similarly, an alkyl transfer can be initiated with the use of a Lewis acid such as  $\text{BF}_3$  or  $\text{SbCl}_5$  or alkylating agents ( $\text{R}_3\text{O}^+$ ). The mechanism is believed to involve a disproportionation reaction (Scheme 1.5).<sup>2</sup> This mechanism is supported by the detection of alkene dimers in the product mixture and by the fact that the reaction yields are never greater than 50%.



Scheme 1.5

Alkoxide transfer from a cyclic orthoester is another example of a route 1 synthesis which has been widely used (Eqn. 1.3).<sup>1a,8</sup>



(ii) Route 2

The second common route towards the 1,3-dioxolan-2-ylum ion system takes advantage of the neighbouring group participation reaction of ester carbonyl groups.<sup>9-11</sup> The reaction takes place as illustrated in Eqn. 1.4 where A is an acceptor for the anionic leaving group Y.

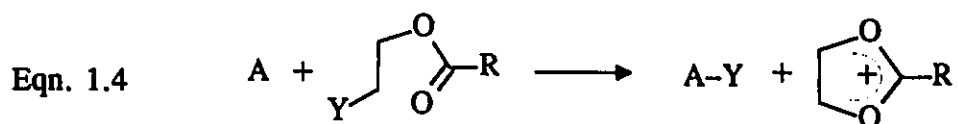


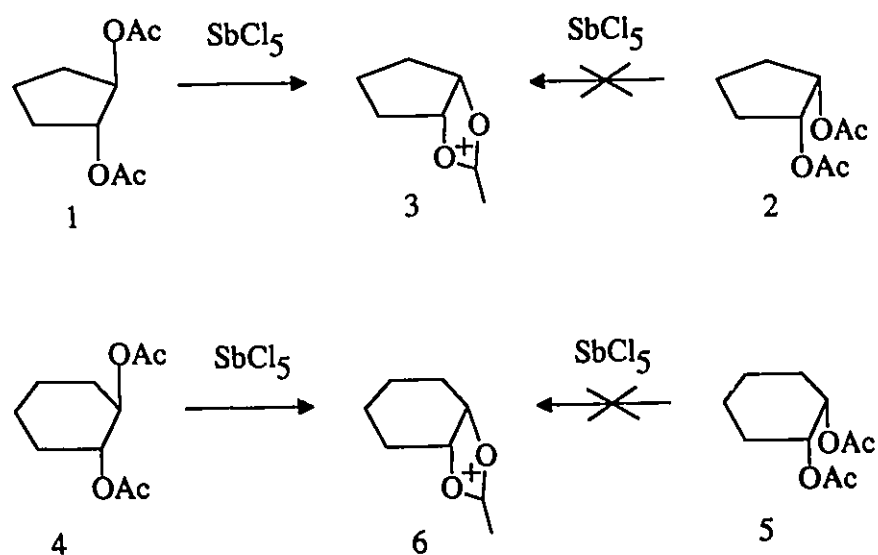
Table 1.4 lists some examples of leaving groups and acceptors which are of preparative importance.<sup>1a</sup>

Table 1.4: Leaving Groups and Acceptors for the Preparation of 1,3-Dioxolan-2-ylum Ions via Route 2.

Leaving Group	Acceptor
Cl, Br	AgBF <sub>4</sub> , AgSbF <sub>6</sub>
F	BF <sub>3</sub>
OR	BF <sub>3</sub> , SbCl <sub>5</sub> , R <sub>3</sub> O <sup>+</sup> FSO <sub>3</sub> H, CH <sub>3</sub> OSO <sub>2</sub> F
OH	FSO <sub>3</sub> H, HClO <sub>4</sub>
R(CO)O	FSO <sub>3</sub> H, SbCl <sub>5</sub>

Some examples of this route towards the 1,3-dioxolan-2-ylum ion are given in Scheme 1.6 which also serves to illustrate the stereochemical requirements of the reaction.<sup>11</sup> Antimony pentachloride reacts with the *trans* diesters 1 and 4 to give the corresponding dioxolanylium ions, 3 and 6. Under the same conditions the *cis* diesters 2 and 5 give only partially soluble adducts from which unchanged starting material can be recovered upon hydrolytic work-up. In the *trans* isomers, the acetate group can readily approach the orientation favoured for the back-side, nucleophilic attack and the neighbouring group reaction is facilitated. Further evidence is provided by noting that the cyclopentane derivative 1 reacts faster than the cyclohexane derivative 4. In 4 the ester groups are initially in a diequatorial relationship and must be brought into a diaxial orientation before the neighbouring group reaction can take place. The *cis* compound 5 can be converted to the dioxolanylium ion 6 in liquid HF.<sup>12</sup> The mechanism of this so-called "front-side attack" is unclear.

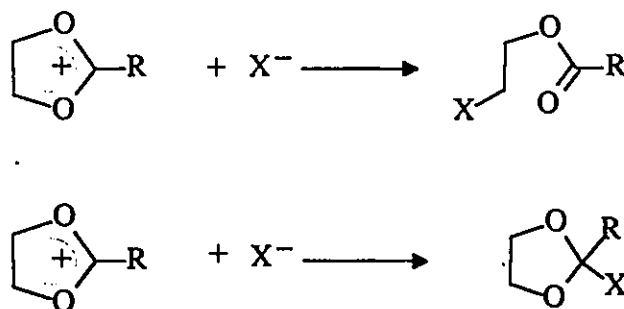




Scheme 1.6

### 1.3 Role of the Anion

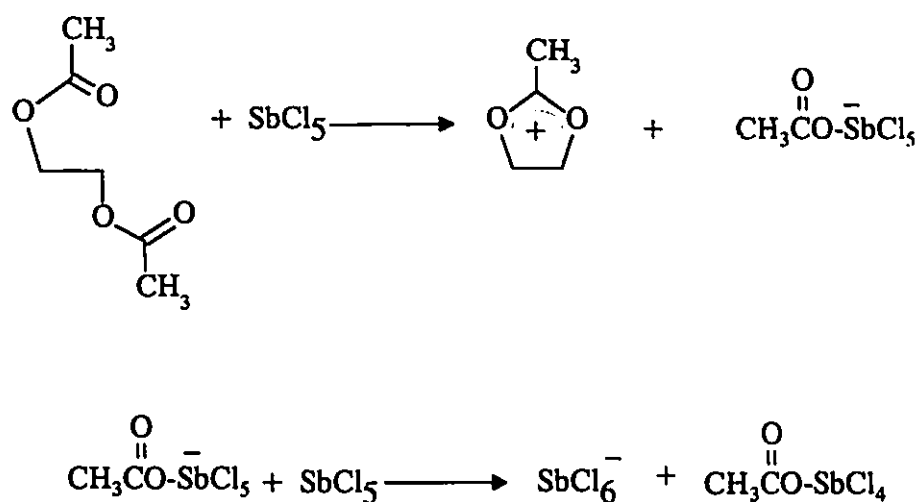
Many of the anions accompanying 1,3-dioxolan-2-ylum cations are halogen complexes of the general formula  $\text{Z}(\text{Hal})_n^-$ , the most important examples of which are  $\text{BF}_4^-$  and  $\text{SbCl}_6^-$ . In general, the anions in the presence of oxonium ions should be of low polarizability and weak nucleophilicity to avoid the following nucleophilic addition reactions (Scheme 1.7):<sup>1a</sup>



Scheme 1.7

Even with the use of the most favourable complex anions, the above decomposition reactions may take place to some extent. Recently, the rate of decay of the 2-phenyl-1,3-dioxolan-2-ylum cation in the presence of a series of anions was measured.<sup>13</sup> The rate of decay is slow (on the order of  $10^{-6}$  to  $10^{-5} \text{ s}^{-1}$  at 288 K) and the stability sequence  $\text{SbCl}_6^- > \text{AsF}_6^- > \text{SbCl}_3\text{Br}^-$  was established. This order is similar to that reported for trialkyloxonium salts.<sup>14</sup>

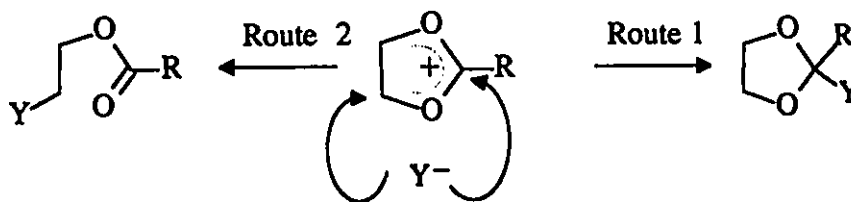
The formation of the complex anion  $\text{SbCl}_6^-$  is an example of a disproportionation reaction<sup>2</sup> which occurs in the presence of excess  $\text{SbCl}_3$  (Scheme 1.8).



Scheme 1.8

#### 1.4 Reaction with Nucleophiles

A nucleophile may add to a 1,3-dioxolan-2-ylum ion in one of two ways, and thus oxonium ions of this and related types are said to be ambident. These pathways are labelled Route 1 and Route 2 in Scheme 1.9 and correspond to the reverse reactions for the formation of the ion already discussed.



Scheme 1.9

Hunig<sup>15</sup> has reviewed the reactions of ambident cations and has explained their behaviour by considering the reaction profiles for the two different routes (Fig 1.1). Route 1 represents the kinetically controlled path since it involves the attack of the nucleophile at the carbon with the lowest electron density and requires the least amount of bond re-organization. The kinetic product can be isolated when the gain in energy from the formation of the bond is large enough. If an equilibrium can be established between the addition product 8 and the 1,3-dioxolan-2-ylum ion 7, then attack via route 2 will result to give the thermodynamically favoured product, 9. In route 2, the energy cost of extensive bond re-organization is more than compensated for by charge neutralization and the resonance stabilization provided by the generation of the ester function.

(i) The Effect of the Nucleophile on the Course of the Reaction

When highly nucleophilic anions are used, reaction by route 1 predominates. This is a result of the high gain in energy in  $\Delta G_1$ . On the other hand, with weak nucleophiles  $\Delta G_1$  is small. The resulting adduct, 8, may easily dissociate to reform the cation 7 which may then react further via route 2. This analysis assumes that the effect of the nucleophile on  $\Delta G_2$ ,  $\Delta G_2^\ddagger$ , and  $\Delta G_1^\ddagger$  are negligible in comparison to its effect on  $\Delta G_1$ . These rules are generally obeyed so that strongly nucleophilic or basic reagents such as  $\text{CH}_3\text{O}^-$ ,  $\text{CN}^-$ , and  $\text{HO}^-$  give the kinetic product (route 1) while weaker nucleophiles such as  $\text{I}^-$ ,  $\text{Br}^-$  and  $\text{Et}_3\text{N}$  give the thermodynamic product (route 2).<sup>3</sup>

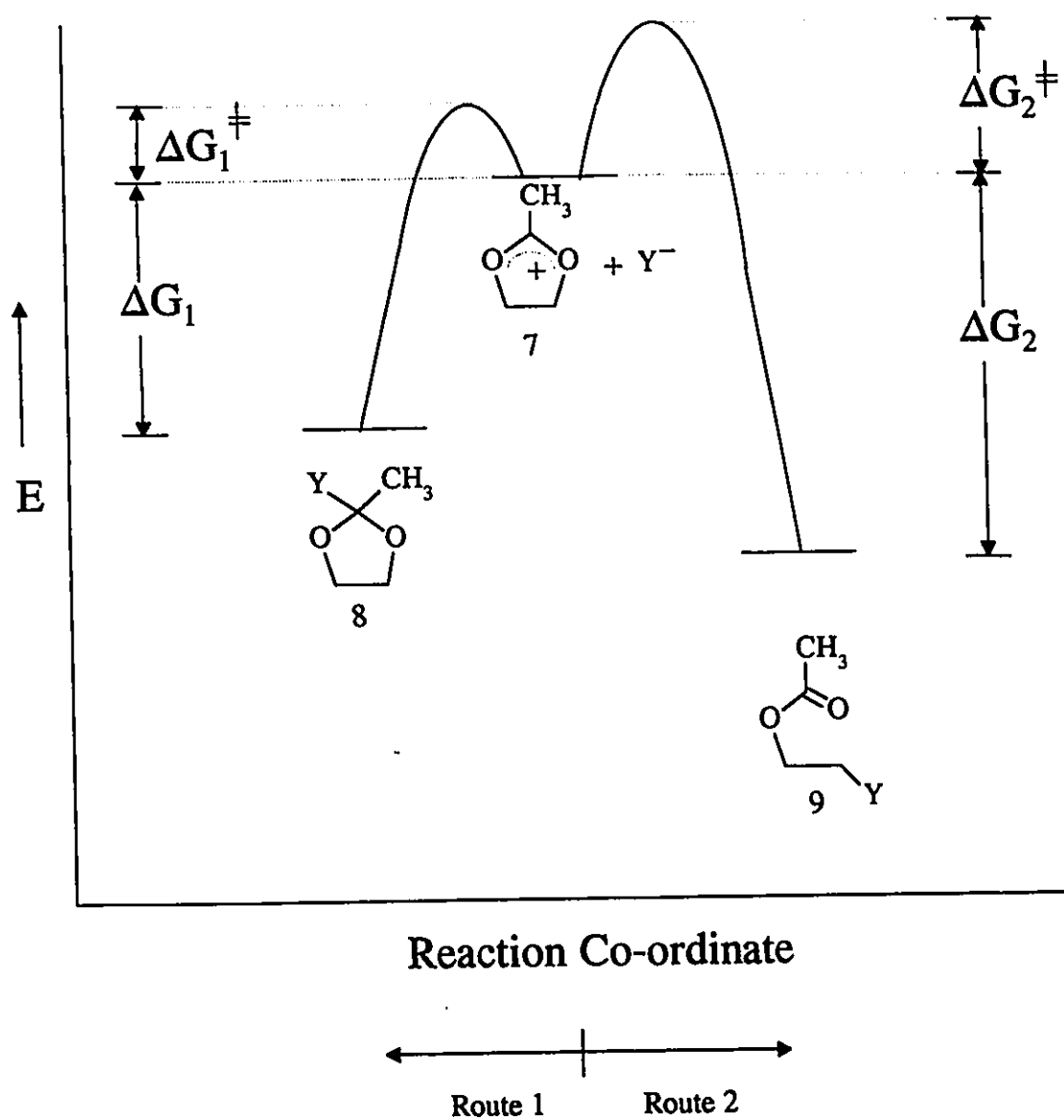


Fig. 1.1: Reaction of ambident cations with nucleophiles.<sup>15</sup>

(ii) The Effect of Ambident Cation Stability on the Course of the Reaction

In principle, the relative position of the cation **7** with respect to the addition products **8** and **9** within the energy profile could also determine whether the kinetic product may be isolated (Fig. 1.2).<sup>15</sup> For high energy (less stable) cations, the magnitude of  $\Delta G_1$  becomes greater. As the cation is increasingly stabilized, the kinetic route becomes less attractive because  $\Delta G_1$  becomes less exothermic. These considerations may be important for extremely stable ambident cations for which even strong nucleophiles react to give the thermodynamic addition product. However, even the very stable 2-aryl-1,3-dioxolan-2-ylum ions are of high enough energy that only kinetically controlled additions are observed with strong nucleophiles.<sup>2</sup>

(iii) Other Factors<sup>15</sup>

Temperature plays an important role in determining the addition of a nucleophile to an ambident cation. Running the reaction at higher temperatures favours the thermodynamic pathway while lower temperatures facilitate the isolation of kinetic products. Longer reaction times favour thermodynamic addition. Steric interactions may reverse the expected course of the reaction. If the site of nucleophilic attack which is normally favoured under a given set of conditions is made sterically inaccessible, then the other route will predominate.

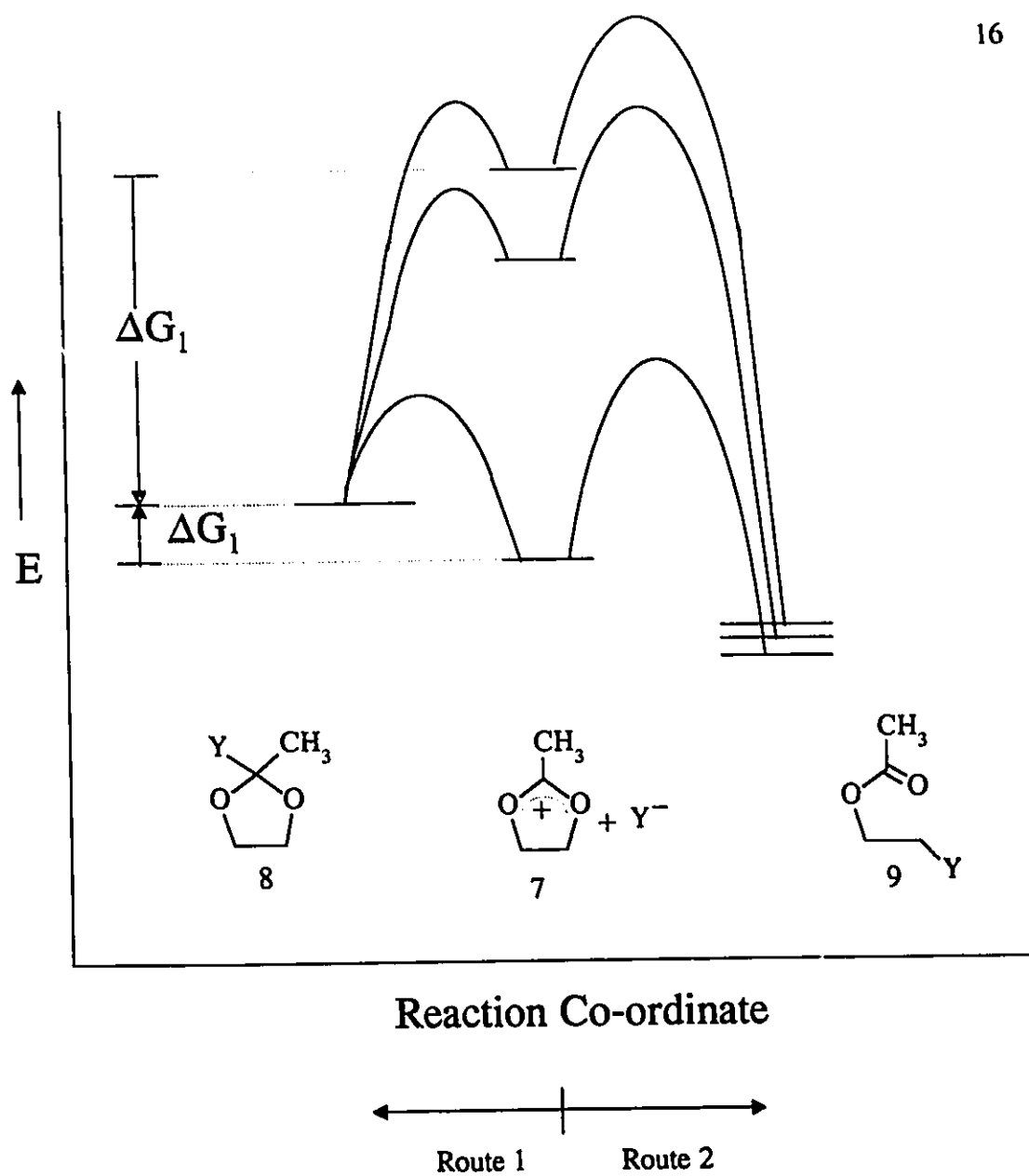


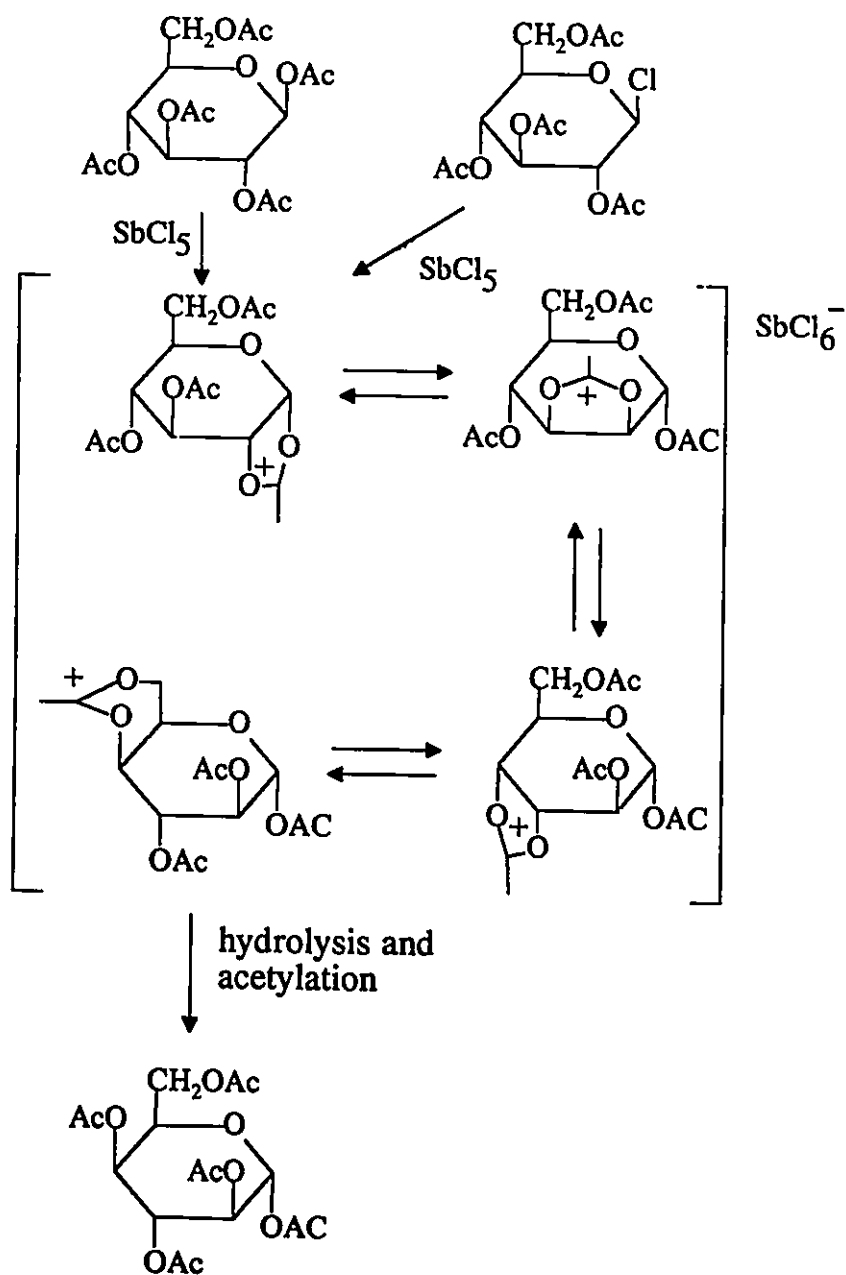
Fig. 1.2: Effect of cation stability on nucleophilic addition.<sup>15</sup>

### 1.5 Dioxolanylium Ions as Intermediates in Carbohydrate Rearrangements

Paulsen has investigated a large number of transformations of carbohydrate and polyol compounds which proceed through 1,3-dioxolan-2-ylum ions.<sup>8,11</sup> These reactions involve the intramolecular attack of a nucleophilic substituent within the sugar molecule and serve as further examples of neighbouring group participation.<sup>10,16</sup> If the polyfunctional compound contains neighbouring groups that are favourably situated, then a complex sequence of transformations can be observed. An impressive example of this is the transformation of D-glucose to D-idose (Scheme 1.10).<sup>17</sup>

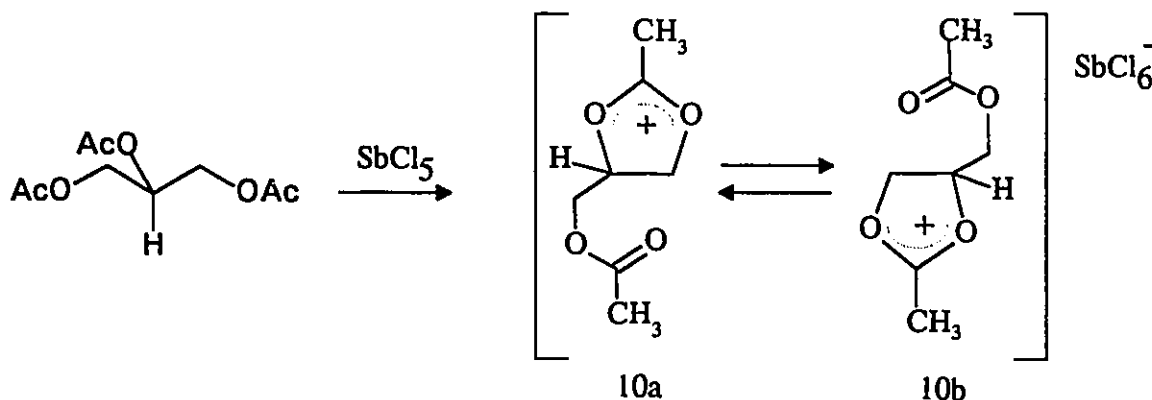
Treatment of tetra-*O*-acetyl- $\beta$ -D-glucopyranosyl chloride with antimony pentachloride yields a crystalline 4,6-acetoxonium salt of idopyranose. The reaction manifold consists of the formation of a gluco 1,3-dioxolan-2-ylum salt which rearranges to a manno ion and then to an altro ion by fast 1,2-neighbouring group reactions. The ido ion is formed from a 1,3-neighbouring group reaction and has low solubility in methylene chloride and continually crystallizes from the equilibrium mixture. In general, the synthetic utility of such transformations is limited since with most other saccharides, the hexachlorantimonate salts obtained contain a mixture of isomeric ions. However, with careful consideration of the stereochemical requirements of the 1,3-dioxolan-2-ylum ion rearrangement, many useful transformations are possible.<sup>17-21</sup> This continues to be an important area of carbohydrate research.





Scheme 1.10

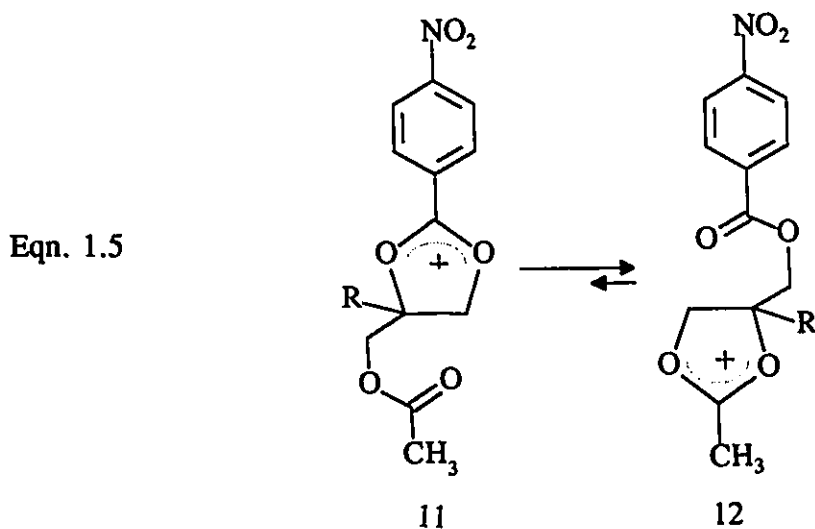
Paulsen has also investigated the reaction dynamics of the 1,2- (and 1,3-) neighbouring group rearrangement. The basic template for the 1,2-rearrangement is provided by 10a  $\rightleftharpoons$  10b which may be prepared by treating glycerol triacetate with antimony pentachloride (Scheme 1.11).<sup>22</sup>



Scheme 1.11

The room temperature  $^1\text{H}$  NMR spectrum of these species contain two separate methyl signals corresponding to the acetoxonium methyl on the dioxolanylium ion ring and the methyl of the acetate group. Upon warming, these methyl signals broaden and eventually coalesce at 365 K. From this, the barrier to isomerization,  $\Delta G^\ddagger$ , was calculated to be 18.7 kcal/mol. This represents the barrier to the 1,2-neighbouring group reaction.

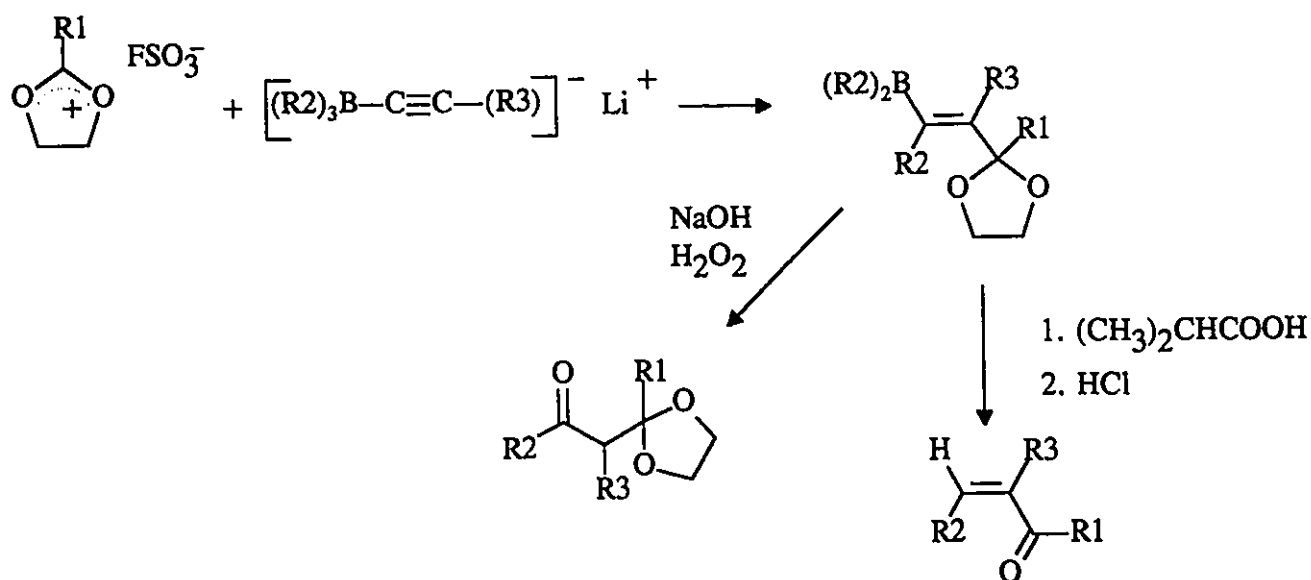
In addition to the degenerate rearrangement described above, the mixed ester system  $11 \rightleftharpoons 12$  was also observed to give rise to a 1,2-rearrangement (Eqn. 1.5).<sup>23</sup> In this case, the stability of the cations involved is different. The electron withdrawing *p*-nitrophenyl group destabilizes the cation in 11, and hence the equilibrium is shifted almost entirely towards 12.



## 1.6 Synthetic Utility

While the occurrence of 1,3-dioxolan-2-ylum ions in carbohydrate chemistry is ubiquitous, the use of these ions in other areas of synthetic organic chemistry is less extensive. One recent example is the preparation of functionalized ketones (Scheme 1.12).<sup>24</sup> The reaction of 2-alkyl-1,3-dioxolan-2-ylum fluorosulphonates with

alkynyltrialkyl borates gives  $\alpha,\beta$ -unsaturated ketones or mono-protected 1,3-diketones depending on the work-up conditions.



Scheme 1.12

Other synthetically useful reactions include the addition of 1,3-dioxolan-2-ylum ions to cyclic ketones<sup>25</sup>, enamines<sup>26,27</sup>, ketene silyl acetals<sup>27</sup>, and lithium organocuprates and lithium organoaluminates<sup>28</sup>. Recent attention has also been given to the use of 1,3-dioxolan-2-ylum ions as initiators for the polymerization of 1,3-dioxane<sup>29</sup>, THF<sup>30</sup>, and 1,3-dioxolane<sup>31</sup>.

## 1.7 X-ray Crystallographic Studies

### (i) Background

Single crystal x-ray crystallography is the most powerful and direct method presently available for the determination of molecular structures. The value of examining a series of closely related molecules has been demonstrated by the structure-correlation method of Burgi and Dunitz.<sup>32a,b</sup> The strategy is to collect as many structures as possible which contain a structural fragment or molecule of interest. Each structure represents a "snapshot" of the fragment in a particular environment and these are ordered in a sequence which represents a gradual deformation of the fragment. The observation of systematic structural changes serves as an experimental basis for mapping the reaction coordinate of a dynamic process. Dunitz has used this method to examine the approach of nucleophiles to an electrophilic center.<sup>33</sup>

Kirby has employed the structure-correlation method to examine the heterolytic cleavage of a C-O bond.<sup>34a-f</sup> An analysis of a series of ethers and esters from the crystallographic literature revealed that the length of the bond in the R<sup>1</sup>-OR<sup>2</sup> system increases with increasing electron withdrawal in the OR<sup>2</sup> group and as the R<sup>1</sup> group changes from methyl through primary, secondary and tertiary alkyl (Table 1.5) This was attributed to an ionic contribution to this bond in the ground state description of the system (Eqn. 1.6).<sup>34c</sup>

Eqn. 1.6

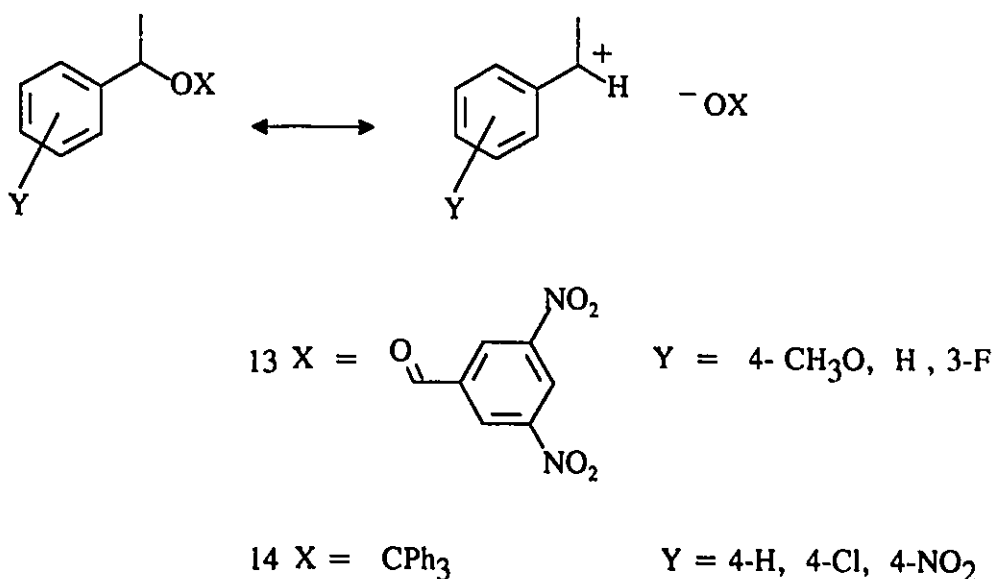


Table 1.5: C-O Bond Lengths ( $R^1$ -OR<sup>2</sup>) in Ethers and Esters

R <sup>1</sup>	Ethers		Esters
	R <sup>2</sup> = alkyl	R <sup>2</sup> = aryl	R <sup>2</sup> = acyl
CH <sub>3</sub>	1.418(2)	1.424(1)	1.450(1)
RCH <sub>2</sub>	1.426(2)	1.437(3)	1.452(2)
R <sub>2</sub> CH	1.432(2)	1.444(6)	1.460(2)
R <sub>3</sub> C	1.450(2)	1.478(4)	1.475(2)

The structure correlations of Burgi and Dunitz<sup>32a,b</sup> are structure-structure relationships between geometrical parameters such as bond lengths and angles. Kirby and co-workers have built upon this concept to establish meaningful structure-*reactivity* relationships which correlate geometrical parameters with rate or equilibrium constants. The structure-reactivity correlation for the S<sub>N</sub>1 cleavage of 1-arylethanol derivatives is a particularly illuminating example.<sup>34b,c</sup> The C-OX bond lengths in a series of esters (13) and ethers (14) of 1-arylethanol were examined. An increase in this bond length was observed for better leaving groups <sup>-</sup>OX, and this increase was inhibited by electron withdrawing substituents Y. An ionic contribution to the C-OX bond in the resonance description of this system was used to account for these observations (Scheme 1.13). Furthermore, the C-OX bond lengths in each of the two series were found to correlate with Hammett  $\sigma$  constants to give the structure-reactivity relationship. From this and other examples, Kirby has defined two working rules relating bond length and reactivity.<sup>34a</sup>

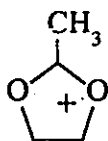
1. The longer the bond, in a given system, the faster it breaks.
2. The more reactive the system, the more sensitive is the length of the bond to structural variation.



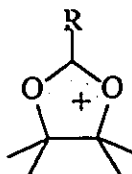
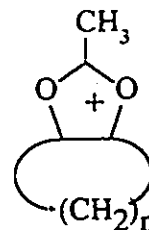
Scheme 1.13

(ii) Structure of the 1,3-dioxolan-2-ylum Ion

Despite the wealth of information provided by x-ray crystallography, relatively few structure determinations of 1,3-dioxolan-2-ylum salts have been carried out. One reason for this may be the difficulty involved in obtaining good quality crystalline samples. To date, a total of nine 1,3-dioxolan-2-ylum ion structures (15-23) have been reported in the literature.<sup>35-40</sup> Selected bond lengths from these ions are given in Table 1.6.

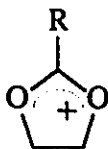
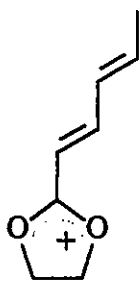


15

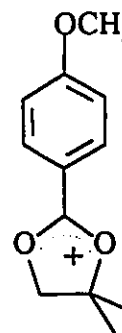
16 R = CH<sub>3</sub>17 R = C<sub>6</sub>H<sub>5</sub>

18 n = 3

19 n = 4

20 R = C<sub>6</sub>H<sub>5</sub>21 R = *p*-CH<sub>3</sub>O-C<sub>6</sub>H<sub>4</sub>

22



23

For most cations in this series, the 1,3-dioxolan-2-ylum ring is planar. The exception is 19 in which the 5-membered ring adopts a slight twist conformation. In each of 15, 16, 18, and 19 the acetoxonium methyl group is co-planar with the ring. An approximate coplanarity also exists for the phenyl and the dioxolanylium rings in each of 17, 20, 21, and 23. In 22, the polyene chain adopts an *s-trans* conformation about both of the formal single bonds. This chain is planar and the angle between this plane and the ring is small.



Table 1.6 Selected Bond Lengths (Å) for Dioxolanylium Salts 15-23.

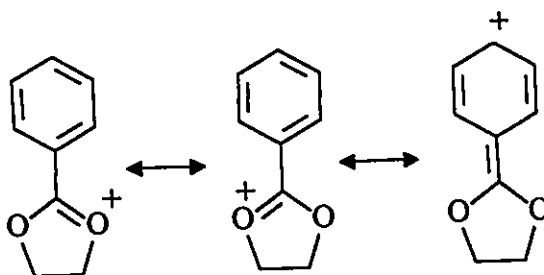
Compound	Bond						
	O(1)C(2)	C(2)O(3)	O(3)C(4)	C(4)C(5)	C(5)O(1)	C(2)C(1')	C(2)C(6)
15 <sup>37</sup>	1.250(6)	1.263(6)	1.470(7)	1.497(6)	1.477(6)	-	1.452(9)
16 <sup>36</sup>	1.277(18)	1.241(2)	1.520(19)	1.566(10)	1.521(15)	-	1.504(18)
17 <sup>35</sup>	1.29(1)	1.29(1)	1.52(1)	1.56(2)	1.52(1)	1.47(2)	-
18 <sup>39</sup>	1.257(3)	1.253(3)	1.479(2)	1.516(4)	1.496(3)	-	1.481(4)
19 <sup>38</sup>	1.269(2)	1.280(8)	1.481(4)	1.535(4)	1.497(6)	-	1.479(7)
20 <sup>40</sup>	1.281(3)	1.282(3)	1.472(3)	1.505(5)	1.480(3)	1.422(3)	-
21 <sup>40</sup>	1.292(8)	1.294(9)	1.475(9)	1.504(11)	1.468(9)	1.413(9)	-
22 <sup>40</sup>	1.288(5)	1.290(5)	1.469(5)	1.515(6)	1.472(5)	1.417(5)	-
23 <sup>40</sup>	1.30(2)	1.29(2)	1.51(2)	1.58(2)	1.46(2)	1.40(2)	-

The cyclopentane ring in 18 adopts an endo-envelope conformation. The cyclohexane ring in 19 lies between a chair and half-chair conformation. The methyl groups at C(4)/C(5) in both 16 and 17 are in a sterically unfavourably two-fold eclipsed configuration due to the planarity of the dioxolanylium ring. The presence of this eclipsed conformation provides evidence for the strong resonance energy of the O(1)-C(2)-O(3)  $\pi$  system which requires total planarity for maximum stabilizing orbital overlap.<sup>36</sup> This mesomeric stabilization outweighs the combined effects of the steric interaction of the two pairs of methyl groups.

For all the dioxolanylium ions 15-23, the O(1)-C(2) and O(3)-C(2) bonds are intermediate in length between those of a C-O single bond in 1,3- dioxolanes (1.41 Å) and a C-O double bond (1.22 Å).<sup>41</sup> The cations can be grouped into two classes with respect to the substituent at C(2).<sup>40</sup> Those with an alkyl group at C(2) (15, 16, 18, 19) have a mean O(1)-C(2)/O(3)-C(2) bond distance of 1.261(5) Å.<sup>41</sup> Cations 17 and 20-23 in which the C(2) substituent is an aryl or unsaturated group, have significantly longer O(1)-C(2)/O(3)-C(2) bond lengths with a mean distance of 1.291(2) Å. The longer O(1)-C(2)/O(3)-C(2) bond lengths for the latter group of cations is indicative of delocalization of positive charge onto the aryl or unsaturated substituent at C(2). This results in a reduction in the double bond character in these C-O bonds (Scheme 1.14).<sup>40</sup>

---

<sup>a</sup>The errors for mean bond lengths are given by  $\sigma_b = [\sum_i (D-d_i)^2/n(n-1)]^{1/2}$  where D is the mean bond distance of n independent variables.

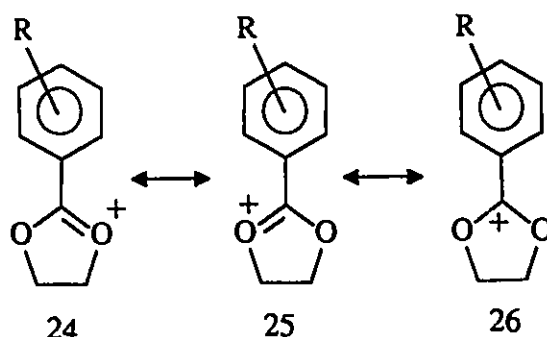


Scheme 1.14

Further evidence for the importance of conjugation between the C(2) substituent and the charged system was provided by examination of the C-C bond lengths within the aryl substituent. As charge is delocalized onto the phenyl substituent, distortions in the benzenoid ring are expected. The non-equivalence of the C-C bonds in the aryl rings of 20 and 21 are in support of this. A similar analysis of the C-C bond lengths in the dienyl chain in 22 also reveals that the positive charge is delocalized to some extent in the unsaturated substituent.<sup>40</sup>

These findings seem to contradict the conclusions of Hart and Tomalia.<sup>42</sup> The dependence of the <sup>1</sup>H NMR chemical shifts of the C(4)/C(5) protons on the C(2) substituent in a series of 2-aryl-1,3-dioxolan-2-ylum ions was investigated. The chemical shifts were found to correlate better with the Hammett  $\sigma$  values ( $r=0.966$ ) than with  $\sigma'$

values ( $r = 0.944$ ). The authors concluded that resonance interactions between electron-releasing substituents and the electron deficient 1,3-dioxolan-2-ylum ring are not strong. It was postulated that the important contributors to the resonance hybrid are 24 and 25 rather than 26 (Scheme 1.15). These findings can perhaps be reconciled with the recent crystallographic investigations by stating that while 26 may not be a major resonance contributor, its contribution is still significant and detectable.



Scheme 1.15

The effect of the C(2) substituent on the O(3)-C(4)/O(1)-C(5) bond lengths is also of interest. Comparison of these C-O bond lengths in 15, 20 and 21 show no significant differences as the C(2) substituent is varied from methyl, through phenyl and *p*-methoxyphenyl. Thus, the chemical shift dependence observed for the C(4)/C(5) protons on the nature of the C(2) substituent is not reflected as a detectable change in the O(3)-C(4)/O(1)-C(5) bond lengths.<sup>40</sup>

The cations 15-23 may be grouped according to the number of alkyl substituents attached to the C(4)/C(5) carbon atoms.<sup>40</sup> This allows three types of O(3)-C(4)/O(1)-C(5)

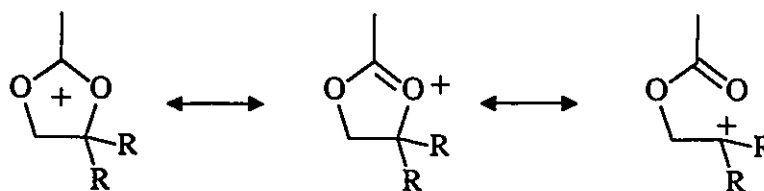
bonds to be identified:  $\text{O-CH}_2\text{R}$ ,  $\text{OCHR}_2$ , and  $\text{OCR}_3$ . The mean bond lengths for each type of C-O bond in the cations is given in Table 1.7. For comparison, the O-C(alkyl) bond lengths observed in alkyl esters are also given.<sup>40,34c</sup>

Table 1.7: Mean O-C(alkyl) Bond Lengths

O-C Bond Type	Bond Length (Å)	
	Dioxolanylium Ion	Ester
O-CR <sub>3</sub>	1.525(5)	1.475(2)
O-CHR <sub>2</sub>	1.491(5)	1.460(2)
O-CH <sub>2</sub> R	1.474(2)	1.452(2)
O-CH <sub>3</sub>	-	1.450(1)

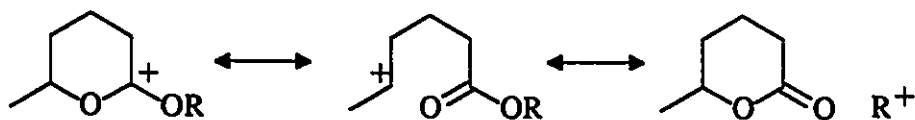
Inspection of the values in Table 1.7 reveals several interesting features.

The O-C(alkyl) bond lengths within the dioxolanylium ring are longer than the corresponding bonds found in the neutral esters. Secondly, substitution at the alkyl carbons in the dioxolanylium rings has a greater effect on the O-C(alkyl) bond lengths than does substitution in the esters. Finally, the O-C(alkyl) bond lengths in the dioxolanylium ions increase as the degree of substitution at the alkyl carbons is increased. This last point was taken as evidence for an ionic contribution to the O-C(alkyl) bond with positive charge residing on the alkyl carbon atom. Increased substitution at C(4)/C(5) allows the alkyl carbon atom to accept more positive charge due to the stabilization provided by these substituents (Scheme 1.16).<sup>40</sup>



Scheme 1.16

Thus, the concept of an ionic contribution to the O-C(alkyl) bonds in ethers and esters proposed by Kirby<sup>34</sup>, can now be extended to include the dioxolanylium ion system as well. A further example has been provided by Childs and co-workers<sup>43</sup>, who have observed a similar substituent effect in tetrahydropyranylium cations. Long O-C(alkyl) bonds were attributed to an ionic contribution to this bond, with positive charge residing on the alkyl carbon atom (Scheme 1.17).



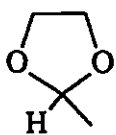
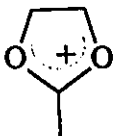
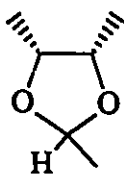
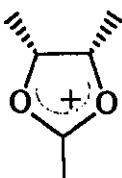
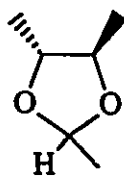
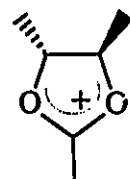
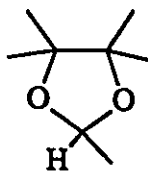
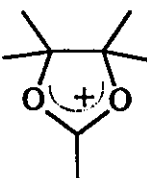
Scheme 1.17

## 1.8 $^{13}\text{C}$ NMR Investigations

The non-bonded resonance structures depicted in Schemes 1.16 and 1.17 are not usually included in the resonance description of alkoxy carbenium ions. There is further experimental evidence, however, that a portion of the positive charge in 1,3-dioxolan-2-ylum cations resides on the C(4)/C(5) alkyl carbon atoms. Paulsen<sup>37</sup> has undertaken a detailed  $^{13}\text{C}$  NMR study of dioxolanylium ions with alkyl substituents at the C(2), C(4) and C(5) carbon atoms. The effect of increased substitution at the alkyl carbons was probed by calculating the chemical shift difference ( $\Delta\delta$ ) for the C(4)/C(5) resonances between the 1,3-dioxolan-2-ylum ion and the corresponding neutral 1,3-dioxolane (Table 1.8). As one and then two methyl groups were placed at each of the C(4) and C(5) carbon atoms, the value of  $\Delta\delta$  grew progressively larger. This was attributed to an increase in positive charge density at C(4)/C(5) with increased substitution.

It would be of interest to apply the same analysis to the C(2) chemical shifts in 1,3-dioxolan-2-ylum ions and 1,3-dioxolanes. This might allow an assessment of how increased substitution at C(4)/C(5) affects charge at C(2). The authors did not perform this calculation, but from the data provided,<sup>37</sup> such an analysis is possible and the results are listed in Table 1.8. A systematic dependence of  $\Delta\delta$  for C(2) on the degree of methyl substitution at C(4)/C(5) is absent. A decrease in C(2) charge density is expected to accompany an increase in charge density at C(4)/C(5) based on the resonance description of the ions given in Scheme 1.16.

Table 1.8:  $^{13}\text{C}$  Chemical Shift Differences in 1,3-dioxolan-2-ylum Ions and 1,3-dioxolanes in  $\text{CH}_3\text{CN}$ .

1,3-dioxolane	1,3-dioxolanylium	$\Delta\delta \text{ C(4)/C(5)}$	$\Delta\delta \text{ C(2)}$
		11.1	91.6
		14.2	81.0
		13.0	81.7
		20.3	89.9



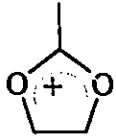
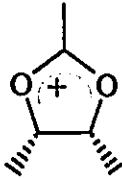
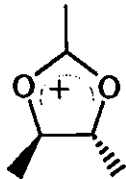
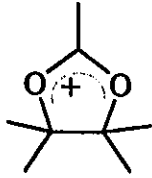
Olah<sup>44</sup> has correlated the  $^{13}\text{C}$  NMR chemical shifts with  $\pi$  electron density on the positively charged carbon atom of oxonium ions (Eqn 1.7).

$$\text{Eqn. 1.7} \quad \delta_{\text{CS}_2} = -306(1-q_r) + 160$$

In this equation,  $\delta_{\text{CS}_2}$  denotes the chemical shift relative to the  $\text{CS}_2$  signal in the  $^{13}\text{C}$  NMR spectrum,  $q_r$  is the electron density, and  $(1-q_r)$  is the formal positive charge on the carbon atom for which  $\delta_{\text{CS}_2}$  is measured. This equation has been applied to the C(2), C(4) and C(5)  $^{13}\text{C}$  NMR chemical shifts of dioxolanylium ions.<sup>37,45</sup> Although the latter two alkyl carbon atoms were included in the analysis, only the C(2) carbon atom is of the correct type to be used in this equation. An increase in the formal positive charge at the C(4)/C(5) carbon atoms was observed with increased methyl substitution (Table 1.9). The charge distribution calculated using Eqn. 1.7 for the 2,4,4,5,5-pentamethyldioxolan-2-ylum cation is similar to that obtained from its ESCA spectrum,<sup>37</sup> thus providing some support for the use of this equation.

The charge densities calculated for C(2) are nearly constant throughout this series. As discussed earlier, the resonance structures shown in Scheme 1.16 suggest that a decrease in positive charge density at the C(2) carbon atom would result from increased substitution at the alkyl carbon atoms. Once again, the  $^{13}\text{C}$  NMR data appear to be at odds with x-ray crystallographic studies.

Table 1.9: Charge Densities Calculated from  $^{13}\text{C}$  Chemical Shifts.

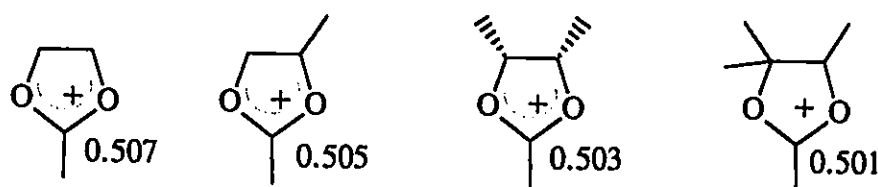
Compound	Positive Charge Density	
	C(4)/C(5)	C(2)
	0.14	0.52
	0.18	0.51
	0.19	0.51
	0.23	0.51

### 1.9 Semi-Empirical Calculations

Pittman has performed SCF-MO calculations in the INDO approximation on a series of 2-substituted 1,3-dioxolan-2-ylum ions.<sup>46</sup> The  $\pi$ -bond orders for the O(1)-

C(2)/O(3)-C(2) bonds were found to be in the range of 0.50 to 0.65 depending on the nature of the C(2) substituent. Thus, both MO calculations and x-ray crystal structure data show the importance of the oxonium resonance structure which gives partial double bond character to these C-O bonds.

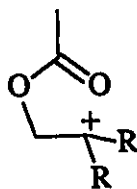
Paulsen has examined the charge distribution in a series of 2-methyl-1,3-dioxolan-2-ylum ions with a varying degree of methyl substitution at C(4)/C(5).<sup>47</sup> Using the MINDO/3 approximation, the positive charge density at C(2) was found to decrease with increased substitution at the C(4)/C(5) carbon atoms (Scheme 1.18). Furthermore, the <sup>13</sup>C NMR chemical shifts of the C(2) carbon atoms were found to correlate well with the calculated C(2)  $\pi$ -charge densities for this series. This supports the notion that there is a contribution from the non-bonded resonance structure to the ground state description of the ion (Scheme 1.16), and that this contribution can be enhanced by increased substitution at the C(4)/C(5) alkyl carbons. However, the dependence of the positive charge density residing on the C(2) carbon atom on C(4)/C(5) substitution is small. This might explain the failure to observe this substituent effect in the <sup>13</sup>C NMR studies<sup>37,43</sup> of these ions due to the limited resolution of those experiments.



C(2) charge density  
Scheme 1.18

### 1.10 Objectives

Despite the considerable attention paid to 1,3-dioxolan-2-ylum ions in the literature, some discrepancies remain regarding the effect of substituents on the structure of the system. It has been suggested<sup>40</sup> that the ground state description of the dioxolanylium ion should include resonance structure 27 based on crystallographic evidence. Some support for this is provided by NMR spectroscopic and theoretical investigations in which increased positive charge density was seen to accompany alkyl substitution on the C(4) carbon atoms.<sup>37,45,47</sup> However, the possibility of observing systematic changes in C(4) charge density with substitution is made difficult due to the differing steric requirements of the substituents employed in these studies. Furthermore, the effect of C(4) substitution on the charge density at other positions in the 1,3-dioxolan-2-ylum ion ring has not been adequately demonstrated. While semi-empirical calculations<sup>47</sup> have suggested a decrease in charge density at C(2) upon alkyl substitution at the C(4)/C(5) carbon atoms, <sup>13</sup>C NMR investigations<sup>37,45</sup> have failed to reveal such a substituent effect.



27

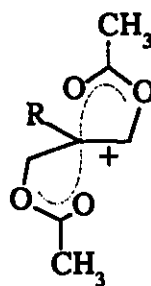
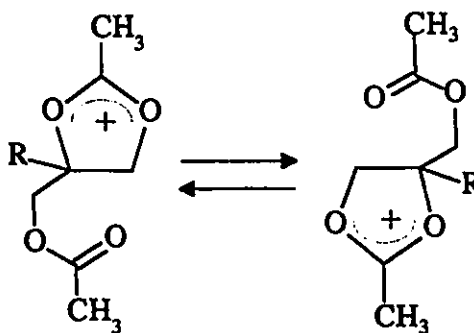
It was proposed that various *p*-substituted phenyl substituents at C(4) could be used to moderate electron density within the dioxolanylium ion ring with minimal effect on the steric requirements of the system. The distribution of positive charge throughout the 1,3-dioxolan-2-ylum ion system could be assessed by  $^{13}\text{C}$  NMR spectroscopy. The electron donating power of aryl substituents are readily identified by their Hammett-type substituent constants. It was intended, therefore, that the use of aryl substituents at C(4) would provide a more quantitative assessment of substituent effects than has been possible in previous studies.

It was further proposed that by a suitable choice of the C(4) substituent, the contribution of the ionic resonance contributor **27** could be enhanced. This could be detected in systematic structural changes using semi-empirical calculations and, where possible, by x-ray crystallography.

The effect of substituents on the reactivity of the 1,3-dioxolan-2-ylum ion towards nucleophilic substitution was also of interest. Building upon the isomerization reaction reported by Paulsen<sup>22</sup>, the effect of substituents on the intramolecular nucleophilic attack of an acetate group on the 1,3-dioxolan-2-ylum ion system could be investigated (Eqn.1.8). It was proposed that the barrier to this isomerization reaction could be systematically reduced by the introduction of better charge stabilizing substituents at C(4). In this way, the nucleophilic substitution reaction could be "mapped out", with the structure of each dioxolanylium ion representing a point along the reaction co-ordinate, with the aim of gaining information about the transition state structure. This was

intended to increase the scope of the nucleophilic addition studies of Dunitz<sup>32,33</sup> and the ionization studies of Kirby,<sup>34</sup> to include cationic systems. In particular, it was thought that when the C(4) substituent was sufficiently electron-donating, then the ion might adopt a structure with a high degree of carbenium ion character with a greater portion of the positive charge residing on C(4). Since the acetate moieties provide good internal Lewis bases, the possibility exists that the system might adopt the trigonal-bipyramidal structure 28, and hence serve as a model for the S<sub>N</sub>2 transition state.<sup>48-50</sup>

Eqn. 1.8



28

## Chapter 2

### NMR Study

Described in this chapter are  $^1\text{H}$  and  $^{13}\text{C}$  NMR investigations of 1,3-dioxolan-2-ylum ion structure and reactivity. In Part A, the syntheses of the 1,3-dioxolan-2-ylum ion systems chosen for study are outlined. Part B describes the intramolecular nucleophilic attack of an acetate group on the 1,3-dioxolan-2-ylum ion. A homologous series of ions were investigated in a systematic attempt to reduce the barrier to this isomerization reaction, and explore the possibility of generating a cation whose structure resembles that of an  $\text{S}_{\text{N}}2$  transition state. The mechanism of isomerization was determined with the aid of dynamic NMR techniques. In Part C, the results of a  $^{13}\text{C}$  NMR correlation analysis on a series of aryl substituted 1,3-dioxolan-2-ylum ions are presented. The dependence of the carbon chemical shifts on the electron donating capability of the aryl substituent was examined. These substituent effects were used to determine the important resonance contributors to the ground state description of the 1,3-dioxolan-2-ylum ion system.

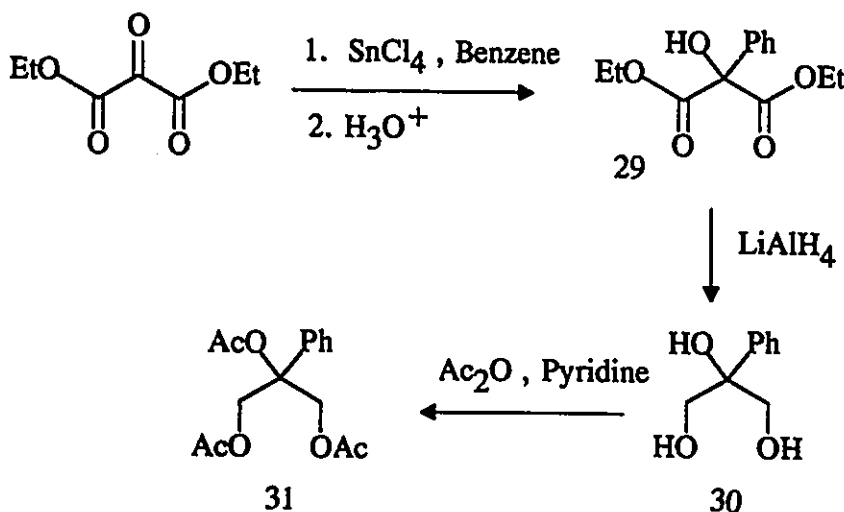
## Part A: Syntheses

### 2.1 Routes Toward Dioxolanylium Ion Precursors

A common strategy was employed to obtain the 1,3-dioxolan-2-ylum salts described in this work. Triacetates of 1,2,3-propanetriol with various substituents at the C(2) position, provided convenient precursors. The syntheses of the triacetates were achieved using one of the following methods.

#### (a) Via Diethylketomalonate

Scheme 2.1 illustrates the route towards **31**. The first step is the condensation of benzene with diethylketomalonate in the presence of  $\text{SnCl}_4$ .<sup>51</sup> Reduction of the diester **29** with  $\text{LiAlH}_4$  afforded the triol **30** which was then acetylated. The second step proved to be the most difficult reaction, the diester resisting reduction even with long reaction times at elevated temperatures. Furthermore, isolation of the triol from the reaction mixture required continuous extraction into ether which was time consuming and inefficient.

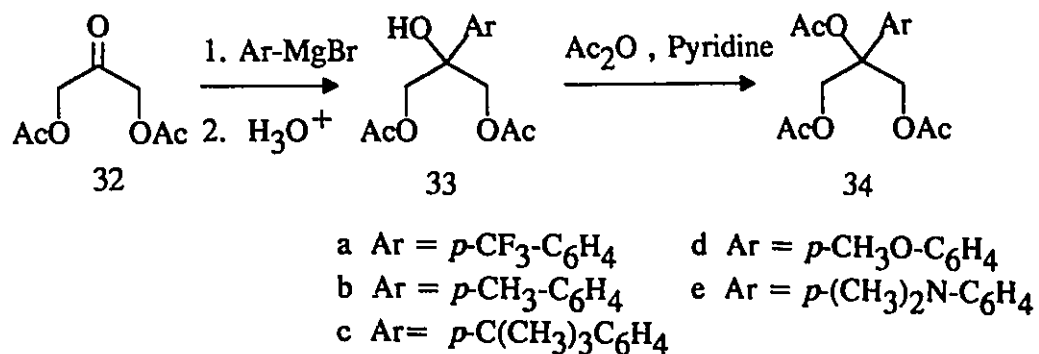


Scheme 2.1



## (b) Via 1,3-Dihydroxypropan-2-one-1,3-diacetate

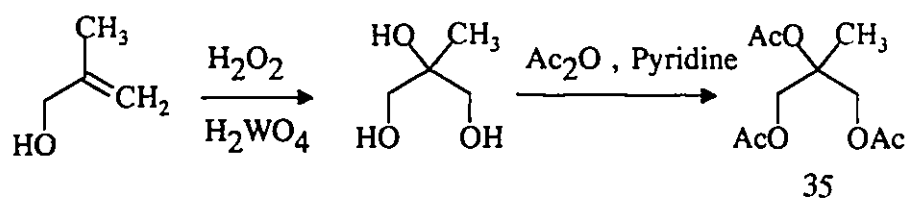
A more successful route towards the triacetate precursors is given in Scheme 2.2. Addition of the appropriate aryl Grignard reagent to 1,3-dihydroxypropan-2-one-1,3-diacetate (32)<sup>32</sup> was performed at  $-60^{\circ}\text{C}$  to allow reaction at the ketone function instead of at the ester carbonyls.<sup>33</sup> This regioselectivity was further enhanced by ensuring that 32 was always present in excess during the addition. Acetylation of the resulting tertiary alcohol 33a-e afforded the triacetate precursor 34a-e.



Scheme 2.2

## (c) Via Dihydroxylation of an Olefin

The triacetate 35 was efficiently prepared via the dihydroxylation of the commercially available 2-methyl-2-propene-1-ol. As illustrated in Scheme 2.3, the olefin was treated with hydrogen peroxide in the presence of tungstic acid acting as a catalyst.<sup>34</sup> Acetylation of the triol gave the desired triacetate.

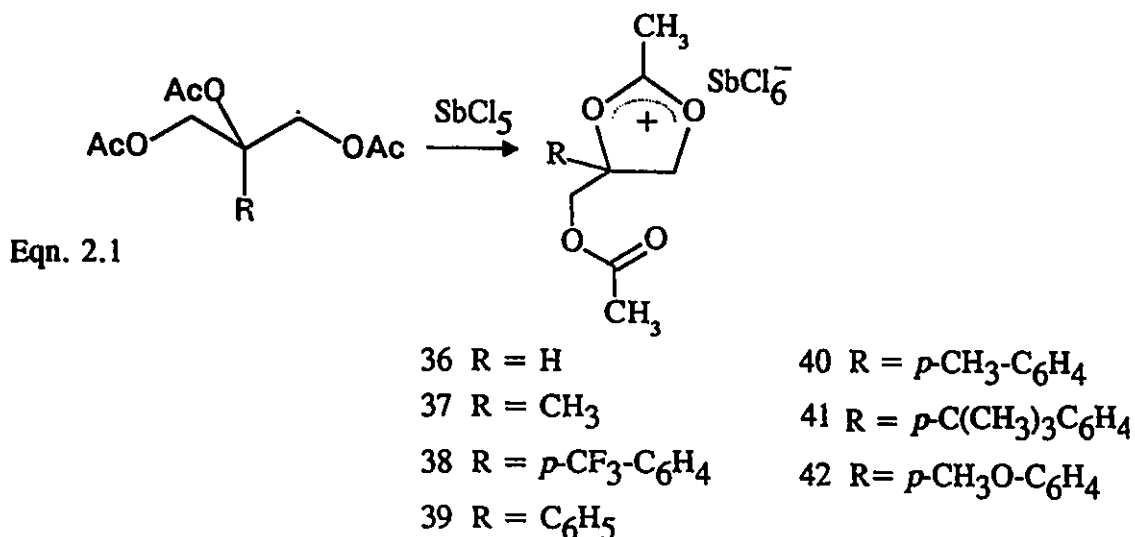


Scheme 2.3

## 2.2 Generation of the Dioxolanylium Ion

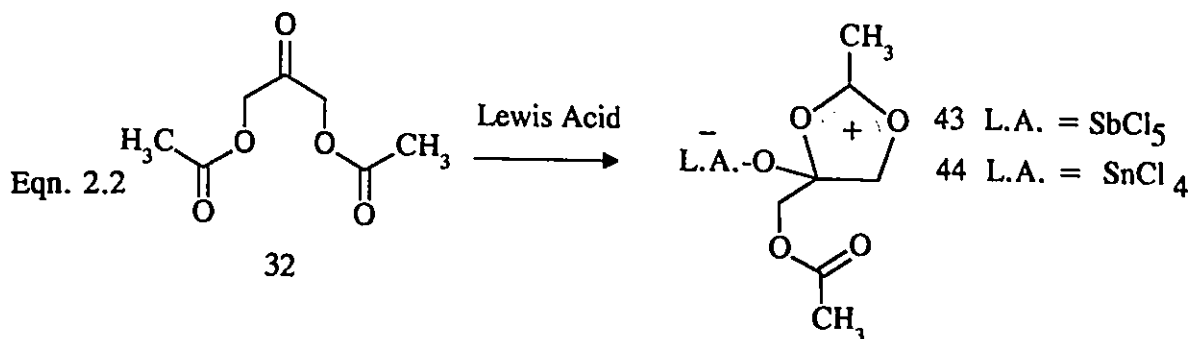
### (a) Hexachloroantimonate ( $\text{SbCl}_6^-$ ) salts

Dioxolanylium ion salts containing an aryl, methyl or hydrogen atom substituent at C(4) were each generated from the corresponding triacetate precursor following the method of Paulsen.<sup>22</sup> Ionization of the triacetates with  $\text{SbCl}_5$  in  $\text{CH}_2\text{Cl}_2$  afforded the dioxolanylium ions as their hexachloroantimonate salts (36-42) (Eqn 2.1). The salts could be isolated and handled at room temperature under a dry nitrogen atmosphere for short periods without decomposition but hydrolysed quickly when exposed to atmospheric moisture. The salts could be stored indefinitely in sealed vials at  $-30^\circ\text{C}$ . The  $^1\text{H}$  and  $^{13}\text{C}$  NMR spectral data for 36 - 42 are presented in Tables 2.1 to 2.3.



## (b) Lewis Acid Adducts

The complexation-cyclization reaction of 1,3-dihydroxypropane-2-one-1,3-diacetate **32** with Lewis acids provided an alternative means of generating the 1,3-dioxolan-2-ylum ion system (Eqn. 2.2). The NMR data for the  $\text{SbCl}_5$  and  $\text{SnCl}_4$  adducts, **43** and **44** respectively, are presented in Table 2.4.



## Part B: Dynamic NMR Studies

2.3  $^1\text{H}$  NMR of Aryl Dioxolanylium Ion Salts

The  $^1\text{H}$  NMR spectra of the C(4)-aryl substituted dioxolanylium ions **38-42** were recorded as their  $\text{SbCl}_6^-$  salts in  $\text{CD}_3\text{NO}_2$  at low temperature. As can be seen from the data presented in Table 2.1, all the salts had similar spectra and were consistent with previously reported spectra for other dioxolanylium ion systems.<sup>3</sup>

Table 2.1: NMR Data for 36 and 37 in CD<sub>3</sub>NO<sub>2</sub>.**<sup>13</sup>C NMR**

Carbon Atom	Compound	
	36	37
C(2)	193.78	192.80
C(4)	92.92	101.98
C(5)	89.88	81.76
C(6)	15.87	15.94
C(7)	77.82	66.67
C(9)	171.74	171.44
C(11)	20.45	20.38
other	-	20.68

**<sup>1</sup>H NMR**

Proton	Compound	
	36	37
H(4)	6.12 -6.22 (m)	-
H(5a)		5.47 (d)
	5.35 - 5.63 (m)	
H(5b)		5.20 (d)
		(10.2 Hz)
H(6)	2.97 (s)	2.95 (s)
H(7a)		4.52 (d)
	4.32 - 4.71 (m)	
H(7b)		4.46 (d)
		(13.5 Hz)
H(11)	2.10 (s)	2.10 (s)
other	-	1.95 (s)

Table 2.2: <sup>1</sup>H chemical shifts<sup>a</sup> of 38-42.

Proton	Compound				
	38	39	40 <sup>b</sup>	41	42
H(5a)	5.88 (d)	5.83 (d)	5.91 (d)	5.81 (d)	5.75 (d)
H(5b)	5.49 (d)	5.49 (d) (9.8 Hz)	5.65 (d) (10.2 Hz)	5.51 (d) (9.8 Hz)	5.51 (d) (9.8 Hz)
H(6)	3.00 (s)	2.98 (s)	3.08 (s)	2.97 (s)	2.94 (s)
H(7a)	4.46 (d)	4.36 (m)	4.69 (d)	4.45 (d)	4.48 (d)
H(7b)	4.40 (d) (13.7 Hz)		4.64 (d) (13.6 Hz)	4.40 (d) (13.6 Hz)	4.40 (d) (13.6 Hz)
H(11)	2.04 (s)	2.04 (s)	2.12 (s)	2.05 (s)	2.06 (s)
H(4')	-		-	-	-
H(3'/5')		7.31-7.55 (m)		7.30 (d)	7.38 (d)
	7.53-7.75 (m)		7.42 (s br.)		
H(2'/6')				7.50 (d) (8.4 Hz)	6.97 (d) (8.8 Hz)
R	-	-	2.40 (s)	1.20 (s)	3.75 (s)

<sup>a</sup> In CD<sub>3</sub>NO<sub>2</sub>/CD<sub>2</sub>Cl<sub>2</sub> at -98 °C except where noted.<sup>b</sup> In CD<sub>3</sub>NO<sub>2</sub> at -21 °C

Table 2.3:  $^{13}\text{C}$  chemical shifts<sup>a</sup> (ppm) of 38-42.

Carbon Atom	Compound					
	38	39 <sup>b</sup>	39	40 <sup>c</sup>	41	42
C(2)	190.73	191.90	190.29	192.71	190.12	189.99
C(4)	98.94	100.10	99.72	102.55	100.07	100.32
C(5)	79.66	82.66	79.58	81.58	79.41	79.27
C(6)	15.42	17.48	15.36	15.96	15.32	15.32
C(7)	66.12	69.22	66.54	67.60	66.34	66.48
C(9)	169.59	171.90	170.00	171.38	169.63	170.25
C(11)	19.88	21.14	19.98	20.39	19.96	20.05
C(1')	134.88	132.10	130.65	129.80	127.58	121.58
C(2'/6')	124.94	125.24	124.13	126.32	124.12	126.34
C(3'/5')	125.87	<sup>d</sup>	128.98	131.23	126.01	113.86
C(4')	121.80	131.91	130.47	143.07	153.51	160.34
R	<sup>d</sup>	-	-	21.18 29.89	34.21	55.09

<sup>a</sup> In  $\text{CD}_3\text{NO}_2/\text{CD}_2\text{Cl}_2$  at  $-98^\circ\text{C}$  except where noted. Chemical shifts given at a precision of  $\pm 0.02$  ppm.

<sup>b</sup> CPMAS spectrum at  $21^\circ\text{C}$ . Chemical shifts given at a precision of  $\pm 0.06$  ppm.

<sup>c</sup> In  $\text{CD}_3\text{NO}_2$  at  $-21^\circ\text{C}$ .

<sup>d</sup> Not detected.

Table 2.4: NMR data for Lewis acid complexes 43 and 44.

**<sup>1</sup>H NMR**

Compound	Chemical Shifts (ppm)
43	2.22 (s br., H11) <sup>a</sup> 2.93 (s br., H6) 4.81 (s br., H7) 5.29 (s br., H5)
44	2.65 (s. br) <sup>b</sup> 5.06 (s. br)

**<sup>13</sup>C NMR**

Compound	Chemical Shifts (ppm)	
	Solution	CPMAS
44	20.99 <sup>c</sup> 68.28 179.62 192.35	21.05 <sup>d</sup> 71.76 183.00 195.38

<sup>a</sup> In CD<sub>2</sub>Cl<sub>2</sub> at -62 °C (250 MHz).<sup>b</sup> In CD<sub>2</sub>Cl<sub>2</sub> at -100 °C (500 MHz).<sup>c</sup> In CD<sub>2</sub>Cl<sub>2</sub> at -100 °C (125.7 MHz).<sup>d</sup> At 25 °C (25.1 MHz).

A sharp singlet for the H(6) methyl protons was consistently observed around 3.0 ppm. The resonance of the H(11) protons corresponding to the methyl group of the acetate moiety, occurred as a sharp singlet around 2.0 ppm. The H(7) methylene protons are magnetically non-equivalent and occurred as a quartet (AB spin system), with a coupling constant of about 13.6 Hz. A second AB spin system was observed for the H(5) methylene protons at lower field than that of the H(7) protons. The coupling constants observed (9.8-10.2 Hz) for the geminal H(5) protons are very similar to those reported for other related dioxolanylium ions.<sup>3</sup>

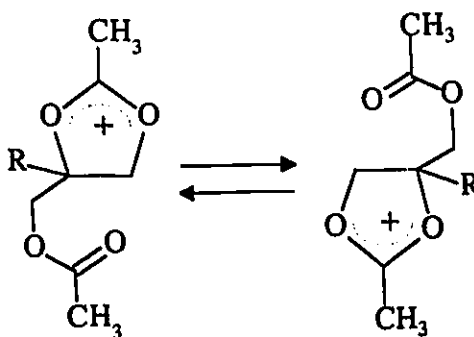
For <sup>1</sup>H NMR spectra recorded at higher temperatures, the acetate and acetoxonium signals (H(11) and H(6) respectively) began to broaden. Similarly the H(5) and H(7) pairs of methylene protons also broadened. The temperature at which these broadenings first became noticeable was system dependent, usually occurring just above room temperature. As the temperature was increased further, broadening continued and in the case of 42, coalescence of the H(11) and H(6) signals was observed with the eventual formation of a single sharp resonance.

These observations are consistent with a degenerate isomerization reaction as shown in Eqn. 2.3.<sup>22</sup> The product of this reaction is identical to the starting material. This process may be viewed as an intramolecular nucleophilic displacement reaction at C(4): the acetate group which is bound as the dioxolanylium moiety is the leaving group and the unbound acetate group acts as an internal nucleophile. In effect, the end result of this isomerization is that the acetate methyl group is "exchanged" for the acetoxonium



methyl group. Similarly, the ring methylene protons H(5) are exchanged for the acyclic methylene protons H(7). When the rate of isomerization is sufficiently fast with respect to the NMR time scale, broadening of these two pairs of signals is observed. This broadening is the consequence of a given proton spending time in two different magnetic environments during the time required to collect each scan. As the temperature is increased further, each pair of signals eventually coalesces into a single resonance. This time-averaged signal appears at point between the chemical shifts in the static condition; that is, when no exchange is occurring. The chemical shift of the averaged peak is dependent upon the population of the spins involved. Since the population of the acetate and acetoxonium methyl resonances are equal, the averaged peak should appear midway between these two chemical shifts.

Eqn. 2.3



## 2.4 Measurement of Isomerization Rate Constants by Total Bandshape Analysis

It is possible to extract rate information from the NMR spectrum of a system undergoing a dynamic exchange process using total bandshape analysis.<sup>55</sup> Using various computer programs, calculated line shapes at various rates of exchange are visually

compared to the actual spectrum obtained at a given temperature. This simple trial and error approach will produce the value of the rate constant which gives the closest fit of the model to the actual spectrum. Typically, the following input parameters are required: number of exchanging sites, frequency and relative population of each site, estimate of the spectrometer line width (in Hz) in the absence of exchange, the estimated rate of exchange, and exchange map which defines which sites exchange with each other. In practice, the visual comparison of the simulated and actual spectrum results in a range of rate constants which reproduce the spectrum equally well.

Using this approach, the rate of isomerization was investigated for the series of dioxolanylium ions with aryl substituents at C(4) (38-42). For each compound, the  $^1\text{H}$  NMR spectrum in  $\text{CD}_3\text{NO}_2$  was recorded over a suitable range of temperatures. In order for a series of variable temperature spectra to be useful for line shape analysis, the temperature range was chosen such that the rate of exchange was fast enough to observe line broadening but not so fast as to produce a completely averaged (sharp) signal.

Two computer simulation programs were employed: DNMR3<sup>36</sup> and Exchange.<sup>37</sup> The former program allowed for the simulation of exchanging spin systems which were coupled; that is, the exchange of the methylene protons H(5) with H(7). This was the case for the *p*-methylphenyl substituted dioxolanylium ion, 40. It was convenient to simulate the methylene groups in this instance since the coalescence of the acetoxonium methyl with the acetate methyl group was somewhat obscured by the resonance at 2.40 ppm of the *p*-methyl group on the phenyl ring. In all other cases, the exchange of the

acetate methyl with the acetoxonium methyl group was simulated with either DNMR3 or Exchange. The rate of exchange of the *p*-CF<sub>3</sub>phenyl compound 38 was too slow to observe any broadening up to 100 °C. In this case, an upper limit for the rate constant was estimated. Figure 2.1 compares the actual and simulated <sup>1</sup>H NMR spectra for the coalescence of the acetate and acetoxonium resonances of 42. The rate constants obtained in this way for the aryl substituted dioxolanylium ions (38-42) are given in Table 2.5.

Table 2.5: Rates of isomerization for 38-42 in CD<sub>3</sub>NO<sub>2</sub>.

Compound	Substituent at C(4)	Temperature (K)	Rate (s <sup>-1</sup> )
38	<i>p</i> -CF <sub>3</sub> C <sub>6</sub> H <sub>4</sub>	373	< 10 (est.)
39	C <sub>6</sub> H <sub>5</sub>	303	10 ± 1
		313	20 ± 1
		323	55 ± 5
		333	100 ± 10
40	<i>p</i> -CH <sub>3</sub> C <sub>6</sub> H <sub>4</sub>	308	100 ± 10
		318	200 ± 25
		323	390 ± 40
41	<i>p</i> -C(CH <sub>3</sub> ) <sub>3</sub> C <sub>6</sub> H <sub>4</sub>	294	15 ± 2
42	<i>p</i> -CH <sub>3</sub> OC <sub>6</sub> H <sub>4</sub>	249	670 ± 30
		254	1170 ± 50
		260	1800 ± 100
		264	4000 ± 250
		270	5600 ± 500

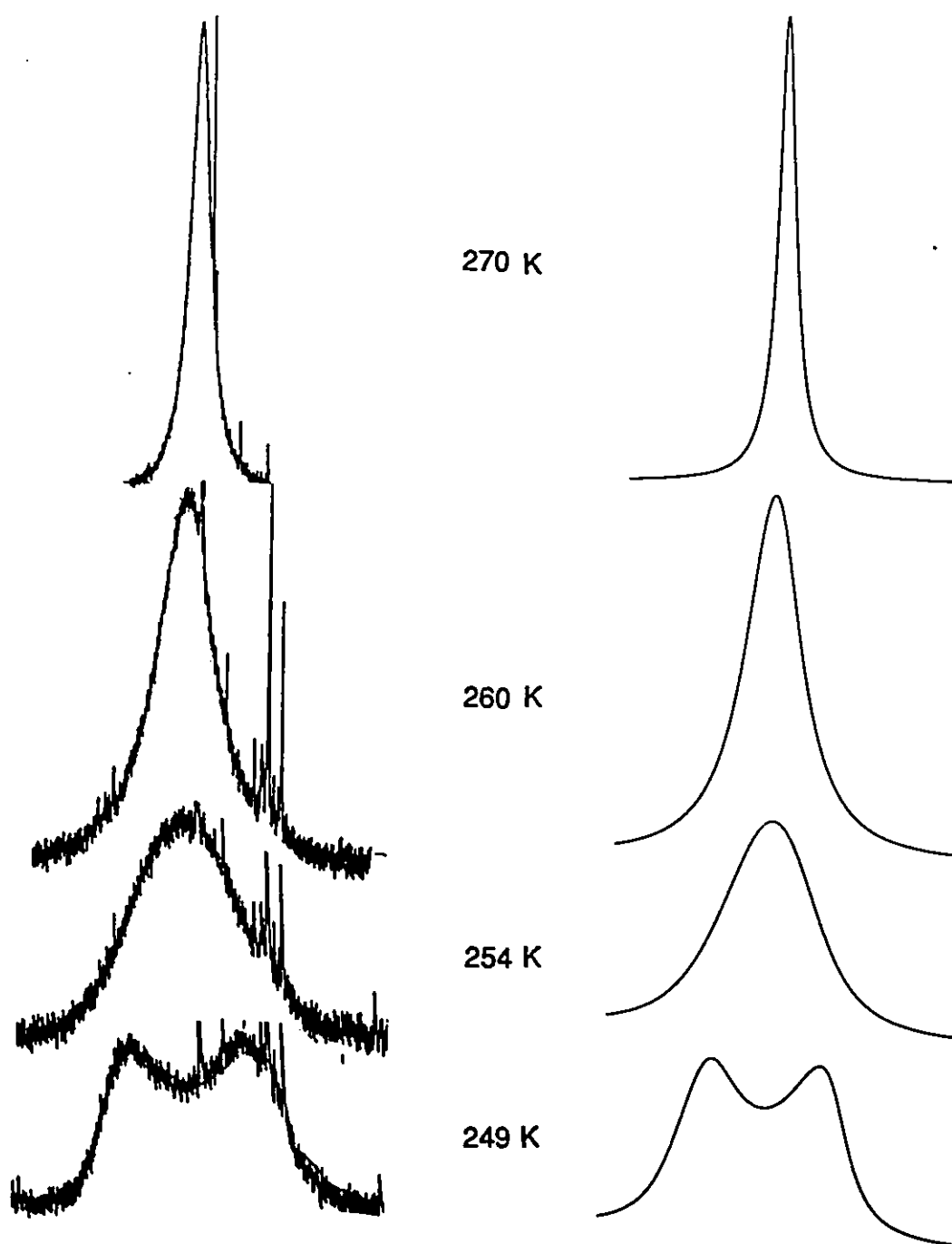


Fig. 2.1: Variable temperature  $^1\text{H}$  NMR spectra of **42** in  $\text{CD}_3\text{NO}_2$ : coalescence of acetate and acetoxonium methyl resonances.

## 2.5 Mechanism of Isomerization for Aryl Dioxolanylium Ions

### (i) Hammett Study

By fitting the kinetic data (Table 2.5) to one of the available Hammett type equations,<sup>38</sup> information about the mechanism of the isomerization reaction could be obtained. The best correlation was obtained with the Okamoto and Brown  $\sigma'$  substituent parameters<sup>39</sup> in a modified Hammett equation (Eqn. 2.4). The plot obtained by fitting the data to Eqn. 2.4 is given in Figure 2.2. The slope,  $\rho$ , was found to be -5.4.

$$\text{Eqn. 2.4} \quad \log(k_x/k_H) = \rho\sigma'$$

The  $\sigma'$  substituent parameters were developed using the solvolysis of cumyl chlorides at 25 °C in 90% aqueous acetone as the model reaction. This form of the Hammett equation is generally used for reactions in which a resonance interaction is possible between the substituent and the reactive centre of an electron demanding transition state. For these reactions, Eqn. 2.4 gives a better fit than the original form of the Hammett equation which was developed using the ionization of benzoic acids. Thus, in the present study, a transition state in which there is a strong resonance interaction between the para substituent on the phenyl ring and an electron deficient reactive center is indicated.

A similar conclusion about the nature of the transition state may be arrived at by considering the value of  $\rho$  obtained. The quantity  $\rho$  is a measure of the sensitivity of the

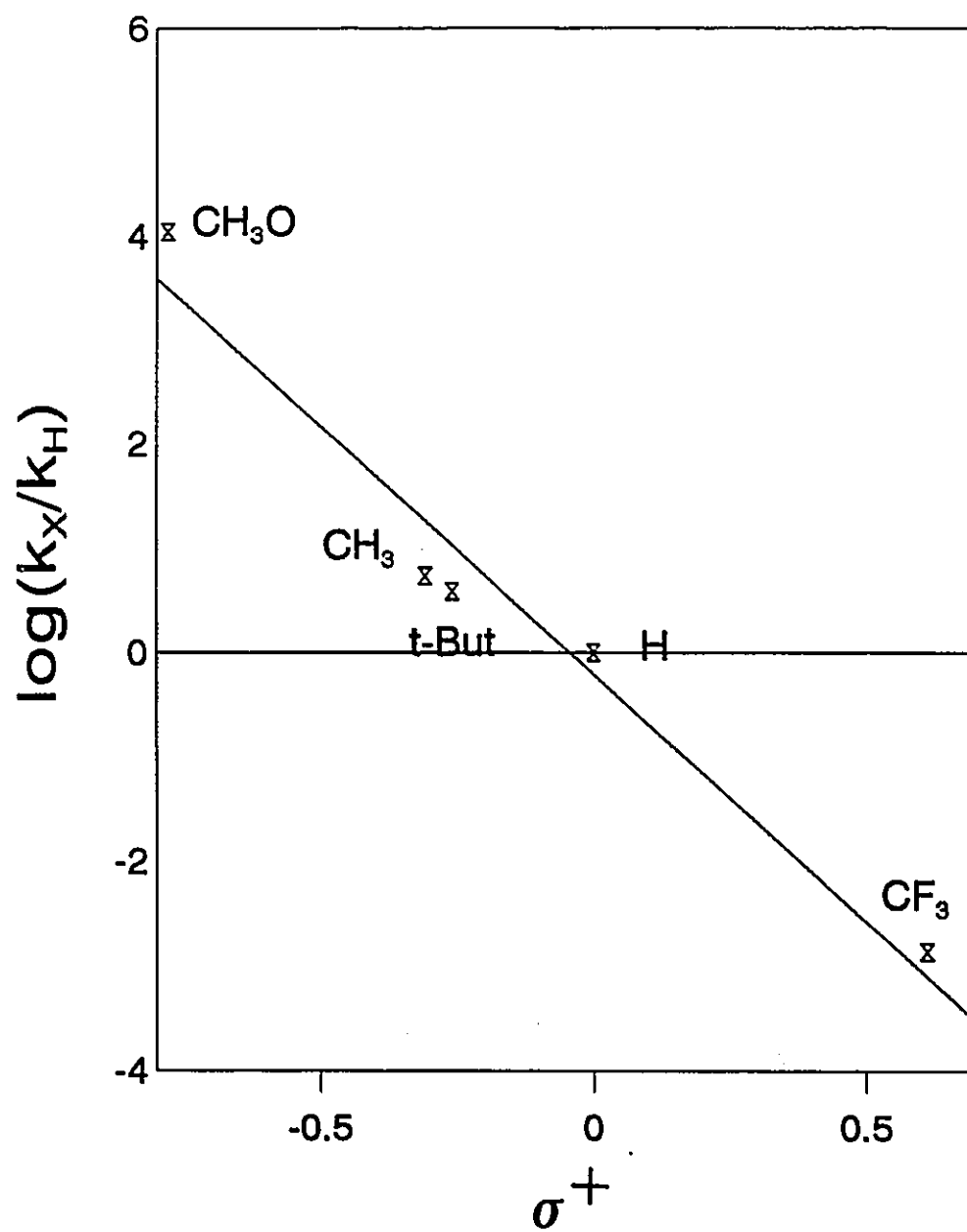


Fig. 2.2: Hammett plot for C(4)-aryl substituted dioxolanylium ion isomerization.

reaction to substituent changes.<sup>38</sup> The negative value for  $\rho$  is indicative of an electron demanding transition state which is stabilized by electron releasing substituents. Furthermore, the magnitude of  $\rho$  suggests a highly polarized transition state in which the degree of bond breaking far exceeds that of bond formation.

There are two possible mechanisms by which the intramolecular displacement reaction can occur as shown in Figure 2.3. The first is via a concerted mechanism in which the C(4)-O(3) bond of the dioxolanylium ring is stretched while the carbonyl oxygen of the free acetate group approaches the C(4) carbon atom. This is analogous to the  $S_N2$  reaction in an intermolecular nucleophilic displacement. The alternative mechanism is a stepwise process. A rate determining heterolytic cleavage of the C(4)-O(3) bond yields a carbenium ion intermediate in the first step. This carbenium ion then collapses with a free acetate group to reform the dioxolanylium ion in the second step. This two step process is analogous to the  $S_N1$  reaction in an intramolecular displacement.

In the case of the step-wise mechanism, cleavage of the C(4)-O(3) bond results in the migration of the positive charge from the O(1)-C(2)-O(3) oxocarbenium system to C(4). The resultant carbenium ion is stabilized by the adjacent aromatic ring. Thus, the step-wise pathway should be particularly sensitive to the electron donating capability of the aromatic ring which serves to stabilize the charge both in the transition state and in the carbenium ion intermediate.

In the concerted mechanism, development of positive charge at C(4) is mitigated by the interaction of the carbonyl oxygen of the approaching nucleophile. In effect, the

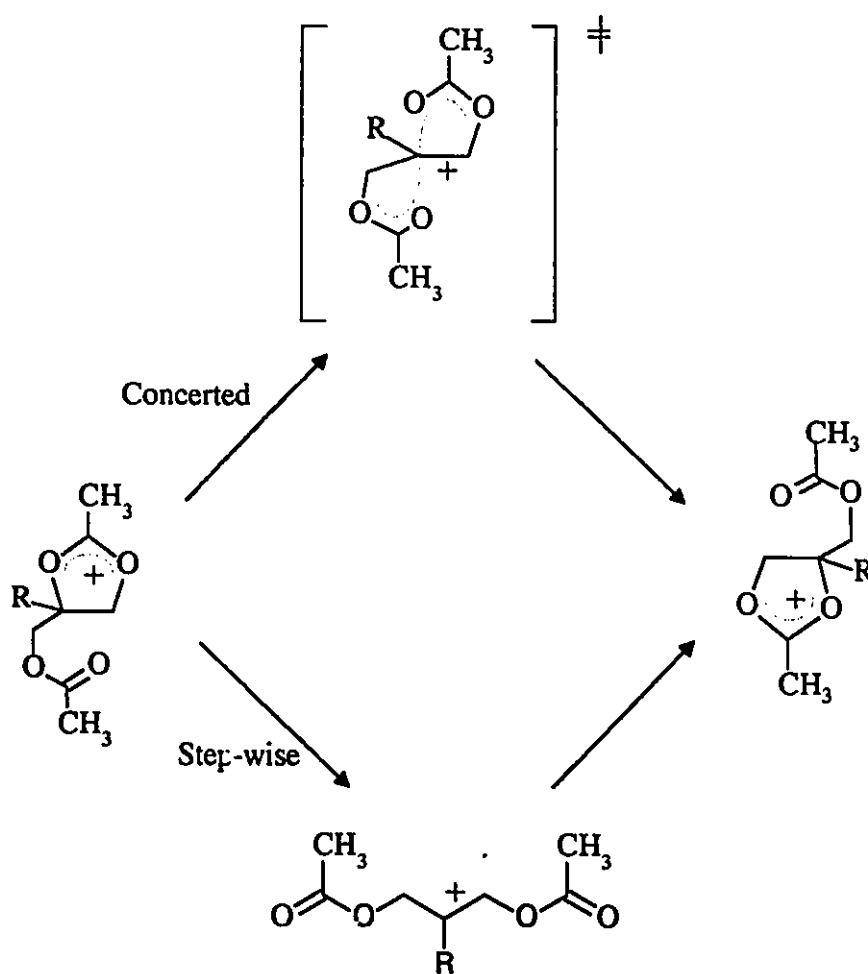


Fig. 2.3: Isomerization mechanisms.



positive charge in the transition state is shared by two partially formed dioxolanylium ions. Thus, the role of the aromatic ring at C(4) is reduced with respect to the step-wise mechanism. This fact may serve as a convenient and measurable distinction between the two pathways.

Any proposed mechanism for the isomerization of the dioxolanylium ions must be consistent with observations noted in the Hammett study. In particular, it must account for the value of  $\rho$ . It is instructive to compare the  $\rho$  values reported in the literature for other displacement reactions with that obtained here. Known  $\rho$  values do not fall into clear groupings for  $S_N1$ -like and  $S_N2$ -like mechanisms. Rather, there exists a spectrum of values that reflect the variable nature of displacement reactions which seldom exhibit limiting  $S_N1$  or  $S_N2$  behaviour. Nevertheless, the  $\rho$  value of -5.4 obtained in this study is sufficiently large that there can be no doubt that the reaction proceeds via a step-wise mechanism.<sup>38</sup>

## (ii) The Baker-Nathan Effect

It is interesting to note the effectiveness of the methyl versus the tertiary butyl substituent on the phenyl ring in accelerating the rate of isomerization. The increase in the rate of isomerization afforded by the introduction of the *p*-methyl substituent onto the phenyl ring is given by  $k_{p-Me}/k_H = 5.4$  at 25 °C. Similarly, the effectiveness of the *p*-*t*-butyl substituent on facilitating the isomerization is  $k_{p-t-Bu}/k_H = 3.85$  at 25 °C. Thus, in this instance, the methyl substituent is more effective than the *t*-butyl substituent in

enhancing the rate of isomerization.

This reversal of the inductive order is termed the Baker-Nathan effect and has been observed for many reactions at electron deficient sites.<sup>60</sup> The origin of the effect, as advanced by Baker and Nathan and subsequently refined by others,<sup>61-63</sup> was attributed to a greater effectiveness of C-H hyperconjugation over C-C hyperconjugation in stabilizing a positive charge. An alternative explanation proposed by Shubert<sup>64</sup> and vigorously defended by Dewar,<sup>65</sup> attributes the effect to differential solvation. Steric inhibition to solvation for *t*-butyl-substituted compounds may be severe enough to counteract its greater stabilizing power via induction in some instances. Whether the inductive order or the Baker-Nathan order is observed is dependent on the importance of solvation in a given reaction. While differential solvation appears to offer an attractive explanation for the Baker-Nathan effect, a contribution from hyperconjugation can not be discounted. It has also been suggested that hyperconjugation itself may be solvent-dependent.<sup>66</sup>

The data collected in the present investigation cannot settle the long standing debate as to the origin of the Baker-Nathan effect. However, two observations are particularly noteworthy. First, it has already been shown that the isomerization reaction proceeds via a transition state structure characterized by a large amount of the positive charge being dispersed into the aromatic ring. This condition often accompanies the observation of a Baker-Nathan effect. Secondly, the use of nitromethane as a solvent has been shown to give rise to a particularly large Baker-Nathan effect.<sup>65</sup> Given the operation

of these two contributing factors, it is therefore not surprising that the Baker-Nathan effect was observed in this system.

(iii) Evaluation of Activation Parameters

In order to compare the effects of the other substituents on the isomerization reaction, it is useful to calculate the activation parameters. An Arrhenius plot of the data presented in Table 2.5 was used to determine the entropy of activation,  $\Delta S^\ddagger$ , for the isomerization of each compound. Not enough data could be collected in the case of the *p*-*t*-butylphenyl and *p*-CF<sub>3</sub>phenyl substituted dioxolanylium ions (41 and 38 respectively) to allow accurate determinations of  $\Delta S^\ddagger$ . The free energy of activation,  $\Delta G^\ddagger$ , was calculated for all compounds using the Eyring equation. The results are presented in Table 2.6.

Inspection of the  $\Delta G^\ddagger$  values reveals that the barrier to the dioxolanylium isomerization is lowered as better electron releasing substituents are placed on the phenyl ring. Using the isomerization of the unsubstituted phenyl compound 39 as a reference, ( $\Delta G^\ddagger=16.4$ ), the *p*-methoxy substituted dioxolanylium ion 42 ( $\Delta G^\ddagger=10.9$ ) exhibited a greatly reduced barrier. This is attributed to the ability of the methoxy group to stabilize the developing positive charge at the C(4) carbon atom in the transition state via a strong resonance interaction.

Table 2.6      Activation parameters<sup>a</sup> for the isomerization of 38-42.

Compound	C(4) substituent	$\Delta G^\ddagger$ (kcal/mol)	$\Delta S^\ddagger$ (e.u.)
38	<i>p</i> -CF <sub>3</sub> C <sub>6</sub> H <sub>4</sub>	(20.3) <sup>b</sup>	-
39	C <sub>6</sub> H <sub>5</sub>	16.4 ± 0.1	-1.3 ± 1.8
40	<i>p</i> -CH <sub>3</sub> C <sub>6</sub> H <sub>4</sub>	15.4 ± 0.1	4.8 ± 1.0
41	<i>p</i> -(CH <sub>3</sub> ) <sub>3</sub> C <sub>6</sub> H <sub>4</sub>	15.6 ± 0.1 <sup>c</sup>	-
42	<i>p</i> -CH <sub>3</sub> OC <sub>6</sub> H <sub>4</sub>	10.9 ± 0.1	9.0 ± 1.0

<sup>a</sup> In CD<sub>3</sub>NO<sub>2</sub> at 25 °C unless otherwise noted.<sup>b</sup> Estimated at 100 °C.<sup>c</sup> At 21 °C.

With the introduction of the *p*-CF<sub>3</sub> substituent (38) the barrier to the isomerization was raised by at least 5 kcal/mol relative to the unsubstituted phenyl dioxolanylium cation 39. This is a result of the powerful electron withdrawing effect of the CF<sub>3</sub> group. The electron demanding transition state is destabilized inductively and hence the barrier is increased.

The value of  $\Delta S^\ddagger$  obtained in all cases was small. This is consistent with unimolecular reactions which exhibit lower values of  $\Delta S^\ddagger$  than their bimolecular counterparts. It is interesting to note that  $\Delta S^\ddagger$  increases as better electron donating

groups are put on the phenyl ring. A looser transition state might be expected when a good electron donating substituent is present on the phenyl ring. The ionization could proceed to a greater extent imparting more internal freedom to the transition state compared to the constrained dioxolanylium ring of the reactant.

(iv) The "Frozen"  $S_N2$  Transition State

A steady reduction in  $\Delta G^\ddagger$  was observed as the *para* substituent on the phenyl ring was made more electron donating. A linear correlation of  $\Delta G^\ddagger$  with  $\sigma'$  is expected since the Eyring equation provides a nexus between the Hammett equation and the desired linear free energy relationship. Such a correlation does indeed exist as shown in Figure 2.4 in which  $\Delta G^\ddagger$  at 25 °C is plotted against the Okamoto-Brown  $\sigma'$  substituent constants. By extrapolation, a substituent with a  $\sigma'$  value of -2.3 would reduce the isomerization barrier to zero. While no known substituent has such a negative value of  $\sigma'$ , the N,N-dimethylamino group is one of the best electron donating groups available with  $\sigma' = -1.7$ . This suggests that the corresponding dioxolanylium ion with a *p*-N,N-dimethylaminophenyl group at C(4) (45) would adopt a conformation which exhibits a high degree of carbenium ion character. It is possible that simultaneous co-ordination by both carbonyl oxygens would result, and thus the ion could serve as a model for the trigonal bipyramidal transition state of the  $S_N2$  reaction.

Attempts at generating this ion via  $SbCl_5$  ionization of the corresponding triacetate 34e (Eqn. 2.5) were unsuccessful. Presumably, Lewis acid co-ordination to the amine

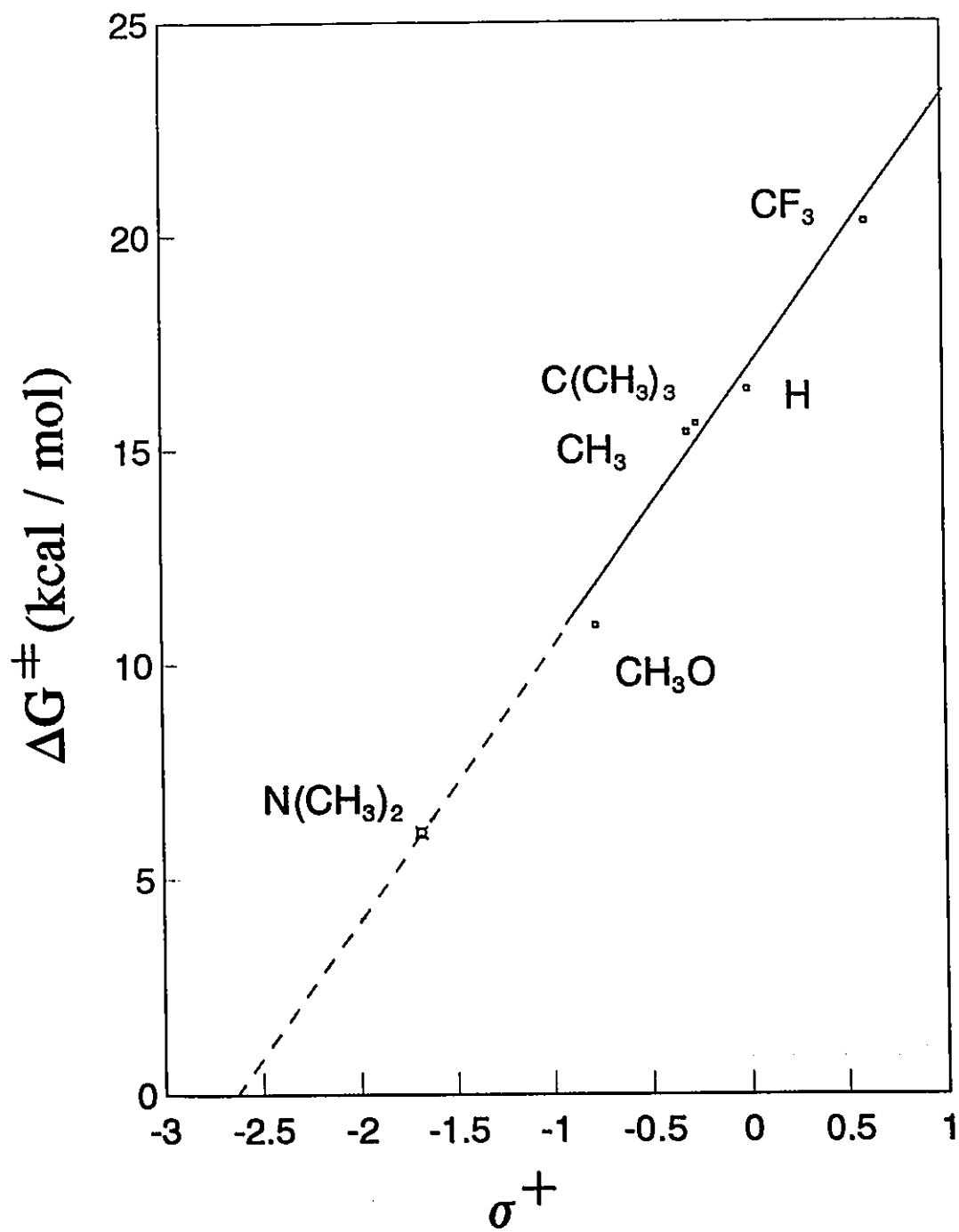
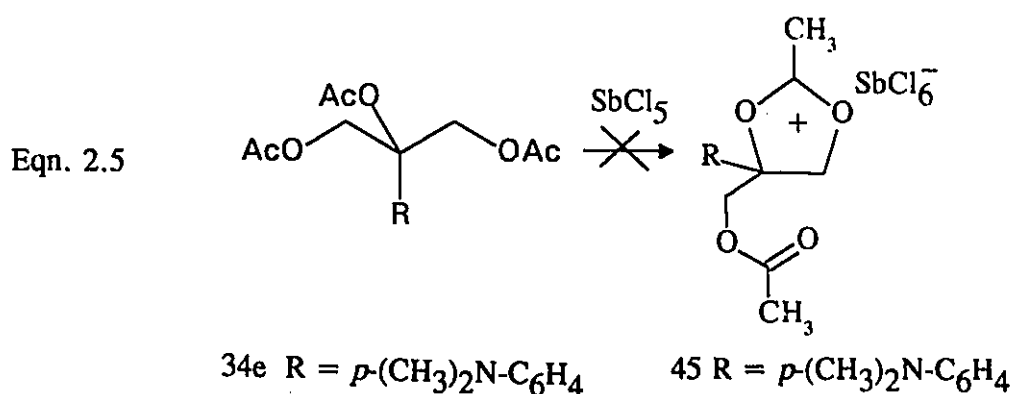


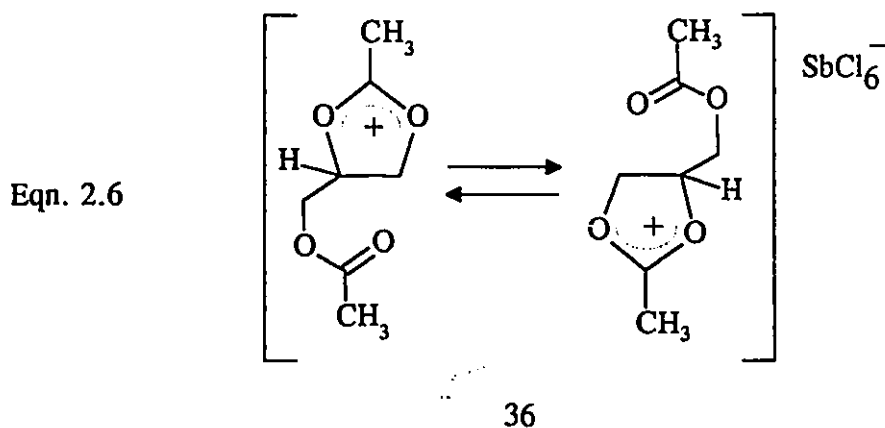
Fig. 2.4: Plot of isomerization barrier vs  $\sigma^+$  for aryl dioxolanylium ions.

function interfered with the ionization reaction. However, the prediction of a low reaction barrier for this compound was tested by the use of semi-empirical calculations. The results of that study are presented in Chapter 4.



## 2.6 Isomerization of the Non-Aryl Dioxolanylium Ion Salts

It was of interest to examine the effect of non-aryl substituents at C(4) on the rate of the dioxolanylium ion isomerization. Paulsen<sup>22</sup> has reported a barrier ( $\Delta G^\ddagger$ ) of 18.7 kcal/mol for the isomerization of **36** (Eqn. 2.6). This is more than 2 kcal/mol higher in energy than the isomerization barrier determined for **39** ( $\Delta G^\ddagger = 16.4 \pm 0.1$  kcal/mol). Thus, the phenyl substituent at C(4) provides an effective means of lowering the reaction barrier. While the aryl dioxolanylium ions **38-42** isomerize via a step-wise pathway, Paulsen has suggested an S<sub>N</sub>2-like (concerted) mechanism for **36**.<sup>22</sup> However, no evidence was given in support of this assertion. In order to help determine which mechanism, step-wise or concerted, controls the isomerization of the non-aryl system, the isomerization of **37** was investigated, in which the C(4) substituent is a methyl group.



It was not convenient to use NMR line shape analysis to obtain the rate of isomerization of the C(4)-methyl substituted dioxolanylium ion 37. At a field strength of 200 MHz no significant broadening of the  $^1\text{H}$  signals was observed at temperatures below 100  $^{\circ}\text{C}$ . It was not practical to try to exceed this temperature due to decomposition of the sample. Furthermore, the use of  $\text{CD}_3\text{NO}_2$  as a solvent imposed its own limit as to which temperatures were accessible. The use of a higher boiling solvent would have interfered with making comparisons with other systems in  $\text{CD}_3\text{NO}_2$ .

(i) Measurement of Isomerization Rate Constants by Selective Inversion

The use of the one-dimensional (1D) magnetization transfer methods allows for the investigation of exchange processes occurring at much slower rates than does the line shape method.<sup>67</sup> The basic experiment involves selective excitation of a spin system to



generate a transient, and then monitoring the magnetization intensity of the exchange-coupled sites using a variable delay. There are two 1D magnetization transfer techniques: selective saturation and selective inversion.<sup>68,69</sup> In selective saturation, the transient is generated by constant irradiation at one site so that the magnetization intensity at that site remains at zero throughout the experiment, while the intensity of the unperturbed site is monitored.<sup>70</sup> In the selective inversion technique, a  $180^\circ$  pulse is applied to one site to invert the magnetization at that site. The advantage of this technique is that the magnetization intensities of both the perturbed and unperturbed signals may be monitored. Thus, selective inversion is often the preferred technique<sup>67</sup> and was the method of choice for the present investigation.

The two site exchange for the isomerization of **36** was investigated using the selective inversion technique as described by Bain.<sup>67</sup> The  $^{13}\text{C}$  resonance of the C(2) carbon atom (see Table 2.1) was inverted with an  $180^\circ$  pulse. The intensity of this spin as a function of time is plotted in Figure 2.5, which illustrates the recovery of the signal to its positive value as governed by the relaxation-exchange processes. Isomerization of the dioxolanylium ion exchanges sites C(2) and C(9), and hence the magnetization intensity of the C(9) signal also is affected. An initial decrease in intensity of the C(9) resonance is observed as magnetization is transferred to this site from C(2), followed by a recovery to the equilibrium condition. Figure 2.6 illustrates the time dependent behaviour of the C(9) signal.

Knowing the magnetization intensities of the signals for the C(2) and C(9) carbon

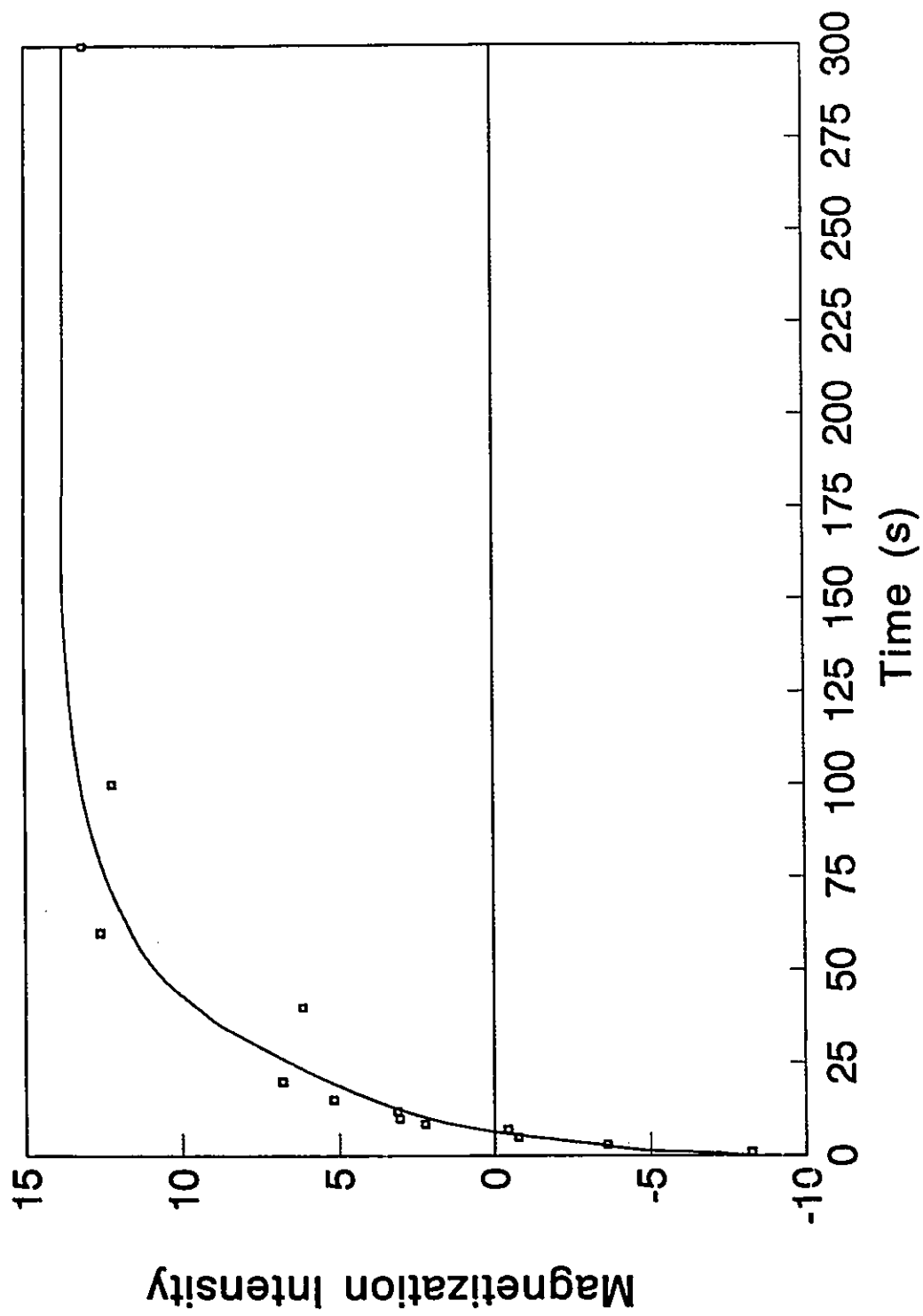


Fig. 2.5: Selective inversion experiment: response of C(2) resonance for 36.

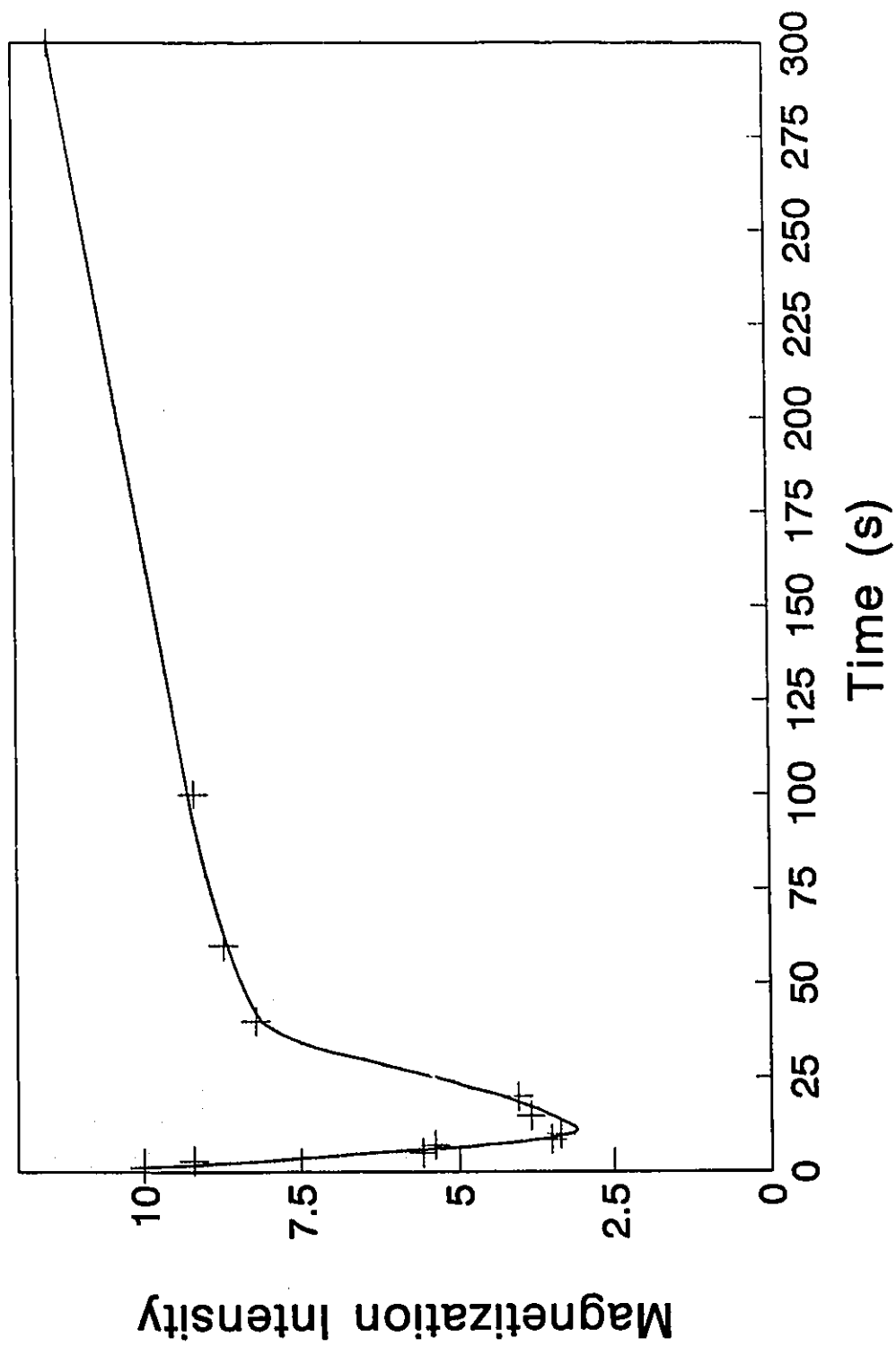


Fig. 2.6: Selective inversion experiment: response of C(9) resonance for 36.

atoms as a function of time, the Bloch equations for the selective inversion experiment can be solved.<sup>71</sup> This involves estimating the value of the exchange rate ( $k$ ) and relaxation rate ( $T_1$ ). The data are then computer-fitted to the Bloch equations using an iterative approach until a good match between the predicted and experimentally determined curves is achieved. The results are presented in Table 2.7 along with those for the isomerization of 37, which was investigated using the same procedure.

Table 2.7: Rate of isomerization of 36 and 37 in  $\text{CD}_3\text{NO}_2$ .

Compound	C(4) substituent	Temperature ( $^{\circ}\text{C}$ )	Rate ( $\text{s}^{-1}$ )	$\Delta G^{\ddagger}$ (kcal/mole)
36	H	25	$0.12 \pm 0.02$	$18.7 \pm 0.1$
37	$\text{CH}_3$	42	$0.02 \pm 0.01$	$21.0 \pm 0.3$

(ii) Mechanism of Isomerization for 36 and 37.

The value of  $\Delta G^{\ddagger}$  obtained for 36 was  $18.7 \pm 0.1$  kcal/mol at  $25^{\circ}\text{C}$ , which is in agreement with that determined by Paulsen using a one-point coalescence approximation method.<sup>22</sup> This was taken as a validation of the experimental procedure. An increase in  $\Delta G^{\ddagger}$  of more than 2 kcal/mol was found in going from a hydrogen to a

methyl substituent at C(4). This effectively rules out the possibility that both of these compounds isomerize by the step-wise pathway. If this were the case, the methyl substituted dioxolanylium should have had the lower barrier because of the greater ability of the methyl group to stabilize the charge at C(4) in the transition state.

In the concerted pathway, however, charge development at C(4) is less pronounced. Therefore, if both compounds isomerized by this pathway, then the inductive stabilization provided by the methyl group would not play a key role. The higher barrier for 37 could be accounted for by the hinderance of the methyl group to the approach of the nucleophile -- an interaction which is absent for 36.

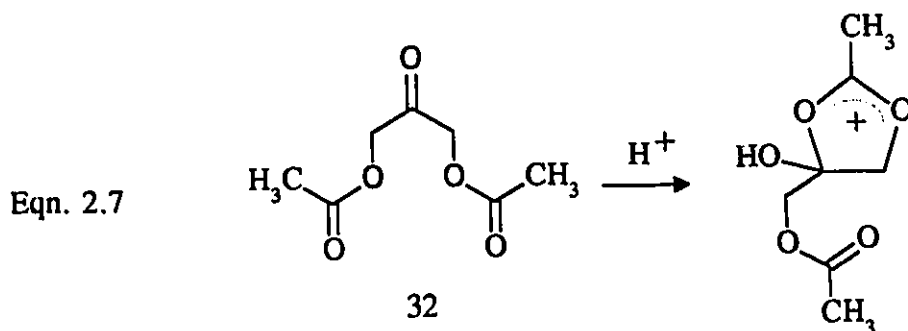
The possibility that 36 isomerizes by the concerted pathway while 37 isomerizes by the step wise pathway must also be addressed. In this case, the higher barrier for 37 is merely accidental. That is, the step-wise pathway has an intrinsically higher barrier than does the concerted pathway. A simple comparison of the values of  $\Delta G^\ddagger$  cannot distinguish this situation from the one discussed above in which both compounds isomerize by the concerted pathway. Semi-empirical AM1 calculations were employed to tackle this problem and the results are presented in Chapter 4.

## 2.7 Lewis Acid Adducts

The C(4)-aryl substituted dioxolanylium ions described in the previous sections were investigated as part of a systematic approach to lowering the isomerization barrier, with the ultimate goal of obtaining a model for the  $S_N2$  transition state. Since aryl

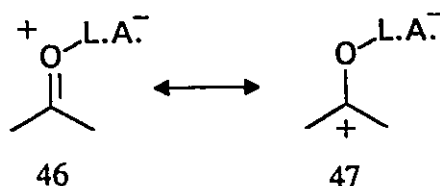
substituents of sufficient electron-donating power could not be successfully introduced onto the dioxolanylium ring, other charge stabilizing substituents were investigated.

An oxygen atom bound directly to the C(4) carbon atom would be a very effective means of stabilizing a positive charge at this site. One way of incorporating such a functionality would be via the protonation-cyclization reaction of 1,3-dihydroxypropan-2-one-1,3-diacetate **32** shown in Eqn. 2.7. However, no dioxolanylium ions could be isolated from the reaction of **32** with  $\text{FSO}_3\text{H}$  and  $\text{CF}_3\text{SO}_3\text{H}$ . The  $^1\text{H}$  NMR spectra obtained on solution of **32** in these acids showed that the protonation did not proceed cleanly and the spectra could not be assigned. Presumably, protonation at the ester carbonyl oxygen atoms was also taking place.



It was thought that the use of a Lewis acid in place of protic acids would allow greater control over the intended reaction. A Lewis acid scale has been proposed based on the ability of the Lewis acid to induce chemical shift changes ( $\Delta\delta$ ) in the base upon complexation.<sup>72</sup> These chemical shift changes reflect the ability of the Lewis acid to

modify atomic charge as illustrated in resonance structures 46 and 47.



The order established using this approach is as follows:<sup>72</sup>



increasing relative power  $\rightarrow$

(i)  $\text{SbCl}_5$  Complex

Treatment of 32 with 1.5 equivalents of  $\text{SbCl}_5$  at  $-78^\circ \text{C}$  in  $\text{CD}_2\text{Cl}_2$ , afforded a dark coloured complex which was not isolated, but was analyzed in situ (Eqn. 2.8). The  $^1\text{H}$  NMR spectrum at  $-62^\circ \text{C}$  (Table 2.4) was consistent with the desired dioxolanylium ion 43. However, all the proton signals were broadened due to the viscosity of the solution at this temperature. As the temperature was increased, an isomerization reaction was observed with broadening of the methyl and methylene resonances. Using the total line shape method previously described, the rate of isomerization and the associated reaction barrier were determined (Table 2.8). The  $\text{SbCl}_5$  complex exhibited a lower barrier to isomerization than any of the aryl-substituted dioxolanylium ions discussed

previously. However, the reaction barrier was still appreciable, suggesting that the complex bears a closer resemblance to a typical dioxolanylium ion rather than a "frozen"  $S_N2$  transition state. Attempts to obtain a single crystal of the complex suitable for x-ray crystallography were unsuccessful.

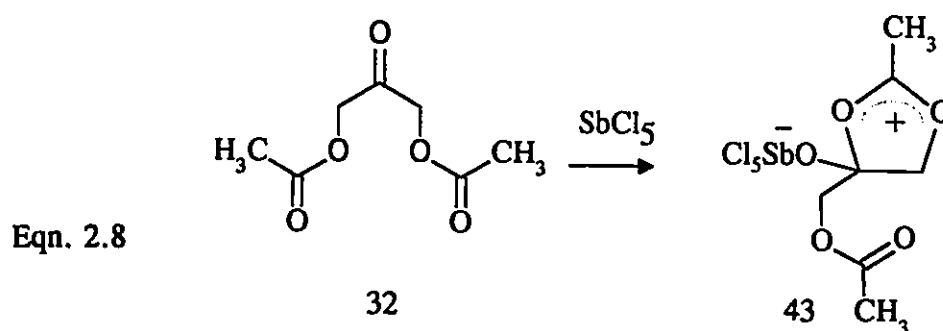


Table 2.8: Rate of isomerization of 43 in  $CD_2Cl_2$ .

Temperature (K)	Rate ( $s^{-1}$ )	$\Delta G^\ddagger$ @ 25 C (kcal/mol)
230	$30 \pm 2$	$8.5 \pm 0.1$
235	$100 \pm 2$	
245	$550 \pm 50$	
250	$1800 \pm 100$	

## (ii) $SnCl_4$ Complex

In an attempt to lower the isomerization barrier even further, a  $SnCl_4$  complex was also investigated. According to the ordering of the Lewis acids discussed previously,



$\text{SnCl}_4$  is significantly weaker than  $\text{SbCl}_5$  in its ability to induce chemical shift changes in the complexed base.<sup>72</sup> This would suggest that the use of  $\text{SnCl}_4$  would reduce the amount of positive charge at C(4) compared to the  $\text{SbCl}_5$  complex. A reduction of positive charge density at C(4) should reduce the isomerization barrier, and may be sufficient to promote the "frozen"  $\text{S}_{\text{N}}2$  transition state structure rather than the typical dioxolanylium ion structure. Treatment of 32 with  $\text{SnCl}_4$  at  $-78^\circ\text{C}$  afforded a white precipitate which was collected. The  $^1\text{H}$ ,  $^{13}\text{C}$  (solution) and CPMAS NMR data for the  $\text{SnCl}_4$  complex 44 are presented in Table 2.4.

Only two signals were detected in the  $^1\text{H}$  NMR spectrum of the complex at  $-100^\circ\text{C}$ : broad singlets centered at 2.60 ppm and 5.10 ppm. This may be consistent with an averaged spectrum for a rapidly isomerizing dioxolanylium ion. If this is indeed the case, the barrier to isomerization must be exceedingly low. The simplicity of the solution  $^{13}\text{C}$  NMR spectrum may also be indicative of a rapid isomerization. However, the similarity between the solution  $^{13}\text{C}$  and CPMAS spectra would require that the isomerization is equally fast in the solid state, which seems unlikely.

An alternative view is that the complex resembles the sought after "frozen"  $\text{S}_{\text{N}}2$  transition state. In solution, complexes of carbonyl compounds with Sn derived Lewis acids prefer to form either 1:2 or 1:1 (acid:carbonyl) chelated adducts.<sup>73,74</sup> For  $\text{SnCl}_4$ , the 1:1 complexes are possible when the ligand is bidentate.<sup>74</sup> For both stoichiometries, crystallographic investigations have demonstrated an octahedral geometry about the Sn atom in  $\text{SnCl}_4$  complexes.<sup>74</sup> With these considerations in mind, a structure may be

proposed for 44, which is also consistent with the NMR data (Fig. 2.7). Unfortunately, single crystals of the complex suitable for x-ray crystallography could not be obtained, and so the structure remains in question.

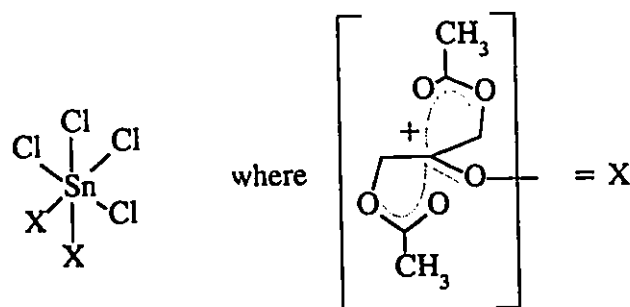


Fig. 2.7 Possible structure of 44

### Part C: <sup>13</sup>C NMR Correlation Analysis

#### 2.8 <sup>13</sup>C NMR of Aryl Dioxolanylium Salts

Similar <sup>13</sup>C NMR spectra were observed for the aryl dioxolanylium salts 38-42 (Table 2.3). Assignments of the <sup>13</sup>C resonances were accomplished using spin-sorts and by comparison with the chemical shifts reported for analogous carbon atoms in other dioxolanylium ion systems and 1,4-disubstituted benzenes.<sup>37,75</sup> In all cases, the lowest

field signal was for the C(2) carbon atom which is consistent with positive charge at this site. The C(2) resonance was typically 20 ppm further downfield than the C(9) resonance, the carbonyl carbon of the free acetate group. The C(5) resonance was about 13 ppm further downfield than that for the C(7) carbon atom. The C(6) resonance was about 4.5 ppm further upfield compared to that of the C(11) carbon atom. Similar upfield shifts have been reported for the resonances of carbon atoms adjacent to the carbonyl carbon of esters,<sup>76</sup> ketones,<sup>73</sup> aldehydes,<sup>72</sup> ethers<sup>77</sup> and imines<sup>78</sup> upon complexation or protonation.

Close inspection of the values listed in Table 2.3 reveals subtle variations in the <sup>13</sup>C chemical shifts for analogous carbons within the five-membered ring. There is an apparent dependence of these chemical shifts on the electron-donating ability of the *para* substituent of the phenyl ring. Successive replacement with better electron donating substituents generally produced an upfield shift for the C(2), C(5) and C(6) resonances and a downfield shift for the C(4) resonances. Since the chemical shifts being considered are for carbons that are far removed from the substituent on the phenyl ring, the effect is clearly electronic in nature and not due to a steric interaction. A detailed analysis of the trends was undertaken in order to gain a better understanding of these substituent effects and to identify their significance in determining the structure and charge distribution within the dioxolanylium ions.

## 2.9 NMR Correlation Analysis

### (a) Background

A linear dependence of the  $^{13}\text{C}$  chemical shift of a given carbon atom and the charge density on that atom was first recognized by Spiess and Schneider.<sup>79</sup> This relationship has provided an invaluable tool for the study of the structure and stability of carbenium ions.<sup>80</sup> It is not surprising that correlations of  $^{13}\text{C}$  NMR substituent effects with Hammett  $\sigma$  parameters may also be found.<sup>81</sup> In general, a linear dependence between  $^{13}\text{C}$  chemical shifts and structure-reactivity constants (i.e.  $\sigma$  values) is found since both of these quantities respond in a similar way to changes in electron density.<sup>82</sup>

Single parameter correlations take the form:<sup>83</sup>

$$\text{Eqn. 2.9} \quad \delta = \rho\sigma + \delta_0$$

where  $\delta$  is the chemical shift,  $\sigma$  is one of the many classical Hammett parameters ( $\sigma_1$ ,  $\sigma_p$ ,  $\sigma_p^+$ ,  $\sigma_m$ ,  $\sigma_m^+$ ,  $\sigma_p^-$ ,  $\sigma_p^{0-}$ ,  $\sigma_p^{+}$ , or  $\sigma_p^{\text{BA}}$ ),  $\rho$  is a proportionality constant, and  $\delta_0$  is an adjustable constant. A constraint that is often applied is  $\delta_0 = \delta_{\text{H}}$ , the chemical shift of the unsubstituted parent compound, and the single parameter Hammett equation becomes:<sup>84</sup>

$$\text{Eqn. 2.10} \quad \Delta\delta = \rho\sigma$$

Use of the substituent-induced chemical shift,  $\Delta\delta = \delta - \delta_0$ , forces zero-intercept behaviour

for Eqn. 2.10 and avoids giving unwarranted freedom to fitting the data resulting from the adjustable parameter  $\delta_0$ .

For many chemical systems, single-parameter equations do not give valid correlations.<sup>81a,82,83,85</sup> Therefore, dual-substituent parameter (DSP) equations have been proposed, the most widely accepted being Taft's DSP equation:<sup>81b</sup>

$$\text{Eqn. 2.11} \quad \Delta\delta = \rho_I\sigma_I + \rho_R\sigma_R$$

The DSP equation separates the inductive,  $\rho_I\sigma_I$ , and the mesomeric,  $\rho_R\sigma_R$ , components of the substituent effect. Taft argued that a single set of  $\sigma_R$  substituent parameters could not adequately describe substituent effects in all systems. Therefore, he set out to define four  $\sigma_R$  scales which reflect the different types of resonance effects that are possible:  $\sigma(\text{BA})$ ,  $\sigma^\circ$ ,  $\sigma^+$ , and  $\sigma^-$ . In general, it is necessary to try each of the four  $\sigma_R$  parameters in the DSP equation in order to obtain the best fit at a given probe site. This procedure must be repeated for all positions of interest in the molecule since not all probe sites respond in the same way to a change in substitution. It is hoped that the  $\sigma_R$  scale which best correlates with the data also has chemical significance.

The  $\sigma_I$  scale is widely accepted as having general applicability. Despite the use of the term "inductive", that part of the substituent effect which is not a result of through resonance, should not be solely attributed to electrical induction through the bonds of the molecular framework. The possibility that the dipole of a substituent can affect another

point in the same molecule, such as a reactive centre, by a through space or field effect is not excluded. Shorter<sup>81c</sup> has argued that both inductive and field effects are simplifications for the way in which a substituent can modify the overall electron distribution in a molecule. They are both convenient models but neither is satisfactory for describing substituent effects in all cases. It is stressed that the DSP equation makes no attempt to address the relative importance of inductive versus field effects.

(b) Evaluation of Correlation Models

In the present study of substituent effects in dioxolanylium ions, the  $^{13}\text{C}$  NMR chemical shifts of 38, 39, 41, and 42 (Table 2.3) were considered. The spectra for this set of compounds were recorded at  $-98^\circ\text{C}$  in  $\text{CD}_2\text{Cl}_2/\text{CD}_3\text{NO}_2$ . This temperature was chosen to ensure that the rate of isomerization was negligible compared to the NMR time scale so that the static dioxolanylium ions could be observed. The solubility of the salts in  $\text{CD}_2\text{Cl}_2$  alone was not high enough to give good spectra in a reasonable amount of time. While the salts have appreciable solubility in  $\text{CD}_3\text{NO}_2$ , the temperature required for this study was far below its freezing point. A combination of these two solvents was used to achieve the required solubility and liquid temperature range. The  $^{13}\text{C}$  NMR spectrum of 40 was originally recorded in  $\text{CD}_3\text{NO}_2$  at  $-21^\circ\text{C}$ . Limited availability of this compound prevented recording the spectrum under the same conditions as the other dioxolanylium salts in this series. The  $^{13}\text{C}$  chemical shifts of the salts were noted to exhibit a dependence on the nature of the solvent, so 40 was excluded from this study.

Correlations between the substituent-induced  $^{13}\text{C}$  chemical shifts ( $\Delta\delta$ ) and various substituent parameters ( $\sigma$ ) were sought using the single and dual substituent parameter equations (Eqn. 2.10 and 2.11). All the appropriate  $\sigma$  parameters<sup>86,87</sup> were tried in each equation for each position in the dioxolanylium ion ring. The goodness of fit at a particular carbon atom for a given equation and a set of values is given by the value of  $F$  (defined as the mean square due to regression divided by the residual mean square).<sup>88</sup> The larger the value of  $F$  obtained (for specified degrees of freedom) the better the fit.

The single substituent parameter equation gave acceptable fits (significant at the 99% confidence level) for positions C(2) and C(4) with  $\sigma_p$  (Table 2.9). Less satisfactory correlations (significant at the 90 % confidence level) were obtained for the C(5) carbon atom with  $\sigma_p^+$  and for the C(6) carbon atom with  $\sigma_p$ .

Table 2.9: Evaluation of the single (SSP) and dual (DSP) substituent parameter correlation models.

Atomic Position	SSP		DSP	
	Parameter	F	Parameters	F
C(2)	$\sigma_p$	483	$\sigma_I, \sigma_R^0$	9483
C(4)	$\sigma_p$	214	$\sigma_I, \sigma_R^0$	32517
C(5)	$\sigma_p^+$	23	$\sigma_I, \sigma_R^0$	70
C(6)	$\sigma_p$	54	$\sigma_I, \sigma_R^0$	147

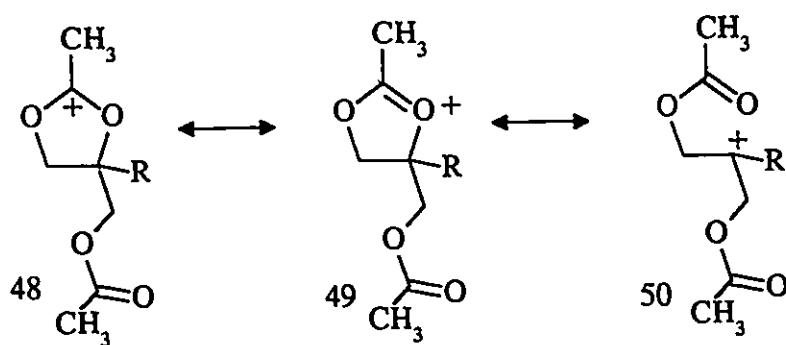
With the DSP equation (using  $\sigma_R^0$  as the resonance parameter), improved correlations were obtained for each of the C(2), C(4), C(5) and C(6) carbon atoms; however, the confidence levels for these correlations remained unaffected. With this limited data set, it is impossible to judge whether the use of the DSP equation provides any significant improvement over the single parameter equation. The apparent improvement in the correlations with the DSP equation may solely be due to the inclusion of a second parameter thereby removing one degree of freedom when fitting the data. However, it has been shown using larger data sets that the increased complexity of the DSP equation is both necessary and sufficient to describe NMR substituent effects.<sup>45,49</sup> The predominant use of the DSP equation in the recent literature further illustrates its usefulness in correlating spectral data.<sup>90-93</sup> Even when the DSP equation does not appear to provide a significantly better correlation, its use will allow at least a qualitative discussion of resonance and inductive effects in a given system. For these reasons, the following interpretation of substituent effects in dioxolanylium ions will be within the context of the DSP equation.

### (c) Significance of the Sensitivity Factors in the DSP Equation

The sensitivity factors,  $\rho_I$  and  $\rho_R$ , for each position in the dioxolanylium ion ring are given in Table 2.10. At C(2), the positive signs for  $\rho_I$  and  $\rho_R$  reveal that electron donating substituents give rise to an upfield shift while electron withdrawing substituents cause a downfield shift relative to the unsubstituted phenyl compound 39. As stated



earlier, differences in chemical shifts (within a series of structurally related compounds) can be related to a change in the electron density. Thus, the upfield shift provided by electron releasing substituents is attributed to an increase in electron density at C(2). This change in electron density at C(2) can be thought of as involving the resonance structures 48 to 50 (Scheme 2.4).



Scheme 2.4

Table 2.10: Dual Substituent Parameter Correlations.

Atomic Position	$\rho_I$	$\rho_R$	$\lambda = \rho_R / \rho_I$
C(2)	$0.78 \pm 0.02$	$1.13 \pm 0.02$	1.5
C(4)	$-1.36 \pm 0.02$	$-2.16 \pm 0.02$	1.6
C(5)	$0.05 \pm 0.1$	$0.75 \pm 0.1$	15.0
C(6)	$0.13 \pm 0.03$	$0.18 \pm 0.03$	1.4

Resonance contributor 50 is used to depict an ionic contribution to the O(3)-C(4) bond. The importance of an ionic resonance contributor to C-O bonds in 1,3-dioxolan-2-ylum ions and related 6-ethoxytetrahydropyrylium ions has been suggested previously by Childs<sup>40,43</sup> based on x-ray crystallographic investigations. Kirby has proposed similar ionic resonance structures for the C-O bonds in neutral systems.<sup>34</sup> An increased contribution from resonance contributor 50 is possible when the *para* substituent on the phenyl ring is made more electron donating. This would result in a reduction in the amount of positive charge at C(2) with an attendant upfield shift for the <sup>13</sup>C resonance of this carbon atom, as was observed.

The negative values for  $\rho_I$  and  $\rho_R$  at C(4) are taken as particularly strong evidence for the increasing contribution of 50 to the resonance description of dioxolanylium ions. Electron donating *para* substituents give rise to a downfield shift with the opposite effect observed for the electron withdrawing substituent, CF<sub>3</sub>. This is a complete reversal of the roles for these substituents reported for *para*-substituted ethylbenzenes and ethylnaphthalenes.<sup>34</sup> In these neutral systems, the <sup>13</sup>C resonance for the CH<sub>2</sub> carbon of the ethyl group experiences a downfield shift when the *para*-substituent is electron withdrawing and an upfield shift when substituent is electron donating. In the present investigation, the observation that electron donating substituents are apparently deshielding while CF<sub>3</sub> effectively shields the C(4) carbon atom may be accounted for by an increasing contribution from 50. The presence of electron donating substituents on the phenyl ring stabilize charge at C(4) thus allowing a greater contribution from 50.

The overall effect is to increase positive charge density at C(4) which results in the shift of the C(4) carbon resonance to lower field.

The chemical shifts for the C(5) carbon atom also exhibited a dependence on the substituent on the phenyl ring. As was the case for the C(2) carbon atom, electron donating substituents induce an upfield shift of the C(5) carbon resonance with positive values for both  $\rho_I$  and  $\rho_R$ . In terms of resonance structure 50, this can be reconciled with a slight opening of the dioxolanylium ring to yield more open chain character. A fully open, symmetrical carbenium ion would give identical resonances for C(5) and C(7) carbon atoms. The observed shift of the C(5) carbon resonance to higher field towards the C(7) carbon resonance of the acetate chain is attributed to the increased importance of 50 when charge stabilizing substituents are present on the phenyl ring. It should be noted that the correlation for the C(5) carbon atom is only significant at the 90% confidence level. Despite the only modest success of the DSP equation in describing the substituent effect at the C(5) carbon atom, the general trend is consistent across the series.

The correlation of the C(6) carbon atom chemical shifts were also significant only at the 90% confidence level. The positive values obtained for  $\rho_I$  and  $\rho_R$  demonstrate that electron donating substituents on the phenyl ring induce an upfield shift. It is tempting to attribute this shift to higher field to an increase in electron density at C(6). In terms of the resonance structures shown in Scheme 2.4, an increase in the contribution from 50 would reduce the amount of positive charge at C(2) and hence, C(6) as well. This would

be consistent with the observed trend in the C(6) carbon atom chemical shifts.

However, it is clear that charge density is not the only factor which contributes to the chemical shifts observed at this site. Comparison of the chemical shifts of the C(11) carbon atom with the C(6) carbon atom for each of the dioxolanylium ions under investigation (Table 2.3), reveals that on going from an acetate methyl group to an acetoxonium methyl group, an upfield shift is observed. The direction and magnitude of this change in chemical shift are similar to those reported for other dioxolanylium ions and for the protonation or alkylation of the carbonyl oxygen of esters<sup>76</sup> and lactones.<sup>43</sup> This upfield shift is not what would be expected when a formal positive charge is introduced adjacent to a methyl group. A powerful neighbouring group effect appears to be operating in the opposite sense to the inductive effect described above. Without a clear understanding of all the factors which contribute to the chemical shift of the C(6) carbon atom, it is difficult to draw any conclusions about the electron density at this site. In principle, charge density calculations would be helpful in identifying these effects. However, as will be seen in Chapter 4, calculations at the AM1 level were inconclusive regarding this point.

The success of  $\sigma_R^0$  in the DSP equation for all positions in the dioxolanylium ion ring is consistent with the structure of the ion. The structure of **39** as determined by x-ray crystallography (see Chapter 3) reveals that the phenyl ring is twisted so as to prevent a full conjugative interaction with the dioxolanylium ring. Based on the similarity of the <sup>13</sup>C solution and solid state CPMAS spectra for **39** (Table 2.3), this orientation is also the

preferred conformation in solution. While the  $\sigma_R'$  scale is useful for positively charged systems, it is most effective when there is a strong resonance interaction between the substituent and the probe site. The lack of a fully delocalized  $\pi$ -system precludes its use here. A more detailed analysis of the transmission of substituent effects and the attendant geometrical requirements is presented in Chapter 4.

(d) **Relative Importance of the Inductive and Mesomeric Substituent Effects**

The parameter  $\lambda$  is defined as  $\rho_R / \rho_I$  and is indicative of the relative importance of the mesomeric effect versus the inductive effect on the chemical shift differences observed. The value of  $\lambda$  is not constant for all positions in a given molecule. This is a consequence of the fact that both the magnitude and sign of the inductive, field, and mesomeric effects are dependent on the position of the substituent relative to the probe site. Since  $\lambda$  is defined as a blending of these effects, it follows that this parameter is also position dependent. Similar values of  $\lambda$  (1.4 to 1.6) were obtained for positions C(2), C(4) and C(6) (Table 2.10). At these carbon atoms the inductive effect makes an important contribution to the observed substituent effects. At C(5) however, the mesomeric effect of the substituents predominates with  $\lambda = 15.0$ .

## 2.10 Summary

The isomerization reaction of a dioxolanylium ion with an internal nucleophile was shown to be extremely sensitive to the nature of the substituent at the displacement

center. Both the ease and mechanism of reaction can be controlled by choice of substituent at C(4). Evidence was presented to suggest that the system may adopt a trigonal bi-pyramidal geometry about the C(4) carbon atom, when substituents of sufficient electron-donating ability are present.

The variation in the ground state structure of the dioxolanylium ion system as a function of the electronic nature of the C(4) substituent was assessed. The effect of the aryl substituent on the charge distribution within the ion was rationalised in terms of a contribution from an ionic resonance structure. Consistent with this, charge-stabilizing substituents at C(4) increase the amount of positive charge at this position while reducing charge at C(2).

## Chapter 3

### Crystallographic Study of Dioxolanylium Ion Structure

The results of the solid state study of the 1,3-dioxolan-2-ylum ion structure are presented in this chapter. Further evidence was obtained to support the inclusion of an ionic resonance contributor to the ground state description of the 1,3-dioxolan-2-ylum ion system.

#### 3.1 X-ray Structure Determinations

Single crystals of **36** and **39** suitable for x-ray crystallographic studies were obtained by vapour diffusion of diethyl ether into  $\text{CH}_2\text{Cl}_2$  solutions of the respective compounds at  $-20\text{ }^\circ\text{C}$ . The crystals were found to be moisture sensitive but otherwise stable at room temperature. Accordingly, all manipulations were performed under a dry nitrogen atmosphere. Experimental details pertaining to the data collection and to the solution of the structures are described in the Experimental section. Selected bond lengths and bond angles for **36** and **39** are presented in Tables 3.1 to 3.4. Selected least squares plane data for the dioxolanylium ion ring in **36** and **39** are presented in Table 3.5. Figures 3.1 to 3.3 illustrate the geometry of the cation, packing and stereoscopic view of the unit cell contents for **36**. Similar plots pertaining to **39** are presented in Figures 3.4 to 3.8.

Table 3.1: Selected bond lengths (Å) for 36.

Sb(1)-Cl(1)#1	2.353(2)	Sb(1)-Cl(1)	2.353(2)
Sb(1)-Cl(3)	2.356(2)	Sb(1)-Cl(3)#1	2.356(2)
Sb(1)-Cl(2)#1	2.376(3)	Sb(1)-Cl(2)	2.376(3)
Sb(2)-Cl(4)	2.35(2)	Sb(2)-Cl(4)#2	2.35(2)
Sb(2)-Cl(5)#2	2.374(4)	Sb(2)-Cl(5)	2.374(3)
Sb(2)-Cl(4A)	2.38(2)	Sb(2)-Cl(4A)#2	2.38(2)
O(1)-C(2)	1.279(9)	O(1)-C(5)	1.480(10)
O(3)-C(2)	1.283(9)	O(3)-C(4)	1.497(11)
O(8)-C(9)	1.358(10)	O(8)-C(7)	1.45(2)
O(10)-C(9)	1.195(10)	C(2)-C(6)	1.48(4)
C(4)-C(7)	1.480(11)	C(4)-C(5)	1.512(12)
C(9)-C(11)	1.496(14)		

Table 3.2: Selected bond angles (°) for 36.

Cl(1)#1-Sb(1)-Cl(1)	180.0	Cl(1)#1-Sb(1)-Cl(3)	89.4(3)
Cl(1)-Sb(1)-Cl(3)	90.6(3)	Cl(1)#1-Sb(1)-Cl(2)#1	90.6(3)
Cl(1)-Sb(1)-Cl(3)#1	89.4(3)	Cl(3)-Sb(1)-Cl(3)#1	180.0
Cl(1)#1-Sb(1)-Cl(2)#1	93(2)	Cl(1)-Sb(1)-Cl(2)#1	87(2)
Cl(3)-Sb(1)-Cl(2)#1	90.76(14)	Cl(3)#1-Sb(1)-Cl(2)#1	89.24(14)
Cl(1)#1-Sb(1)-Cl(2)	87(2)	Cl(1)-Sb(1)-Cl(2)	93(2)
Cl(3)-Sb(1)-Cl(2)	89.24(14)	Cl(3)#1-Sb(1)-Cl(2)	90.76(14)
Cl(2)#1-Sb(1)-Cl(2)	179.998(1)	Cl(4)-Sb(2)-Cl(4)#2	180.000(2)
Cl(4)-Sb(2)-Cl(5)#2	90(2)	Cl(4)#2-Sb(2)-Cl(5)#2	90(2)
Cl(4)-Sb(2)-Cl(5)	90(2)	Cl(4)#2-Sb(2)-Cl(5)	90(2)
Cl(5)#2-Sb(2)-Cl(5)	179.999(5)	Cl(4)-Sb(2)-Cl(4A)	89.80(10)
Cl(4)#2-Sb(2)-Cl(4A)	90.20(10)	Cl(5)#2-Sb(2)-Cl(4A)	90(2)
Cl(5)-Sb(2)-Cl(4A)	90(2)	Cl(4)-Sb(2)-Cl(4A)#2	90.20(10)
Cl(4)#2-Sb(2)-Cl(4A)#2	89.80(10)	Cl(5)#2-Sb(2)-Cl(4A)#2	90(2)
Cl(5)-Sb(2)-Cl(4A)#2	90(2)	Cl(4A)-Sb(2)-Cl(4A)#2	179.999(2)
C(2)-O(1)-C(5)	108.3(6)	C(2)-O(3)-C(4)	109.1(6)
C(9)-O(8)-C(7)	113.8(10)	O(1)-C(2)-O(3)	116.3(7)
O(1)-C(2)-C(6)	122.8(13)	O(3)-C(2)-C(6)	121.0(14)
C(7)-C(4)-O(3)	106.9(7)	C(7)-C(4)-C(5)	117.1(8)
O(3)-C(4)-C(5)	101.3(6)	O(1)-C(5)-C(4)	103.9(7)
O(8)-C(7)-C(4)	106.2(7)	O(10)-C(9)-O(8)	123.5(11)
O(10)-C(9)-C(11)	125.9(9)	O(8)-C(9)-C(11)	110.5(11)

Symmetry transformations used to generate equivalent atoms:

#1 -x,-y,-z #2 -x,-y+1,-z+1



Table 3.3: Selected bond lengths (Å) for 39.

SbCl(1)	2.356(3)	SbCl(2)	2.355(2)
SbCl(3)	2.372(2)	SbCl(4)	2.370(2)
SbCl(5)	2.358(3)	SbCl(6)	2.376(3)
O(1)C(2)	1.311(9)	O(1)C(5)	1.458(10)
O(3)C(2)	1.277(9)	O(3)C(4)	1.514(8)
O(8)C(7)	1.445(9)	O(8)C(9)	1.349(9)
O(10)C(9)	1.187(10)	C(2)C(6)	1.433(12)
C(4)C(5)	1.556(11)	C(4)C(7)	1.503(10)
C(4)C(1')	1.497(10)	C(9)C(11)	1.503(11)
C(1')C(2')	1.389(12)	C(1')C(6')	1.386(11)
C(2')C(3')	1.383(13)	C(3')C(4')	1.366(15)
C(4')C(5')	1.408(15)	C(5')C(6')	1.394(12)
Cl(1')C(12)	1.681(12)	Cl(2')C(12)	1.741(13)

Table 3.4: Selected bond angles (°) for 39.

Cl(1)SbCl(2)	90.6(1)	Cl(1)SbCl(3)	89.8(1)
Cl(2)SbCl(3)	179.5(1)	Cl(1)SbCl(4)	178.1(1)
Cl(2)SbCl(4)	90.5(1)	Cl(3)SbCl(4)	89.1(1)
Cl(1)SbCl(5)	91.3(1)	Cl(2)SbCl(5)	89.9(1)
Cl(3)SbCl(5)	89.8(1)	Cl(4)SbCl(5)	90.2(1)
Cl(1)SbCl(6)	89.0(1)	Cl(2)SbCl(6)	91.5(1)
Cl(3)SbCl(6)	88.9(1)	Cl(4)SbCl(6)	89.5(1)
Cl(5)SbCl(6)	178.7(1)	C(2)O(1)C(5)	108.8(6)
C(2)O(3)C(4)	109.9(5)	C(7)O(8)C(9)	116.2(5)
O(1)C(2)O(3)	115.5(7)	O(1)C(2)C(6)	121.9(7)
O(3)C(2)C(6)	122.6(7)	O(3)C(4)C(5)	99.7(5)
O(3)C(4)C(7)	104.6(5)	C(5)C(4)C(7)	113.4(6)
O(3)C(4)C(1')	109.9(6)	C(5)C(4)C(1')	115.7(6)
C(7)C(4)C(1')	112.1(6)	O(1)C(5)C(4)	103.7(6)
O(8)C(7)C(4)	107.7(6)	O(8)C(9)O(10)	122.3(7)
O(8)C(9)C(11)	112.0(7)	O(10)C(9)C(11)	125.6(8)
C(4)C(1')C(2')	120.7(7)	C(4)C(1')C(6')	119.7(7)
C(2')C(1')C(6')	119.5(7)	C(1')C(2')C(3')	119.3(8)
C(2')C(3')C(4')	122.6(10)	C(3')C(4')C(5')	118.2(9)
C(4')C(5')C(6')	119.8(9)	C(1')C(6')C(5')	120.6(8)
Cl(1')C(12)Cl(2')	116.8(7)		

Table 3.5: Selected least-squares plane data for 36 and 39.

Atom	Distance (Å) from plane	
	36	39
O(1)	0.042 (5)	0.070 (5)
C(2)	0.000 (4)	-0.007 (4)
O(3)	-0.040 (5)	-0.056 (4)
C(4)	0.059 (5)	0.085 (4)
C(5)	-0.060 (5)	-0.092 (5)
C(6)	-0.012 (23)	0.011 (15)

Atoms O(1), C(2), O(3), C(4), and C(5) used to define the plane.

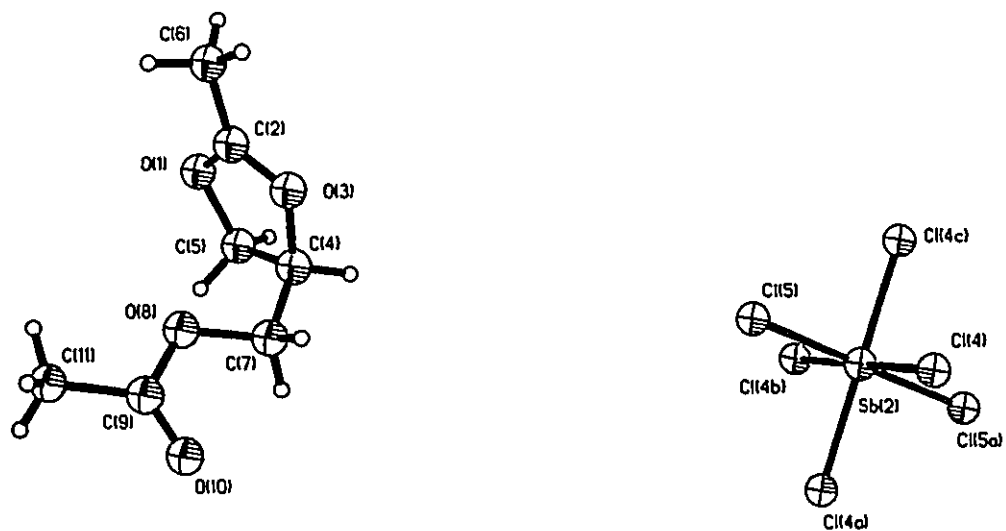


Figure 3.1: Conformation of 36.

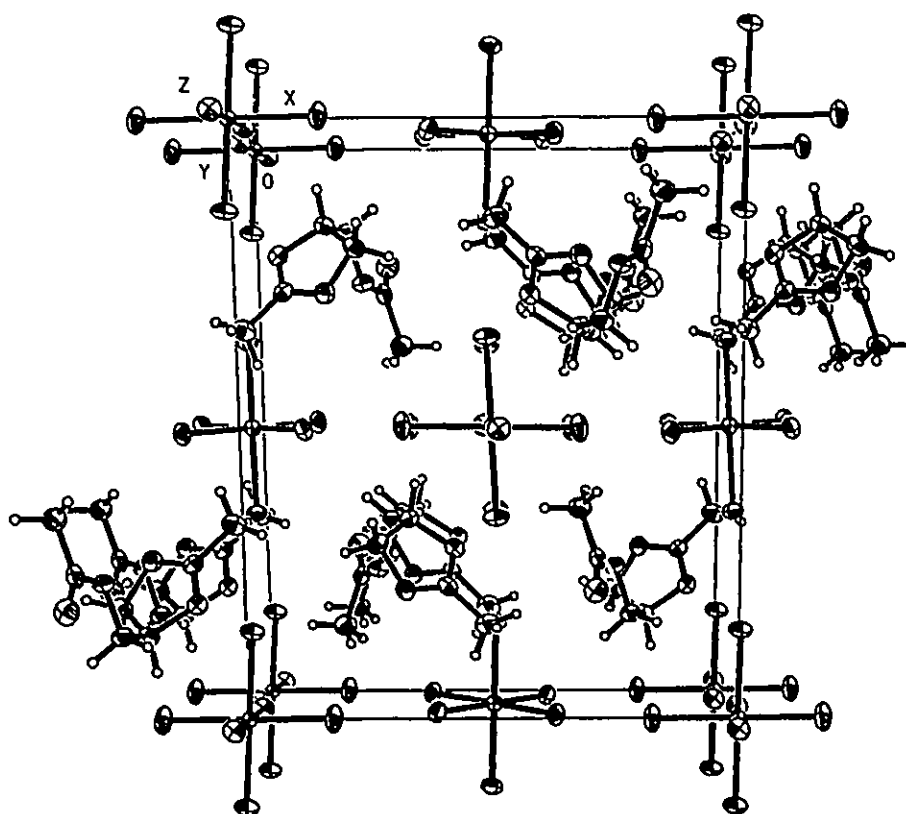


Figure 3.2: Unit cell packing in 36 (viewed along z axis).

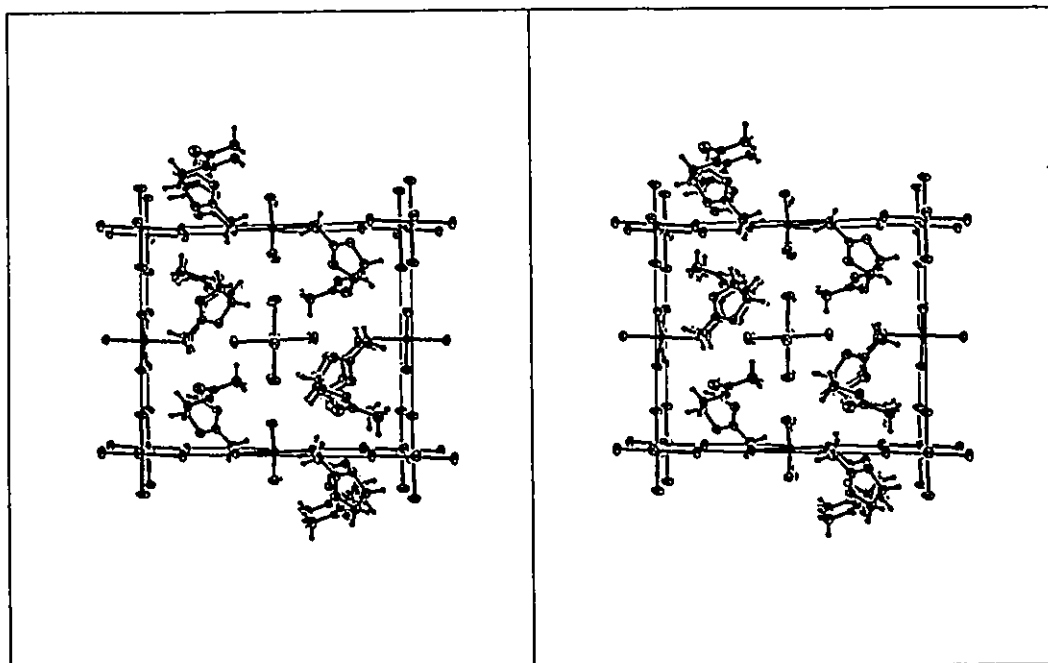


Figure 3.3: Stereoscopic view of unit cell contents for 36 (viewed along z axis).

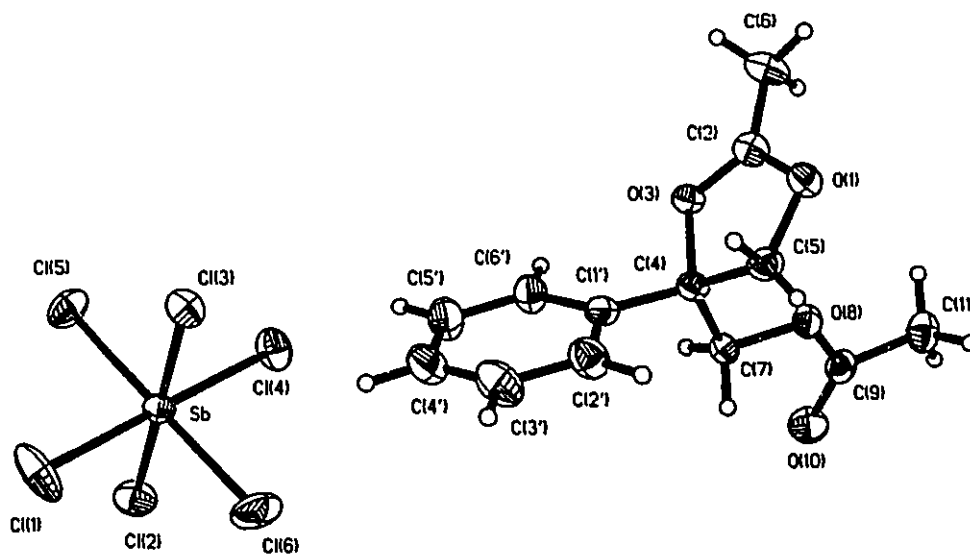


Figure 3.4: Conformation of 39.

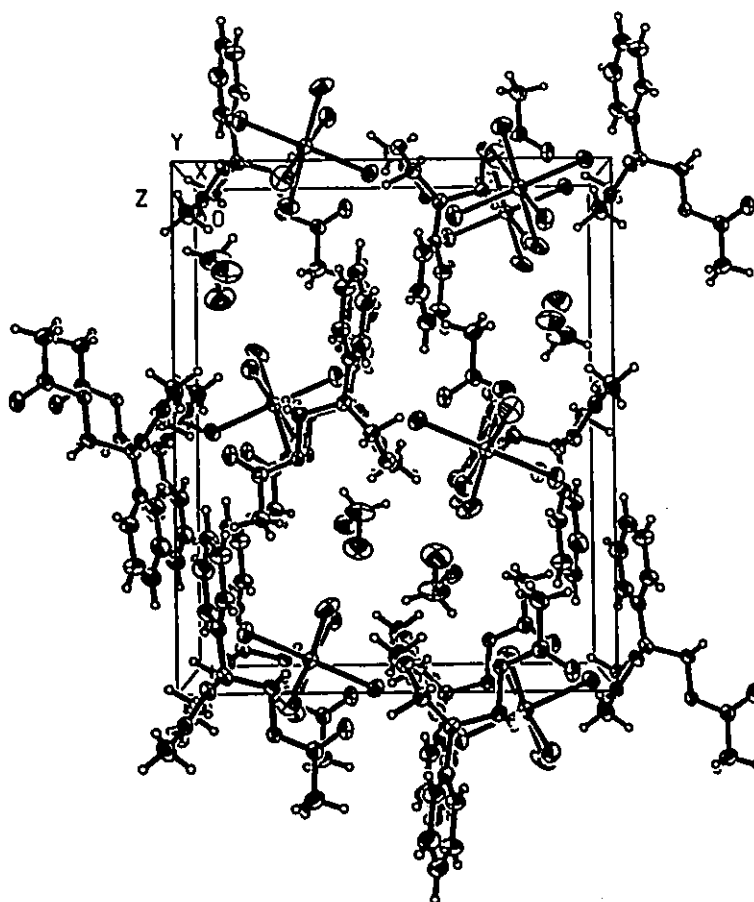


Figure 3.5: Unit cell packing in 39 (viewed along x axis).

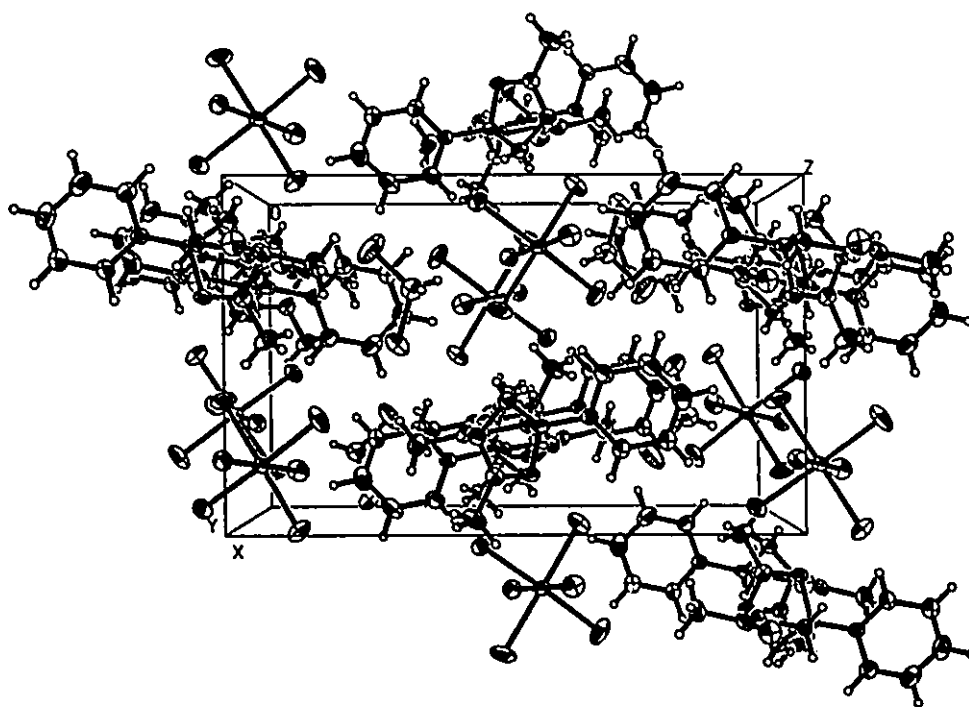


Figure 3.6: Unit cell packing in 39 (viewed along z axis).



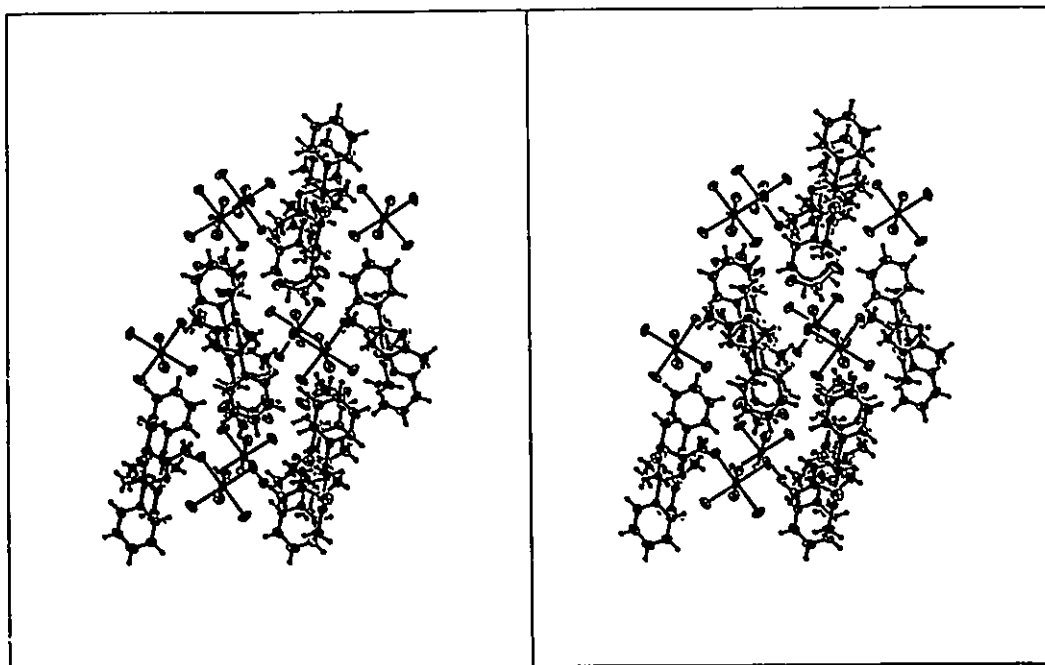


Figure 3.7: Stereoscopic view of unit cell contents for **39** (viewed along z axis).

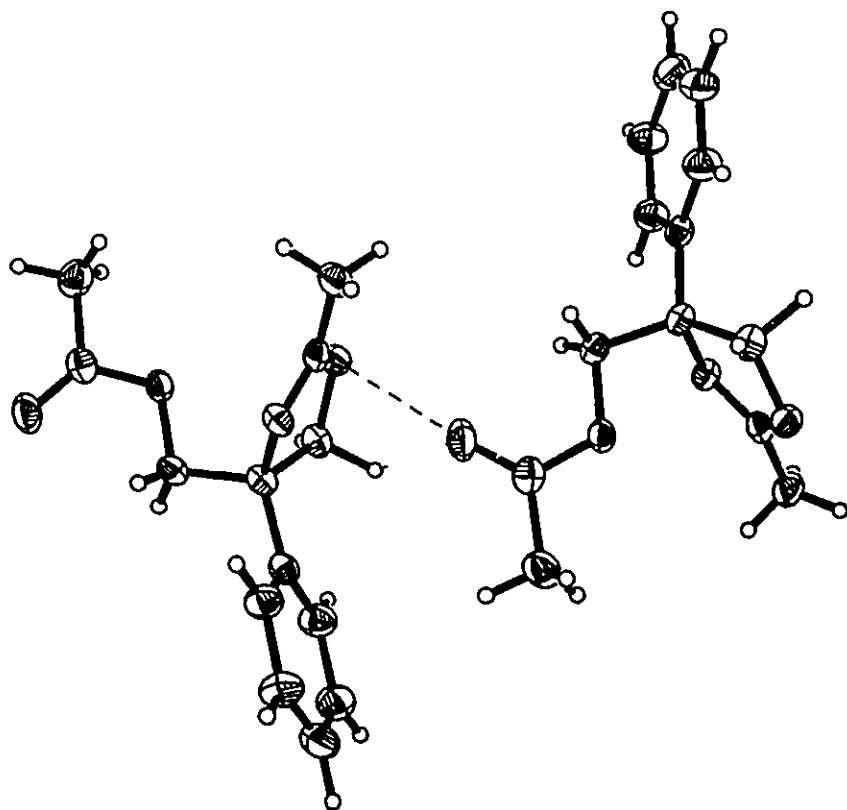
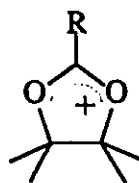
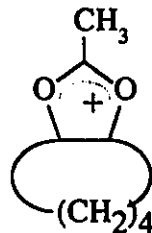


Figure 3.8: Intermolecular interaction in 39.

### 3.2 Conformation of the Dioxolanylium Cation

#### (a) Conformation of 36

The overall structure of 36 (Fig. 3.1) is similar to those previously reported for other cations of this type.<sup>35-40</sup> The dioxolanylium ring adopts a planar conformation (Table 3.5), with the maximum displacement from the least-squares plane being 0.060 (5) Å for the C(5) carbon atom. In nearly all of the known structures of dioxolanylium ions, the five-membered ring is planar. The tendency for the dioxolanylium system to remain planar, even in the presence of large steric interactions acting in opposition, is clearly illustrated by the structures reported for 16<sup>36</sup> and 17.<sup>35</sup> In each of these structures, planarity of the dioxolanylium ring forces the methyl groups into an unfavourable double eclipsed conformation. Deviations in planarity are not easily achieved due to the resulting cost in resonance energy to the O(1)-C(2)-O(3)  $\pi$  system. The only exception to this rule has been the structure reported by Paulsen and Dammeyer<sup>38</sup> for 2-methyl-4,5-tetramethylene-1,3-dioxolan-2-ylum perchlorate, 19. Fusion with the six-membered ring forces the dioxolanylium ion ring to adopt a twist conformation with an O(1)-C(5)-C(4)-O(3) torsional angle of 25.9°. The O(1)-C(5)-C(4)-O(3) torsional angle in 36 is only 10.0°.

16 R = CH<sub>3</sub>17 R = C<sub>6</sub>H<sub>5</sub>

19

One of the principle reasons for undertaking the crystallographic study of these dioxolanylium ions, was to determine if the ground state structure reflected the reactivity of the ions. The concerted isomerization of **36** involves the approach of the O(10) carbonyl oxygen atom to the displacement center, C(4). In the solid state structure, the O(10) oxygen atom is far removed from the C(4) atom and not in the proper alignment to attack this position. Instead, the free acetate chain lies in an *s-cis* conformation (Fig 3.1).

The closest contact of the  $\text{SbCl}_6^-$  anion with the dioxolanylium ion cation of **36** occurs between the Cl(3) chlorine atom on the counter ion and the H(4) hydrogen atom, and has a distance of 2.582 Å. Possible interactions between a halogen atom on the counter ion and the positively charged C(2) carbon atom of dioxolanylium ions<sup>35,40</sup> and in related systems<sup>43,95</sup> have been previously suggested. In these studies, interatomic distances ranging from 3.206 Å to 3.495 Å for C<sup>+</sup> and chlorine atoms have been observed. In **36**, the closest approach between C(2) and the counter ion is achieved with the Cl(2) chlorine atom at a distance of 3.353 Å. Since a good value for the van der Waal radius for a C<sup>+</sup> atom is not available, it is difficult to determine whether this type of interaction is significant, although it is shorter than that observed for neutral carbon atoms with chlorine (3.50 Å). On the other side of the cationic plane approaching the C(2) carbon atom, is the O(8) oxygen atom, at a distance of 3.170 Å. This distance is achieved by the folding over of the free acetate chain onto the dioxolanylium ring. Again, without a reliable value for the van der Waal radius of a C<sup>+</sup> carbon atom, it is

difficult to determine if this is a significant interaction.

(b) Conformation of 39

The structure of 39 also contains a planar dioxolanylium ring (Figure 3.4). The acetate side chain in 39 adopts a similar orientation with respect to the dioxolanylium ring as was observed in 36. The ester group lies in an *s-cis* conformation and is folded over the dioxolanylium ion ring, bringing the O(8) oxygen atom close to the positively charged C(2) atom (2.977 Å).

The closest anion-cation contact for 39 occurs between the H(7b) hydrogen atom and Cl(6) chlorine atom with a distance of 2.771 Å. The anion is far removed from the positively charged C(2) carbon atom. The closest approach by the anion to the C(2) carbon atom is by the Cl(4) chlorine atom at a distance of 3.822 Å. Approaching the C(2) atom from the other side of the cationic plane is an O(10b) carbonyl oxygen from an adjacent dioxolanylium cation within the crystalline lattice (Fig 3.8). The C(2)-O(10b) intermolecular distance is quite short at 2.681 Å. Despite this close approach of a Lewis base to one side of a positively charged carbon atom, there is no distortion of the C<sup>+</sup> carbon out of the plane of the cation in 39. A distortion of the C<sup>+</sup> atom towards the Lewis base is sometimes observed in such cases.<sup>43,95</sup>

The interaction of the O(10b) oxygen atom with the C(2) carbon atom may be considered an early "snap-shot" of the dynamic process of a nucleophile attacking a cationic center. The concept of examining non-bonded interactions within the crystal

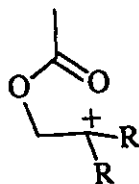
environment as a means of investigating dynamic processes has been advanced by Burgi and Dunitz. These authors and their co-workers have systematically applied this technique to investigate the approach of oxygen- and nitrogen-containing nucleophiles to a carbonyl group.<sup>32,33</sup> The present example and other work in our laboratory,<sup>40,43,95</sup> has extended this concept to the approach of nucleophiles to charged systems.

The orientation of the phenyl group in **39** is also of interest. The angle between the normals to the plane of the phenyl group and the best fit plane of the dioxolanylium ring is  $42.4^\circ$ . In the step-wise isomerization of **39**, rupture of the O(3)-C(4) bond produces a carbenium ion intermediate in which the phenyl ring is coplanar with the plane of the  $sp^2$  hybridized C(4) atom (see Chapter 4). A similar orientation should be evident in the transition state structure. In the ground state structure, the O(3)-C(4)-C(1')-C(2') torsional angle reveals that the phenyl group is not yet in the proper orientation to maximally delocalize the positive charge which will develop at C(4) during the course of the isomerization. It should be borne in mind, however, that while total planarity between  $\pi$  systems maximizes orbital overlap, significant delocalization can still occur in non-planar systems. This concept is presented in greater detail in Chapter 4.

### 3.3 C-O Bond lengths in **36** and **39**.

The O(1)-C(2)/O(3)-C(2) bond lengths in both **36** and **39** are intermediate in length between those of C-O single and double bonds (Tables 3.1 and 3.3). This is a common feature of all dioxolanylium ions, and is a consequence of resonance

delocalization of positive charge across the O(1)-C(2)-O(3)  $\pi$  system.<sup>35-40</sup> In 36, the O(1)-C(2) and O(3)-C(2) bond lengths are not significantly different.<sup>41</sup> In Chapter 2, evidence was presented which supported the inclusion of resonance structure 50 in the ground state description of the dioxolanylium ion system. In light of this, some differentiation might be expected for these two bond lengths; that is, more double bond character for the O(3)-C(2) bond and hence a shorter bond length compared to the O(1)-C(2) bond.



50

The difference in the O(1)-C(2) and O(3)-C(2) bond lengths in 39 just fail to be significant at the 99% confidence level. These bond lengths differ by  $2.7\sigma$  which is,

---

The statistical treatment used to determine the difference between two directly comparable bond lengths,  $d_1(\sigma_1)$  and  $d_2(\sigma_2)$ , is as follows:

$$\sigma = [(\sigma_1)^2 + (\sigma_2)^2]^{1/2}$$

where  $\sigma_1$  and  $\sigma_2$  are the standard deviations of the two observed bond lengths,  $d_1$  and  $d_2$ , and  $\sigma$  is the standard deviation between the two values. The bond lengths are significantly different at the 99% confidence level if the following inequality holds:

$$|d_1 - d_2| > 3\sigma$$

however, a significant difference at better than the 95% confidence level. To completely dismiss this difference as insignificant, would be to give far too much weight to only a 4% change in confidence level.<sup>9a</sup> It is suggested that the difference observed in the O(1)-C(2)/O(3)-C(2) bond lengths in **39** represents an increased contribution from resonance structure **50**, relative to that found in **36**.

The O(3)-C(4)/O(1)-C(5) bond lengths also provide a means of assessing the contribution from **50** to the ground state description of dioxolanylium ions. In **36**, the length of the O(3)-C(4) bond is not significantly different from that of the O(1)-C(5) bond. This illustrates the difficulty of detecting meaningful differences in bond lengths within a single dioxolanylium ion. However, it has been shown<sup>40</sup> by comparing the structures of a series of dioxolanylium ions reported in the literature, that an increase in the degree of substitution at the alkyl carbon atoms is accompanied by an increase in the O-C(alkyl) bond lengths. The O(3)-C(4) and the O(1)-C(5) bond lengths in **36** are consistent with the average values reported for O-CHR<sub>2</sub> and O-CH<sub>2</sub>R bonds respectively.

The effect of substitution at the alkyl carbon atoms in dioxolanylium ions can be more easily appreciated in the structure of **39**. For this cation, the O(3)-C(4) bond is significantly longer ( $4.4\sigma$ ) than the O(1)-C(5) bond. The importance of resonance contributor **50** is clearly indicated by the structure of this cation. Furthermore, the O(3)-C(4) and O(1)-C(5) bond lengths are in agreement with the average values reported<sup>40</sup> for O-CR<sub>3</sub> and O-CH<sub>2</sub>R bonds respectively, in related systems. In principle, steric interactions may also contribute to the differences observed in bond lengths, when the



bonds being compared differ in their substitution pattern. This is only likely to be of concern in the most severely crowded systems, since bond lengths are the least likely among the geometrical parameters to experience perturbation from steric strain.<sup>34a,96b</sup>

### 3.4 Summary

Further evidence was found to support the inclusion of the ionic resonance contributor **50** in the ground state description of dioxolanylium ions. The environments around the positively charged C(2) carbon atoms in each of **36** and **39** contain Lewis bases situated nearby. As such, these structures represent early "snap-shots" of nucleophilic addition reactions at positively charged centers. The solid state conformations of **36** and **39** bear little resemblance to the respective transition state structures for the isomerizations of these compounds. Dioxolanylium ions which are more reactive towards isomerization, may adopt structures which represent points further along the reaction co-ordinate. This possibility was explored with the use of semi-empirical calculations, and the results are presented in the following chapter.

## Chapter 4

### Semi-Empirical Investigation of Dioxolanylium Ion Structure and Isomerization

The use of x-ray crystallography and NMR spectroscopy have provided evidence for the structure, charge distribution, and mechanism of reaction for the dioxolanylium ions studied. It was of interest to compare the results obtained experimentally with those predicted from theoretical calculations. Also, theoretical studies can in principle be used to extend the correlations to cations beyond the ones which could be obtained experimentally. Further insight can be provided by modelling the intermediates or transition states for the dioxolanylium isomerizations, yielding more direct evidence than that which could be inferred from the spectroscopic investigations.

#### 4.1 Structure of the Aryl Substituted Dioxolanylium Ions

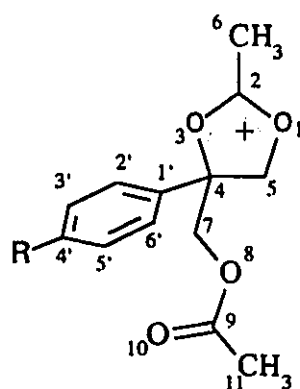
AM1 geometry optimizations were performed on cations 38-42, and 45. The fractional co-ordinates corresponding to the crystal structure geometry of the cation in 39 were first transformed into cartesian orthogonal co-ordinates for input into PCMODEL<sup>57</sup>. Modifications to the base structure of 39 were performed within PCMODEL to obtain

the initial geometries of the remaining cations. The cations were assigned a charge of +1 and AM1 geometry optimizations were carried out using the semi-empirical modelling program AMPAC<sup>98</sup>. In each case, the convergence criteria for the optimum geometry were set to achieve an energy gradient of better than 0.01 Kcal/Å. Selected bond distances and bond angles for the optimized cations are given in Table 4.1 and 4.2 respectively. For simplicity, the numbering scheme used to refer to the dioxolanylium ion salts in previous chapters has been retained, although only the cation (in absence of the counter ion) is considered here.

The AM1-optimized conformations of 38-42 and 45 are similar. The five membered dioxolanylium ring of 39 is planar to achieve maximum orbital overlap within the O(1)-C(2)-O(3)  $\pi$ -system (Fig. 4.1).<sup>36</sup> The C(6) carbon atom of the acetoxonium methyl group is coplanar with this ring. The ester function of the acetate side chain lies in an *s-cis* conformation and no interaction of this side chain with the dioxolanylium ring is apparent. The phenyl ring is twisted with respect to the dioxolanylium ring to give a O(3)-C(4)-C(1')-C(2') dihedral angle of 32.2 °. The remaining aryl-substituted dioxolanylium ions (38, 40-42, and 45), share the same basic conformation as that of 39.

Table 4.1: Selected AM1 optimized bond lengths (Å) for cations 38-42 and 45.

Bond	Compound					
	38	39	40	41	42	45
O(1)C(2)	1.329	1.330	1.330	1.330	1.330	1.332
C(2)O(3)	1.321	1.319	1.318	1.318	1.317	1.314
O(3)C(4)	1.509	1.513	1.516	1.517	1.520	1.530
C(4)C(5)	1.542	1.541	1.541	1.540	1.540	1.539
O(1)C(5)	1.470	1.469	1.470	1.470	1.469	1.469
C(2)C(6)	1.469	1.470	1.470	1.470	1.470	1.471
C(4)C(7)	1.529	1.528	1.528	1.528	1.528	1.527
C(7)O(8)	1.429	1.430	1.430	1.430	1.430	1.431
O(8)C(9)	1.390	1.389	1.388	1.388	1.388	1.387
C(9)C(11)	1.485	1.484	1.484	1.484	1.484	1.485
C(9)O(10)	1.226	1.226	1.226	1.226	1.226	1.227
C(4)C(1')	1.493	1.490	1.488	1.488	1.486	1.479
C(1')C(2')	1.400	1.401	1.401	1.399	1.406	1.405
C(2')C(3')	1.395	1.394	1.392	1.394	1.385	1.382
C(3')C(4')	1.397	1.395	1.400	1.400	1.413	1.427
C(4')C(5')	1.396	1.396	1.403	1.406	1.404	1.427
C(5')C(6')	1.394	1.393	1.389	1.390	1.391	1.382
C(6')C(1')	1.400	1.402	1.402	1.401	1.399	1.402
C(4')R	1.531	1.102	1.480	1.506	1.368	1.377

38 R = CF<sub>3</sub>

39 R = H

40 R = CH<sub>3</sub>41 R = C(CH<sub>3</sub>)<sub>3</sub>42 R = OCH<sub>3</sub>45 R = N(CH<sub>3</sub>)<sub>2</sub>

Table 4.2: Selected AM1 optimized bond angles ( $^{\circ}$ ) for 38-42 and 45.

Angle	Compound					
	38	39	40	41	42	45
O(3)C(4)C(5)	101.37	101.22	101.21	101.20	101.07	100.85
O(3)C(4)C(7)	105.69	105.48	105.34	105.34	105.22	104.71
O(3)C(4)C(1')	107.99	107.74	107.67	107.59	107.24	106.85
C(7)C(4)C(5)	114.18	114.14	114.19	114.18	114.09	114.01
C(7)C(4)C(1')	111.45	111.62	111.68	111.70	111.77	112.03
C(5)C(4)C(1')	115.02	115.38	115.44	115.50	116.01	116.69
O(1)C(2)O(3)	112.46	112.48	112.54	112.59	112.55	112.60
C(6)C(2)O(1)	123.34	123.19	123.14	123.07	123.02	122.74
C(6)C(2)O(3)	124.21	124.32	124.32	124.35	124.43	124.65
C(2)O(3)C(4)	111.07	111.09	111.01	110.97	111.02	110.98
O(1)C(5)C(4)	104.28	104.39	104.41	104.43	104.51	104.68
C(2)O(1)C(5)	110.81	110.79	110.80	110.80	110.83	110.88
Dihedral Angle						
O(3)C(4)C(1')C(2')	29.33	32.21	32.95	33.53	37.24	42.34

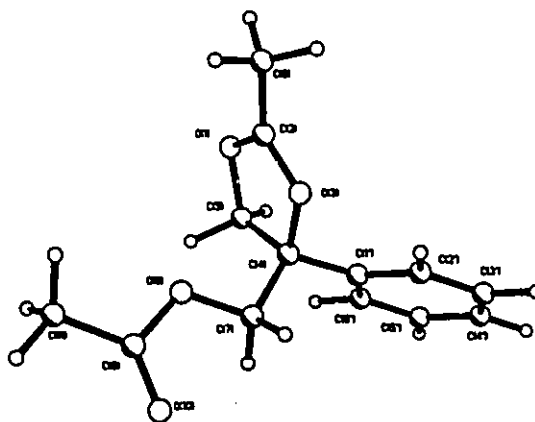
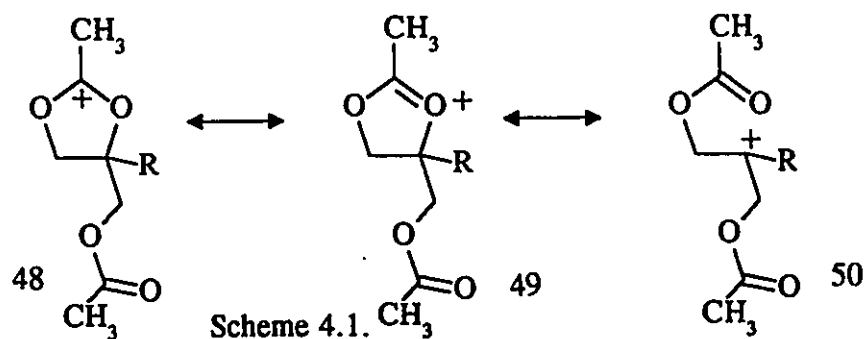


Fig. 4.1: AM1 optimized geometry of 39.

The corresponding bond distances within cations **38-42** and **45** are similar (Table 4.1). Again using cation **39** as a typical example, the O(1)-C(2) and O(3)-C(2) bond distances were found to be intermediate in length between those of single and double C-O bonds. Similar results have been previously reported for crystallographic studies<sup>35,40</sup> and SCF-MO calculations<sup>46</sup> of other dioxolanylium ion systems. The partial double bond character for these C-O bonds is consistent with charge delocalization across the O(1)-C(2)-O(3) system. Similarly, the O(1)-C(2)/O(3)-C(2) bond lengths in the other cations in this series (**38**, **40-42** and **45**), are also indicative of positive charge delocalization.

Despite the overall similarity of the structures of **38-42** and **45**, some systematic variations in several bond lengths are apparent. A contraction of the C(2)-O(3) bond was observed as the *para* substituent on the phenyl ring is made more electron donating. As was discussed in Chapters 2 and 3, the effect of the *para* substituent on the phenyl ring can be viewed in terms of the relative importance of the non-bonded resonance structure **50** to the ground state description of the ion (Scheme 4.1).

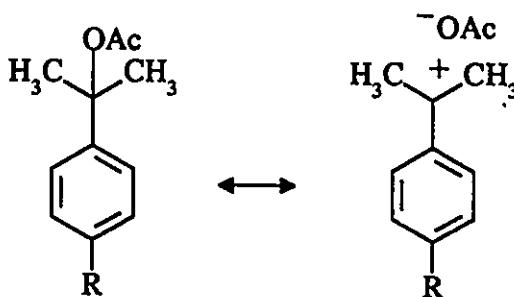


An increase in the contribution of **50** would be expected as the substituent on the phenyl ring is made better electron donating so as to better stabilize the formal positive charge

at C(4). The contraction of C(2)-O(3) bond length across the series is consistent with an increasing contribution of 50 to the resonance description of these cations. Furthermore, the C(2)-O(3) bond lengths for this series was found to correlate well ( $r = 0.996$ ) with the Okamoto-Brown  $\sigma^+$  constants for the *para* substituents on phenyl ring (Fig. 4.2).

While variation of the aromatic substituent at C(4) has only a small effect on the C(2)-O(3) bond length, it is necessary to establish a suitable point of reference when assessing the importance of this substituent effect. To this end, the AM1-optimized structures of the benzylic esters 51a-f were computed. In light of Kirby's investigations of 1-arylethanol derivatives<sup>34</sup> (see Chapter 1), an ionic contribution to the resonance structure description of the neutral ester system is expected as well (Scheme 4.2). The O(3)-C(2) bond distances in 51a-f were found to contract slightly as the aromatic ring was made more electron donating while the O(1)-C(2) bond length was essentially constant across the series (Table 4.3). In comparison then, the trend observed for the C(2)-O(3) bond length in the dioxolanylium ion system, is more pronounced than in the neutral system.

Scheme 4.2



51

- |                         |  |
|-------------------------|--|
| (a) R = CF <sub>3</sub> | (d) R = C(CH <sub>3</sub> ) <sub>3</sub> |
| (b) R = H               | (e) R = OCH <sub>3</sub>                 |
| (c) R = CH <sub>3</sub> | (f) R = N(CH <sub>3</sub> ) <sub>2</sub> |

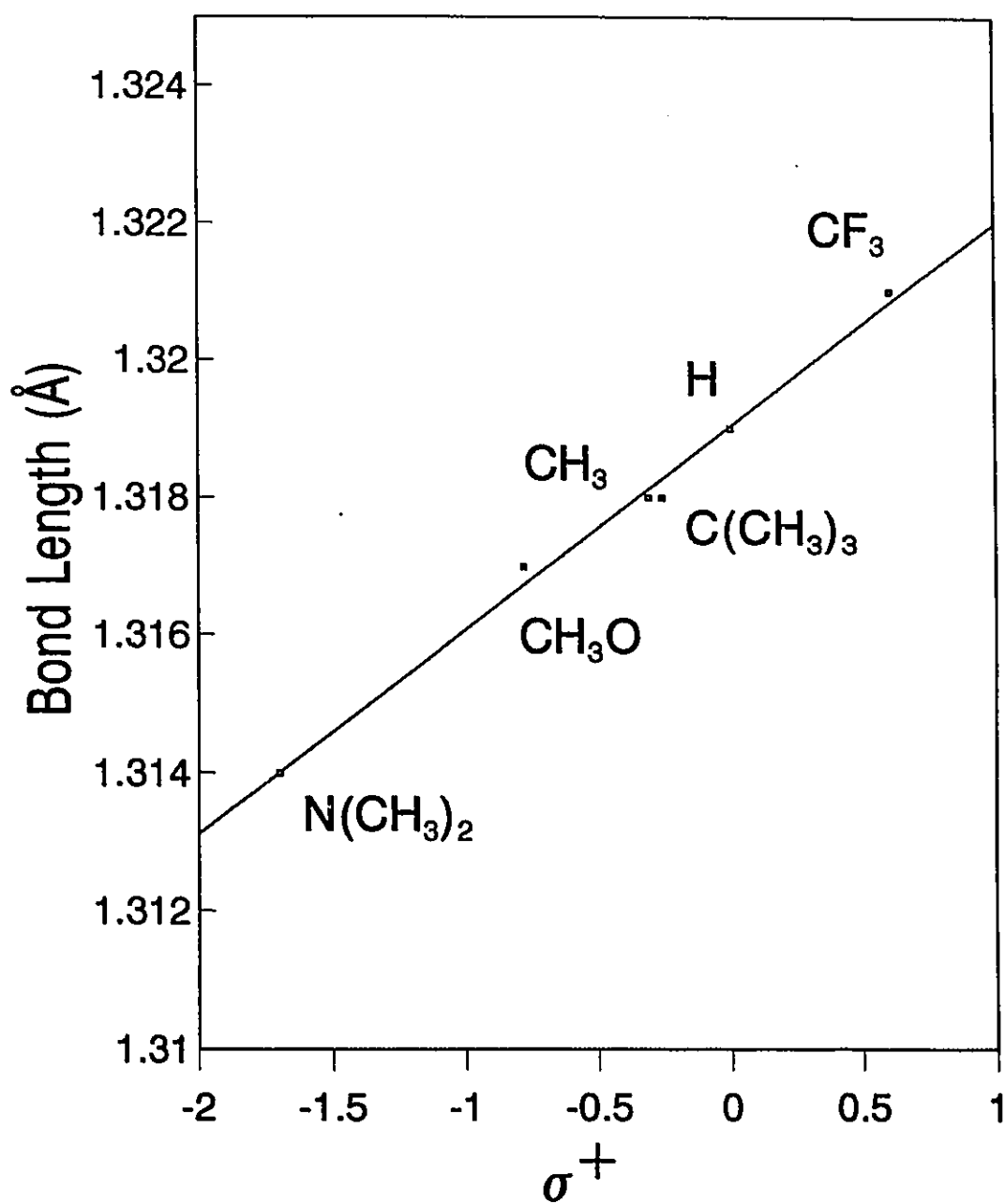
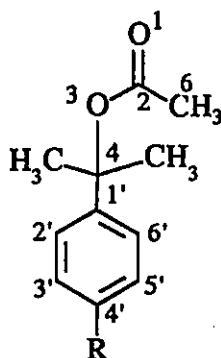


Fig. 4.2: Plot of C(2)-O(3) bond lengths in 38-42 and 45 vs  $\sigma^+$ .



Table 4.3: Selected AM1 optimized bond lengths (Å) for 51a-f.

Bond	Compound					
	51a	51b	51c	51d	51e	51f
O(1)C(2)	1.234	1.235	1.235	1.235	1.235	1.235
C(2)O(3)	1.374	1.372	1.372	1.371	1.371	1.371
O(3)C(4)	1.441	1.443	1.443	1.443	1.444	1.445
C(2)C(6)	1.487	1.488	1.488	1.487	1.488	1.488
C(4)C(1')	1.509	1.507	1.506	1.506	1.506	1.504
C(1')C(2')	1.398	1.399	1.398	1.396	1.397	1.397
C(2')C(3')	1.395	1.394	1.394	1.396	1.395	1.390
C(3')C(4')	1.394	1.394	1.398	1.398	1.394	1.417
C(4')C(5')	1.398	1.395	1.401	1.404	1.409	1.417
C(5')C(6')	1.392	1.393	1.391	1.390	1.387	1.387
C(6')C(1')	1.403	1.402	1.402	1.402	1.405	1.401
C(4')R	1.524	1.100	1.481	1.506	1.380	1.406



A further trend was observed for the O(3)-C(4) bond lengths in the dioxolanylium ions 38-42 and 45. Successive replacement of the *para*-substituent on the aromatic ring with better electron donating groups produced an elongation of the O(3)-C(4) bond. A good correlation ( $r = -0.993$ ) of these bond lengths with  $\sigma^+$  constants was obtained (Fig. 4.3). This provides additional support for the use of an ionic resonance contributor (50)

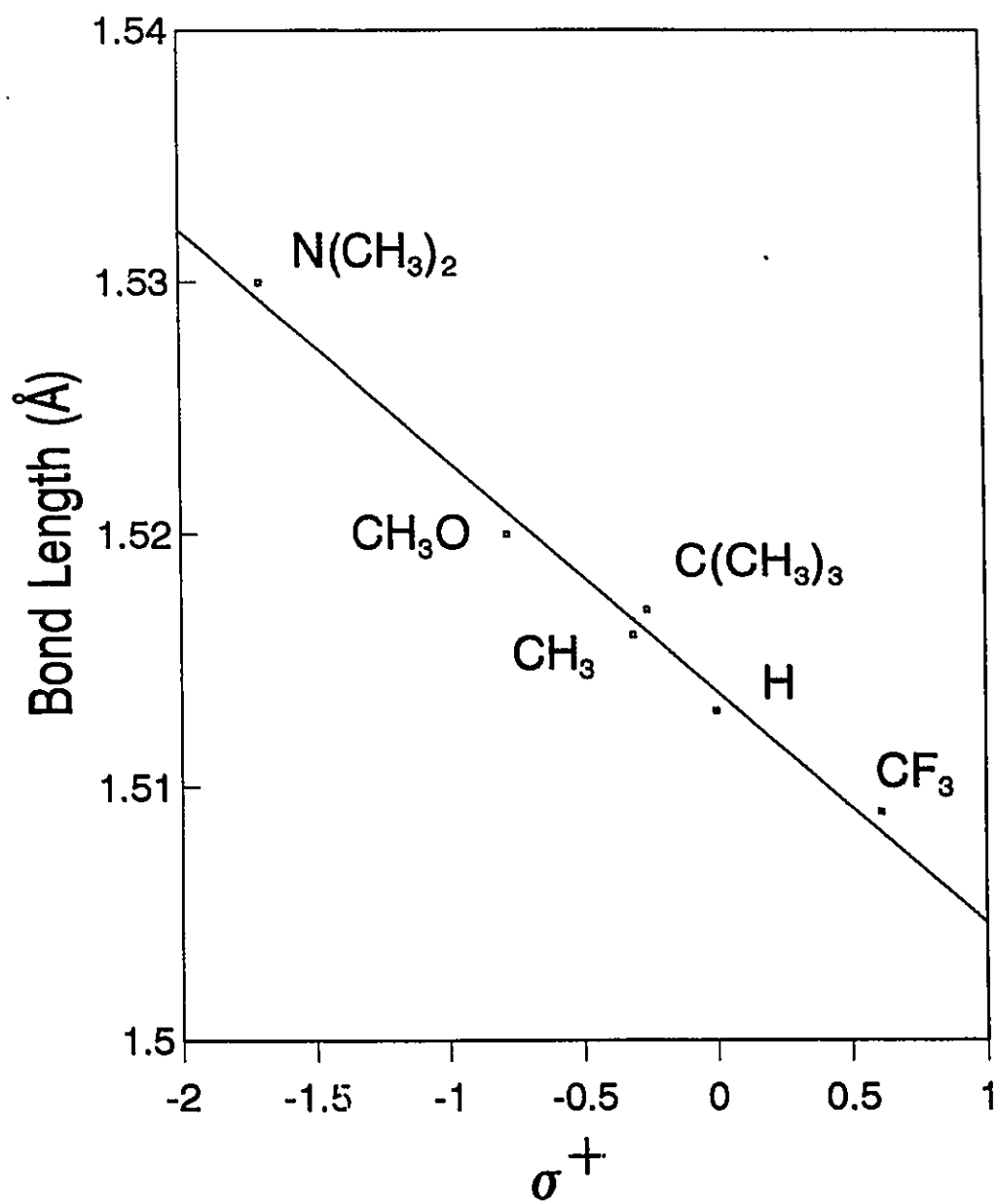


Fig. 4.3: Plot of C(4)-O(3) bond lengths in 38-42 and 45 vs  $\sigma^+$ .

in the description of dioxolanylium ions. Comparison with the O(3)-C(4) bond lengths in the ester series 51a-f (Table 4.3), again reveals that the dioxolanylium ion system exhibits a greater sensitivity to the substituent effect.

This difference in sensitivity is a reflection of the better "leaving group" ability of the oxonium ion moiety compared to the ester function. That is, formal cleavage of the O(3)-C(4) bond in the dioxolanylium ions produces a neutral "leaving group", which is preferred to the cleavage of the O(3)-C(4) bond in the ester system which would expel a carboxylate anion. While these considerations are of particular importance to the reactivity of these systems towards C-O bond cleavage, the same factors also play a role in determining the ground state structures. Indeed, this effect forms the basis for Kirby's structure-reactivity correlations.<sup>34</sup>

An elongation of the C(2)-O(1) bond in 38-42 and 45 is expected with increasing carbenium ion character as depicted by resonance contributor 50. However, this bond was found to be relatively insensitive to the nature of the substituent on the phenyl ring. Similarly, the O(1)-C(5) bond length is essentially constant across the series. Thus, not all bond lengths respond to substitution to the same degree. A similar conclusion has been reached by examining the effect of C(2)-substituents on dioxolanylium ion structure.<sup>40</sup> The situation is analogous to that observed in the <sup>13</sup>C NMR study (Chapter 2) in which the value of  $\lambda$  was position dependent.

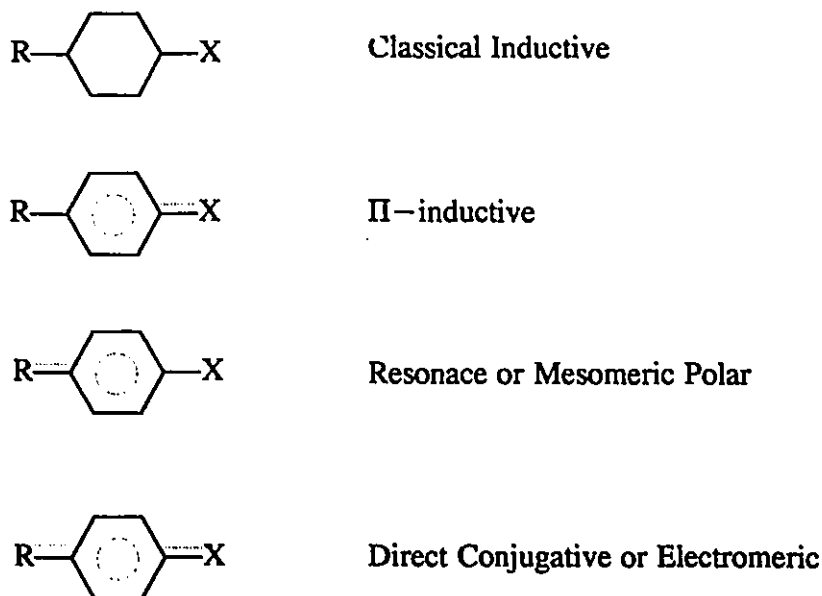
In addition to the trends observed for the bond lengths within the dioxolanylium ion ring, many systematic variations in the bond angles about C(4) were also observed.

As the electron-donating ability of the aryl substituent is increased, the C(7)-C(4)-C(1') and the C(5)-C(4)-C(1') bond angles increase (Table 4.2). The C(7)-C(4)-C(5) bond angle showed only small random fluctuations across the series. As greater weight is given to resonance contributor **50**, the orbitals on C(4) approach formal  $sp^2$  hybridization. The observation of a steady increase in C-C-C bond angles towards  $120^\circ$  is consistent with this view. Systematic decreases in the O(3)-C(4)-C(5), O(3)-C(4)-C(7) and O(3)-C(4)-C(1') bond angles were noted. As the geometry of the carbon atoms bound to C(4) approaches trigonal planar, the O(3)-C(4) bond approaches an orthonormal orientation with respect to this plane.

Various theories for the modes of transmission of substituent effects in organic systems have recently been reviewed.<sup>81d</sup> The familiar concepts of induction, resonance and field effects are often sufficient in accounting for both the nature of a substituent effect (whether stabilizing or destabilizing) and its magnitude. This approach, within the context of a dual substituent parameter equation, was successful in describing the effect of substituents on the  $^{13}\text{C}$  chemical shifts of the dioxolanylium ion system (Chapter 2). With the detailed knowledge of the structures of the C(4)-aryl substituted dioxolanylium ions as provided by the AM1 calculations, a more in depth view into the transmission of substituent effects is now possible.

Wells and co-workers<sup>81a</sup> have presented simplified component interaction models for the propagation and distribution of substituent electronic effects. Four types of interactions were identified: classical inductive,  $\pi$ -inductive, resonance or mesomeric

polar, and direct conjugative or electromeric (Scheme 4.3). The direct conjugative (and to some extent, the  $\pi$ -inductive) interaction is sensitive to deviation from planarity of the  $\pi$  system.



Scheme 4.3

The resonance energy can be related to the torsional angle,  $\theta$ , between the interacting  $\pi$  systems as follows.<sup>99,100</sup>

Eqn. 4.1 
$$E_r^\theta = E_r^0 \cos^2 \theta$$

The resonance energy can be taken as an indication of the degree of interaction of the  $\pi$  orbitals. It is a maximum when the torsional angle between the interacting  $\pi$  orbitals is

0 (i.e., total planarity) and a minimum (no interaction) when the  $\pi$  systems are perpendicular. Similar  $\cos^2\theta$  laws have been suggested to account for the dependence of various spectral properties on the torsional angle,  $\theta$ .<sup>99,101</sup>

Are the substituent effects observed in 38-42 and 45 at least partly due to direct conjugative and  $\pi$ -inductive interactions? Resonance structure 50 provides the most convenient way of visualizing how such interactions may take place. In order for the system to derive the maximum benefit from resonance delocalization, the aryl ring in 50 must be orthogonal to the formal p-orbital at C(4). Alternatively, the same geometric relationship should hold for the O(3)-C(4) bond with respect to the aryl ring when considering the more conventional resonance structures 48 and 49 (Scheme 4.1). Thus the O(3)-C(4)-C(1')-C(2') dihedral angle  $\phi$  provides a criterion for determining the likelihood of effective conjugative interactions (Fig. 4.4).

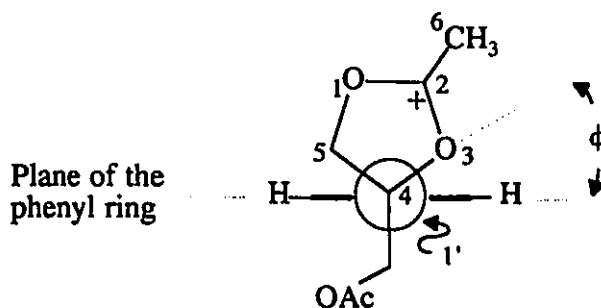


Fig. 4.4: Dihedral angle  $\phi$  in aryl dioxolanylium ions.

The dihedral angle,  $\phi$  is related to the torsional angle  $\theta$  between the interacting orbitals by the following simple relationship:

Eqn. 4.2

$$\theta = 90^\circ - \phi$$

Substituting the values for the O(3)-C(4)-C(1')-C(2') dihedral angles in 38-42 and 45 (Table 4.2) into Eqn. 4.2, gives values of  $\theta$  in the range from  $48^\circ$  to  $61^\circ$ . While the interacting orbitals are far from coplanar, Eqn 4.1 indicates some orbital overlap is still possible. While it is true that Eqn. 4.1 strictly applies only to the interaction of p-orbitals, its use (at least in a qualitative sense) is justified here, given the increasing  $sp^2$ -character for the C(4) hybridization noted earlier.

Indeed, there is evidence for the operation of a direct conjugative interaction when the *para* phenyl substituent is methoxy (42) and N,N-dimethylamino (45), the only two substituents in the series which have a lone pair of electrons capable of participating in such an interaction. For these two dioxolanylium ions, the bond which joins the heteroatom to the aryl ring is significantly shorter than the corresponding bond in the reference esters (51a-f). Similarly, a contraction of the C(4)-C(1') in 45 with respect to the neutral ester 51f was observed. Some distortion in the benzenoid ring in 45 is also apparent. These results suggest a "quinanoid" structure for the aryl ring in 45 and, to a lesser extent, in 42 as well.

It is interesting to note that the dihedral angle,  $\phi$ , (and hence,  $\theta$ ) is not constant throughout the series (Table 4.2). In fact,  $\phi$  varies linearly with the  $\sigma^+$  value for the *para* substituent on the aryl ring ( $r = -0.991$ ) as illustrated by Figure 4.5. It is precisely because this relationship holds, that all other correlations of the various quantities with

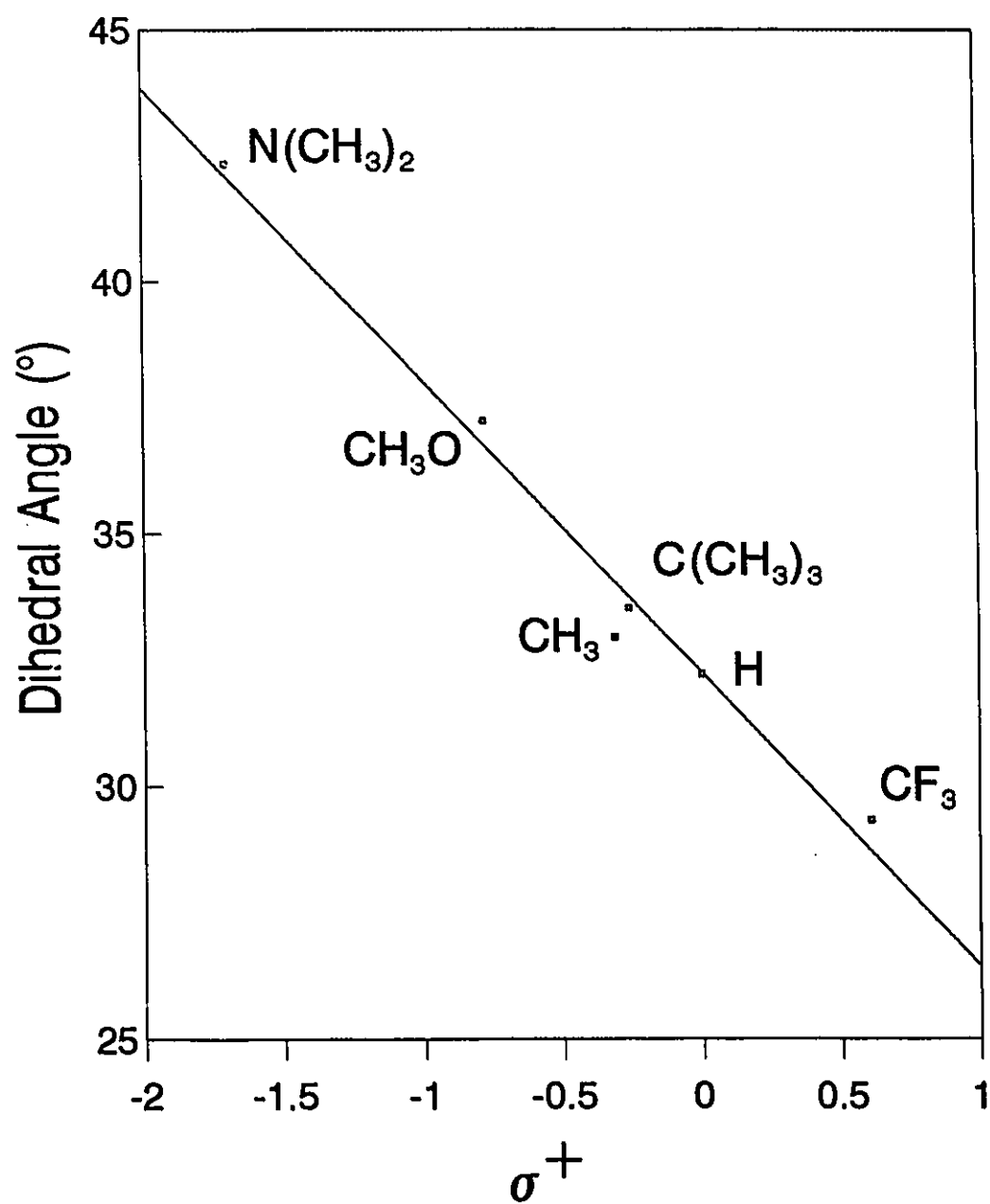


Fig. 4.5: Plot of O(3)-C(4)-C(1')-C(2') dihedral angles in 38-42 and 45 vs  $\sigma^+$ .



$\sigma^*$  were possible. Had  $\phi$  varied randomly, then a correction for this variable would be necessary in any attempted correlation with the substituent parameters.<sup>34a</sup> At any rate, the most favourable alignment of the aryl ring with respect to a potential conjugative interaction is achieved when the substituent is N,N-dimethylamino ( $\phi = 42.3^\circ$ ,  $\theta = 47.7^\circ$ ). Not coincidentally, this is the system best suited to take advantage of such an interaction.

## 4.2 Charge Distribution

The atomic charge densities for cations 38-42 and 45 are available from the AM1 optimized structures (Table 4.4). Like all calculated quantities, atomic charge densities are dependent upon the basis set used for the calculation, and so care should be taken not to ascribe too much importance to the individual values.<sup>102</sup> However, it is worthwhile to examine trends in charge density as a result of substitution across a series of compounds. When this is done, two important features emerge. First, as the *para* substituent on the phenyl ring is made more electron donating, the amount of positive charge residing on the O(1)-C(2)-O(3) fragment steadily decreases. This is in accord with the increasing importance of resonance structure 50, in which positive charge is syphoned away from the acetoxonium moiety.

Table 4.4 : Selected AM1 calculated charge densities for 38-42 and 45.

Atom	Compound					
	38	39	40	41	42	45
O(1)	-0.1447	-0.1485	-0.1496	-0.1497	-0.1512	-0.1557
C(2)	0.3781	0.3749	0.3740	0.3735	0.3736	0.3698
O(3)	-0.1562	-0.1555	-0.1561	-0.1562	-0.1578	-0.1617
C(4)	0.1170	0.1255	0.1295	0.1303	0.1378	0.1509
C(5)	-0.0514	-0.0517	-0.0514	-0.0516	-0.0516	-0.0511
C(6)	-0.2189	-0.2176	-0.2175	-0.2174	-0.2173	-0.2163

The other notable feature of the values presented in Table 4.4 is the response of the C(4) charge densities to substitution. Better electron donating groups on the aryl ring produce an increase in the amount of positive charge residing on the C(4) carbon atom. Again, this is consistent with an increasing contribution from 50 to the resonance description of these ions. The same trend was noted for the  $^{13}\text{C}$  chemical shifts of C(4) in the NMR spectra of these compounds (Chapter 2). Furthermore, the calculated charge densities at C(4) show a correlation ( $r = 0.975$ ) with the  $^{13}\text{C}$  chemical shifts at this site for which data could be collected (Fig. 4.6). This link between theory and experiment demonstrates that SCF-MO calculations at the AM1 level generally perform well in describing the response of the dioxolanylium ion to substitution.

Charge density at the C(5) carbon atom appears to be relatively insensitive to the nature of the aryl substituent, with the value remaining close to zero across the series. The values obtained for C(6) are more intriguing. A slight increase in positive charge density was observed with increasing electron donating capability of the aryl substituent,

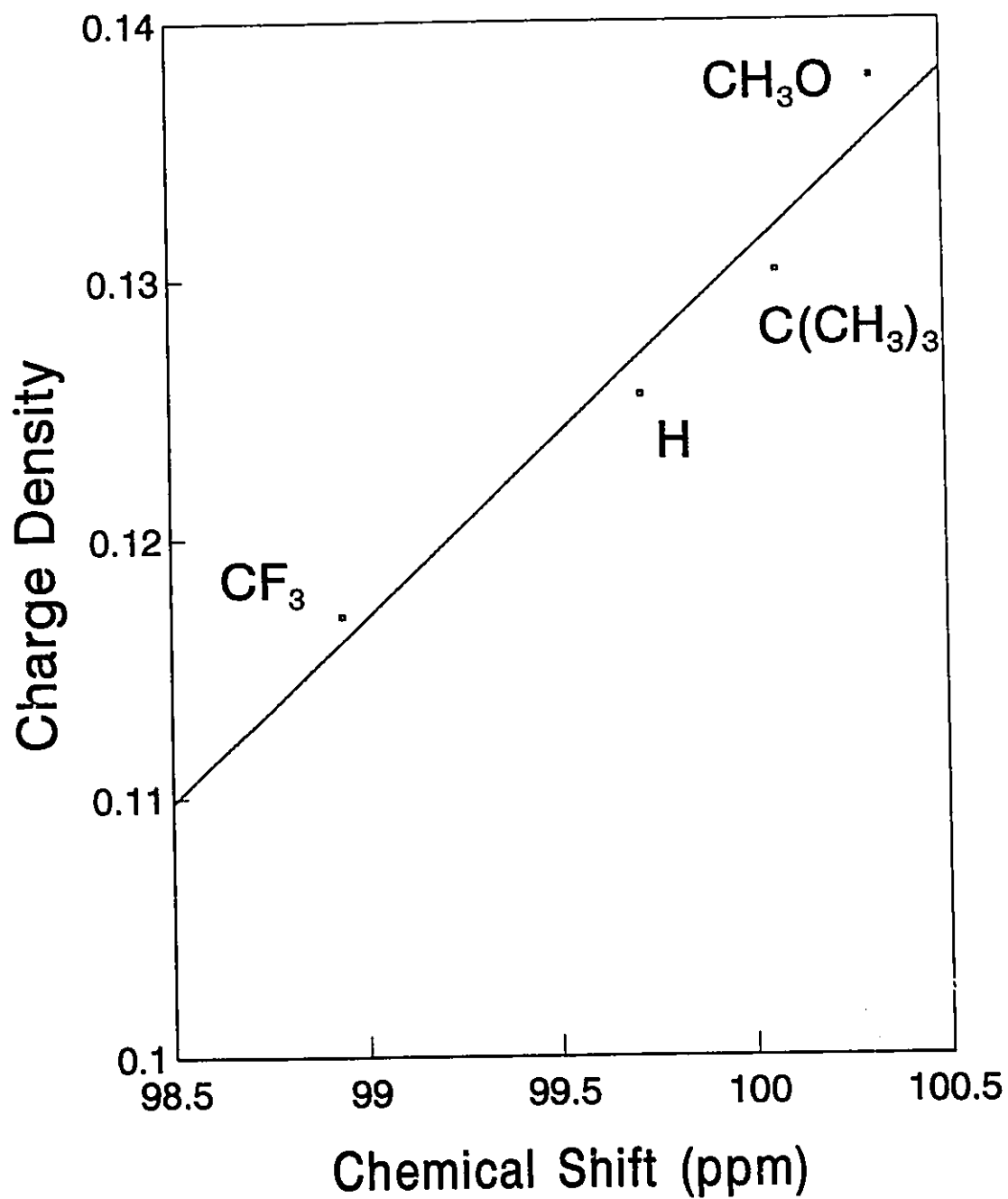


Fig. 4.6: Plot of calculated charge density vs. C(4) chemical shift for aryl dioxolanylium ions.

contrary to what would be expected based on the resonance description advanced in this thesis. However, no linear correlation of the C(6) charge densities could be found with any of the Hammett type substituent constants. In light of this, it would be difficult to assign much significance to this apparent trend.

#### 4.3 Modelling the Isomerization Reaction of the Aryl System

In addition to providing detailed structural information of the dioxolanylium ion ground state, SCF-MO calculations also provided a means to examine the reaction dynamics of the isomerization process. The reaction barrier can be calculated from the heat of formation of the ground state and that of the transition state model. Using this approach, both the concerted and step-wise mechanism could be modelled to determine which pathway was of lowest energy for each system. Comparison with the experimentally determined reaction barriers provides a means of deducing the mechanism of isomerization.

##### (a) The Step-Wise Pathway

A schematic representation of the reaction co-ordinate diagram for the step-wise isomerization mechanism is given in Figure 4.7. It resembles the typical two-stepped process for the intermolecular  $S_N1$  reaction. The first barrier is encountered as the O(3)-C(4) bond is ruptured to give the carbenium ion intermediate. The second barrier is traversed as the carbenium ion collapses with the acetate group to reform the

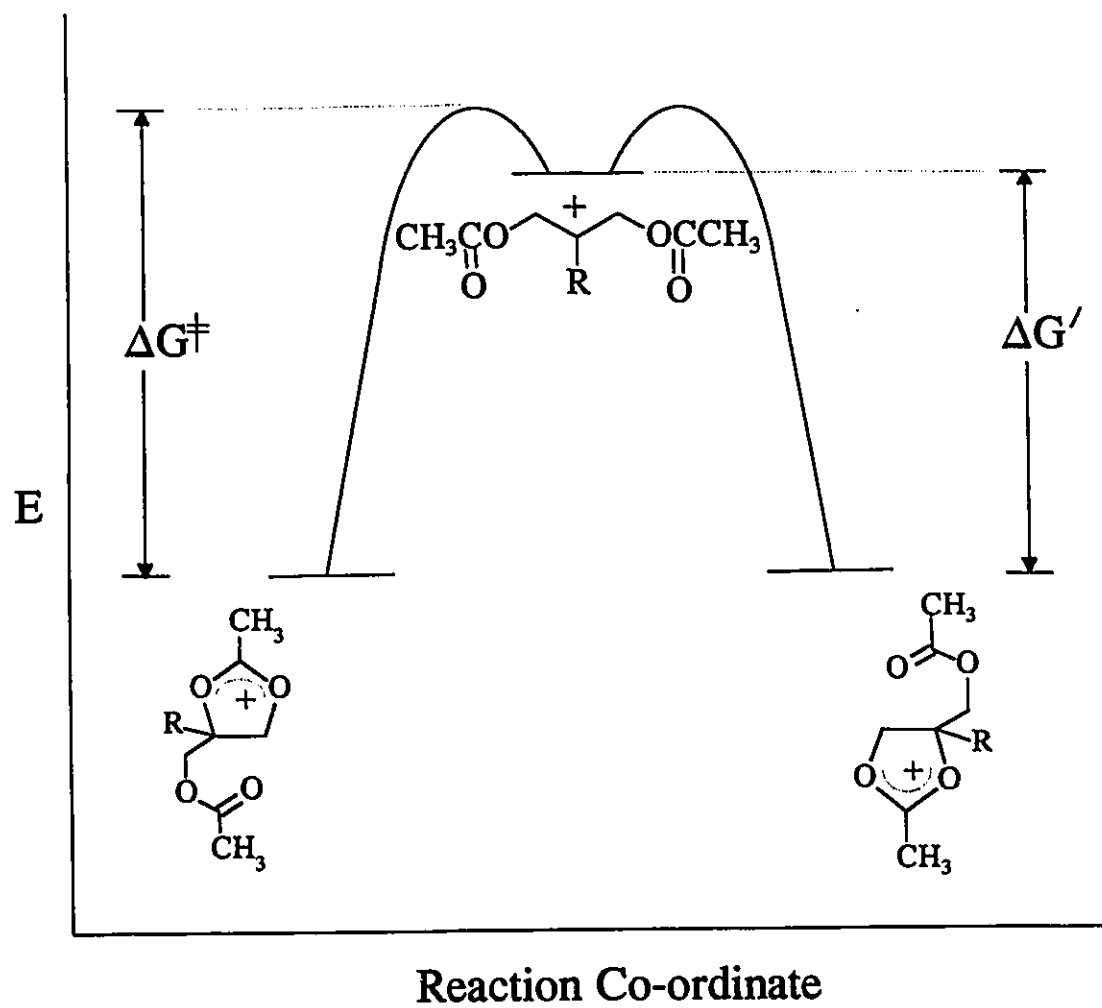


Fig. 4.7: Reaction co-ordinate diagram for step-wise isomerization.

dioxolanylium ion. Because the isomerization is a degenerate process, the carbenium ion intermediate is presented with identical reaction barriers for the forward and reverse processes.

In order to calculate the reaction barrier for this process, it is necessary to obtain the heat of formation of the transition state for the rate-determining step. This corresponds to a structure in which the O(3)-C(4) bond is partially broken. The determination of the point at which this bond stretching results in an energy maximum is a difficult and time-consuming process. However, because the rate determining O(3)-C(4) bond cleavage is endothermic, the transition state structure should resemble the carbenium ion intermediate. That is, the O(3)-C(4) bond is almost completely broken in the transition state. Consequently the electronic requirement of the transition state and that of the intermediate are similar. It was reasoned, therefore, that the structure of the intermediate represents a suitable approximation for the true transition state structure, at least for the purposes of the present study. This postulate has been a valuable tool in many investigations of solvolysis reactions.<sup>103</sup> This approach greatly simplified the calculation by substituting a simple energy minimization for a more complicated transition state structure determination.

The fully optimized geometries of the open carbenium ion intermediates, **52a-f**, in the absence of the counter ions, were determined. Selected bond lengths and bond angles are presented in Table 4.5. All the carbenium ions have similar structures and conformations, and **52b** provides a typical example (Fig. 4.8). The C(1)-C(2)-C(3)

system adopts a trigonal planar conformation which is coplanar with the phenyl ring. The ion is asymmetrical with respect to the two acetate side chains, with one ester adopting an *s-cis* conformation and the other an *s-trans* conformation. This arrangement presumably minimizes the steric interactions of the ester functions with each other and with the phenyl ring.

As the *para* substituent is made more electron-donating across the series, increased bond alternation is evident in the aryl rings of 52a-f. This is consistent with increased charge delocalization into the aryl ring. The observation of this trend is facilitated by comparison with the aryl bond lengths in the neutral ester system (Table 4.3) which exhibit much less differentiation.

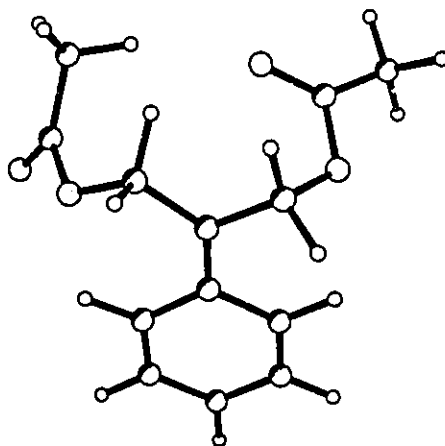
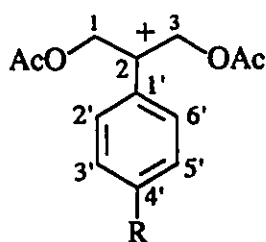


Fig. 4.8: AM1 optimized geometry of 52b.

Table 4.5: Selected bond lengths (Å) and bond angles (°) for the AM1 optimized geometries of carbenium ions 52a-f.

Bond	Compound					
	52a	52b	52c	52d	52e	52f
C(1')-C(2')	1.438	1.442	1.444	1.442	1.449	1.451
C(2')-C(3')	1.380	1.377	1.372	1.373	1.363	1.356
C(3')-C(4')	1.404	1.408	1.416	1.417	1.433	1.453
C(4')-C(5')	1.395	1.398	1.408	1.412	1.420	1.452
C(5')-C(6')	1.390	1.384	1.378	1.377	1.370	1.357
C(6')-C(1')	1.431	1.436	1.439	1.438	1.445	1.449
C(2)-C(1')	1.396	1.388	1.383	1.382	1.376	1.367
C(4')-R	1.541	1.105	1.472	1.502	1.339	1.345
Bond Angle						
C(1)C(2)C(3)	111.44	111.50	111.42	111.82	111.54	111.98
C(1)C(2)C(1')	127.81	127.54	127.46	127.14	127.40	126.72
C(3)C(2)C(1')	120.68	120.90	121.06	120.95	120.99	121.22
C(3)C(2)C(1')C(2')	4.95	6.00	5.66	6.85	6.29	6.42



- (a) R = CF<sub>3</sub>    (d) R = C(CH<sub>3</sub>)<sub>3</sub>  
 (b) R = H        (e) R = OCH<sub>3</sub>  
 (c) R = CH<sub>3</sub>    (f) R = N(CH<sub>3</sub>)<sub>2</sub>

Further evidence for this is provided by the calculated charge densities of the carbenium ions 52a-f (Table 4.6). The amount of positive charge residing on C(2) is diminished as the charge stabilizing power of the aryl substituent is increased. A similar trend was reported by Olah and co-workers who calculated charge distributions in the



PM1 approximation for a series of benzylic cations.<sup>104</sup>

Table 4.6: Selected AM1 calculated charge densities for 52a-f.

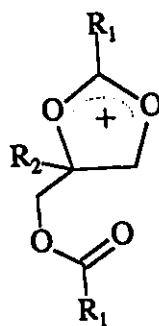
Atom	Compound					
	52a	52b	52c	52d	52e	52f
C(1)	-0.0483	-0.0428	-0.0394	-0.0387	-0.0319	-0.0219
C(2)	0.1956	0.1667	0.1427	0.1412	0.1031	0.0445
C(3)	-0.0469	-0.0427	-0.0372	-0.0372	-0.0302	-0.0193
C(1')	-0.1664	-0.1683	-0.1649	-0.1628	-0.1654	-0.1382

From the heat of formation of the carbenium ions and the corresponding dioxolanylium ions, the values of  $\Delta G'$  listed in Table 4.7 were obtained. It should be noted that the barrier calculated in this way is not a true reaction barrier, but rather represents the enthalpy of reaction for the first step of the isomerization. Explicitly, this quantity is equal to the difference between the heat of formation between the dioxolanylium ion ground state and that of the carbenium ion intermediate. This energy difference is labelled  $\Delta G'$  in Figure 4.7. An important consequence of this is that the calculated value will likely be of lower magnitude than the actual reaction barrier,  $\Delta G^\ddagger$ . For ease of comparison, the experimental values of  $\Delta G^\ddagger$ , where available, are also given in Table 4.7.

As expected from the above considerations, the calculated values of  $\Delta G'$  are indeed lower than the experimentally determined values of  $\Delta G^\ddagger$ . Taking this into

Table 4.7 Calculated Isomerization Barriers

Substituents		Compound	Calculated Barrier, $\Delta G'$		$\Delta G^\ddagger$
R1	R2		Step-wise	Concerted	
CH <sub>3</sub>	<i>p</i> -CF <sub>3</sub> C <sub>6</sub> H <sub>4</sub>	38	19.1		(20.3)
CH <sub>3</sub>	C <sub>6</sub> H <sub>5</sub>	39	14.2		16.4
CH <sub>3</sub>	<i>p</i> -CH <sub>3</sub> C <sub>6</sub> H <sub>4</sub>	40	11.2		15.4
CH <sub>3</sub>	<i>p</i> -C(CH <sub>3</sub> ) <sub>3</sub> C <sub>6</sub> H <sub>4</sub>	41	11.1		15.6
CH <sub>3</sub>	<i>p</i> -CH <sub>3</sub> OC <sub>6</sub> H <sub>4</sub>	42	5.8	17.7	10.9
CH <sub>3</sub>	<i>p</i> -N(CH <sub>3</sub> ) <sub>2</sub> C <sub>6</sub> H <sub>4</sub>	45	-2.2		
CH <sub>3</sub>	H	36	50.7	23.0	18.7
CH <sub>3</sub>	CH <sub>3</sub>	37	36.5	24.3	21.0
CF <sub>3</sub>	H	57	32.1	17.5	
CF <sub>3</sub>	CH <sub>3</sub>	58	20.3	19.4	



account, there exists a reasonable correspondence between the experimental and theoretical values. While there exists some discrepancy between the individual values of  $\Delta G'$  and  $\Delta G^\ddagger$ , the calculated values as a whole reproduce the dependence of the isomerization barrier on the aryl substituent. A linear correlation exists ( $r = 0.967$ ) between the experimental and calculated reaction barriers (Fig. 4.9). This demonstrates that the model successfully describes the response of the system to substitution even though it may be less accurate in absolute terms.

Having established the reliability of the theoretical model, it was used to extend the study of substituent effects to compounds which could not be obtained experimentally. The results of Chapter 2 suggested that for 45, in which the *para* substituent on the aryl ring is an N,N-dimethylamino group, the barrier to isomerization would be extremely low. This prediction was tested further by modelling the step-wise reaction for this compound. The negative value of  $\Delta G'$  indicates that the open carbenium ion is more stable than the corresponding dioxolanylium ion. Allowing for the difference between  $\Delta G'$  and  $\Delta G^\ddagger$ , this is in support of the value of  $\Delta G^\ddagger$  obtained from the extrapolation of the experimental results.

#### (b) The Concerted Pathway

The concerted pathway for the dioxolanylium ion isomerization is also amenable to study by the semi-empirical method. The reaction co-ordinate diagram for this process, shown in Figure 4.10, resembles that of the analogous intermolecular  $S_N2$

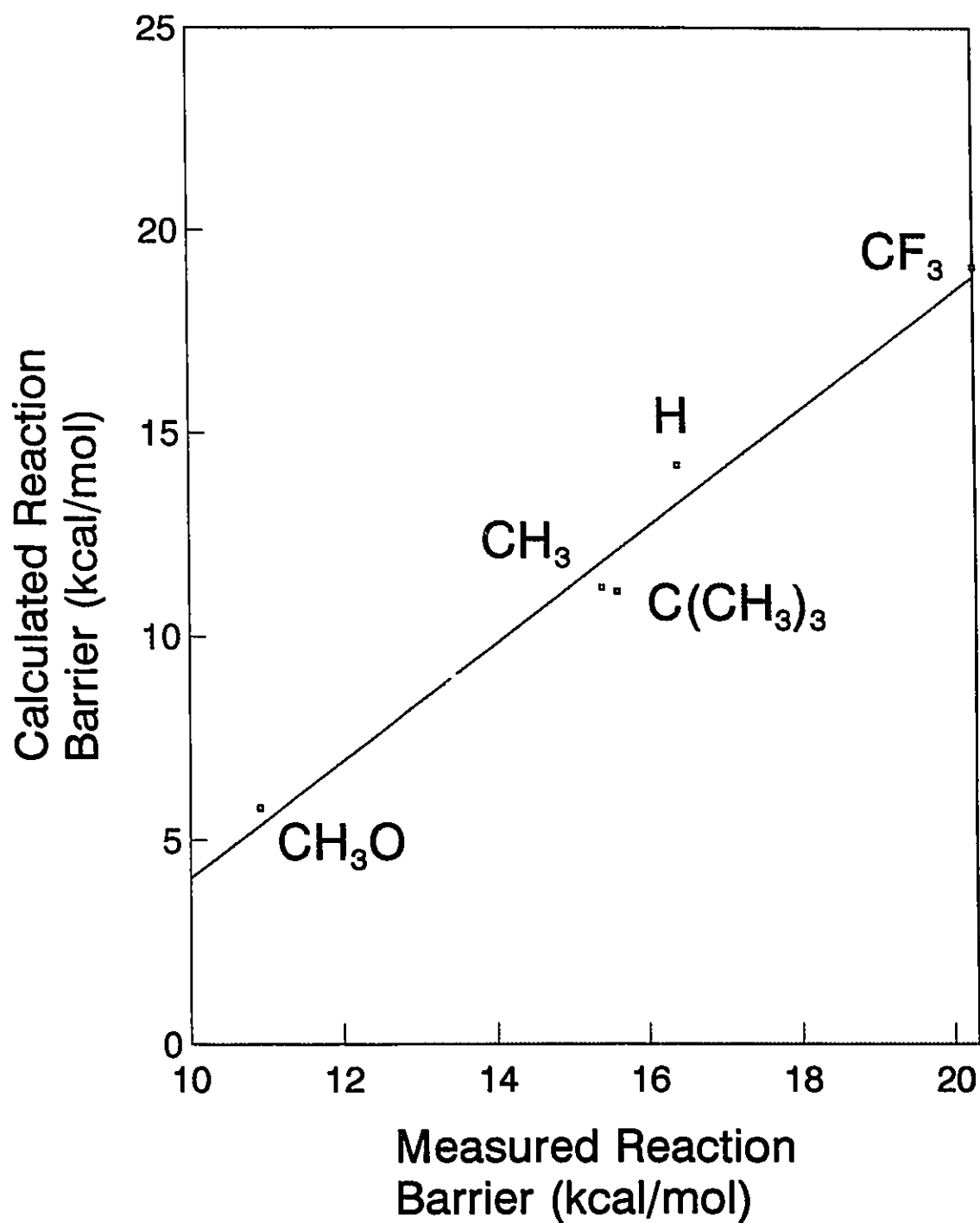


Fig. 4.9: Plot of calculated vs. experimental reaction barriers for aryl dioxolanylium ion isomerization

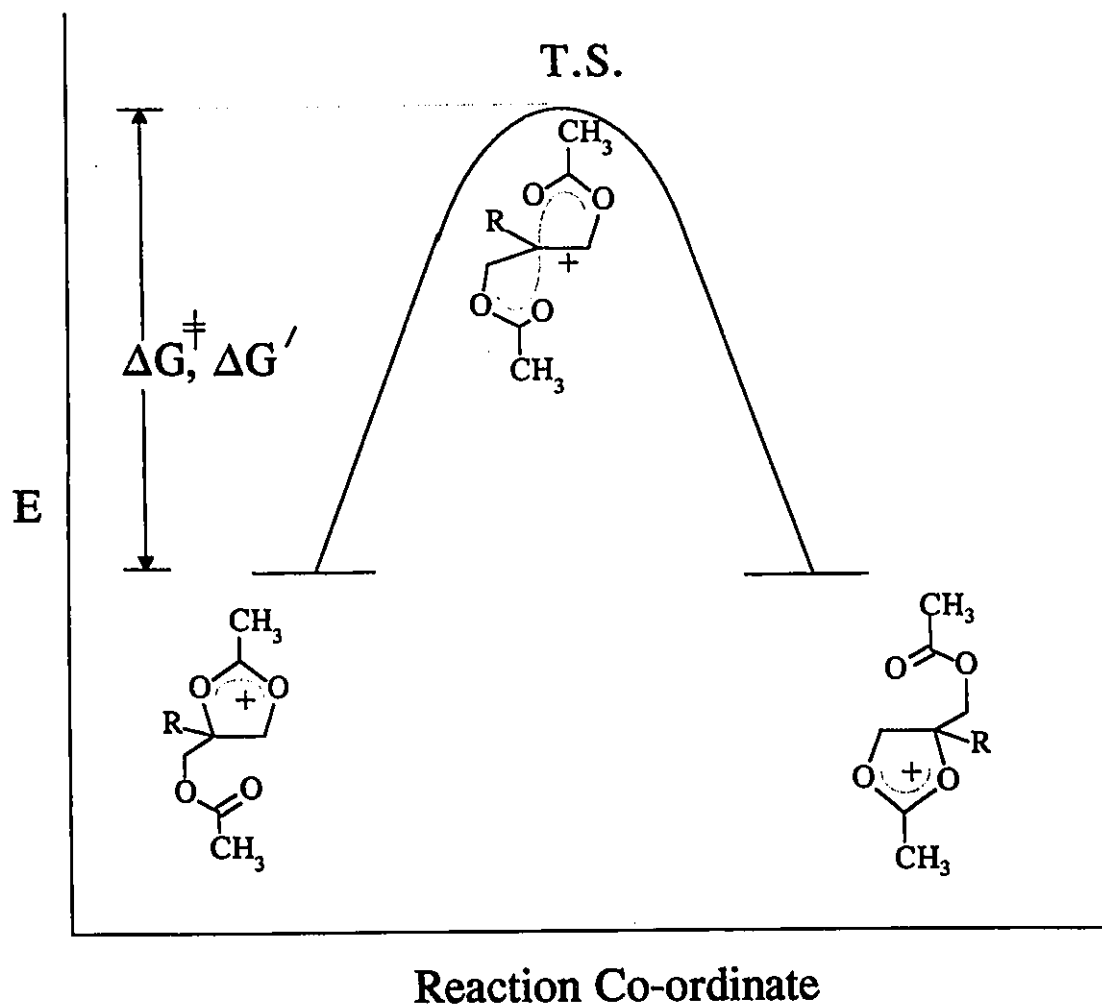


Fig. 4.10: Reaction co-ordinate diagram for concerted isomerization.

reaction. Only a single reaction barrier is traversed in this pathway.

The structure of the transition state was assumed to be symmetrical. That is, a trigonal bi-pyramidal arrangement about the C(4) carbon atom is adopted with the nucleophilic carbonyl oxygen and the departing carbonyl oxygen equidistant from the displacement center. The result is the symmetrical curve depicted in Figure 4.10 wherein the transition state is reached at exactly the mid-way point along the reaction co-ordinate. While it is commonplace to make this assumption for degenerate reactions such as this one,<sup>105</sup> its validity has recently been challenged on theoretical grounds.<sup>106</sup> However, no experimental evidence is available to support the existence of an asymmetrical transition state for a degenerate rearrangement.

The acceptance of a symmetrical transition state provides an important practical benefit. The transition state may be located by a partially constrained geometry optimization. Thus, as was the case for the step-wise pathway, a simple minimization is substituted for a more difficult calculation. The reaction barrier for the concerted pathway model is defined as the difference in the heat of formation of the transition state structure and that of the ground state. This quantity is labelled  $\Delta G'$  in Figure 4.10.

Using this procedure, the concerted pathway was modelled for 42 in which the *para* substituent on the aryl ring is a methoxy group. The resulting value of  $\Delta G'$  was found to be 17.7 kcal/mol (Table 4.7). This reaction barrier far exceeds the calculated barrier for the step-wise pathway (5.8 kcal/mol). This is in support of the Hammett study (Chapter 2) which demonstrated that the stepwise pathway is preferred for the aryl-

substituted dioxolanylium ion isomerization.

#### 4.4 Modelling the Isomerization Barrier of the Non-aryl system

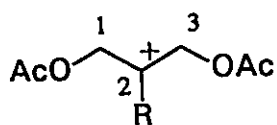
The methodology developed to model the isomerization of the aryl system was also applied to the reaction of the C(4)-hydrogen and C(4)-methyl substituted dioxolanylium ions, **36** and **37**. The aim of this study was to determine whether the step-wise or concerted isomerization pathway is favoured by comparing the calculated and experimentally determined reaction barriers.

##### (a) Step-Wise Pathway

The open carbenium ion intermediates **53** and **54** were used to approximate the transition states for the step-wise isomerizations of **36** and **37** respectively. The bond angles (Table 4.8) of the carbenium ions are consistent with charge localization on an sp<sup>2</sup>-hybridized C(2) carbon atom. In **53** the carbon/oxygen skeleton is planar with one ester function adopting an *s-cis* orientation and the other *s-trans* (Fig. 4.11). A similar conformation was determined for **54**.

Table 4.8: Selected bond angles ( $^{\circ}$ ) for the AM1 optimized geometries of carbenium ions 53 and 54.

Bond Angle	53	54
C(1)C(2)C(3)	121.61	118.64
C(1)C(2)R	119.08	120.25
C(3)C(2)R	119.31	121.11



53 R = H

54 R = CH<sub>3</sub>

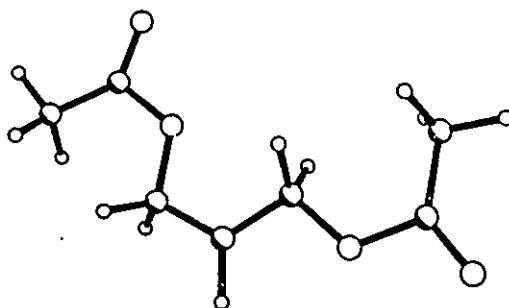


Fig. 4.11: AM1 optimized geometry of 53.

From the heats of formation of carbenium ions 53 and 54 and the corresponding dioxolanylium ions (36 and 37), the barriers for the step-wise isomerization pathways were calculated (Table 4.7). The step-wise barrier for 36 is exceptionally high (50.7 kcal/mol). The replacement of the hydrogen atom at C(4) for a methyl substituent on going from 36 to 37, lowers the step-wise barrier by about 14 kcal/mol. This value



compares well with that reported by Arnett,<sup>107</sup> who has measured the difference in the enthalpies of ionization of *t*-butyl chloride and 2-chloropropane to be  $15.8 \pm 1.4$  kcal/mol.

(b) Concerted Pathway

It was again useful to assume symmetrical transition state geometries, 55 and 56, for the concerted isomerizations of 36 and 37 respectively. Selected interatomic distances and bond angles for 55 and 56 obtained by partially constrained geometry optimization are presented in Table 4.9. The geometry about the C(4) carbon atom in 55 is trigonal bipyramidal (Fig. 4.12). A similar conformation was calculated for 56. A tighter transition state was observed in 55 in which the O(3)-C(4)/O(10)-C(4) distances are 1.898 Å compared to 1.946 Å in 56. Presumably, this is a result of an unfavourable steric interaction in 56, in which the presence of the methyl group at C(4) prevents a closer association of the nucleophile and the leaving group with the displacement center.

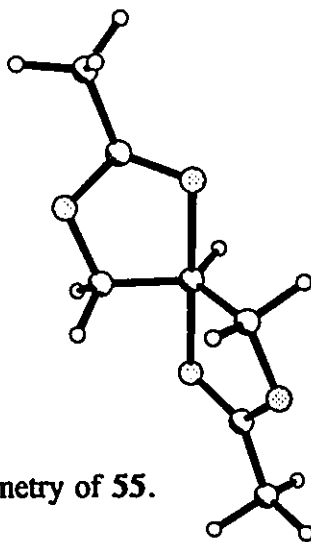
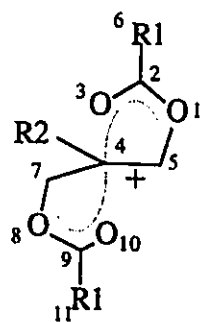


Fig. 4.12: AM1 optimized geometry of 55.

Table 4.9: Selected AM1 optimized bond lengths (Å) for the concerted transition state structures 55, 56, 61 and 62.

Bond	55	56	61	62
O(1)C(2)	1.355	1.357	1.343	1.344
C(2)O(3)	1.263	1.259	1.252	1.248
O(3)C(4)	1.898	1.946	1.940	1.986
C(4)C(5)	1.518	1.516	1.514	1.516
O(1)C(5)	1.441	1.439	1.448	1.446
C(2)C(6)	1.476	1.477	1.566	1.565
C(4)C(7)	1.518	1.516	1.514	1.514
C(7)O(8)	1.441	1.440	1.447	1.446
O(8)C(9)	1.355	1.358	1.343	1.346
C(9)C(11)	1.476	1.477	1.566	1.565
C(9)O(10)	1.263	1.259	1.252	1.248
C(4)O(10)	1.898	1.946	1.940	1.986
C(4)R2	1.110	1.497	1.111	1.490



	R1	R2
55	CH <sub>3</sub>	H
56	CH <sub>3</sub>	CH <sub>3</sub>
61	CF <sub>3</sub>	H
62	CF <sub>3</sub>	CH <sub>3</sub>

From the heats of formation of transition states 55 and 56 and the corresponding ground states (36 and 37), the reaction barriers for the concerted isomerizations of 36 and 37 were calculated (Table 4.7). Replacement of the hydrogen atom at the C(4) carbon atom for a methyl group raised the reaction barrier by 1.3 kcal/mol. This is

attributed once again to the increased steric requirements for nucleophilic displacement occurring at the 3° C(4) carbon atom in 37.

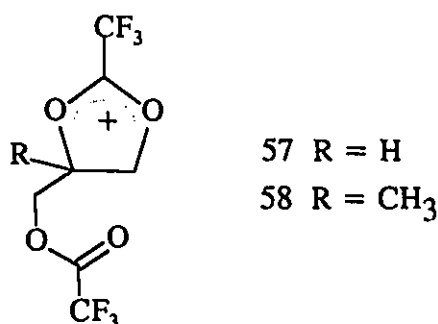
The barriers to isomerization of 36 and 37 in the concerted pathway are substantially lower in energy than those encountered in the step-wise pathway (Table 4.7). Thus, the concerted mechanism should be the preferred mode of reaction for these systems. In addition, there is a good correspondence between the calculated concerted barriers and the experimentally determined values of  $\Delta G^\ddagger$ . On the basis of these observations, it can be concluded that the isomerizations of 36 and 37 occur via the concerted pathway.

#### 4.5 Effect of the Trifluoroacetate Group

The discussion to this point regarding the reduction of the dioxolanylium ion isomerization barrier, has focused on the stabilization of the transition state by introducing electron donating substituents at C(4). Charge releasing substituents at C(4) stabilize the step-wise transition state and carbenium ion intermediate. For the concerted transition state, however, the stabilization achieved by the introduction of a charge releasing substituent at C(4) is balanced against increased steric crowding at the displacement site.

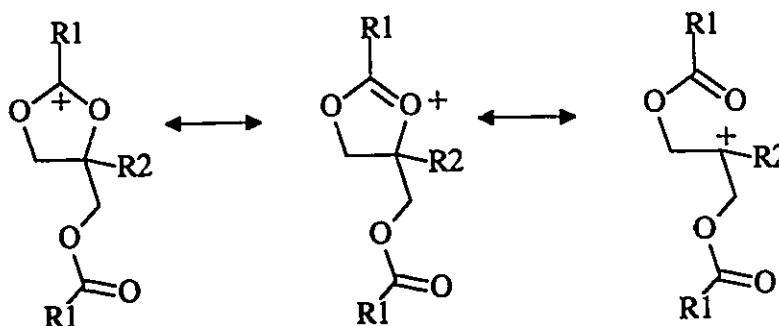
An alternative approach to reducing the reaction barrier is the destabilization of the ground state. The most direct approach to destabilizing the dioxolanylium ion system is to introduce a charge withdrawing substituent at C(2). The trifluoromethyl group was chosen for this study since it is one of the most powerful electron withdrawing

substituents known. Using **57** and **58** as model compounds, the feasibility of this approach to lowering the reaction barrier was tested. Both the acetate and acetoxonium methyl groups were replaced with  $\text{CF}_3$  groups to retain the degeneracy of the isomerization. The effect of  $\text{CF}_3$  substituents was probed both in the ground state structures and in the isomerization reactions.



(a) Ground State Structure

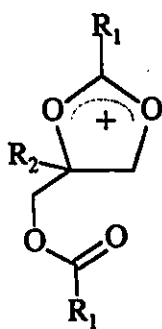
The effect of the  $\text{CF}_3$  groups and the C(4) substituent on the ground state structure of the dioxolanylium ion is readily observable. Calculated bond lengths in the optimized geometries for **36**, **37**, **57**, and **58** are compared in Table 4.10. Similar to the trend observed for the C(4)-aryl substituted series, replacement of the hydrogen atom for a methyl group at C(4) resulted in consistent changes in various bond lengths within the dioxolanylium ring system. An elongation of the O(3)-C(4) bond and contraction of the C(2)-O(3) bond was noted on going from **36** to **37** and from **57** to **58**. Once again, this is attributed to the increased importance of an ionic resonance contributor (Scheme 4.4), due to the inductive stabilization provided by the methyl group.



Scheme 4.4

Table 4.10 Selected AM1 optimized bond lengths (Å) for 36, 37, 57 and 58.

Bond	36	37	57	58
O(1)C(2)	1.332	1.333	1.314	1.317
C(2)O(3)	1.325	1.320	1.314	1.308
O(3)C(4)	1.482	1.496	1.500	1.528
C(4)C(5)	1.534	1.542	1.536	1.539
O(1)C(5)	1.473	1.468	1.484	1.480
C(2)C(6)	1.467	1.469	1.581	1.579
C(4)C(7)	1.528	1.533	1.523	1.536
C(7)O(8)	1.418	1.418	1.425	1.423
O(8)C(9)	1.384	1.383	1.368	1.373
C(9)C(11)	1.483	1.484	1.562	1.559
C(9)O(10)	1.235	1.232	1.225	1.220



	R1	R2
36	CH <sub>3</sub>	H
37	CH <sub>3</sub>	CH <sub>3</sub>
57	CF <sub>3</sub>	H
58	CF <sub>3</sub>	CH <sub>3</sub>

The effect of the  $\text{CF}_3$  group can be assessed by the comparison of the structures of 36 to 57, as well as, 37 to 58. For each pair of dioxolanylium ions, the presence of the trifluoromethyl substituent produces an elongation of the  $\text{O}(3)\text{-C}(4)$  bond relative to the acetate derivative. The more open-like structure for the trifluoromethyl derivatives is a direct result of the destabilization of the positive charge at  $\text{C}(2)$ .

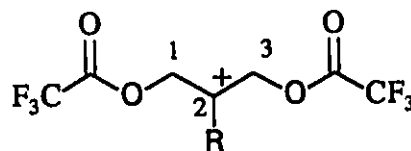
(b) Modelling the Isomerization Barriers for Trifluoroacetate Derivatives

(i) Step-wise pathway

The open carbenium ions 59 and 60 were used to approximate the transition states for the step-wise isomerization of dioxolanylium ions 57 and 58 respectively. The optimized structures of these ions are similar to those obtained for the methyl analogues 53 and 54 discussed earlier. The bond angles are consistent with a trigonal planar carbenium ion (Table 4.11).

Table 4.11: Selected bond angles ( $^\circ$ ) for the AM1 optimized geometries of carbenium ions 59 and 60.

Bond Angle	59	60
$\text{C}(1)\text{C}(2)\text{C}(3)$	122.10	118.79
$\text{C}(1)\text{C}(2)\text{R}$	119.34	121.45
$\text{C}(3)\text{C}(2)\text{R}$	118.56	119.76

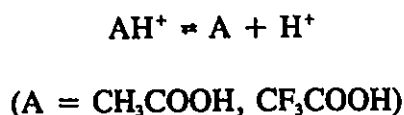


59 R = H

60 R =  $\text{CH}_3$

The reaction barriers for the isomerization of **57** and **58** via the step-wise pathway were calculated using the method previously described. The step-wise isomerization barriers,  $\Delta G'$ , are substantially lower than those of the methyl-substituted analogues **36** and **37** (Table 4.7). The presence of the  $\text{CF}_3$  groups lowered the barriers by 16-18 kcal/mol. This difference compares well with that reported for the relative proton affinities of acetic acid and trifluoroacetic acid (15.4 kcal/mol),<sup>108</sup> where proton affinity is defined as the heat of reaction of Eqn 4.3:

Eqn. 4.3



Dissociation of  $\text{AH}^+$  is analogous to unassisted C-O bond cleavage of the dioxolanylium ions.

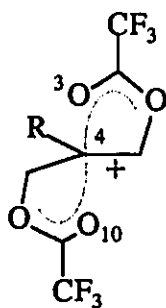
The observation of the above substituent effect is indicative of the destabilization brought about by placing a  $\text{CF}_3$  group adjacent to a positive charge.<sup>109</sup> However, neither the values for proton affinities nor  $\Delta G'$  should be confused for absolute measurements of the destabilization brought about by the  $\text{CF}_3$  group. Both these quantities reflect a substituent effect in a "reactant" relative to a "product". An absolute value for the destabilization of cationic center brought about by an adjacent  $\text{CF}_3$  group has been arrived at by *ab initio* calculations of isodesmic reactions. Carbenium ions and hydroxycarbenium ions are destabilized by  $\alpha\text{-CF}_3$  groups by 37 kcal/mol and 36 kcal/mol respectively.<sup>110</sup> The fact that the value of  $\Delta G'$  is lowered by only 16-18 kcal/mol for the

trifluoroacetate derivatives suggests that the transition states are destabilized as well. The net effect, however, is a lowering of the reaction barrier.

The lower barrier for the isomerization of **58** relative to that of **57** can again be attributed to the greater stability of the tertiary carbenium ion intermediate (and of the transition state) encountered in the isomerization of the former compound. It is not surprising therefore, that the difference between  $\Delta G'$  of **36** and **37** is similar in magnitude to the difference between that of **57** and **58**.

(ii) Concerted Pathway

The transition states for the concerted isomerizations of **57** and **58** are represented by **61** and **62** respectively, and were obtained by partially constrained geometry optimizations as previously described. The trigonal bi-pyramidal structure of **61** exhibits shorter O(3)-C(4)/O(10)-C(4) bond distances than does **62** (Table 4.9). As was the case for the acetate analogues **55** and **56**, the tighter transition state for **61** is attributed to less steric crowding at the displacement center than is encountered in **62**.



**61** R = H

**62** R = CH<sub>3</sub>



A further comparison may be made between the transition state structures of the acetate and the trifluoroacetate systems. The O(3)-C(4)/O(10)-C(4)) bond distances in **61** (1.940 Å) are longer than in **55** (1.898 Å). Similarly, these C-O bonds are longer in **62** than in **56**. Thus, looser transition states were found for the trifluoroacetate derivatives which minimize inductive destabilization of the charge at the C(2) and C(9) carbon atoms.

The effect of replacing the hydrogen atom at C(4) in **57** with a methyl group (**58**) results in a small increase in the concerted reaction barrier. This effect was also observed in the acetate systems **36** and **37**. The barriers to concerted isomerization of **57** and **58** are lower than the corresponding values of  $\Delta G'$  for **36** and **37** (Table 4.7). However, the effect of the CF<sub>3</sub> groups on the concerted barrier is not nearly as pronounced as it is in the step-wise pathway. The destabilizing effect of the CF<sub>3</sub> group in the ground state is offset by substantial destabilization of the transition state. The net effect is only a relatively small reduction in the concerted barrier.

The use of trifluoroacetate derivatives yields a reduction in the barrier to the dioxolanylium isomerization. In theory, this approach provides a means of obtaining a system whose ground state structure resembles a classical S<sub>N</sub>2 transition state. In practice, however, this cannot be considered an effective means of doing so. Decreasing the stability of the dioxolanylium ion increases the difficulty of its isolation. Despite the synthetic challenges, the use of electron releasing substituents attached to the C(4) carbon atom (the transition state stabilization approach) remains as the only viable option.

#### 4.6 Comparison of X-ray Crystal Structures with AM1-Optimized Geometries

In Chapter 3, the results of the x-ray crystallographic study of dioxolanylium ions 36 and 39 (in which the C(4) substituent is hydrogen and phenyl respectively) were presented. There are substantial differences between the bond lengths determined experimentally with those calculated at the AM1 level. However, the use of semi-empirical calculations has provided useful insight into the nature of dioxolanylium ions. While there exists some discrepancy between the optimized structures obtained at this level of theory and those obtained by experimental methods, the value of this approach was demonstrated by examining a given trend across a series of ions. In so doing, systematic errors arising from various approximations effectively cancelled out. Thus while the structure of a particular dioxolanylium ion may not be reproduced satisfactorily, the response of that ion to substitution was successfully modelled. This is particularly true for the modelling of the isomerization barriers which were in good agreement with the experimentally determined values.

#### 4.7 Summary

The isomerization mechanisms proposed for the aryl and non-aryl substituted dioxolanylium ions on the basis of the dynamic NMR studies, were confirmed by modelling these reactions at the AM1 level. Systematic structural variations within the aryl series of dioxolanylium ions were correlated with Hammett substituent constants. These structural variations provided further support for the inclusion of an ionic

resonance contributor to the ground state description of this system. Introducing better electron donating substituents at C(4) systematically increased the weight given to this ionic resonance contributor.

## General Summary

The role played by substituents in determining the structure and reactivity of the 1,3-dioxolan-2-ylum ion system has been presented in this thesis. Using a variety of complementary techniques, it was shown that an ionic resonance contributor should be included in the ground state description of the system. The weight given to this ionic resonance contributor is dependent upon the electron-donating power of the C(4)-substituent. The C(4)-substituent also plays an important role in determining the mechanism and ease of nucleophilic attack on the 1,3-dioxolan-2-ylum ion.

It has been demonstrated that the use of aryl substituents at C(4) represents one strategy by which an S<sub>N</sub>2 transition state-like structure might be obtained. In addition, the Lewis acid complexes described in this thesis show particular promise in achieving such a structure. It is suggested that future investigations explore the use of other hetero atoms (such as sulfur or nitrogen), by incorporating functionality which places these charge stabilizing groups adjacent to the C(4) carbon atom.

The use of AM1 calculations proved to be an effective tool in determining the effect of substituents on the structure and reactivity of the 1,3-dioxolan-2-ylum ion system. To date, no *ab initio* studies have been carried out on this system. It would be of interest to investigate the system further at a higher level of theory. It is hoped that the calculated and experimentally determined structures might show a closer correspondence than can be achieved using semi-empirical methods.

## Chapter 5

### Experimental

#### 5.1 Materials

Diethyl ether was refluxed over  $\text{LiAlH}_4$  and distilled under a dry nitrogen atmosphere. Similarly, dioxane and benzene were distilled from sodium,  $\text{CH}_2\text{Cl}_2$  and  $\text{CCl}_4$  from  $\text{P}_2\text{O}_5$ . Toluene was washed with concentrated  $\text{H}_2\text{SO}_4$  and distilled. When not used immediately, dry solvents were stored in a glove bag which was continuously purged with nitrogen in the presence of  $\text{P}_2\text{O}_5$ . Deuterated solvents for use in NMR experiments were used without further purification. The Lewis acids  $\text{SnCl}_4$  and  $\text{SbCl}_5$  were distilled prior to use while 1.0 M  $\text{SbCl}_5$  in  $\text{CH}_2\text{Cl}_2$  (Aldrich) was used without further purification.

#### 5.2 Instrumentation

##### (a) NMR Spectroscopy

$^1\text{H}$  NMR spectra were collected using a Varian EM390 (90 MHz), Bruker AM200 (200 MHz), Bruker WM250 (250 MHz), Bruker AM300 (300 MHz), or Bruker AM500 (500 MHz) spectrometers. Spectra collected in deuterated solvents were referenced using the residual proton signals. Tetramethylsilane (TMS) was used as an internal reference for spectra collected in  $\text{CCl}_4$ . Solution  $^{13}\text{C}$  NMR spectra were collected on a Bruker AM500 (125.7 MHz), Bruker AM300 (75.1 MHz), or Bruker AM200 (50.3 MHz)

spectrometers. Solid state  $^{13}\text{C}$  NMR spectra were obtained by the cross polarization magic angle spinning (CPMAS) technique on a Bruker MSL100 (25.1 MHz) spectrometer at room temperature. Samples were mixed with KBr and packed in alumina rotors under a dry nitrogen atmosphere. Adamantane was used as an external reference.

(b) X-ray Crystallography

(i) Data Collection and Reduction

Crystals of **36** and **39** were obtained by vapour diffusion of diethyl ether into  $\text{CH}_2\text{Cl}_2$  solutions of the respective compounds at  $-20^\circ\text{C}$ . Suitable crystals were selected and sealed in Lindemann capillaries under a nitrogen atmosphere. Diffraction experiments were performed at low temperature on a Siemens R3m/V diffractometer for **36** (173 K) using  $\text{AgK}\alpha$  ( $\lambda = 0.56086 \text{ \AA}$ ) and a Nicolet P3 diffractometer for **39** (173 K) using  $\text{MoK}\alpha$  ( $\lambda = 0.71069 \text{ \AA}$ ). The initial orientation matrices were obtained from 25 machine centred reflections for **36** ( $17.3^\circ < 2\theta < 37.6^\circ$ ) and 15 machine centred reflections for **39** ( $20.61^\circ < 2\theta < 26.77^\circ$ ). For **36**, c-centred h,k,  $\pm 1$  data ( $2\theta \leq 50^\circ$ ) were collected, while h,k,  $\pm 1$  data ( $2\theta \leq 45^\circ$ ) were collected for **39**. In each case, standard reflections were monitored and showed no statistically significant change during data collection. For **36**, data were collected with a scan range of  $0.6^\circ$  below  $\text{K}\alpha_1$  and  $0.6^\circ$  above  $\text{K}\alpha_2$ . For **39**, data were collected with a scan range of  $1.0^\circ$  below  $\text{K}\alpha_1$  and  $1.0^\circ$  above  $\text{K}\alpha_2$ . The background scan time was 50% of the total scan time for both **36** and

39. Corrections were made for Lorentz-polarization factors for all data. Semi-empirical absorption corrections were applied to the data for 39 and DIFABS<sup>III</sup> for 36.

(ii) Structure Solution and Refinement

The observed extinctions were consistent with the monoclinic space group  $C2/m$  for 36 and the orthorhombic space group  $P2_12_12_1$  for 39. The coordinates of the antimony atoms were found from three dimensional Patterson syntheses for 36 and 39. Full-matrix least-squares refinements of these coordinates, followed by a three dimensional electron density synthesis, in each case, revealed the positional parameters of all the non-hydrogen atoms and confirmed those of the heavy atoms.

A packing disorder was observed for 36. It was later determined that the proper space group for 36 was  $P2_1/a$ , using the same cell. This gave a completely ordered, well-behaved refinement. Since the original crystal had decayed with time, and another non-twinned crystal could not be found, the refinement was completed using only the  $h+k = 2n$  data. The only problem that resulted from the absence of the weak  $h+k = 2n+1$  data was that the two antimony atoms in the model could not be refined anisotropically. This would result in a divergence of the least-squares refinement. The results obtained from the partial data set were suitable for the purposes of the present investigation.

The refinements were carried out using full-matrix least-squares. The temperature factors of the non-hydrogen atoms, which were previously isotropic, were made

anisotropic, and further cycles of refinement revealed the positional parameters of the hydrogen atoms. The hydrogen atoms were included in the final cycles using a riding model and calculated positions. For **39**, the phenyl protons were constrained with respect to the carbons to which they were bonded with U values fixed at 0.08. The methyl protons were fixed as rigid groups with U values of 0.108. For **36**, the hydrogen U values were fixed at 1.2 or 1.5 times the  $U_{eq}$  of the attached carbon atom. Throughout the refinement, anomalous dispersion corrections were applied to the scattering curves for antimony, chlorine, and oxygen. Programs used for **39** included XTAL<sup>112</sup> for data reduction and SHELXTL PLUS<sup>113</sup> for structure solution and refinement. For **36**, the software used included Siemens P3, Siemens SHELXTL PLUS and SHELX 93. All thermal ellipsoid plots were created using SHELXTL PLUS. Information pertinent to the data collection and final structure solutions of **36** and **39** is presented in Table 5.1 and Table 5.2 respectively. Tabulated in the Appendix section (Tables A1 to A8) are: atomic co-ordinates and equivalent isotropic displacement coefficients for non-hydrogen atoms; anisotropic displacement coefficients for non-hydrogen atoms; atomic co-ordinates and isotropic displacement coefficients for all hydrogen atoms; and  $F_oF_c$  values for both **36** and **39**.



Table 5.1: Structure determination summary for 36.

**Crystal Data**

Empirical formula	C <sub>7</sub> H <sub>11</sub> Cl <sub>6</sub> O <sub>4</sub> Sb
-------------------	--

Colour; Habit	colourless prism
---------------	------------------

Crystal size (mm)	0.3 x 0.2 x 0.2
-------------------	-----------------

Crystal system	monoclinic
----------------	------------

Space group	P2 <sub>1</sub> /a
-------------	--------------------

Unit cell dimensions	a = 16.387(2) Å b = 13.390(2) Å c = 7.8350(10) Å
----------------------	--

	β = 105.770(10) °
--	-------------------

Volume	1654.5(4) Å <sup>3</sup>
--------	--------------------------

Z	4
---	---

Formula weight	493.61
----------------	--------

Density (calculated)	1.982 Mg/m <sup>3</sup>
----------------------	-------------------------

Absorption coefficient	1.373 mm <sup>-1</sup>
------------------------	------------------------

F(000)	952
--------	-----

**Data Collection**

Diffractometer Used	Siemens R3m/V
---------------------	---------------

Radiation	AgKα (λ = 0.56086 Å)
-----------	----------------------

Temperature	173 K
-------------	-------

Monochromator	Highly oriented graphite crystal
---------------	----------------------------------

Table 5.1 (cont.)

2 $\theta$ Range	2.04 to 25.07 °
Scan Type	$\theta 2\theta$
Scan Speed	variable; 2.00° to 29.30 °/min in $\omega$
Scan Range ( $\omega 2\theta$ )	$\pm 0.6^\circ$
Background Measurement	Stationary crystal and stationary counter at beginning and end of scan, each for 25 % of total scan time
Standard Reflections	3 measure every 100 reflections
Index Ranges	$0 \leq h \leq 24$ , $0 \leq k \leq 20$ , $-11 \leq l \leq 11$
Reflections Collected	3207
Independent Reflections	3107 ( $R_m = 2.01\%$ )
Observed Reflections	3100 ( $F^2 > -3\sigma(F^2)$ )
Absorption Correction	DIFABS
<b>Solution and Refinement</b>	
System Used	Siemens SHELXTL
Solution	Patterson
Refinement method	Full-Matrix Least-Squares on $F^2$
Quantity Minimized	$\Sigma w(F_o^2 - F_c^2)^2$
Absolute Structure	N/A

Table 5.1 (cont.)

Extinction Correction	0.000597
Hydrogen Atoms	Riding model; for H(4), H(5a/b), and H(7a/b) U is greater than 20 % of $U_{eq}$ of attached carbon atom; for all other protons, U is greater than 50 % of $U_{eq}$ of attached carbon atom.
Weighting Scheme	$w^{-1} = \sigma^2(F_o^2) + (0.0001P)^2 + 9.88P$ where $P = [\max(F_o^2, 0) + 2 F_c^2] \div 3$
Number of Parameters Refined	157
Final R indices ( $I > 2\sigma(I)$ )	R1 = 3.94 %, wR2 = 6.85 %
R indices (all data)	R1 = 6.89 %, wR2 = 8.25 %
Goodness-of-fit on $F^2$	1.106
Largest and Mean $\Delta/\sigma$	0.003, < 0.001
Data-to-Parameter Ratio	19.7:1
Largest Difference Peak	2.053 eÅ <sup>-3</sup>
Largest Difference Hole	-2.623 eÅ <sup>-3</sup>
Extinction coefficient	0.00060(13)

Table 5.2: Structure determination summary for 39.

**Crystal Data**

Empirical Formula	$C_{13} H_{15} Cl_6 O_4 Sb \cdot (CH_2Cl_2)$
Colour; Habit	colourless prism
Crystal size (mm)	0.3 x 0.2 x 0.2
Crystal System	Orthorhombic
Space Group	$P2_12_12_1$
Unit Cell Dimension	$a = 10.410(4) \text{ \AA}$ $b = 16.901(5) \text{ \AA}$ $c = 14.109(5) \text{ \AA}$
Volume	$2482.3(12) \text{ \AA}^3$
Z	4
Formula weight	652.1
Density(calc.)	$1.745 \text{ Mg/m}^3$
Absorption Coefficient	$1.983 \text{ mm}^{-1}$
F(000)	1274.96
<b>Data Collection</b>	
Diffractometer Used	Nicolet P3
Radiation	$MoK\alpha (\lambda = 0.71069 \text{ \AA})$
Temperature	173 K

Table 5.2 (cont.)

Monochromator	Highly oriented graphite crystal
2 $\theta$ Range	7.0 to 45.0°
Scan Type	$\omega$
Scan Speed	Variable; 2.00 to 29.30°/min. in $\omega$
Scan Range ( $\omega$ )	$\pm 1.0^\circ$
Background Measurement	Stationary crystal and stationary counter at beginning and end of scan, each for 25 % of total scan time
Standard Reflections	3 measured every 100 reflections
Index Ranges	$0 \leq h \leq 11$ , $0 \leq k \leq 18$ $-15 \leq l \leq 15$ , or Fridel mate
Reflections Collected	3718
Independent Reflections	3205 ( $R_{int} = 1.35\%$ )
Observed Reflections	3205 ( $F \geq 0$ )
Absorption Correction	$\psi$ Scan
<b>Solution and Refinement</b>	
System Used	Siemens SHELXTL PLUS (PC Version)
Solution	Patterson
Refinement Method	Full-Matrix Least-Squares on F
Quantity Minimized	$\Sigma w(F_o - F_c)^2$

Table 5.2 (cont.)

Absolute Structure	N/A
Extinction Correction	N/A
Hydrogen Atoms	Riding model, fixed isotropic U
Weighting Scheme	$w^{-1} = \sigma^2(F) + 0.0028F^2$
Number of Parameters Refined	208
Final R Indices (obs. data)	R = 4.80 %, wR = 6.19 %
R Indices (all data)	R = 4.80 %, wR = 6.19 %
Goodness-of-Fit	1.05
Largest and Mean $\Delta/\sigma$	both less than 0.001
Data-to-Parameter Ratio	15.4:1
Largest Difference Peak	1.09 eÅ <sup>-3</sup>
Largest Difference Hole	-1.43 eÅ <sup>-3</sup>

(c) Infrared Spectroscopy

Samples were mixed with KBr and pressed into thin disks under a dry nitrogen atmosphere. Infrared spectra were collected on a Biorad FTIR spectrometer.

### 5.3 Syntheses

*2-phenyl-2-hydroxydiethylmalonate (29)*: Following the method of Riebsomer,<sup>51</sup> dry benzene (11 g, 141 mmol) was mixed with diethyl ketomalonate (5.0 g, 28.7 mmol) in a 3-necked flask under a dry nitrogen atmosphere. With vigorous stirring, anhydrous SnCl<sub>4</sub> (5.75 mL) was added dropwise over 30 minutes at 0 °C. Stirring was continued for 2 hours at room temperature. The reaction mixture was poured into 300g of crushed ice containing 1 mL of concentrated HCl. After standing until most of the ice had melted, the mixture was extracted into ether. The ether layer was washed with water until free from chlorides. The ether layer was dried over Na<sub>2</sub>SO<sub>4</sub>, filtered, and the solvent removed on a rotary evaporator. The residue was distilled at 160 °C / 5 mm Hg. Yield: 2.85 g (40 %) of a colourless oil. <sup>1</sup>H NMR (CCl<sub>4</sub>, 90 MHz): δ 7.25-7.77 ppm (m, Ar, 5H); 4.35 ppm (s, OH, 1H); 4.25 ppm (q, J = 7.5 Hz, CH<sub>2</sub>, 4H); 1.23 ppm (t, J = 7.5 Hz, CH<sub>3</sub>, 6H).

*2-phenyl-1,2,3-propanetriol (30)*: To a 3-necked flask fitted with a condenser, dropping funnel, and a nitrogen bubbler was added 1.08 g (28.4 mmol) of lithium aluminum hydride in dry ether. The diester 29 (2.7 g, 10.7 mmol) was added slowly with stirring

and cooling. After the initial reaction subsided, the mixture was heated at reflux for 24 hours. After the reaction was complete, excess LAH was decomposed by the addition of 10 mL of ethyl acetate, followed by approximately 80 mL of 6N HCl. The aqueous layer was separated and made basic by the addition of approximately 120 mL of 6N NaOH. This solution was extracted several times with ether, and the combined extracts were dried over  $K_2CO_3$ . The solvent was removed on a rotary evaporator and the residue was taken up in  $CCl_4$ . A white precipitate was collected. Yield: 0.80 g (44 %). The compound was used immediately in the next step without further purification.

*2-phenyl-1,2,3-propanetrioltriacetate (31)*: The triol **30** (0.80 g, 4.76 mmol) was dissolved in 3 mL of acetic anhydride and 0.5 mL of pyridine. The solution was stirred overnight. The reaction mixture was poured into a 5%  $NaHCO_3$  solution and extracted with ether. The ether layer was washed with dilute HCl and then water until the aqueous extracts were neutral. The organic layer was dried over  $Na_2SO_4$ , followed by removal of the solvent on a rotary evaporator. Yield: 0.50 g (36 %).  $^1H$  NMR ( $CCl_4$ , 90 MHz):  $\delta$  7.30 ppm (s br., Ar, 5H); 4.60 ppm (s,  $CH_2$ , 4H); 2.03 ppm (s,  $CH_3$ , 3H); 1.95 ppm (s,  $CH_3$ , 6H).

*2-(4-methoxyphenyl)-1,2,3-propanetriol-1,3-diacetate (33d)*: 8.95 g (47.9 mmol) of *p*-bromoanisole was reacted with 1.74 g (71.6 mmol) of magnesium turnings in 125 mL of dry THF for 24 hours. The Grignard reagent was added dropwise with stirring to 10.0



g (57.5 mmol) of 1,3-dihydroxypropan-2-one-1,3-diacetate<sup>32</sup> dissolved in 500 ml of THF and 300 mL of toluene at -65 °C. The addition was conducted over 2 hours followed by 1 hour of additional stirring. The reaction mixture was brought up to 0 °C and quenched with 10 mL of 25% H<sub>2</sub>SO<sub>4</sub> and 30 mL of water. The solution was extracted into ether and the organic layer was washed with 5% NaHCO<sub>3</sub> and water until neutral. Drying over NaSO<sub>4</sub> and removal of the solvent gave an oil which was taken up in ether/hexanes. Upon standing at 5 °C, 4.72 g (29 %) of a white precipitate (m.pt. 67 °C, uncorrected) was collected. <sup>1</sup>H NMR (CCl<sub>4</sub>, 90 MHz): δ 7.35 ppm (d, J = 9.0 Hz, Ar, 2H); 6.80 ppm (d, J = 9.0 Hz, Ar, 2H); 4.20 ppm (s, CH<sub>2</sub>, 4H); 3.75 ppm (s, OCH<sub>3</sub>, 3H); 2.85 ppm (s, OH, 1H); 2.00 ppm (s, CH<sub>3</sub>, 6H). MS (relative intensity, %): m/z 282 (2) M<sup>+</sup>; 209 (45); 167 (100); 149 (27); 121 (52); 77 (18). Calculated mass for C<sub>14</sub>H<sub>18</sub>O<sub>6</sub>: 282.11034. Observed mass: 282.11030.

The following diesters were prepared using analogous procedures.

*2-(4-trifluoromethylphenyl)-1,2,3-propanetriol-1,3-diacetate (33a)* was prepared from *p*-bromotrifluorotoluene. Recrystallized from ether/hexanes to give a white solid. Yield: 7.5 g (53 %). <sup>1</sup>H NMR (200 MHz, CDCl<sub>3</sub>): δ 7.51 - 7.70 ppm (m, Ar, 4H), 4.29 - 4.42 ppm (m, CH<sub>2</sub>, 4H); 3.10 ppm (s br., OH, 1H); 2.03 ppm (s, CH<sub>3</sub>, 6H).

*2-(4-methylphenyl)-1,2,3-propanetriol-1,3-diacetate (33b)* was prepared from *p*-

bromotoluene. The product was distilled at 140 °C / 1mm Hg to give 5.0 g (27 %) of a colourless oil. <sup>1</sup>H NMR (90 MHz, CCl<sub>4</sub>): δ 7.35 ppm (d, J = 9.0 Hz, Ar, 2H); 7.10 ppm (d, J = 9.0 Hz, Ar, 2H); 4.25 ppm (s br., CH<sub>2</sub>, 4H); 3.15 ppm (s br., OH, 1H); 2.35 ppm (s, CH<sub>3</sub>, 3H); 1.95 (s, CH<sub>3</sub>, 6H).

*2-(4-*t*-butylphenyl)-1,2,3-propanetriol-1,3-diacetate (33c)* was prepared from *p*-bromo-*t*-butylbenzene. Yield: 2.5 g (43 %) of a yellow oil. <sup>1</sup>H NMR (90 MHz, CDCl<sub>3</sub>): δ 7.30 - 7.55 ppm (m, Ar, 4H); 4.31 ppm (s, CH<sub>2</sub>, 4H); 2.95 ppm (s br., OH, 1H); 2.00 ppm (s, CH<sub>3</sub>, 6H); 1.25 ppm (s, CH<sub>3</sub>, 9H).

*2-(4-*N,N*-dimethylaminophenyl)-1,2,3-propanetriol-1,3-diacetate (33e)* was prepared from *p*-bromodimethylaniline. The product was purified on a silica column eluted with ether/hexanes. Yield: 1.5 g (12 %) of a pale green oil. <sup>1</sup>H NMR (500 MHz, CD<sub>2</sub>Cl<sub>2</sub>): δ 7.29 ppm (d, J = 8.9 Hz, Ar, 2H); 6.71 ppm (d, J = 8.9 Hz, Ar, 2H); 4.29 ppm (d, J = 11.5 Hz, CH(H), 2H); 4.25 ppm (d, J = 11.5 Hz, CH(H), 2H); 2.92 ppm (s, N-CH<sub>3</sub>, 6H); 2.00 ppm (s, CH<sub>3</sub>, 6H). A signal for OH was not detected. MS (relative intensity, %): 295 (27) M<sup>+</sup>; 222 (64); 180 (100); 134 (71). Calculated mass for C<sub>15</sub>H<sub>21</sub>NO<sub>5</sub>: 295.14197. Observed mass: 295.14400.

The following triesters were prepared from the corresponding diesters, using a procedure similar to that already described for the acetylation of 2-phenyl-1,2,3-propanetriol (30).

*2-(4-trifluoromethylphenyl)-1,2,3-propanetrioltriacetate (34a)*: Yield: 4.0 g (71 %) of oil. No further purification was necessary.  $^1\text{H}$  NMR (90 MHz,  $\text{CDCl}_3$ ):  $\delta$  7.35 - 7.70 ppm (m, Ar, 4H); 4.55 ppm (s,  $\text{CH}_2$ , 4H); 2.00 ppm (s,  $\text{CH}_3$ , 3H); 1.90 ppm (s,  $\text{CH}_3$ , 6H).

*2-(4-methylphenyl)-1,2,3-propanetrioltriacetate (34b)*: Yield: 3.5g (60%) of a pale yellow oil. No further purification was necessary.  $^1\text{H}$  NMR (90 MHz,  $\text{CCl}_4$ ):  $\delta$  7.00-7.31 ppm (m, Ar, 4H); 4.55 ppm (s,  $\text{CH}_2$ , 4H); 2.35 ppm (s,  $\text{C}_{\text{Ar}}\text{-CH}_3$ , 3H); 2.02 ppm (s,  $\text{CH}_3$ , 3H); 1.97 ppm (s,  $\text{CH}_3$ , 6H). MS (relative intensity, %):  $m/z$  308 (3)  $\text{M}^+$ ; 249 (100); 193 (71); 151 (100). Calculated mass for  $\text{C}_{16}\text{H}_{20}\text{O}_6$ : 308.12599. Observed mass: 308.12530.

*2-(4-*t*-butylphenyl)-1,2,3-propanetrioltriacetate (34c)*: Yield: 2.5 g (88 %) of a pale yellow oil. No further purification was necessary.  $^1\text{H}$  NMR (200 MHz,  $\text{CDCl}_3$ ):  $\delta$  7.40 ppm (s, Ar, 4H); 4.37 ppm (s,  $\text{CH}_2$ , 4H); 2.06 ppm (s,  $\text{CH}_3$ , 9H); 1.33 ppm (s,  $\text{CH}_3$ , 9H). MS (relative intensity, %):  $m/z$  350 (32)  $\text{M}^+$ ; 335 (15); 295 (57); 277 (55). Calculated mass for  $\text{C}_{19}\text{H}_{26}\text{O}_6$ : 350.17294. Observed mass: 350.17380.

*2-(4-methoxyphenyl)-1,2,3-propanetrioltriacetate (34d)*: Recrystallized from ether/hexanes. Yield: 1.5 g (22 %).  $^1\text{H}$  NMR (200 MHz,  $\text{CCl}_4$ ):  $\delta$  7.20 ppm (d,  $J$  = 8.7 Hz, Ar, 2H); 6.79 ppm (d,  $J$  = 8.7 Hz, Ar, 2H); 4.54 - 4.64 ppm (m,  $\text{CH}_2$ , 4H);

3.76 ppm (s, OCH<sub>3</sub>, 3H); 2.02 ppm (s, CH<sub>3</sub>, 3H); 1.98 ppm (s, CH<sub>3</sub>, 6H). MS (relative intensity, %): m/z 324 (5) M<sup>+</sup>; 209 (73); 167 (100). Calculated mass for C<sub>16</sub>H<sub>20</sub>O<sub>7</sub>: 324.12090. Observed mass: 324.12080.

*2-(4-N,N-dimethylaminophenyl)-1,2,3-propanetrioltriacetate (34e)*: Yield: 0.85g (74 %) of oil. No further purification was necessary. <sup>1</sup>H NMR (200 MHz, CDCl<sub>3</sub>): δ 7.33 ppm (d, J = 8.6 Hz, Ar, 2H); 6.72 ppm (d, J = 8.6 Hz, Ar, 2H); 4.35 ppm (s, CH<sub>2</sub>, 4H); 2.96 ppm (s, N-CH<sub>3</sub>, 6H); 2.07 ppm (s, CH<sub>3</sub>, 9H).

*2-methyl-1,2,3-propanetrioltriacetate (35)*: Following the method of Saegebarth,<sup>34</sup> 100 mg of tungstic acid was added to 10 mL of 30% H<sub>2</sub>O<sub>2</sub> with stirring until the catalyst dissolved. The solution was diluted with 20 mL of water and 5 g (69.4 mmol) of 2-methyl-2-propene-1-ol (Aldrich) was added dropwise with stirring at 0 °C. Stirring was continued for 2 hours after the addition. The solvent was removed on a rotary evaporator to give a colourless oil. The residue was not characterized but was immediately used in the following step. The oil was dissolved in 50 mL of acetic anhydride and 1 drop of conc. H<sub>2</sub>SO<sub>4</sub> was added to produce a highly exothermic reaction. The solution was left to stand at room temperature for 3 hours. A small amount of Na<sub>2</sub>CO<sub>3</sub> was added to neutralize the mixture which was then filtered and concentrated on a rotary evaporator. The residue was dissolved in 100 mL of water and extracted with 3 x 100 mL of ether. The combined extracts were washed with 50 mL of 10% NaHCO<sub>3</sub>, 100 mL of water, and

then dried over  $\text{Na}_2\text{SO}_4$ . Filtration and removal of the solvent gave 9.07 g (56 % from 2-methyl-2-propene-1-ol) of a pale yellow oil. No further purification was necessary.  $^1\text{H}$  NMR (200 MHz,  $\text{CDCl}_3$ ):  $\delta$  4.30 ppm (d,  $J = 11.5$  Hz, CH(H), 2H); 4.17 ppm (d,  $J = 11.5$  Hz, CH(H), 2H); 1.99 ppm (s,  $\text{CH}_3$ , 6H); 1.93 ppm (s,  $\text{CH}_3$ , 3H); 1.42 ppm (s,  $\text{CH}_3$ , 3H).

*2-methyl-4-phenyl-4-acetoxymethyl-1,3-dioxolan-2-ylum hexachloroantimonate (39):*

Following the method of Paulsen,<sup>22</sup> 0.470 g of the triacetate 31 in 2 mL of dry  $\text{CH}_2\text{Cl}_2$  was cooled to  $-30^\circ\text{C}$  and 0.36 ml of  $\text{SbCl}_5$  in 5 mL of  $\text{CH}_2\text{Cl}_2$  was added dropwise with stirring under a dry nitrogen atmosphere. The solution was slowly brought to room temperature to give a white precipitate. The solid was collected, washed with dry ether, and recrystallized from  $\text{CH}_2\text{Cl}_2$ /ether. IR (KBr disc):  $\nu$  1742  $\text{cm}^{-1}$  (C=O); 1548  $\text{cm}^{-1}$ ; 1513  $\text{cm}^{-1}$ .  $^1\text{H}$  NMR data is presented in Table 2.2.  $^{13}\text{C}$  NMR data is presented in Table 2.3. The assigned structure was confirmed by xray crystallography.

The following dioxolanylium ions salts were prepared by ionization of the corresponding triacetates using similar procedures.

*2-methyl-4-acetoxymethyl-1,3-dioxolan-2-ylum hexachloroantimonate (36):*  $^1\text{H}$  and  $^{13}\text{C}$  NMR data are presented in Table 2.1. Assigned structure was confirmed by xray crystallography.

*2,4-dimethyl-4-acetoxymethyl-1,3-dioxolan-2-ylum hexachloroantimonate (37)*:  $^1\text{H}$  and  $^{13}\text{C}$  NMR data are presented in Table 2.1.

*2-methyl-4-(4-trifluoromethylphenyl)-4-acetoxymethyl-1,3-dioxolan-2-ylum hexachloroantimonate (38)*: IR (KBr disc):  $\nu$  1742  $\text{cm}^{-1}$  (C=O), 1544  $\text{cm}^{-1}$ , 1505  $\text{cm}^{-1}$ .  $^1\text{H}$  NMR data is presented in Table 2.2.  $^{13}\text{C}$  NMR data is presented in Table 2.3.

*2-methyl-4-(4-methylphenyl)-4-acetoxymethyl-1,3-dioxolan-2-ylum hexachloroantimonate (40)*:  $^1\text{H}$  NMR data is presented in Table 2.2.  $^{13}\text{C}$  NMR data is presented in Table 2.3.

*2-methyl-4-(4-*t*-butylphenyl)-4-acetoxymethyl-1,3-dioxolan-2-ylum hexachloroantimonate (41)*: IR (KBr disc):  $\nu$  1750  $\text{cm}^{-1}$  (C=O); 1542  $\text{cm}^{-1}$ ; 1509  $\text{cm}^{-1}$ .  $^1\text{H}$  NMR data is presented in Table 2.2.  $^{13}\text{C}$  NMR data is presented in Table 2.3.

*2-methyl-4-(4-methoxyphenyl)-4-acetoxymethyl-1,3-dioxolan-2-ylum hexachloroantimonate (42)*: IR (KBr disc):  $\nu$  1739  $\text{cm}^{-1}$  (C=O); 1611  $\text{cm}^{-1}$ ; 1584  $\text{cm}^{-1}$ ; 1543  $\text{cm}^{-1}$ ; 1515  $\text{cm}^{-1}$ .  $^1\text{H}$  NMR data is presented in Table 2.2.  $^{13}\text{C}$  NMR data is presented in Table 2.3.

The following complexes are for the Lewis acid adducts of 1,3-dihydroxypropan-2-one-1,3-diacetate (32):

SbCl<sub>3</sub> complex, 43: To a cooled (-78 ° C) NMR tube containing a solution of 32 (20 mg) in CD<sub>2</sub>Cl<sub>2</sub>, was added 1.5 equivalents of SbCl<sub>3</sub> dissolved in a small amount of CD<sub>2</sub>Cl<sub>2</sub>. The addition was carried out slowly, under an atmosphere of dry nitrogen, with occasional agitation to allow the contents of the NMR tube to mix thoroughly. The resulting dark coloured complex was analyzed in situ by <sup>1</sup>H NMR (Table 2.4).

SnCl<sub>4</sub> complex, 44: To 0.87 g of 32 in 2 mL of dry CH<sub>2</sub>Cl<sub>2</sub> was added 1.32 g of SnCl<sub>4</sub> in 3 mL of CH<sub>2</sub>Cl<sub>2</sub> at -30 ° C and under a dry nitrogen atmosphere. Upon standing overnight at -10 ° C colourless white crystals of the complex were collected and washed with CCl<sub>4</sub>. <sup>1</sup>H NMR, <sup>13</sup>C NMR (solution) and CPMAS data are presented in Table 2.4.

#### 5.4 AM1 Calculations

The fractional co-ordinates corresponding to the cation in the crystal structure of 39 were converted to cartesian co-ordinates within SHELXTL PLUS<sup>113</sup> and exported to PCMODEL.<sup>97</sup> The latter program was used to modify the structure to add the *para* substituents to the phenyl ring and thus generate the co-ordinates for the remaining aryl-substituted dioxolanylium ions. An input file was created for use in AMPAC<sup>98</sup> by assigning an overall charge of +1 to the cations.

Similarly, the co-ordinates of the cation in the crystal structure of 36 were used to create an AMPAC input file. The starting geometry of 37 was obtained by replacement of the hydrogen atom at C(4) in 36 with a methyl group within PCMODEL.

The cartesian co-ordinates so obtained were exported to AMPAC. The starting geometries of all neutral species, intermediates and transition state structures described in Chapter 4 were created in PCMODEL.

Full AM1 geometry optimization was carried out for the neutral species, dioxolanylium ions and carbenium ion intermediates, while partially constrained optimizations were carried out for the concerted transition states as previously described. All AM1 calculations were performed on an IBM RISC System/6000 computer.



## Appendix

Table A1: Atomic coordinates ( $\times 10^4$ ) and equivalent isotropic displacement parameters ( $\text{\AA}^2 \times 10^3$ ) for 36.

Atom	x	y	z	U(eq)
Sb(1)	0	0	0	24(1)
Sb(2)	0	5000	5000	30(1)
Cl(1)	-20(12)	1752(1)	207(17)	52(1)
Cl(2)	1505(1)	-79(49)	820(2)	45(5)
Cl(3)	32(1)	-145(5)	3014(2)	39(1)
Cl(4)	-36(12)	6177(14)	2763(26)	40(2)
Cl(4A)	-100(12)	3687(14)	2899(25)	44(2)
Cl(5)	1502(1)	4936(66)	5684(3)	43(5)
O(1)	7778(4)	3240(5)	9229(7)	41(1)
O(3)	7104(3)	4235(4)	7118(7)	36(1)
O(8)	7517(11)	2589(13)	5254(12)	33(2)
O(10)	7153(4)	2138(5)	2379(8)	4(2)
C(2)	7740(5)	4092(6)	8473(9)	33(2)
C(4)	6591(6)	3296(7)	6730(11)	38(2)
C(5)	7007(5)	2669(7)	8334(11)	44(2)
C(6)	8382(5)	4883(37)	9107(10)	49(7)
C(7)	651(5)	2931(7)	4985(11)	40(2)
C(9)	7676(6)	2204(6)	3773(12)	39(2)
C(11)	8571(7)	1838(9)	4174(17)	58(3)

Equivalent isotropic U defined as one third of the trace of the orthogonalized  $U_{ij}$  tensor.

Table A2: Anisotropic displacement parameters ( $\text{\AA}^2 \times 10^3$ ) for 36.

Atom	$U_{11}$	$U_{22}$	$U_{33}$	$U_{12}$	$U_{13}$	$U_{23}$
Cl(1)	76(2)	29(1)	67(5)	-5(1)	47(4)	-3(2)
Cl(2)	26(1)	65(15)	43(1)	-2(3)	11(1)	4(4)
Cl(3)	48(1)	50(4)	24(1)	1(1)	17(1)	4(1)
Cl(4)	47(3)	35(4)	35(2)	1(2)	7(2)	-6(3)
Cl(4A)	53(3)	33(4)	42(5)	-12(3)	7(2)	-2(2)
Cl(5)	28(1)	50(17)	47(1)	0(2)	5(1)	4(5)
O(1)	43(3)	41(3)	39(3)	10(3)	10(2)	2(3)
O(3)	38(3)	38(3)	33(2)	0(2)	10(2)	3(2)
O(8)	29(2)	48(6)	20(6)	-6(4)	5(5)	4(4)
O(10)	65(4)	58(4)	38(3)	-7(3)	13(3)	5(3)
C(2)	35(4)	38(4)	27(3)	0(3)	14(3)	6(3)
C(4)	33(4)	43(5)	37(4)	-4(4)	10(4)	-4(4)
C(5)	44(5)	46(5)	45(4)	0(4)	18(4)	-9(4)
C(6)	43(4)	60(20)	42(3)	3(6)	9(3)	-7(7)
C(7)	33(4)	49(5)	36(4)	-3(4)	5(3)	4(4)
C(9)	49(5)	27(4)	45(4)	-3(3)	20(4)	-7(3)
C(11)	45(6)	57(6)	79(8)	-21(7)	28(6)	0(5)

The anisotropic displacement exponent takes the form:

$$-2\pi^2(h^2a^{*2}U_{11} + \dots + 2hka^*b^*U_{12})$$

Table A3: Hydrogen coordinates ( $\times 10^4$ ) and isotropic displacement parameters ( $\text{\AA}^2 \times 10^3$ ) for 36.

Atom	x	y	z	U(eq)
H(4)	5987(6)	3435(7)	6691(11)	45
H(5A)	6629(5)	2591(7)	9119(11)	53
H(5B)	7156(5)	1999(7)	7976(11)	53
H(6A)	8233(5)	5472(37)	8342(10)	73
H(6B)	8940(5)	4636(37)	9071(10)	73
H(6C)	8399(5)	5065(37)	10328(10)	73
H(7A)	6248(5)	2376(7)	4564(11)	48
H(7B)	6521(5)	3475(7)	4096(11)	48
H(11A)	8865(7)	1985(9)	5414(17)	88
H(11B)	8861(7)	2174(9)	3395(17)	88
H(11C)	8572(7)	1115(9)	3976(17)	88

Table A4: Atomic coordinates ( $\times 10^4$ ) and equivalent isotropic displacement coefficients ( $\text{\AA}^2 \times 10^3$ ) for 39.

Atom	x	y	z	U(eq)
Sb	3165(1)	4544(1)	2049(1)	33(1)
Cl(1)	1827(3)	3482(1)	1608(2)	74(1)
Cl(2)	3405(2)	4007(1)	3579(1)	55(1)
Cl(3)	2944(2)	5089(1)	508(1)	44(1)
Cl(4)	4459(2)	5642(1)	2476(2)	54(1)
Cl(5)	5009(2)	3850(1)	1546(2)	55(1)
Cl(6)	1311(2)	5262(2)	2522(2)	71(1)
Cl(1')	6996(4)	2488(2)	931(3)	114(2)
Cl(2')	9682(3)	2059(2)	1213(3)	90(1)
O(1)	2266(5)	10674(3)	174(4)	38(2)
O(3)	3389(5)	9738(3)	855(3)	32(2)
O(8)	2262(5)	10616(3)	2264(3)	36(2)
O(10)	2110(7)	10537(4)	3833(4)	54(2)
C(2)	3397(8)	10365(5)	351(5)	36(2)
C(4)	2031(7)	9554(4)	1170(5)	32(2)
C(5)	1278(8)	10136(5)	521(6)	38(3)
C(6)	4561(9)	10724(5)	20(6)	51(3)
C(7)	2000(8)	9779(4)	2200(5)	34(2)
C(9)	2313(8)	10923(5)	3146(6)	39(3)
C(11)	2631(10)	11790(5)	3137(6)	53(3)
C(12)	8135(12)	1784(7)	878(11)	89(5)
C(1')	1750(7)	8694(4)	1021(5)	34(2)
C(2')	535(9)	8446(5)	742(6)	50(3)
C(3')	298(10)	7646(6)	632(7)	62(4)
C(4')	1203(12)	7081(6)	816(7)	63(4)
C(5')	2423(10)	7330(5)	1127(7)	55(3)
C(6')	2683(9)	8134(4)	1225(6)	46(3)

Equivalent isotropic U defined as one third of the trace of the orthogonalized  $U_{ij}$  tensor

Table A5: Anisotropic displacement coefficients ( $\text{\AA}^2 \times 10^3$ ) for 39.

Atom	$U_{11}$	$U_{22}$	$U_{33}$	$U_{12}$	$U_{13}$	$U_{23}$
Sb	25(1)	37(1)	35(1)	-2(1)	-2(1)	1(1)
Cl(1)	83(2)	55(1)	85(2)	-36(1)	-49(2)	28(1)
Cl(2)	59(1)	69(1)	36(1)	-5(1)	-2(1)	8(1)
Cl(3)	46(1)	46(1)	41(1)	-1(1)	-10(1)	9(1)
Cl(4)	47(1)	47(1)	66(1)	-11(1)	-17(1)	-5(1)
Cl(5)	55(1)	64(1)	47(1)	28(1)	2(1)	-1(1)
Cl(6)	37(1)	93(2)	84(2)	19(1)	20(1)	6(1)
Cl(1')	108(3)	87(2)	146(3)	59(2)	-14(3)	-11(2)
Cl(2')	62(2)	66(2)	141(3)	-24(1)	-4(2)	4(2)
O(1)	36(3)	38(3)	40(3)	-2(2)	-3(2)	7(2)
O(3)	24(3)	40(3)	32(3)	2(2)	-1(2)	8(2)
O(8)	49(3)	33(3)	27(3)	5(2)	-1(2)	1(2)
O(10)	70(4)	63(4)	29(3)	2(3)	4(3)	0(3)
C(2)	39(5)	43(4)	28(4)	-3(4)	-6(3)	0(3)
C(4)	23(4)	38(4)	34(4)	3(3)	1(3)	8(3)
C(5)	34(5)	43(4)	38(4)	4(4)	3(4)	4(4)
C(6)	47(5)	63(6)	42(5)	-18(5)	1(4)	12(4)
C(7)	38(4)	31(4)	34(4)	2(3)	2(4)	6(3)
C(9)	38(4)	42(4)	39(5)	13(4)	-1(3)	5(4)
C(11)	65(6)	42(4)	52(5)	7(4)	-5(5)	-8(4)
C(12)	56(7)	57(6)	156(13)	0(6)	-9(9)	-8(7)
C(1')	30(4)	39(4)	33(4)	0(4)	3(3)	5(3)
C(2')	42(5)	47(5)	59(5)	-6(4)	-5(4)	5(4)
C(3')	60(6)	61(6)	63(6)	-24(5)	-13(5)	7(5)
C(4')	86(8)	46(5)	55(6)	-9(5)	17(5)	7(5)
C(5')	53(6)	40(5)	71(6)	0(4)	-2(5)	-1(4)
C(6')	46(5)	38(5)	53(5)	2(4)	-2(4)	0(4)

The anisotropic displacement exponent takes the form:

$$-2\pi^2(h^2a^{*2}U_{11} + \dots + 2hka^*b^*U_{12})$$

Table A6: H-Atom coordinates ( $\times 10^4$ ) and isotropic displacement coefficients ( $\text{\AA}^2 \times 10^3$ ) for 39.

Atom	x	y	z	U
H(5A)	952	9845	-126	70
H(5B)	754	10322	713	70
H(6A)	4373	11065	-506	108
H(6B)	5235	10364	-153	108
H(6C)	4831	11036	552	108
H(7A)	2642	9487	2541	52
H(7B)	1169	9666	2462	52
H(11A)	2813	11935	3781	108
H(11B)	1922	12098	2907	108
H(11C)	3374	11889	2752	108
H(12A)	7872	1356	1281	300
H(12B)	8177	1603	234	300
H(2'A)	-131	8827	627	80
H(3'A)	-533	7482	412	80
H(4'A)	1007	6529	741	80
H(5'A)	3078	6947	1267	80
H(6'A)	3514	8306	1438	80

Table A7: Observed and calculated structure factors for 36.

h	k	l	10Fo	10Fc	10s	h	k	l	10Fo	10Fc	10s	h	k	l	10Fo	10Fc	10s
2	0	0	1985	1908	8	17	7	0	66	49	65	20	6	1	152	126	26
4	0	0	3394	3406	13	19	7	0	76	13	75	22	6	1	421	428	12
6	0	0	3845	3881	16	21	7	0	85	34	64	-21	6	1	349	376	12
8	0	0	2924	2865	15	0	8	0	1973	1982	15	-19	7	1	481	472	11
10	0	0	1271	1252	10	2	8	0	1555	1568	12	-17	7	1	350	336	12
12	0	0	1770	1736	15	4	8	0	1188	1206	10	-15	7	1	790	793	9
14	0	0	1650	1652	15	6	8	0	1608	1643	14	-13	7	1	969	955	10
16	0	0	490	489	10	8	8	0	1399	1368	12	-11	7	1	740	732	8
18	0	0	693	685	9	10	8	0	673	658	11	-9	7	1	977	992	10
20	0	0	756	742	10	12	8	0	1074	1047	11	-7	7	1	1567	1569	13
22	0	0	62	276	18	14	8	0	783	775	9	-5	7	1	1348	1321	11
3	1	0	0	0	4	16	8	0	477	482	10	-3	7	1	606	615	6
5	1	0	0	14	1	18	8	0	505	498	11	-1	7	1	2208	2228	14
7	1	0	0	78	91	20	8	0	503	485	7	3	7	1	976	988	8
9	1	0	0	24	80	22	1	9	325	299	8	5	7	1	1096	1105	10
11	1	0	0	0	2	24	3	9	430	386	8	7	7	1	1121	1139	10
13	1	0	0	80	116	26	5	9	95	149	47	9	7	1	495	493	7
15	1	0	0	6	1	28	7	9	96	135	40	11	7	1	413	409	9
17	1	0	0	36	75	30	9	9	153	146	24	13	7	1	855	861	9
19	1	0	0	0	41	32	11	9	104	60	42	15	7	1	215	208	16
21	1	0	0	0	27	34	13	9	0	0	64	17	7	1	209	215	17
23	1	0	0	2206	2180	36	15	9	0	198	189	21	7	1	351	381	13
2	2	0	2570	2546	11	17	9	0	118	33	38	19	7	1	219	208	18
4	2	0	658	658	6	19	9	0	20	7	20	22	8	1	110	26	44
6	2	0	2587	2566	13	21	9	0	1472	1490	12	-20	8	1	53	32	52
8	2	0	1437	1409	11	23	9	0	849	716	8	-18	8	1	128	77	30
10	2	0	1093	1095	10	25	9	0	1222	1219	11	-16	8	1	165	151	22
12	2	0	1158	1139	11	27	9	0	859	850	9	-14	8	1	119	124	32
14	2	0	356	362	11	29	9	0	495	494	9	-12	8	1	298	264	12
16	2	0	463	476	10	31	9	0	695	676	10	-10	8	1	319	300	10
18	2	0	607	585	10	33	9	0	677	684	10	-8	8	1	408	397	8
20	2	0	255	278	17	35	9	0	256	250	16	-6	8	1	241	238	10
22	2	0	354	345	5	37	9	0	324	332	15	-4	8	1	697	696	7
24	2	0	1232	1208	10	39	9	0	370	370	12	-2	8	1	276	260	7
2	3	0	785	773	7	41	9	0	523	556	8	0	8	1	454	431	4
4	3	0	90	35	19	43	9	0	566	589	7	2	8	1	337	310	7
6	3	0	761	759	7	45	9	0	395	413	9	4	8	1	427	414	6
8	3	0	194	218	13	47	9	0	459	490	9	6	8	1	319	281	10
10	3	0	162	191	18	49	9	0	275	291	12	8	8	1	0	7	1
12	3	0	192	239	17	51	9	0	264	318	15	10	8	1	36	7	35
14	3	0	115	164	31	53	9	0	105	160	42	12	8	1	0	16	1
16	3	0	0	0	0	55	9	0	130	188	32	14	8	1	0	5	1
18	3	0	0	0	0	57	9	0	97	88	49	16	8	1	57	86	57
20	3	0	87	90	1	59	9	0	45	87	40	18	8	1	0	16	1
22	3	0	35	81	34	61	9	0	971	979	10	20	8	1	383	372	13
24	3	0	2508	2506	8	63	9	0	444	442	8	22	8	1	356	373	13
2	4	0	189	205	8	65	9	0	485	483	8	24	8	1	197	203	20
4	4	0	382	339	5	67	9	0	680	693	8	26	8	1	603	618	9
6	4	0	1410	1407	11	69	9	0	571	574	8	28	8	1	713	720	9
8	4	0	1060	1053	9	71	9	0	2537	2534	13	30	8	1	366	360	10
10	4	0	115	132	22	73	9	0	1303	1290	10	32	8	1	707	711	8
12	4	0	897	901	9	75	9	0	1234	1232	10	34	8	1	550	558	8

Table A7 (cont.)

14	4	0	762	755	9	14	12	0	453	458	11	-1	1	1	1	2175	2160	9	-9	5	5	1	946	950	9	-7	9	1	1060	1084	11		
16	4	0	264	277	13	16	12	0	205	186	20	3	1	1	1	1	2682	2691	11	-5	5	5	1	1600	1612	12	-5	9	1	551	578	7	
18	4	0	283	299	14	18	12	0	227	180	20	3	1	1	1	1	890	884	11	-3	9	9	1	1031	1033	8	-3	9	1	588	605	7	
20	4	0	538	548	10	20	12	0	191	232	16	7	1	1	1	1	1742	1745	12	-3	5	5	1	1288	1294	10	-1	9	1	1054	1076	10	
22	4	0	135	168	34	22	13	0	203	240	15	5	1	1	1	1	1804	1776	13	-1	5	5	1	1761	1774	12	3	9	1	905	906	8	
24	5	0	1407	1400	11	24	13	0	259	281	13	9	1	1	1	1	418	417	16	3	5	5	1	1719	1711	12	3	9	1	207	232	11	
26	5	0	1251	1253	10	26	13	0	13	98	13	11	1	1	1	1	860	847	8	3	5	5	1	1036	1028	9	5	9	1	864	905	9	
28	5	0	883	882	6	28	13	0	196	236	17	15	1	1	1	1	900	890	8	5	5	5	1	1459	1490	11	7	9	1	720	730	8	
30	5	0	1098	1095	9	30	13	0	115	151	33	17	1	1	1	1	485	472	8	5	5	5	1	1511	1493	11	9	9	1	277	289	11	
32	5	0	519	540	6	32	13	0	0	19	18	19	1	1	1	1	142	153	24	9	5	5	1	740	720	8	11	9	1	409	414	9	
34	5	0	539	559	7	34	13	0	116	71	37	19	1	1	1	1	509	510	10	11	5	5	1	788	788	9	13	9	1	565	563	9	
36	5	0	421	444	9	36	13	0	585	590	8	23	1	1	1	1	200	288	14	13	5	5	1	941	962	10	15	9	1	249	247	15	
38	5	0	214	250	16	38	14	0	344	362	10	-24	2	2	2	1	64	55	31	15	5	5	1	502	291	13	17	9	1	143	170	28	
40	5	0	226	255	16	40	14	0	333	331	10	-22	2	2	2	1	130	22	64	17	5	5	1	290	291	13	19	9	1	313	328	14	
42	5	0	77	132	76	42	14	0	508	508	9	-20	2	2	2	1	90	39	61	17	5	5	1	501	499	10	-20	10	1	0	58	1	
44	5	0	43	131	43	44	14	0	341	352	11	-18	2	2	2	1	56	7	56	19	5	5	1	290	326	16	-18	10	1	95	31	51	
46	5	0	2605	2627	14	46	14	0	268	273	14	-16	2	2	2	1	0	14	1	21	5	5	1	70	74	69	-16	10	1	132	72	28	
48	5	0	2105	2097	13	48	14	0	321	311	13	-12	2	2	2	1	56	76	55	-22	6	6	1	0	40	1	-12	10	1	88	70	46	
50	5	0	888	913	8	50	14	0	322	326	14	-14	2	2	2	1	130	145	20	-16	6	6	1	128	148	26	-10	10	1	0	64	1	
52	5	0	2413	2409	16	52	14	0	157	154	28	-10	2	2	2	1	550	557	6	-12	6	6	1	81	10	60	-8	10	1	0	11	1	
54	5	0	1500	1494	12	54	14	0	221	194	15	-8	2	2	2	1	304	274	6	-12	6	6	1	204	213	14	-4	10	1	0	86	33	
56	5	0	661	657	7	56	15	0	174	136	18	-6	2	2	2	1	478	475	5	-10	6	6	1	173	156	15	-4	10	1	0	13	1	
58	5	0	1167	1150	11	58	15	0	175	131	19	-4	2	2	2	1	624	603	6	-8	6	6	1	130	148	19	-2	10	1	0	15	1	
60	5	0	1043	1023	11	60	15	0	200	165	18	-2	2	2	2	1	572	565	5	-6	6	6	1	186	199	11	0	10	1	110	88	23	
62	5	0	356	329	11	62	15	0	134	38	27	0	2	2	2	1	205	221	4	-4	6	6	1	401	399	5	2	10	1	77	149	44	
64	5	0	478	466	10	64	15	0	52	70	51	4	2	2	2	1	1083	1073	9	-2	6	6	1	98	76	17	6	10	1	230	184	12	
66	5	0	510	502	11	66	15	0	84	30	84	6	2	2	2	1	474	447	5	0	6	6	1	453	450	10	8	10	1	79	60	47	
68	5	0	213	240	20	68	15	0	673	684	8	8	2	2	2	1	135	137	12	2	6	6	1	23	41	32	10	10	1	0	56	1	
70	5	0	233	246	8	70	16	0	610	626	9	10	2	2	2	1	289	274	7	6	6	6	1	65	610	6	12	10	1	59	21	59	
72	5	0	102	102	1	72	16	0	491	502	10	12	2	2	2	1	373	347	18	8	6	6	1	303	321	9	14	10	1	121	71	31	
74	5	0	248	205	9	74	16	0	632	623	9	14	2	2	2	1	18	91	18	10	6	6	1	0	30	1	16	10	1	0	31	1	1
76	5	0	0	0	88	76	16	0	516	501	10	16	2	2	2	1	260	234	12	10	6	6	1	0	92	1	18	10	1	25	3	24	
78	5	0	0	0	0	78	16	0	373	357	12	18	2	2	2	1	0	26	1	14	6	6	1	47	40	46	20	10	1	100	244	59	
80	5	0	12	23	12	80	16	0	401	386	12	20	2	2	2	1	94	54	53	12	6	6	1	62	34	62	-19	11	1	112	244	59	
82	5	0	28	28	22	82	16	0	340	323	14	22	2	2	2	1	101	123	41	11	5	5	2	0	57	1	13	9	2	107	103	33	
84	5	0	0	0	1	84	16	1	0	6	1	15	1	1	1	2	93	123	41	11	5	5	2	363	132	18	15	9	2	97	71	41	
86	5	0	404	280	11	86	16	1	64	18	63	1	1	1	1	2	0	79	1	13	5	5	2	164	132	18	17	9	2	85	71	60	
88	5	0	555	546	10	88	16	1	0	14	14	21	1	1	1	2	50	44	49	15	5	5	2	255	206	13	19	9	2	87	60	67	
90	5	0	434	424	10	90	16	1	65	38	65	21	1	1	1	2	49	49	1	15	5	5	2	96	95	43	19	9	2	266	279	17	
92	5	0	928	931	10	92	16	1	0	14	1	-24	2	2	2	1	67	45	67	17	5	5	2	75	73	75	-20	10	2	207	186	19	
94	5	0	651	651	8	94	16	1	0	21	1	1	1	1	1	2	366	349	13	19	5	5	2	0	27	1	-16	10	2	277	276	15	
96	5	0	758	764	8	96	16	1	117	70	28	-22	2	2	2	1	438	459	12	21	5	5	2	111	34	37	-16	10	2	611	587	9	
98	5	0	1000	1032	10	98	16	1	0	65	65	-14	2	2	2	1	70	99	69	-22	6	6	2	345	370	14	-12	10	2	334	313	11	
100	5	0	926	938	8	100	16	1	82	102	70	-16	2	2	2	1	422	417	10	-20	6	6	2	420	445	15	-10	10	2	441	420	9	
102	5	0	723	740	8	102	16	1	0	56	58	-14	2	2	2	1	907	913	10	-18	6	6	2	238	239	15	-8	10	2	719	734	9	
104	5	0	853	853	9	104	16	1	1	56	65	-12	2	2	2	1	334	330	8	-16	6	6	2	475	473	9	-10	10	2	821	831	8	
106	5	0	946	952	10	106	16	1	317	316	15	-10	2	2	2	1	399	394	6	-14	6	6	2	1111	1112	11	-6	10	2	230	220	11	
108	5	0	510	505	9	108	17	1	317	327	14	-8	2	2	2	1	1267	1252	10	-12	6	6	2	425	433	9	-4	10	2	1020	1043	10	
110	5	0	592	592	9	110	17	1	335	327	15	-6	2	2	2	1	1083	1052	9	-10	6	6	2	777	788	8	-2	10	2	862	878	6	
112	5	0	603	605	9	112	17	1	367	370	12	-4	2	2	2	1	274	263	6	-8	6	6	2	1570	1560	14	0	10	2	443	469	7	
114	5	0	379	388	12	114	17	1	470	463	11	-2	2	2	2	1	1753	1769	10	-6	6	6	2	701	699	6	2	10	2	645	656	7	
116	5	0	253	250	15	116	17	1	451	461	10	-5	2	2	2	1	1442	1275	7	-4	6	6	2	1778	1777	14	4	10	2	928	936	10	
118	5	0	333	334	15	118	17	1	420	417	10	-3	2	2	2	1	183	190	8	-2	6	6	2	1778	1777	14	6	10	2	928	936	10	





Table A7 (cont.)

-13	15	1	379	411	14	-19	1	20	4	2	419	62	12	-21	9	2	116	43	40	7	13	2	136	107	26	
-11	15	1	261	266	16	-17	53	-23	5	2	0	38	62	-19	9	2	0	44	1	9	13	2	141	110	25	
-9	15	1	427	419	10	-15	4	-19	5	2	54	55	1	-17	9	2	75	11	75	11	13	2	156	69	24	
-7	15	1	507	504	10	-11	64	-17	5	2	0	97	1	-15	9	2	0	64	1	13	13	2	101	81	50	
-5	15	1	391	402	10	-11	110	-15	5	2	0	167	1	-13	9	2	43	9	43	15	13	2	134	28	29	
-3	15	1	337	356	9	-9	176	-13	5	2	0	507	1	-11	9	2	22	49	22	-16	14	2	224	235	19	
-1	15	1	531	554	9	-7	319	-11	5	2	122	282	10	-9	9	2	0	60	1	-14	14	2	339	333	13	
1	15	1	361	383	10	-5	176	-9	5	2	282	299	10	-7	9	2	270	268	10	-10	14	2	316	318	13	
3	15	1	279	307	12	-3	811	-7	5	2	0	44	6	-5	9	2	170	143	14	-8	14	2	420	415	10	
5	15	1	375	385	10	-1	272	-7	5	2	561	555	1	-5	9	2	0	13	1	-6	14	2	462	471	9	
7	15	1	353	359	11	1	247	-5	5	2	247	267	5	-1	9	2	54	66	54	-4	14	2	507	521	8	
9	15	1	182	209	20	5	547	-3	5	2	557	541	5	3	9	2	63	33	63	0	14	2	395	408	7	
11	15	1	223	229	17	1	315	-1	5	2	477	450	6	5	9	2	40	80	1	2	14	2	320	349	11	
13	15	1	256	271	17	9	324	3	5	2	507	486	6	7	9	2	0	132	39	4	14	2	296	316	12	
15	15	1	169	145	23	11	220	3	5	2	565	563	6	9	9	2	0	133	39	4	14	2	483	489	9	
-14	16	1	63	16	62	11	199	5	5	2	332	302	7	11	9	3	25	57	35	6	14	3	0	35	1	
-12	16	1	57	1	57	13	100	-19	5	2	404	359	12	9	9	3	217	212	14	-14	14	3	0	3	1	
8	14	2	271	280	1	-15	1029	-17	5	3	581	600	9	-11	9	3	726	752	9	-12	14	3	120	38	30	
10	14	2	237	235	15	-13	771	-15	5	3	1097	1111	11	-7	9	3	623	625	8	-10	14	3	0	39	1	
12	14	2	396	377	11	-11	552	-13	5	3	1070	1063	10	-5	9	3	283	290	10	-8	14	3	100	140	37	
14	14	2	241	274	16	-9	1511	-9	5	3	972	976	9	-3	9	3	729	735	8	-6	14	3	54	63	53	
-15	15	2	45	8	45	-7	1511	-9	5	3	1693	1730	14	-1	9	3	916	930	8	-4	14	3	92	75	39	
-13	15	2	37	42	37	-5	1086	-7	5	3	2031	2058	16	1	9	3	370	401	8	-2	14	3	14	20	14	
-11	15	2	66	55	65	-3	1490	-5	5	3	1200	1229	10	5	9	3	626	629	7	0	14	3	0	33	1	
-9	15	2	0	15	57	-1	2315	-3	5	3	2259	2233	14	7	9	3	529	523	8	6	14	3	45	33	45	
-7	15	2	57	67	57	3	1210	-1	5	3	1424	1471	12	11	9	3	455	456	9	8	14	3	40	7	39	
-5	15	2	0	13	1	1	1069	9	5	3	1794	1802	14	13	9	3	553	540	9	10	14	3	0	34	1	
-3	15	2	0	53	1	7	2003	15	5	3	1230	1219	11	15	9	3	346	346	82	-15	15	3	298	139	17	
-1	15	2	39	49	39	9	794	10	5	3	724	725	8	17	9	3	83	69	82	-13	15	3	0	35	1	
3	15	2	0	91	1	11	1003	1009	10	5	1011	1017	10	-20	10	3	27	2	27	-11	15	3	215	164	23	
5	15	2	22	50	22	13	907	912	10	5	768	756	8	-18	10	3	97	86	47	-9	15	3	157	164	23	
7	15	2	48	73	47	15	307	309	12	5	333	330	11	-16	10	3	31	33	30	-11	15	3	324	301	12	
9	15	2	75	103	74	17	474	474	10	5	427	420	11	-14	10	3	61	60	60	-7	15	3	256	242	14	
11	15	2	0	37	1	19	518	10	5	3	408	416	11	-12	10	3	61	60	60	-5	15	3	208	219	15	
13	15	2	0	80	1	21	196	17	19	5	57	52	57	-10	10	3	0	56	1	-3	15	3	230	254	14	
-14	16	2	261	251	17	-24	107	72	72	6	102	108	50	-8	10	3	83	107	49	-1	15	3	383	408	10	
-12	16	2	223	252	20	-20	15	-18	6	3	125	131	31	-6	10	3	166	170	16	1	15	3	205	191	14	
-10	16	2	192	196	20	-20	80	-16	6	3	69	125	68	-2	10	3	23	65	22	3	15	3	312	320	12	
-8	16	2	411	395	11	-16	80	-16	6	3	265	245	13	0	10	3	0	46	1	5	15	3	367	360	10	
-6	16	2	259	264	14	-14	268	-14	6	3	306	298	11	2	10	3	127	129	20	7	15	3	261	280	15	
-4	16	2	323	315	11	-12	68	-14	6	3	291	284	10	6	10	3	139	150	19	9	15	3	243	246	13	
-2	16	2	367	369	10	-10	205	-8	6	3	488	467	7	6	10	3	0	20	1	11	15	3	309	300	13	
0	16	2	183	181	18	-8	79	-6	6	3	411	406	6	6	10	3	46	107	45	-14	16	3	81	116	81	
2	16	2	256	275	14	-4	86	-4	6	3	389	386	6	10	10	3	53	41	53	-12	16	3	85	105	85	
4	16	2	221	312	13	-2	181	-2	6	3	375	671	4	12	10	3	115	0	42	1	16	3	98	174	44	
6	16	2	163	173	19	0	355	0	6	3	262	292	8	16	10	3	123	34	34	-8	16	3	98	91	44	
8	16	2	132	195	21	4	300	6	6	3	520	550	6	18	10	3	306	310	15	-4	16	3	170	212	22	
10	16	2	190	214	21	6	539	6	6	3	268	311	11	-19	11	3	366	383	14	-2	16	3	121	153	30	
-13	17	2	148	120	28	8	130	17	6	3	180	207	14	-19	11	3	0	310	15	15	-4	16	3	159	149	21
-9	17	2	177	173	23	10	98	10	6	3	175	187	16	-17	11	3	3	366	383	14	-2	16	3	121	153	30
-5	17	2	129	168	30	12	130	12	6	3	191	216	16	-15	11	3	642	645	10	0	16	3	89	134	88	



Table A7 (cont.)

-23	1	4	114	147	49	-21	5	4	120	80	37	12	294	270	4	270	294	12	-4	14	4	294	281	12	5	1	5	1086	1088	10	7
-21	1	4	0	33	24	-17	5	4	308	280	12	61	119	61	4	61	119	61	-2	14	4	395	390	9	7	1	5	521	503	7	8
-19	1	4	147	80	21	-17	5	4	308	280	12	13	212	13	4	314	241	10	0	14	4	324	326	12	9	1	5	539	542	8	9
-17	1	4	239	224	30	-15	5	4	200	168	17	10	341	10	4	314	241	10	2	14	4	255	242	12	11	1	5	780	771	10	10
-15	1	4	115	76	30	-13	5	4	155	122	19	8	416	402	8	220	172	12	6	14	4	399	382	10	13	1	5	332	321	16	16
-13	1	4	174	126	16	-11	5	4	205	173	18	8	416	402	8	220	172	12	6	14	4	399	382	10	13	1	5	332	321	16	16
-11	1	4	187	148	14	-9	5	4	205	173	18	8	416	402	8	220	172	12	6	14	4	399	382	10	13	1	5	332	321	16	16
-9	1	4	309	271	8	-7	5	4	606	586	7	7	415	369	8	137	103	19	10	14	4	215	223	13	-24	2	5	399	402	11	11
-7	1	4	106	141	19	-5	5	4	389	386	6	6	415	369	8	137	103	19	10	14	4	215	223	13	-24	2	5	399	402	11	11
-5	1	4	266	213	7	-3	5	4	697	672	7	7	415	369	8	137	103	19	10	14	4	215	223	13	-24	2	5	399	402	11	11
-3	1	4	79	47	21	-1	5	4	413	414	6	6	415	369	8	137	103	19	10	14	4	215	223	13	-24	2	5	399	402	11	11
-1	1	4	264	282	6	1	5	4	499	510	6	6	415	369	8	137	103	19	10	14	4	215	223	13	-24	2	5	399	402	11	11
1	1	4	33	50	33	3	5	4	556	587	7	7	415	369	8	137	103	19	10	14	4	215	223	13	-24	2	5	399	402	11	11
3	1	4	212	184	12	5	5	4	411	439	8	8	415	369	8	137	103	19	10	14	4	215	223	13	-24	2	5	399	402	11	11
5	1	4	175	140	12	7	5	4	411	439	8	8	415	369	8	137	103	19	10	14	4	215	223	13	-24	2	5	399	402	11	11
7	1	4	211	210	10	9	5	4	411	439	8	8	415	369	8	137	103	19	10	14	4	215	223	13	-24	2	5	399	402	11	11
9	1	4	155	126	20	11	5	4	411	439	8	8	415	369	8	137	103	19	10	14	4	215	223	13	-24	2	5	399	402	11	11
11	1	4	159	126	20	11	5	4	411	439	8	8	415	369	8	137	103	19	10	14	4	215	223	13	-24	2	5	399	402	11	11
13	1	4	171	125	19	13	5	4	411	439	8	8	415	369	8	137	103	19	10	14	4	215	223	13	-24	2	5	399	402	11	11
15	1	4	0	37	1	15	5	4	411	439	8	8	415	369	8	137	103	19	10	14	4	215	223	13	-24	2	5	399	402	11	11
17	1	4	80	50	31	17	5	4	411	439	8	8	415	369	8	137	103	19	10	14	4	215	223	13	-24	2	5	399	402	11	11
19	1	4	0	31	1	19	5	4	411	439	8	8	415	369	8	137	103	19	10	14	4	215	223	13	-24	2	5	399	402	11	11
21	1	4	140	178	35	21	5	4	411	439	8	8	415	369	8	137	103	19	10	14	4	215	223	13	-24	2	5	399	402	11	11
23	1	4	140	178	35	21	5	4	411	439	8	8	415	369	8	137	103	19	10	14	4	215	223	13	-24	2	5	399	402	11	11
25	1	4	140	178	35	21	5	4	411	439	8	8	415	369	8	137	103	19	10	14	4	215	223	13	-24	2	5	399	402	11	11
27	1	4	140	178	35	21	5	4	411	439	8	8	415	369	8	137	103	19	10	14	4	215	223	13	-24	2	5	399	402	11	11
29	1	4	140	178	35	21	5	4	411	439	8	8	415	369	8	137	103	19	10	14	4	215	223	13	-24	2	5	399	402	11	11
31	1	4	140	178	35	21	5	4	411	439	8	8	415	369	8	137	103	19	10	14	4	215	223	13	-24	2	5	399	402	11	11
33	1	4	140	178	35	21	5	4	411	439	8	8	415	369	8	137	103	19	10	14	4	215	223	13	-24	2	5	399	402	11	11
35	1	4	140	178	35	21	5	4	411	439	8	8	415	369	8	137	103	19	10	14	4	215	223	13	-24	2	5	399	402	11	11
37	1	4	140	178	35	21	5	4	411	439	8	8	415	369	8	137	103	19	10	14	4	215	223	13	-24	2	5	399	402	11	11
39	1	4	140	178	35	21	5	4	411	439	8	8	415	369	8	137	103	19	10	14	4	215	223	13	-24	2	5	399	402	11	11
41	1	4	140	178	35	21	5	4	411	439	8	8	415	369	8	137	103	19	10	14	4	215	223	13	-24	2	5	399	402	11	11
43	1	4	140	178	35	21	5	4	411	439	8	8	415	369	8	137	103	19	10	14	4	215	223	13	-24	2	5	399	402	11	11
45	1	4	140	178	35	21	5	4	411	439	8	8	415	369	8	137	103	19	10	14	4	215	223	13	-24	2	5	399	402	11	11
47	1	4	140	178	35	21	5	4	411	439	8	8	415	369	8	137	103	19	10	14	4	215	223	13	-24	2	5	399	402	11	11
49	1	4	140	178	35	21	5	4	411	439	8	8	415	369	8	137	103	19	10	14	4	215	223	13	-24	2	5	399	402	11	11
51	1	4	140	178	35	21	5	4	411	439	8	8	415	369	8	137	103	19	10	14	4	215	223	13	-24	2	5	399	402	11	11
53	1	4	140	178	35	21	5	4	411	439	8	8	415	369	8	137	103	19	10	14	4	215	223	13	-24	2	5	399	402	11	11
55	1	4	140	178	35	21	5	4	411	439	8	8	415	369	8	137	103	19	10	14	4	215	223	13	-24	2	5	399	402	11	11
57	1	4	140	178	35	21	5	4	411	439	8	8	415	369	8	137	103	19	10	14	4	215	223	13	-24	2	5	399	402	11	11
59	1	4	140	178	35	21	5	4	411	439	8	8	415	369	8	137	103	19	10	14	4	215	223	13	-24	2	5	399	402	11	11
61	1	4	140	178	35	21	5	4	411	439	8	8	415	369	8	137	103	19	10	14	4	215	223	13	-24	2	5	399	402	11	11
63	1	4	140	178	35	21	5	4	411	439	8	8	415	369	8	137	103	19	10	14	4	215	223	13	-24	2	5	399	402	11	11
65	1	4	140	178	35	21	5	4	411	439	8	8	415	369	8	137	103	19	10	14	4	215	223	13	-24	2	5	399	402	11	11
67	1	4	140	178	35	21	5	4	411	439	8	8	415	369	8	137	103	19	10	14	4	215	223	13	-24	2	5	399	402	11	11
69	1	4	140	178	35	21	5	4	411	439	8	8	415	369	8	137	103	19	10	14	4	215	223	13	-24	2	5	399	402	11	11
71	1	4	140	178	35	21	5	4	411	439	8	8	415	369	8	137	103	19	10	14	4	215	223	13	-24	2	5	399	402	11	11
73	1	4	140	178	35	21	5	4	411	439	8	8	415	369	8	137	103	19	10	14	4	215	223	13	-24	2	5	399	402	11	11
75	1	4	140	178	35	21	5	4	411	439	8	8	415	369	8	137	103	19	10	14	4	215	223	13	-24	2	5	399	402	11	11
77	1	4	140	178	35	21	5	4	411	439	8	8	415	369	8	137	103	19	10	14	4	215	223	13	-24	2	5	399	402	11	11
79	1	4	140	178	35	21	5	4	411	439	8	8	415	369	8	137	103	19	10	14	4	215	223	13	-24	2	5	399	402	11	11
81	1	4	140	178	35	21	5	4	411	439	8	8	415	369	8	137	103	19	10	14	4	215	223	13	-24	2	5	399	402	11	11
83	1	4	140	178	35	21	5	4	411	439	8	8																			

Table A7 (cont.)

-3	3	4	0	165	3	1	3	7	4	63	80	62	-10	12	4	547	549	9	-22	0	5	5	94	21	73	-12	4	5	60	89	60	
-1	3	4	178	130	15	10	13	5	7	191	179	15	-8	12	4	707	707	9	-20	0	5	5	25	110	24	-10	4	5	393	356	8	
1	3	4	220	236	13	9	13	7	7	215	179	13	-6	12	4	388	383	9	-18	0	5	5	119	184	34	-8	4	5	17	133	9	
3	3	4	169	164	1	1	1	7	7	4	0	6	-2	12	4	539	542	8	-16	0	5	5	38	244	42	-4	4	5	259	186	11	
5	3	4	104	142	24	24	13	11	7	119	83	31	0	12	4	678	684	8	-14	0	5	5	220	244	14	-4	4	5	194	163	12	
7	3	4	217	261	13	13	15	7	7	0	24	1	2	12	4	405	413	6	-12	0	5	5	396	424	23	0	4	5	175	159	12	
9	3	4	107	144	28	28	17	7	7	0	22	1	4	12	4	325	341	10	-10	0	5	5	128	213	23	2	4	5	90	51	15	
11	3	4	21	109	20	20	14	22	8	336	320	14	6	12	4	514	516	9	-8	0	5	5	488	590	7	6	4	5	123	139	18	
13	3	4	107	123	30	30	14	-22	8	4	330	320	10	12	4	327	332	11	-6	0	5	5	632	661	7	7	4	5	111	70	22	
15	3	4	0	123	31	31	14	-20	8	4	338	182	8	12	4	281	277	13	-2	0	5	5	885	903	8	8	4	5	109	136	24	
17	3	4	216	215	21	21	14	-16	8	4	602	609	12	12	4	246	267	15	0	0	5	5	316	340	8	12	4	5	52	116	52	
19	3	4	451	467	12	12	9	-12	8	4	583	579	9	14	12	4	76	116	75	2	0	5	5	339	336	8	14	4	5	109	56	29
-22	4	4	260	272	14	14	9	-10	8	4	688	663	8	-17	13	4	102	57	49	6	0	5	5	571	523	11	16	4	5	82	71	48
-24	4	4	812	815	8	8	9	-8	8	4	1156	1159	11	-13	13	4	145	65	28	6	0	5	5	246	197	16	18	4	5	50	42	58
-18	4	4	455	448	8	8	9	-6	8	4	610	613	7	-11	13	4	70	79	70	8	0	5	5	246	197	16	18	4	5	281	267	15
-16	4	4	752	757	8	8	9	-4	8	4	847	843	7	-9	13	4	54	95	53	12	0	5	5	92	86	42	-21	5	5	301	305	15
-12	4	4	435	448	8	8	9	-2	8	4	1396	1365	13	-7	13	4	86	104	47	14	0	5	5	0	24	37	-17	5	5	399	414	11
-10	4	4	1350	1351	12	12	9	2	8	4	930	927	8	-5	13	4	150	183	21	16	0	5	5	108	54	37	-15	5	5	515	515	9
-8	4	4	430	442	6	6	9	6	8	4	1229	1263	12	-3	13	4	115	133	28	18	0	5	5	416	387	13	-13	5	5	244	243	13
-6	4	4	696	698	11	11	9	8	8	4	866	851	9	-1	13	4	78	127	55	23	1	5	5	355	363	14	-11	5	5	310	302	10
-4	4	4	1362	1336	11	11	9	10	8	4	740	722	8	9	13	4	154	168	20	-21	1	5	5	190	202	20	-9	5	5	907	910	9
-2	4	4	698	708	11	11	9	12	8	4	617	592	8	7	13	4	82	133	60	-17	1	5	5	632	630	9	-7	5	5	317	324	8
0	4	4	1098	1118	10	10	9	14	8	4	326	327	12	11	13	4	0	86	1	-13	1	5	5	497	501	8	-3	5	5	298	278	8
2	4	4	516	522	7	7	17	16	8	4	359	349	14	13	13	4	117	55	30	-11	1	5	5	766	763	13	-1	5	5	545	528	7
4	4	4	436	437	8	8	9	-21	9	4	341	377	5	-12	14	4	279	291	16	-9	1	5	5	939	943	8	3	5	5	310	284	7
6	4	4	434	437	8	8	9	-19	9	4	78	0	28	-14	14	4	178	163	21	-5	1	5	5	761	738	7	5	5	5	524	527	7
8	4	4	434	437	8	8	9	-17	9	4	0	0	18	-6	16	5	0	12	1	-3	1	5	5	1619	1640	13	-16	5	5	794	794	6
10	4	4	434	437	8	8	9	-17	9	4	0	0	18	-6	16	5	0	12	1	-3	1	5	5	1619	1640	13	-16	5	5	794	794	6
12	4	4	434	437	8	8	9	-17	9	4	0	0	18	-6	16	5	0	12	1	-3	1	5	5	1619	1640	13	-16	5	5	794	794	6
14	4	4	434	437	8	8	9	-17	9	4	0	0	18	-6	16	5	0	12	1	-3	1	5	5	1619	1640	13	-16	5	5	794	794	6
16	4	4	434	437	8	8	9	-17	9	4	0	0	18	-6	16	5	0	12	1	-3	1	5	5	1619	1640	13	-16	5	5	794	794	6
18	4	4	434	437	8	8	9	-17	9	4	0	0	18	-6	16	5	0	12	1	-3	1	5	5	1619	1640	13	-16	5	5	794	794	6
20	4	4	434	437	8	8	9	-17	9	4	0	0	18	-6	16	5	0	12	1	-3	1	5	5	1619	1640	13	-16	5	5	794	794	6
22	4	4	434	437	8	8	9	-17	9	4	0	0	18	-6	16	5	0	12	1	-3	1	5	5	1619	1640	13	-16	5	5	794	794	6
24	4	4	434	437	8	8	9	-17	9	4	0	0	18	-6	16	5	0	12	1	-3	1	5	5	1619	1640	13	-16	5	5	794	794	6
26	4	4	434	437	8	8	9	-17	9	4	0	0	18	-6	16	5	0	12	1	-3	1	5	5	1619	1640	13	-16	5	5	794	794	6
28	4	4	434	437	8	8	9	-17	9	4	0	0	18	-6	16	5	0	12	1	-3	1	5	5	1619	1640	13	-16	5	5	794	794	6
30	4	4	434	437	8	8	9	-17	9	4	0	0	18	-6	16	5	0	12	1	-3	1	5	5	1619	1640	13	-16	5	5	794	794	6
32	4	4	434	437	8	8	9	-17	9	4	0	0	18	-6	16	5	0	12	1	-3	1	5	5	1619	1640	13	-16	5	5	794	794	6
34	4	4	434	437	8	8	9	-17	9	4	0	0	18	-6	16	5	0	12	1	-3	1	5	5	1619	1640	13	-16	5	5	794	794	6
36	4	4	434	437	8	8	9	-17	9	4	0	0	18	-6	16	5	0	12	1	-3	1	5	5	1619	1640	13	-16	5	5	794	794	6
38	4	4	434	437	8	8	9	-17	9	4	0	0	18	-6	16	5	0	12	1	-3	1	5	5	1619	1640	13	-16	5	5	794	794	6
40	4	4	434	437	8	8	9	-17	9	4	0	0	18	-6	16	5	0	12	1	-3	1	5	5	1619	1640	13	-16	5	5	794	794	6
42	4	4	434	437	8	8	9	-17	9	4	0	0	18	-6	16	5	0	12	1	-3	1	5	5	1619	1640	13	-16	5	5	794	794	6
44	4	4	434	437	8	8	9	-17	9	4	0	0	18	-6	16	5	0	12	1	-3	1	5	5	1619	1640	13	-16	5	5	794	794	6
46	4	4	434	437	8	8	9	-17	9	4	0	0	18	-6	16	5	0	12	1	-3	1	5	5	1619	1640	13	-16	5	5	794	794	6
48	4	4	434	437	8	8	9	-17	9	4	0	0	18	-6	16	5	0	12	1	-3	1	5	5	1619	1640	13	-16	5	5	794	794	6
50	4	4	434	437	8	8	9	-17	9	4	0	0	18	-6	16	5	0	12	1	-3	1	5	5	1619	1640	13	-16	5	5	794	794	6
52	4	4	434	437	8	8	9	-17	9	4	0	0	18	-6	16	5	0	12	1	-3	1	5	5	1619	1640	13	-16	5	5	794	794	6
54	4	4	434	437	8	8	9	-17	9	4	0	0	18	-6	16	5	0	12	1	-3	1	5	5	1619	1640	13	-16	5	5	794	794	6
56	4	4	434	437	8	8	9	-17	9	4	0	0	18	-6	16	5	0	12	1	-3	1	5	5	1619	1640	13	-16	5	5	794	794	6
58	4	4	434	437	8	8	9	-17	9	4	0	0	18	-6	16	5	0	12	1	-3	1	5	5	1619	1640	13	-16	5	5	794	794	6
60	4	4	434	437	8	8	9	-17	9	4	0	0	18	-6	16	5	0	12	1	-3	1	5	5	1619	1640	13	-16	5	5	794	794	6
62	4	4	434	437	8	8	9	-17	9	4	0	0	18	-6	16	5	0	12	1	-3	1	5	5	1619	1640	13	-16	5	5	794	794	6
64	4	4	434	437	8	8	9	-17	9	4	0	0	18	-6	16	5	0	12	1													

Table A7 (cont.)

14	6	5	5	115	39	28	3	11	5	5	5	446	447	8	-14	0	0	6	6	6	6	432	407	9	4	4	4	4	6	1125	1139	11	-7	9	6	6	0	19	1	
16	6	5	5	75	74	16	5	11	5	5	5	419	426	9	-12	0	0	6	6	6	6	792	790	9	6	6	6	6	6	646	625	8	-5	9	6	6	140	115	20	
-11	7	5	5	274	270	14	7	11	5	5	5	234	248	14	-10	0	0	6	6	6	6	1174	1203	12	8	8	8	8	8	617	585	8	-1	9	6	6	58	63	33	
-19	7	5	5	246	234	16	9	11	5	5	5	239	257	15	-8	0	0	6	6	6	6	956	947	10	10	10	10	10	10	817	789	8	1	9	6	6	209	201	13	
-17	7	5	5	447	462	11	11	11	5	5	5	373	352	11	-6	0	0	6	6	6	6	761	759	8	12	12	12	12	12	484	494	13	1	9	6	6	82	113	43	
-15	7	5	5	624	633	9	13	11	5	5	5	175	188	21	-4	0	0	6	6	6	6	1214	1203	11	14	14	14	14	14	286	284	13	3	9	6	6	108	113	27	
-13	7	5	5	363	387	11	13	11	5	5	5	175	188	21	-4	0	0	6	6	6	6	1214	1203	11	14	14	14	14	426	414	10	5	9	6	6	146	165	20		
-11	7	5	5	666	655	8	13	11	5	5	5	135	126	32	-2	0	0	6	6	6	6	388	375	5	-23	5	5	5	5	143	57	33	9	9	6	6	58	126	58	
-9	7	5	5	1001	995	10	13	11	5	5	5	148	107	25	2	0	0	6	6	6	6	798	781	8	-19	5	5	5	5	33	9	33	9	11	9	6	6	0	120	-1
-7	7	5	5	690	689	8	13	11	5	5	5	237	214	15	4	0	0	6	6	6	6	1043	1043	10	-19	5	5	5	5	127	85	30	11	9	6	6	70	65	70	
-5	7	5	5	742	737	8	13	11	5	5	5	178	166	19	8	0	0	6	6	6	6	405	392	8	-17	5	5	5	5	142	165	28	13	9	6	6	168	122	23	
-3	7	5	5	1074	1077	10	13	11	5	5	5	210	227	15	10	0	0	6	6	6	6	397	382	9	-15	5	5	5	5	47	65	46	-20	10	6	6	277	263	15	
-1	7	5	5	995	977	10	13	11	5	5	5	250	241	13	12	0	0	6	6	6	6	584	559	8	-13	5	5	5	5	275	212	11	-18	10	6	6	398	393	12	
1	7	5	5	591	593	7	13	11	5	5	5	241	224	13	12	0	0	6	6	6	6	584	559	8	-13	5	5	5	5	186	87	15	-16	10	6	6	249	242	15	
3	7	5	5	824	818	9	13	11	5	5	5	258	278	12	14	0	0	6	6	6	6	145	116	22	-11	5	5	5	5	183	157	16	-14	10	6	6	336	335	12	
5	7	5	5	942	929	10	13	11	5	5	5	128	131	22	16	0	0	6	6	6	6	260	273	14	-9	5	5	5	5	83	18	31	-10	10	6	6	528	530	9	
7	7	5	5	385	393	9	13	11	5	5	5	280	290	11	-23	1	6	6	6	6	0	31	1	1	-5	5	5	5	5	313	270	9	-8	10	6	6	469	464	9	
9	7	5	5	475	467	9	13	11	5	5	5	129	164	24	-21	1	6	6	6	6	0	35	1	1	-3	5	5	5	5	71	18	54	-6	10	6	6	331	327	10	
11	7	5	5	592	592	8	13	11	5	5	5	199	183	36	-17	1	6	6	6	6	126	66	29	1	-1	5	5	5	5	58	40	57	-4	10	6	6	595	591	8	
13	7	5	5	299	291	11	13	11	5	5	5	236	254	16	-15	1	6	6	6	6	0	102	1	1	1	5	5	5	5	236	246	11	-2	10	6	6	628	610	8	
15	7	5	5	196	196	17	13	11	5	5	5	330	319	11	-13	1	6	6	6	6	49	14	49	12	3	5	5	5	175	160	14	0	10	6	6	310	313	7		
17	7	5	5	290	291	14	13	11	5	5	5	208	228	16	-11	1	6	6	6	6	45	18	45	13	7	5	5	5	36	52	36	2	10	6	6	511	507	8		
19	7	5	5	108	133	42	13	11	5	5	5	273	248	20	-9	1	6	6	6	6	305	251	10	9	5	5	5	5	0	25	64	1	4	10	6	6	539	543	8	
21	7	5	5	60	78	60	13	11	5	5	5	186	144	20	-7	1	6	6	6	6	202	139	12	11	5	5	5	5	65	25	64	6	10	6	6	371	371	10		
23	7	5	5	177	179	22	13	11	5	5	5	236	254	16	-5	1	6	6	6	6	49	14	49	12	11	5	5	5	65	25	64	12	10	6	6	445	411	10		
25	7	5	5	330	319	11	13	11	5	5	5	330	319	11	-3	1	6	6	6	6	313	287	10	13	5	5	5	5	99	2	34	8	10	6	6	243	256	16		
27	7	5	5	254	252	13	13	11	5	5	5	254	252	13	-1	1	6	6	6	6	255	267	10	13	5	5	5	5	166	200	25	12	10	6	6	148	101	26		
29	7	5	5	335	369	11	13	11	5	5	5	398	388	11	-1	1	6	6	6	6	298	300	9	16	5	5	5	5	618	639	9	-17	11	6	6	131	100	33		
31	7	5	5	529	577	8	13	11	5	5	5	318	323	15	3	1	6	6	6	6	159	192	11	14	5	5	5	5	502	506	9	-15	11	6	6	118	89	35		
33	7	5	5	483	500	7	13	11	5	5	5	318	323	15	5	1	6	6	6	244	259	11	14	5	5	5	5	618	639	9	-13	11	6	6	122	119	30			
35	7	5	5	412	445	8	13	11	5	5	5	317	345	12	7	1	6	6	6	198	232	14	28	11	5	5	5	502	506	9	-11	11	6	6	103	99	35			
37	7	5	5	593	590	7	13	11	5	5	5	317	345	12	9	1	6	6	6	112	144	28	33	11	5	5	5	502	506	9	-9	11	6	6	161	161	20			
39	7	5	5	464	463	8	13	11	5	5	5	240	217	15	11	1	6	6	6	103	160	33	32	11	5	5	5	502	506	9	-7	11	6	6	200	200	16			
41	7	5	5	336	329	10	13	11	5	5	5	240	217	15	13	1	6	6	6	103	160	33	32	11	5	5	5	502	506	9	-5	11	6	6	161	161	20			
43	7	5	5	344	307	10	13	11	5	5	5	296	285	13	15	1	6	6	6	105	123	32	32	11	5	5	5	502	506	9	-3	11	6	6	200	200	16			
45	7	5	5	244	208	12	13	11	5	5	5	296	285	13	17	1	6	6	6	105	123	32	32	11	5	5	5	502	506	9	-1	11	6	6	161	161	20			
47	7	5	5	139	158	17	13	11	5	5	5	296	285	13	17	1	6	6	6	105	123	32	32	11	5	5	5	502	506	9	1	11	6	6	161	161	20			
49	7	5	5	210	158	17	13	11	5	5	5	296	285	13	17	1	6	6	6	105	123	32	32	11	5	5	5	502	506	9	3	11	6	6	161	161	20			
51	7	5	5	0	0	1	13	11	5	5	5	296	285	13	17	1	6	6	6	105	123	32	32	11	5	5	5	502	506	9	5	11	6	6	161	161	20			
53	7	5	5	68	39	67	13	11	5	5	5	296	285	13	17	1	6	6	6	105	123	32	32	11	5	5	5	502	506	9	7	11	6	6	161	161	20			
55	7	5	5	254	241	17	13	11	5	5	5	296	285	13	17	1	6	6	6	105	123	32	32	11	5	5	5	502	506	9	9	11	6	6	161	161	20			
57	7	5	5	185	182	22	13	11	5	5	5	296	285	13	17	1	6	6	6	105	123	32	32	11	5	5	5	502	506	9	11	11	6	6	161	161	20			
59	7	5	5	386	396	12	13	11	5	5	5	296	285	13	17	1	6	6	6	105	123	32	32	11	5	5	5	502	506	9	13	11	6	6	161	161	20			
61	7	5	5	504	501	12	13	11	5	5	5	296	285	13	17	1	6	6	6	105	123	32	32	11	5	5	5	502	506	9	15	11	6	6	161	161	20			
63	7	5	5	297	274	12	13	11	5	5	5	296	285	13	17	1	6	6	6	105	123	32	32	11	5	5	5	502	506	9	17	11	6	6	161	161	20			
65	7	5	5	518	512	9	13	11	5	5	5	296	285	13	17	1	6	6	6	105	123	32	32	11	5	5	5	502	506	9	19									

Table A7 (cont.)

Table A7 (cont.)	5	9	5	5	641	639	8	-7	15	5	368	360	11	14	2	6	228	252	15	-3	7	6	134	131	21	4	12	6	538	628	9	
	5	9	5	5	360	346	10	-3	15	5	282	375	10	-23	3	6	338	335	12	-1	7	6	70	27	55	6	12	6	375	365	10	
	9	9	5	5	410	395	10	-3	15	5	463	475	10	-21	3	6	90	42	66	3	7	6	180	194	14	8	12	6	392	385	11	
	11	9	5	5	466	450	16	1	15	5	366	380	11	-19	3	6	0	10	45	5	7	6	135	152	21	-17	13	6	0	22	1	
	13	9	5	5	260	270	16	3	15	5	339	337	11	-17	3	6	95	6	55	7	7	6	98	101	29	-15	13	6	0	22	37	
	15	9	5	5	162	178	22	5	15	5	379	384	11	-15	3	6	84	46	37	9	7	6	180	174	15	-13	13	6	111	25	43	
	20	10	5	5	26	1	25	5	15	5	374	340	11	-13	3	6	93	19	55	7	7	6	112	161	30	-11	13	6	43	25	43	
	-2	10	5	5	0	29	1	12	15	5	285	340	11	-11	3	6	0	65	1	11	7	6	0	99	1	-9	13	6	43	25	43	
	-16	10	5	5	40	58	40	-12	16	5	50	224	17	-9	3	6	192	104	14	13	7	6	0	104	1	-7	13	6	77	60	77	
	-12	10	5	5	0	8	1	-10	16	5	70	37	69	-7	3	6	60	111	6	15	7	6	100	112	40	-5	13	6	30	10	29	
	-10	10	5	5	67	63	66	-8	16	5	55	61	54	-5	3	6	111	47	1	-20	8	6	231	185	15	-3	13	6	67	81	66	
	-1	13	6	6	89	34	39	-4	2	7	355	303	9	-5	7	7	0	532	8	-5	13	7	488	465	9	3	3	8	87	46	30	
	-1	13	6	6	58	40	58	-2	2	7	19	48	18	-3	7	7	707	689	8	-1	13	7	333	357	11	3	3	8	148	151	17	
	3	13	6	6	111	47	30	2	2	7	292	295	6	-1	7	7	355	354	9	-1	13	7	435	406	10	10	7	3	8	109	93	24
	5	13	6	6	116	63	30	2	2	7	0	68	1	1	7	7	405	399	8	-1	13	7	339	396	11	3	3	8	0	0	3	
	7	13	6	6	77	10	77	4	2	7	159	189	16	1	7	7	553	554	8	3	13	7	339	396	11	3	3	8	148	151	17	
	9	13	6	6	21	21	59	6	2	7	0	188	17	7	7	7	344	339	10	5	13	7	357	347	11	11	3	8	0	0	3	
	-14	14	6	6	212	248	15	10	2	7	169	0	42	11	7	7	280	294	19	-12	14	7	0	27	1	-20	4	8	72	23	71	
	-12	14	6	6	263	248	15	8	2	7	53	29	52	11	7	7	74	31	74	-18	4	8	364	374	11	-16	4	8	41	400	11	
	-10	14	6	6	377	366	11	12	2	7	81	89	49	13	7	7	249	237	10	-6	14	7	0	13	1	-14	4	8	209	201	15	
	-8	14	6	6	354	331	11	14	2	7	254	264	16	-20	8	7	71	61	70	-8	14	7	55	10	54	-12	4	8	522	516	9	
	-6	14	6	6	395	379	10	-19	3	7	356	359	12	-18	8	7	210	159	17	-4	14	7	34	17	34	-10	4	8	538	533	9	
	-4	14	6	6	427	416	10	-17	3	7	674	676	9	-16	8	7	118	96	35	-2	14	7	0	22	1	-8	4	8	350	345	9	
	-2	14	6	6	280	288	12	-13	3	7	506	512	9	-14	8	7	200	141	16	0	14	7	48	10	48	-4	4	8	353	351	8	
	0	14	6	6	336	343	11	-11	3	7	559	558	8	-12	8	7	230	212	15	2	14	7	0	28	1	-2	4	8	267	263	10	
	2	14	6	6	376	370	11	-9	3	7	951	947	9	-10	8	7	310	248	11	4	14	7	0	28	1	0	4	8	303	315	6	
	4	14	6	6	264	250	14	-7	3	7	927	911	10	-8	8	7	227	169	12	-9	15	7	180	207	16	2	4	8	468	477	8	
	6	14	6	6	248	236	15	-5	3	7	764	778	6	-6	8	7	341	314	10	-7	15	7	243	168	17	6	4	8	338	335	9	
	8	14	6	6	250	232	15	-7	3	7	930	932	12	-4	8	7	325	298	11	-5	15	7	214	207	15	8	4	8	190	141	13	
	-13	15	6	6	90	32	56	-3	3	7	1292	1248	8	-2	8	7	260	252	17	-3	15	7	204	229	17	8	4	8	306	278	10	
	-11	15	6	6	0	8	1	-1	3	7	766	795	8	0	8	7	277	267	17	-1	15	7	199	203	16	10	4	8	246	258	13	
	-9	15	6	6	115	65	34	-1	3	7	812	804	10	6	8	7	315	312	10	3	15	7	173	132	18	12	4	8	79	95	49	
	-7	15	6	6	45	23	45	3	3	7	1028	1011	8	8	8	7	173	196	16	-4	16	7	126	120	28	12	4	8	0	46	1	
	-5	15	6	6	81	18	75	5	3	7	752	745	8	10	8	7	197	199	18	-6	16	7	135	121	25	-19	5	8	0	51	1	
	-3	15	6	6	75	1	1	7	3	7	512	494	8	12	8	7	109	120	31	-2	16	7	87	115	25	-17	5	8	82	79	50	
	-1	15	6	6	0	1	1	11	3	7	597	585	9	19	8	7	112	98	29	-22	0	8	171	165	25	-15	5	8	0	36	1	
	3	15	6	6	103	49	34	13	3	7	552	552	15	-19	9	7	211	220	19	-20	0	8	115	100	37	-13	5	8	0	107	1	
	5	15	6	6	0	0	0	13	3	7	223	235	34	-17	9	7	293	299	14	-18	0	8	402	404	11	-9	5	8	0	87	31	
	-10	16	6	6	326	13	62	-22	4	7	111	0	20	-15	9	7	368	333	11	-16	0	8	474	466	8	-7	5	8	93	56	15	
	-8	16	6	6	251	264	16	-18	4	7	136	0	90	-13	9	7	203	171	17	-14	0	8	474	466	8	-3	5	8	171	197	15	
	-6	16	6	6	229	243	16	-16	4	7	60	18	60	-11	9	7	466	448	9	-12	0	8	472	467	8	-1	5	8	85	66	1	
	-4	16	6	6	279	284	14	-14	4	7	67	2	2	-9	9	7	397	393	10	-10	0	8	472	467	8	-1	5	8	0	16	1	
	-2	16	6	6	322	306	11	-12	4	7	77	0	0	-7	9	7	299	271	9	-10	0	8	472	467	8	-1	5	8	0	16	1	
	0	16	6	6	188	187	12	-10	4	7	77	36	28	-5	9	7	340	337	10	-6	0	8	315	301	12	3	5	8	67	50	35	
	2	16	6	6	232	232	15	-8	4	7	97	127	28	-3	9	7	535	516	8	-6	0	8	761	769	8	5	5	8	93	50	30	
	4	16	6	6	253	243	15	-6	4	7	0	65	55	-1	9	7	282	282	11	-2	0	8	268	277	16	9	7	5	8	67	50	30
	-7	17	6	6	85	129	59	-4	4	7	56	125	26	3	9	7	254	244	13	-2	0	8	288	277	16	8	5	8	0	18	1	
	-5	17	6	6	23	109	23	-2	4	7	105	125	26	3	9	7	479	455	8	0	0	8	587	583	9	-20	6	8	145	174	27	
	-3	17	6	6	86	109	47	-1	17	6	206	228	8	5	9	7	294	284	14	2	0	8	412	399	9	-20	6	8	0	262	287	15
	-1	17	6	6	0	120	-1	4	4	7	235	235	12	11	9	7	289	275	12	6	0	8	351	352	10	-18	6	8	388	380	11	
	-22	0	7	7	157	141	30	6	4	7	97	75	31	11	9	7	289	273	13	8	0	8	361	352	10	-16	6	8	0	388	380	11

Table A7 (cont.)

-20	0	7	160	115	25	8	4	7	0	52	1	-18	10	7	130	88	32	10	0	8	390	371	10	-14	6	8	182	144	17
-18	0	7	355	313	12	10	4	7	31	36	31	-16	10	7	149	101	25	12	0	8	181	193	18	-12	6	8	394	336	10
-16	0	7	329	249	12	12	4	7	64	75	63	-14	10	7	239	100	14	-19	1	8	0	2	23	-10	6	8	521	521	8
-14	0	7	411	389	9	14	5	7	55	11	54	-12	10	7	152	123	21	-17	1	8	148	38	24	-8	6	8	188	209	9
-12	0	7	404	358	8	19	5	7	240	272	16	-8	10	7	157	123	21	-13	1	8	142	95	24	-6	6	8	365	370	8
-10	0	7	721	647	7	19	5	7	286	398	11	-6	10	7	183	137	16	-17	1	8	0	95	24	-4	6	8	517	513	9
-8	0	7	494	422	7	17	5	7	635	648	9	-4	10	7	98	97	35	-13	1	8	142	78	20	-2	6	8	373	370	9
-6	0	7	654	587	7	15	5	7	633	655	9	-4	10	7	168	162	18	-11	1	8	31	26	31	0	6	8	179	178	8
-4	0	7	805	741	9	13	5	7	567	585	8	-2	10	7	102	108	15	-9	1	8	26	88	26	2	6	8	322	334	10
-2	0	7	509	479	7	11	5	7	945	951	10	0	10	7	131	108	15	-7	1	8	78	56	33	6	6	8	159	159	18
0	0	7	496	483	10	9	5	7	1063	1098	11	2	10	7	118	94	25	-3	1	8	55	72	54	10	6	8	273	257	12
2	0	7	707	686	8	7	5	7	770	722	11	4	10	7	0	67	1	-1	1	8	140	146	16	10	6	8	299	306	12
4	0	7	290	306	10	5	5	7	1105	1122	11	6	10	7	34	30	33	3	1	8	0	4	17	-19	7	8	99	74	44
6	0	7	331	346	11	3	5	7	1177	1162	11	8	10	7	81	90	56	5	1	8	146	96	17	-17	7	8	0	14	1
8	0	7	305	343	11	1	5	7	894	902	9	10	10	7	395	355	14	3	1	8	149	138	17	-15	7	8	92	66	45
10	0	7	229	250	14	3	5	7	765	764	8	10	10	7	0	26	1	5	1	8	146	44	1	-13	7	8	53	6	53
12	0	7	155	194	21	5	5	7	697	684	8	11	11	7	395	393	13	11	1	8	0	72	32	-9	7	8	113	7	24
14	0	7	155	194	21	5	5	7	481	464	8	11	11	7	318	355	14	11	1	8	101	53	67	-9	7	8	90	49	35
16	0	7	390	361	13	9	5	7	657	644	8	11	11	7	554	542	9	11	1	8	68	124	24	-7	7	8	90	49	35
18	0	7	194	230	23	9	5	7	429	430	10	-7	11	7	492	495	9	-20	2	8	359	362	11	-5	7	8	90	49	35
20	0	7	368	355	12	11	5	7	269	269	13	-7	11	7	610	605	8	-18	2	8	380	341	19	-3	7	8	20	59	20
22	0	7	620	605	9	13	5	7	133	97	28	-3	11	7	678	672	8	-16	2	8	161	164	19	-1	7	8	75	21	37
24	0	7	532	544	9	20	6	7	133	83	28	-3	11	7	516	523	8	-14	2	8	385	360	9	1	7	8	37	29	37
26	0	7	420	406	9	18	6	7	266	231	14	-1	11	7	524	512	8	-12	2	8	611	615	8	3	7	8	0	28	1
28	0	7	835	837	9	16	6	7	79	11	59	3	11	7	583	567	8	-10	2	8	168	136	15	5	7	8	52	20	52
30	0	7	853	850	9	14	6	7	370	328	10	5	11	7	446	438	10	-8	2	8	424	423	8	9	7	8	84	48	40
32	0	7	457	437	7	12	6	7	192	134	16	7	11	7	326	325	11	-6	2	8	565	561	8	9	7	8	50	18	50
34	0	7	827	822	8	10	6	7	187	165	16	9	11	7	382	367	11	-4	2	8	387	389	8	-18	6	8	234	236	15
36	0	7	925	920	7	8	6	7	305	250	9	-16	12	7	110	0	3	2	2	8	181	181	23	-16	8	8	111	116	32
38	0	7	503	500	7	6	6	7	253	215	12	-12	12	7	46	20	45	0	2	8	574	568	7	-14	8	8	231	236	15
40	0	7	776	750	8	4	6	7	212	181	13	-12	12	7	64	76	54	4	2	8	400	372	8	-12	8	8	251	246	14
42	0	7	502	497	8	2	6	7	113	86	15	-8	12	7	84	76	54	10	2	8	164	144	16	-10	8	8	345	357	11
44	0	7	502	497	8	0	6	7	307	312	9	-6	12	7	0	32	5	8	2	8	363	350	10	-8	8	8	101	156	33
46	0	7	260	231	11	2	6	7	36	35	36	-4	12	7	0	17	1	10	2	8	302	312	11	-6	8	8	246	237	12
48	0	7	518	495	11	4	6	7	66	79	65	-2	12	7	64	127	63	12	2	8	140	127	22	-4	8	8	438	425	9
50	0	7	358	369	11	8	6	7	52	27	52	0	12	7	45	9	45	12	2	8	97	26	41	-2	8	8	259	249	11
52	0	7	231	244	16	10	6	7	0	40	1	2	12	7	80	51	60	-19	3	8	0	63	1	0	8	8	227	229	17
54	0	7	43	43	42	12	6	7	212	212	19	4	12	7	76	74	75	-17	3	8	85	164	47	2	8	8	399	381	9
56	0	7	110	72	38	21	7	7	232	242	16	6	12	7	35	44	34	-13	3	8	65	127	65	6	8	8	355	343	10
58	0	7	219	175	17	19	7	7	232	242	16	6	12	7	35	44	34	-13	3	8	65	127	65	6	8	8	355	343	10
60	0	7	154	113	22	17	7	7	543	545	10	15	12	7	0	5	1	-11	3	8	218	289	13	10	8	8	333	319	11
62	0	7	217	241	10	15	7	7	315	308	12	15	12	7	0	5	1	-11	3	8	218	289	13	10	8	8	333	319	11
64	0	7	217	241	10	15	7	7	315	308	12	15	12	7	0	5	1	-11	3	8	218	289	13	10	8	8	333	319	11
66	0	7	217	241	10	15	7	7	315	308	12	15	12	7	0	5	1	-11	3	8	218	289	13	10	8	8	333	319	11
68	0	7	217	241	10	15	7	7	315	308	12	15	12	7	0	5	1	-11	3	8	218	289	13	10	8	8	333	319	11
70	0	7	217	241	10	15	7	7	315	308	12	15	12	7	0	5	1	-11	3	8	218	289	13	10	8	8	333	319	11
72	0	7	217	241	10	15	7	7	315	308	12	15	12	7	0	5	1	-11	3	8	218	289	13	10	8	8	333	319	11
74	0	7	217	241	10	15	7	7	315	308	12	15	12	7	0	5	1	-11	3	8	218	289	13	10	8	8	333	319	11
76	0	7	217	241	10	15	7	7	315	308	12	15	12	7	0	5	1	-11	3	8	218	289	13	10	8	8	333	319	11
78	0	7	217	241	10	15	7	7	315	308	12	15	12	7	0	5	1	-11	3	8	218	289	13	10	8	8	333	319	11
80	0	7	217	241	10	15	7	7	315	308	12	15	12	7	0	5	1	-11	3	8	218	289	13	10	8	8	333	319	11
82	0	7	217	241	10	15	7	7	315	308	12	15	12	7	0	5	1	-11	3	8	218	289	13	10	8	8	333	319	11
84	0	7	217	241	10	15	7	7	315	308	12	15	12	7	0	5	1	-11	3	8	218	289	13	10	8	8	333	319	11
86	0	7	217	241	10	15	7	7	315	308	12	15	12	7	0	5	1	-11	3	8	218	289	13	10	8	8	333	319	11
88	0	7	217	241	10	15	7	7	315	308	12	15	12	7	0	5	1	-11	3	8	218	289	13	10	8	8	333	319	11
90	0	7	217	241	10	15	7	7	315	308	12	15	12	7	0	5	1	-11	3	8	218	289	13	10	8	8	333	319	11
92	0	7	217	241	10	15	7	7	315	308	12	15	12	7	0	5	1	-11	3	8	218	289	13	10	8	8	333	319	11
94	0	7	217	241	10	15	7	7	315	308	12	15	12	7	0	5	1	-11	3	8	218	289	13	10	8	8	333	319	11
96	0	7	217	241	10	15	7	7	315	308	12	15	12	7	0	5	1	-11	3</										







Table A8: Observed and calculated structure factors for 39.

h	k	l	10Fo	10Fc	10s	h	k	l	10Fo	10Fc	10s	h	k	l	10Fo	10Fc	10s	h	k	l	10Fo	10Fc	10s
4	0	0	767	862	8	1	9	0	174	179	7	-9	6	1	264	281	9	0	10	1	638	654	11
6	0	0	1406	1774	12	2	9	0	257	231	6	-8	6	1	880	846	10	1	10	1	326	353	7
8	0	0	869	1073	10	10	1	1	561	656	29	-7	6	1	508	484	7	2	10	1	108	86	13
10	0	0	194	248	11	11	1	1	162	148	20	-6	6	1	522	506	7	3	10	1	385	436	7
1	1	0	1580	1421	5	5	9	0	428	432	7	-5	6	1	222	219	7	4	10	1	381	378	7
2	1	0	873	738	7	6	9	0	174	168	10	-4	6	1	719	690	8	5	10	1	371	387	7
3	1	0	565	551	7	7	9	0	701	692	9	-3	6	1	461	439	7	6	10	1	467	440	7
4	1	0	330	323	6	8	9	0	110	84	17	-2	6	1	1379	1325	10	7	10	1	314	337	8
5	1	0	1134	1082	11	9	9	0	397	404	17	-1	6	1	990	999	10	8	10	1	219	336	8
6	1	0	43	19	17	10	10	0	155	152	13	0	6	1	542	522	5	9	10	1	313	314	8
7	1	0	1076	1262	11	11	10	0	604	643	8	-2	6	1	958	1017	10	-8	11	1	216	188	10
8	1	0	409	498	8	12	10	0	1007	1029	11	-1	6	1	1326	1339	10	-7	11	1	63	28	23
9	1	0	487	592	8	13	10	0	215	227	11	3	6	1	462	441	6	-6	11	1	624	595	8
10	1	0	76	103	22	14	10	0	68	79	20	2	6	1	716	682	9	-5	11	1	656	653	8
11	1	0	106	115	20	15	10	0	145	140	11	6	6	1	225	218	7	-4	11	1	218	225	8
1	2	0	823	789	6	16	10	0	485	492	18	7	6	1	508	478	7	-3	11	1	885	891	10
2	2	0	1793	1705	7	17	10	0	160	164	12	4	6	1	832	841	10	-2	11	1	365	371	7
3	2	0	1015	922	9	18	10	0	944	907	11	5	6	1	281	288	8	-1	11	1	334	338	5
4	2	0	783	742	8	19	10	0	96	117	19	6	6	1	415	428	8	0	11	1	364	364	7
5	2	0	1006	980	11	20	10	0	624	617	18	7	6	1	317	305	8	1	11	1	878	923	10
6	2	0	1014	919	10	21	10	0	445	471	7	8	6	1	158	157	12	2	11	1	211	206	8
7	2	0	395	393	6	22	10	0	80	34	34	9	6	1	676	660	9	3	11	1	635	649	8
8	2	0	730	730	9	23	10	0	217	211	9	10	6	1	675	651	8	4	11	1	208	205	9
9	2	0	169	179	11	24	10	0	267	290	8	-7	7	1	390	350	7	5	11	1	611	594	9
10	2	0	270	271	8	25	10	0	556	530	10	-6	7	1	141	148	9	6	11	1	56	28	21
11	2	0	264	265	9	26	10	0	61	11	22	-5	7	1	782	724	9	7	11	1	200	197	11
1	3	0	480	455	5	27	10	0	797	760	9	-4	7	1	801	778	8	8	11	1	130	157	16
2	3	0	117	135	8	28	10	0	596	632	8	-3	7	1	929	893	9	-8	12	1	266	280	9
3	3	0	324	317	6	29	10	0	37	27	17	-2	7	1	792	755	6	-6	12	1	260	272	9
4	3	0	1998	1864	10	30	10	0	216	212	12	-1	7	1	119	119	9	-5	12	1	638	629	7
5	3	0	57	24	17	31	10	0	148	146	12	0	7	1	748	774	9	-4	12	1	305	276	7
6	3	0	138	115	9	32	10	0	216	212	12	1	7	1	893	907	9	-3	12	1	523	538	7
7	3	0	245	227	7	33	10	0	154	159	12	2	7	1	768	790	8	-2	12	1	398	401	7
8	3	0	370	380	7	34	10	0	443	439	8	3	7	1	751	733	9	-1	12	1	260	276	8
9	3	0	607	619	9	35	10	0	270	274	9	4	7	1	153	158	9	0	12	1	75	16	16
10	3	0	108	84	16	36	10	0	215	223	8	5	7	1	374	350	8	1	12	1	258	282	8
11	3	0	1693	1646	8	37	10	0	251	237	8	6	7	1	659	647	11	2	12	1	394	404	7
0	4	0	1693	1646	8	38	10	0	451	419	7	7	7	1	171	157	11	3	12	1	510	517	8
1	4	0	232	203	5	39	10	0	184	184	11	8	7	1	671	661	8	4	12	1	279	288	8
2	4	0	1412	1344	9	40	10	0	1699	1617	9	9	7	1	1284	1237	10	5	12	1	629	613	8
3	4	0	2720	2499	10	41	10	0	193	188	11	10	7	1	518	571	7	6	12	1	268	271	9
4	4	0	260	266	12	42	10	0	340	353	8	-10	8	1	1230	1247	13	7	12	1	275	271	9
5	4	0	1256	1205	12	43	10	0	277	278	9	-9	8	1	795	787	9	8	12	1	182	168	11
6	4	0	57	54	19	44	10	0	402	411	8	-8	8	1	160	169	11	9	12	1	208	212	10
7	4	0	111	81	12	45	10	0	317	321	7	-7	8	1	422	424	7	10	12	1	208	212	10
8	4	0	386	378	7	46	10	0	446	458	7	-6	8	1	331	333	8	-6	13	1	273	282	9
9	4	0	201	210	9	47	10	0	406	390	7	-5	8	1	52	56	21	7	13	1	423	396	7
10	4	0	239	202	9	48	10	0	70	68	23	-4	8	1	222	205	8	-4	13	1	739	719	10
1	5	0	555	544	7	49	10	0	799	746	9	-3	8	1	722	686	8	-3	13	1	310	316	7
2	5	0	1011	941	10	50	10	0	498	477	8	-2	8	1	908	885	10	-2	13	1	369	378	7
3	5	0	276	270	6	51	10	0	193	190	11	-1	8	1	859	795	9	-1	13	1	506	518	8
4	5	0	1422	1304	11	52	10	0	256	281	11	0	8	1	1027	1067	8	0	13	1	366	349	7
5	5	0	384	374	6	53	10	0	461	470	8	1	8	1	818	781	9	1	13	1	520	515	8

Table A8 (cont.)

6	5	0	0	44	32	18	3	15	0	0	308	312	8	-4	4	1	708	655	8	2	8	1	872	875	10	2	13	1	372	381	7
7	5	0	0	142	128	11	5	15	0	0	810	776	10	-3	4	1	1084	1049	10	4	8	1	712	677	8	3	13	1	311	303	8
8	5	0	0	366	361	8	5	15	0	0	245	342	8	-2	4	1	1050	953	9	4	8	1	240	246	7	4	13	1	420	397	10
9	5	0	0	111	85	15	6	15	0	0	244	219	10	-1	4	1	724	658	8	5	8	1	219	238	8	5	13	1	273	283	9
10	5	0	0	538	524	6	6	16	0	0	89	56	21	0	4	1	917	943	26	6	8	1	417	408	7	6	13	1	213	220	10
1	6	0	0	401	395	6	7	16	0	0	233	246	10	1	4	1	606	669	7	7	8	1	300	292	8	7	13	1	79	104	23
2	6	0	0	664	655	6	8	16	0	0	87	71	20	2	4	1	1010	978	7	8	8	1	880	867	11	-7	14	1	325	310	8
3	6	0	0	245	332	11	9	16	0	0	631	585	9	3	4	1	1061	1048	10	10	8	1	262	270	9	-5	14	1	560	521	8
4	6	0	0	556	506	7	10	16	0	0	296	311	9	4	4	1	689	655	8	9	8	1	331	333	8	-4	14	1	204	200	10
5	6	0	0	764	773	9	11	16	0	0	583	543	23	5	4	1	812	751	8	-9	9	1	77	99	22	-3	14	1	546	498	8
6	6	0	0	92	74	15	12	17	0	0	64	8	8	6	4	1	1220	1188	13	-8	9	1	535	538	8	-2	14	1	343	341	8
7	6	0	0	171	159	10	13	17	0	0	554	540	8	7	4	1	532	540	7	-7	9	1	611	606	8	-1	14	1	378	404	5
8	6	0	0	98	127	16	14	17	0	0	53	24	22	8	4	1	666	683	9	-6	9	1	142	159	11	0	14	1	336	340	8
9	6	0	0	376	386	8	15	18	0	0	241	240	10	9	4	1	445	441	7	-5	9	1	360	326	7	1	14	1	397	406	7
10	6	0	0	192	196	11	16	18	0	0	268	279	10	10	4	1	435	434	8	-4	9	1	435	434	7	2	14	1	318	345	8
1	7	0	0	177	179	6	17	0	0	1	68	88	12	-10	5	1	172	180	11	-3	9	1	737	745	8	3	14	1	522	505	8
2	7	0	0	883	877	9	18	0	0	1	538	622	24	-8	5	1	627	625	8	-2	9	1	224	186	6	4	14	1	203	199	10
3	7	0	0	961	967	12	19	0	0	1	1116	1204	53	-9	5	1	101	101	8	-1	9	1	70	54	11	5	14	1	543	524	8
4	7	0	0	1013	971	10	20	0	0	1	131	146	26	-6	5	1	649	594	8	2	9	1	201	226	7	6	14	1	292	328	9
5	7	0	0	257	251	7	21	0	0	1	138	165	14	-5	5	1	161	181	10	3	9	1	416	415	7	-6	15	1	199	186	11
6	7	0	0	414	405	7	22	0	0	1	116	130	13	-4	5	1	861	861	10	4	9	1	345	364	7	-5	15	1	230	217	10
7	7	0	0	605	589	8	23	0	0	1	539	669	10	-3	5	1	911	749	10	5	9	1	181	152	10	-4	15	1	303	291	8
8	7	0	0	96	71	18	24	0	0	1	101	114	23	-2	5	1	675	656	8	6	9	1	593	604	8	-3	15	1	189	205	11
9	7	0	0	64	64	23	25	0	0	1	527	680	7	0	5	1	457	451	4	8	9	1	134	109	14	-1	15	1	470	492	8
10	7	0	0	299	297	8	26	0	0	1	735	676	7	1	5	1	666	699	8	9	9	1	316	326	8	0	15	1	273	271	6
1	8	0	0	827	847	9	27	0	0	1	1623	1490	36	2	5	1	805	789	8	9	10	1	336	309	8	2	15	1	167	150	11
2	8	0	0	106	111	11	28	0	0	1	624	570	6	3	5	1	904	859	11	-9	10	1	349	341	8	3	15	1	207	192	10
3	8	0	0	477	466	11	29	0	0	1	493	455	18	4	5	1	167	175	7	-8	10	1	319	326	8	3	15	1	304	294	8
4	8	0	0	695	678	7	30	0	0	1	564	581	6	5	5	1	609	583	13	6	9	1	467	453	8	4	15	1	218	232	11
5	8	0	0	280	266	7	31	0	0	1	1473	1478	7	7	5	1	107	93	13	-5	10	1	394	383	7	5	15	1	186	176	11
6	8	0	0	89	50	15	32	0	0	1	555	657	7	6	5	1	608	593	8	4	10	1	379	363	7	6	15	1	72	65	23
7	8	0	0	63	39	21	33	0	0	1	1388	1463	84	8	5	1	284	231	7	-3	10	1	424	410	7	-4	16	1	39	20	19
8	8	0	0	555	550	8	34	0	0	1	857	932	46	9	5	1	598	627	8	-2	10	1	94	77	14	-3	16	1	144	155	14
9	8	0	0	256	258	9	35	0	0	1	1370	1473	77	10	6	1	193	170	10	-1	10	1	351	345	6	4	16	1	917	951	9
10	8	0	0	35	90	21	36	0	0	1	462	421	6	-2	8	2	699	698	8	3	13	2	227	219	9	5	2	3	438	489	6
1	16	1	1	129	166	15	37	0	0	2	1109	1001	12	3	8	2	803	790	9	4	13	2	227	219	9	6	2	3	318	353	7
2	16	1	1	316	319	8	38	0	0	2	468	469	7	4	8	2	130	110	11	5	13	2	481	461	8	7	2	3	616	651	8
3	16	1	1	668	666	8	39	0	0	2	1837	1669	10	5	8	2	375	385	7	6	13	2	222	207	10	8	2	3	397	448	18
4	16	1	1	317	325	8	40	0	0	2	473	457	6	6	8	2	266	259	11	7	13	2	324	336	8	9	2	3	407	446	16
5	16	1	1	173	162	12	41	0	0	2	887	865	9	7	8	2	728	717	9	-6	14	2	339	347	8	10	3	3	695	659	9
6	16	1	1	149	155	14	42	0	0	2	349	334	10	8	8	2	267	265	9	-5	14	2	336	366	8	8	3	3	661	634	8
7	16	1	1	35	22	17	43	0	0	2	822	852	9	9	9	2	438	410	8	-4	14	2	336	318	8	-8	3	3	448	446	7
8	16	1	1	85	58	10	44	0	0	2	446	438	6	-8	9	2	490	477	8	-3	14	2	438	430	8	-7	3	3	295	263	7
9	17	1	1	289	293	9	45	0	0	2	1707	1664	10	7	9	2	826	799	9	-2	14	2	435	440	8	-6	3	3	656	592	8
10	17	1	1	595	623	12	46	0	0	2	415	408	10	-6	9	2	569	547	8	0	14	2	441	432	16	-5	3	3	769	693	9
1	17	1	1	123	123	12	47	0	0	2	411	435	7	-5	9	2	580	574	8	1	14	2	57	100	22	-4	3	3	336	307	6
2	17	1	1	590	617	9	48	0	0	2	95	107	15	-4	9	2	601	611	7	2	14	2	426	452	8	-3	3	3	1619	1491	10
3	17	1	1	299	297	9	49	0	0	2	297	278	7	-3	9	2	250	233	10	3	14	2	432	436	8	-2	3	3	224	198	6
4	18	1	1	304	305	10	50	0	0	2	159	164	11	-2	9	2	918	898	10	4	14	2	319	324	8	-1	0	3	264	321	8
5	18	1	1	562	568	13	51	0	0	2	279	298	8	-1	9	2	1152	1146	12	5	14	2	376	358	8	0	3	3	78	85	8
6	18	1	1	304	306	9	52	0	0	2	423	398	8	0	9	2	500	546	11	5	14	2	376	358	8	0	3	3	78	85	8

Table A8 (cont.)

0	0	2	1765	1764	16	-9	5	2	228	229	9	1	2	9	2	1125	1158	12	-6	14	2	356	356	8	1	3	3	3	345	346	6
1	1	2	1433	1477	14	-8	5	2	251	250	8	3	3	9	2	875	886	7	-5	15	2	217	224	11	2	3	3	3	202	207	6
2	0	2	687	707	21	-6	5	2	452	438	7	3	3	9	2	229	230	8	-3	15	2	570	564	9	4	3	3	3	1473	1485	10
3	0	2	404	441	15	-5	5	2	317	296	12	4	5	9	2	595	594	8	-4	15	2	473	463	8	5	3	3	3	306	316	6
4	0	2	324	327	20	-4	5	2	1119	1024	10	5	9	9	2	538	554	8	-3	15	2	426	439	8	8	3	3	3	691	704	8
5	0	2	468	482	26	-5	5	2	2007	1852	11	6	9	9	2	553	543	8	-1	15	2	473	463	8	8	3	3	3	600	594	7
6	0	2	663	736	39	-2	5	2	1661	1531	10	7	9	9	2	805	782	8	-1	15	2	473	457	7	7	3	3	3	256	258	7
7	0	2	418	449	21	-3	5	2	1857	1733	10	8	9	9	2	475	481	8	0	15	2	66	76	17	8	3	3	3	403	419	7
8	0	2	482	534	22	-1	5	2	420	404	6	8	9	9	2	425	406	8	1	15	2	397	450	8	8	3	3	3	598	637	8
9	0	2	468	525	27	0	5	2	208	225	8	-9	10	2	2	53	69	21	2	15	2	263	262	8	10	3	3	3	619	654	9
10	0	2	65	77	16	-7	10	2	1717	1710	10	-8	10	2	2	619	597	9	3	15	2	423	440	8	-10	4	3	3	450	460	8
11	0	2	1032	961	10	3	5	2	1563	1522	10	-7	10	2	2	701	672	9	4	15	2	468	440	8	8	3	3	3	527	490	8
-1	1	2	1026	971	9	3	5	2	1869	1866	11	-6	10	2	2	523	496	8	5	15	2	556	559	10	-8	4	3	3	516	475	7
-2	1	2	470	472	6	5	5	2	1055	1016	10	-5	10	2	2	325	327	8	6	15	2	234	209	10	-7	4	3	3	345	328	6
-1	1	2	1337	1825	32	6	5	2	323	275	6	-4	10	2	2	184	187	10	-5	16	2	347	321	8	-6	4	3	3	329	327	6
0	1	2	647	650	7	7	5	2	424	446	7	-3	10	2	2	255	262	8	-3	16	2	440	427	8	-5	4	3	3	461	432	6
1	1	2	1747	1817	6	8	5	2	234	242	9	-2	10	2	2	637	618	8	-1	16	2	267	277	9	-3	4	3	3	851	786	9
2	1	2	416	449	6	9	5	2	237	208	7	-1	10	2	2	844	848	9	0	16	2	96	98	19	-1	4	3	3	1459	1360	10
3	1	2	922	961	9	10	5	2	396	399	7	0	10	2	2	1045	1065	27	1	16	2	258	276	9	0	4	3	3	894	860	9
4	1	2	900	944	10	-10	5	2	237	208	7	1	10	2	2	802	841	9	1	16	2	358	359	8	1	4	3	3	107	110	6
5	1	2	749	818	26	6	6	2	298	292	8	3	10	2	2	622	622	7	2	16	2	333	359	8	2	4	3	3	833	872	9
6	1	2	255	277	24	-8	6	2	323	323	8	4	10	2	2	425	427	8	3	16	2	425	427	8	2	4	3	3	1339	1366	10
7	1	2	880	936	9	-6	6	2	266	265	14	5	10	2	2	251	263	10	4	16	2	251	263	10	4	4	3	3	418	415	6
8	1	2	310	335	12	-4	6	2	99	103	9	6	10	2	2	355	338	8	5	16	2	355	338	8	5	4	3	3	305	305	6
9	1	2	187	213	12	-5	6	2	814	738	9	8	10	2	2	179	178	11	-2	17	2	179	168	12	6	4	3	3	320	338	6
10	1	2	385	438	16	-3	6	2	1081	1018	12	-8	10	2	2	603	602	8	0	17	2	231	238	13	7	4	3	3	461	460	7
11	1	2	170	186	11	-2	6	2	1560	1479	11	8	10	2	2	664	689	9	-2	17	2	231	238	13	8	4	3	3	561	593	8
-7	2	2	813	767	9	9	6	2	974	942	11	-8	11	2	2	39	63	19	1	17	2	153	145	9	8	4	3	3	470	495	8
-6	2	2	617	585	8	-1	6	2	1224	1191	10	-7	11	2	2	178	184	7	2	17	2	188	195	8	9	4	3	3	427	459	8
-5	2	2	723	666	6	0	6	2	415	428	4	-6	11	2	2	395	398	8	3	17	2	162	153	12	10	4	3	3	215	211	10
-4	2	2	388	360	8	1	6	2	1148	1163	10	-5	11	2	2	299	298	8	2	17	2	230	230	10	-10	5	3	3	598	563	8
-3	2	2	681	631	8	2	6	2	928	916	11	-4	11	2	2	148	147	7	3	17	2	160	174	9	-9	5	3	3	626	592	8
-2	2	2	839	752	8	3	6	2	1497	1475	11	-3	11	2	2	373	389	7	1	0	3	175	174	8	-7	5	3	3	599	549	8
-1	2	2	1631	1515	7	4	6	2	1022	1020	12	-2	11	2	2	614	624	8	0	18	3	1038	1052	8	-7	5	3	3	599	549	8
0	2	2	1920	1897	104	5	6	2	755	757	8	-1	11	2	2	1096	1089	11	3	0	3	57	35	10	-6	5	3	3	391	363	7
1	2	2	1492	1516	7	7	6	2	276	276	7	0	11	2	2	591	588	9	4	0	3	572	571	15	-5	5	3	3	314	310	6
2	2	2	800	796	8	8	6	2	323	324	7	1	11	2	2	1034	1082	11	5	0	3	47	445	24	-4	5	3	3	410	379	6
3	2	2	608	621	7	9	6	2	281	282	8	2	11	2	2	576	607	8	6	0	3	346	391	28	-7	5	3	3	1226	1145	11
4	2	2	339	333	6	10	6	2	437	453	8	3	11	2	2	370	385	7	7	0	3	399	467	29	-1	5	3	3	575	528	7
5	2	2	621	672	8	8	6	2	212	223	10	4	11	2	2	132	146	12	8	0	3	62	49	20	11	5	3	3	941	887	10
6	2	2	545	554	8	-10	7	2	524	509	9	5	11	2	2	281	273	8	9	0	3	489	549	32	0	5	3	3	833	878	8
7	2	2	729	776	6	8	6	2	35	76	17	6	11	2	2	380	410	8	10	0	3	165	176	10	2	5	3	3	493	518	6
8	2	2	482	542	22	-8	7	2	517	511	8	-6	11	2	2	696	689	11	-6	1	3	978	932	10	2	5	3	3	1121	1148	2
9	2	2	348	377	17	-6	7	2	299	263	7	-8	12	2	2	192	167	8	-5	1	3	874	776	10	4	5	3	3	376	382	6
10	2	2	128	130	27	-4	7	2	352	349	7	-7	12	2	2	406	406	8	-4	1	3	347	317	6	5	5	3	3	299	315	6
11	2	2	276	302	16	-5	7	2	1060	1007	12	-6	12	2	2	491	474	8	-3	1	3	459	437	6	6	5	3	3	356	371	7
-10	3	2	280	266	18	-3	7	2	813	769	10	-5	12	2	2	461	431	8	-2	1	3	824	830	9	7	5	3	3	538	549	8
-8	3	2	457	457	7	-1	7	2	580	595	6	-5	12	2	2	229	245	9	-1	1	3	1658	1610	20	8	5	3	3	567	576	8
-6	3	2	332	303	7	7	7	2	282	300	6	0	1	3	3	508	536	8	0	1	3	508	536	8	10	5	3	3	546	571	8
-5	3	2	206	187	7	-1	7	2	282	300	6	-3	12	2	2	129	138	8	1	1	3	1520	1590	20	8	5	3	3	255	198	10
-4	3	2	931	867	10	1	7	2	567	567	7	-2	12	2	2	235	245	9	2	1	3	762	788	6	9	10	5	3	350	345	8
-3	3	2	1418	1305	11	3	7	2	1007	1000	11	-1	12	2	2	493	493	8	3	1	3	433	386	6	-10	6	3	3	360	342	8
-2	3	2	761	665	8	4	7	2	1013	991	10	0	12	2	2	892	920	14	4	4	3	308	333	7	-9	6	3	3	683	618	8

Table A8 (cont.)

-2	3	2	732	672	7	7	330	331	7	2	12	2	472	498	7	6	1	3	857	923	9	-7	6	3	793	750	9	
-1	3	2	1176	1120	8	8	271	283	7	3	12	2	254	240	8	7	1	3	314	352	18	-6	6	3	807	765	9	
0	3	2	510	538	17	17	529	513	7	4	12	2	149	144	12	8	9	1	315	346	29	-5	6	3	364	329	7	
1	3	2	1096	1120	8	8	287	69	20	5	12	2	449	435	8	8	10	1	264	307	13	-4	6	3	572	529	7	
2	3	2	680	687	7	7	208	511	10	6	12	2	481	473	8	8	10	1	518	533	22	-3	6	3	359	318	6	
3	3	2	632	661	7	7	277	259	9	8	12	2	271	286	9	9	-8	2	236	221	8	-2	6	3	636	643	8	
4	3	2	1310	1292	11	11	704	704	9	8	12	2	421	407	8	8	-7	2	201	638	9	-1	6	3	1488	1446	10	
5	3	2	852	865	10	10	257	259	9	-7	13	2	223	201	10	10	-6	2	354	339	6	0	6	3	1177	1200	29	
6	3	2	179	211	7	7	162	157	11	-5	13	2	481	465	8	8	-5	2	501	464	11	2	6	3	1386	1451	10	
7	3	2	315	316	7	7	267	253	8	-5	13	2	231	217	9	9	-3	2	759	678	8	3	6	3	324	314	6	
8	3	2	433	452	7	7	397	396	7	-4	13	2	664	641	9	9	-2	2	689	669	8	4	6	3	535	530	7	
9	3	2	258	266	8	8	807	788	9	-3	13	2	244	250	9	9	-1	2	393	380	21	5	6	3	358	323	6	
-10	4	2	293	303	8	8	726	704	9	-2	13	2	529	555	8	8	0	2	1538	1634	8	6	6	3	738	779	9	
-9	4	2	155	156	12	12	430	424	6	-1	13	2	60	63	15	15	1	2	393	380	21	7	6	3	745	743	9	
-8	4	2	319	291	7	7	1191	1207	9	1	13	2	527	551	8	8	2	2	615	656	7	8	6	3	622	636	9	
-7	4	2	114	91	12	12	402	414	6	2	13	2	259	255	8	8	3	2	660	718	7	9	6	3	331	342	8	
-6	4	2	335	348	8	8	780	801	9	-7	1	4	378	359	7	7	0	5	4	709	749	6	-7	10	4	649	628	9
-5	6	3	81	86	21	21	635	623	9	-5	1	4	1048	996	11	11	1	5	4	548	580	7	-5	10	4	468	461	8
-4	7	3	470	478	8	8	265	303	9	-4	1	4	628	608	7	7	2	5	4	1459	1498	11	-4	10	4	493	473	8
-3	7	3	595	648	8	8	209	227	11	-3	1	4	357	334	6	6	3	5	4	548	580	7	-4	10	4	193	199	9
-2	7	3	585	567	8	8	175	176	12	-2	1	4	448	448	6	6	4	5	4	872	900	10	-3	10	4	545	543	8
-1	7	3	661	657	8	8	170	158	12	-1	1	4	669	654	7	7	5	5	4	196	216	9	-2	10	4	236	223	8
0	7	3	487	467	7	7	393	401	8	0	1	4	1953	1990	67	67	8	5	4	230	267	9	0	10	4	1382	1379	13
1	7	3	418	398	7	7	535	514	8	1	1	4	643	682	6	6	9	5	4	245	259	9	1	10	4	685	710	25
2	7	3	612	589	2	2	731	688	9	2	1	4	416	432	6	6	8	5	4	438	456	8	2	10	4	223	241	8
3	7	3	1278	1189	7	7	323	329	6	3	1	4	323	329	6	6	10	5	4	429	417	8	3	10	4	527	547	8
4	7	3	1278	1189	7	7	323	329	6	3	1	4	323	329	6	6	10	5	4	429	417	8	3	10	4	527	547	8
5	7	3	703	738	8	8	583	607	8	4	1	4	579	608	7	7	-9	6	4	248	244	9	5	10	4	464	459	7
6	7	3	654	680	8	8	599	607	8	5	1	4	952	1003	11	11	-8	6	4	248	244	9	6	10	4	464	459	7
7	7	3	1194	1207	11	11	351	397	7	6	1	4	341	354	7	7	-7	6	4	249	239	8	7	10	4	633	626	8
8	7	3	584	584	7	7	50	26	14	1	1	4	548	576	7	7	-6	6	4	249	239	8	8	10	4	633	626	8
9	7	3	374	418	7	7	384	396	7	8	1	4	548	576	7	7	-6	6	4	249	239	8	8	10	4	633	626	8
10	7	3	374	418	7	7	384	396	7	8	1	4	548	576	7	7	-6	6	4	249	239	8	8	10	4	633	626	8
11	7	3	374	418	7	7	384	396	7	8	1	4	548	576	7	7	-6	6	4	249	239	8	8	10	4	633	626	8
12	7	3	374	418	7	7	384	396	7	8	1	4	548	576	7	7	-6	6	4	249	239	8	8	10	4	633	626	8
13	7	3	374	418	7	7	384	396	7	8	1	4	548	576	7	7	-6	6	4	249	239	8	8	10	4	633	626	8
14	7	3	374	418	7	7	384	396	7	8	1	4	548	576	7	7	-6	6	4	249	239	8	8	10	4	633	626	8
15	7	3	374	418	7	7	384	396	7	8	1	4	548	576	7	7	-6	6	4	249	239	8	8	10	4	633	626	8
16	7	3	374	418	7	7	384	396	7	8	1	4	548	576	7	7	-6	6	4	249	239	8	8	10	4	633	626	8
17	7	3	374	418	7	7	384	396	7	8	1	4	548	576	7	7	-6	6	4	249	239	8	8	10	4	633	626	8
18	7	3	374	418	7	7	384	396	7	8	1	4	548	576	7	7	-6	6	4	249	239	8	8	10	4	633	626	8
19	7	3	374	418	7	7	384	396	7	8	1	4	548	576	7	7	-6	6	4	249	239	8	8	10	4	633	626	8
20	7	3	374	418	7	7	384	396	7	8	1	4	548	576	7	7	-6	6	4	249	239	8	8	10	4	633	626	8
21	7	3	374	418	7	7	384	396	7	8	1	4	548	576	7	7	-6	6	4	249	239	8	8	10	4	633	626	8
22	7	3	374	418	7	7	384	396	7	8	1	4	548	576	7	7	-6	6	4	249	239	8	8	10	4	633	626	8
23	7	3	374	418	7	7	384	396	7	8	1	4	548	576	7	7	-6	6	4	249	239	8	8	10	4	633	626	8
24	7	3	374	418	7	7	384	396	7	8	1	4	548	576	7	7	-6	6	4	249	239	8	8	10	4	633	626	8
25	7	3	374	418	7	7	384	396	7	8	1	4	548	576	7	7	-6	6	4	249	239	8	8	10	4	633	626	8
26	7	3	374	418	7	7	384	396	7	8	1	4	548	576	7	7	-6	6	4	249	239	8	8	10	4	633	626	8
27	7	3	374	418	7	7	384	396	7	8	1	4	548	576	7	7	-6	6	4	249	239	8	8	10	4	633	626	8
28	7	3	374	418	7	7	384	396	7	8	1	4	548	576	7	7	-6	6	4	249	239	8	8	10	4	633	626	8
29	7	3	374	418	7	7	384	396	7	8	1	4	548	576	7	7	-6	6	4	249	239	8	8	10	4	633	626	8
30	7	3	374	418	7	7	384	396	7	8	1	4	548	576	7	7	-6	6	4	249	239	8	8	10	4	633	626	8
31	7	3	374	418	7	7	384	396	7	8	1	4	548	576	7	7	-6	6	4	249	239	8	8	10	4	633	626	8
32	7	3	374	418	7	7	384	396	7	8	1	4	548	576	7	7	-6	6	4	249	239	8	8	10	4	633	626	8
33	7	3	374	418	7	7	384	396	7	8	1	4	548	576	7	7	-6	6	4	249	239	8	8	10	4	633	626	8
34	7	3	374	418	7	7	384	396	7	8	1	4	548	576	7	7	-6	6	4	249	239	8	8	10	4	633	626	8
35	7	3	374	418	7	7	384	396	7	8	1	4	548	576	7	7	-6	6	4	249	239	8	8	10	4	633	626	8
36	7	3	374	418	7	7	384	396	7	8	1	4	548	576	7	7	-6	6	4	249	239	8	8	10	4	633	626	8
37	7	3	374	418	7	7	384	396	7	8	1	4	548	576	7	7	-6	6	4	249	239	8	8	10	4	633	626	8
38	7	3	374	418	7	7	384	396	7	8	1	4	548	576	7	7	-6	6	4	249	239	8	8	10	4	633	626	8
39	7	3	374	418	7	7	384	396	7	8																		

Table A8 (cont.)

Table AB (cont.)	7	8	3	729	732	9	-5	14	3	281	272	9	-10	3	4	56	31	21	-3	7	4	1377	1324	12	-2	12	4	518	516	8	
	8	3	403	410	7	-4	14	3	284	263	8	-8	3	4	108	93	16	-2	7	4	988	928	10	-1	12	4	671	681	8		
	9	8	379	355	8	-3	14	3	295	282	9	-9	3	4	295	282	7	-1	7	4	513	479	7	0	12	4	146	142	26		
	-9	9	526	500	8	-2	14	3	246	229	9	-6	3	4	614	567	8	0	7	4	280	202	10	1	12	4	628	684	8		
	-8	9	345	323	8	-1	14	3	200	203	10	-3	3	4	394	345	7	1	7	4	473	501	6	2	12	4	485	516	8		
	-7	9	501	494	8	0	14	3	349	338	8	-5	3	4	1017	973	10	2	7	4	904	920	10	3	12	4	451	468	8		
	-6	9	358	315	7	-1	14	3	326	256	8	-4	3	4	784	706	8	3	7	4	1304	1329	12	4	12	4	225	194	9		
	-5	9	3	538	510	8	2	14	3	326	359	8	-3	3	4	801	827	9	4	7	4	801	827	9	5	12	4	482	465	8	
	-4	9	3	713	664	8	2	14	3	325	222	9	-2	3	4	1416	1345	9	6	7	4	686	731	8	6	12	4	205	198	10	
	-3	9	3	1085	1051	11	3	14	3	365	390	8	0	3	4	188	151	15	5	7	4	198	205	9	-7	12	4	170	149	12	
	-2	9	3	981	996	11	4	14	3	269	268	9	1	3	4	1275	1346	6	8	7	4	287	288	8	-6	13	4	378	367	8	
	-1	9	3	544	533	7	5	14	3	266	275	9	2	3	4	716	719	8	9	7	4	340	357	8	-5	13	4	321	309	8	
	0	9	3	532	542	7	6	14	3	268	288	9	3	3	4	702	733	8	-9	8	4	455	450	8	-4	13	4	313	299	8	
	1	9	3	936	993	11	-4	15	3	421	399	8	5	3	4	902	964	10	-8	8	4	286	267	8	-3	13	4	405	428	8	
	2	9	3	1038	1052	11	-3	15	3	283	233	9	5	3	4	339	363	7	-7	8	4	517	515	8	-2	13	4	482	459	7	
	3	9	3	669	654	8	-2	15	3	401	410	8	7	3	4	545	500	8	-6	8	4	432	429	7	0	13	4	613	618	9	
	4	9	3	320	319	7	-1	15	3	299	307	6	8	3	4	694	650	8	-5	8	4	432	429	7	1	13	4	430	472	8	
	5	9	3	508	506	8	0	15	3	381	404	7	8	3	4	522	302	8	-4	8	4	504	477	7	3	13	4	393	411	7	
	6	9	3	486	489	8	1	15	3	56	38	21	10	3	4	91	107	18	-3	8	4	634	610	8	3	13	4	301	302	8	
	7	9	3	334	325	8	2	15	3	290	200	8	-8	3	4	526	505	8	-2	8	4	1087	1071	12	4	13	4	313	325	8	
	8	9	3	495	504	8	3	15	3	386	401	8	-10	4	4	4	302	303	8	-1	8	4	841	847	35	5	13	4	212	213	10
	-9	10	3	247	242	10	-8	16	3	284	261	9	-8	4	4	228	209	8	2	8	4	609	620	8	7	13	4	168	150	12	
	-8	10	3	367	335	8	-7	16	3	171	161	12	-7	4	4	790	749	9	3	8	4	484	476	7	-6	14	4	238	244	10	
	-7	10	3	449	436	8	-6	16	3	251	238	10	-6	4	4	353	334	6	4	8	4	418	430	8	-5	14	4	156	159	13	
	-6	10	3	341	298	7	-5	16	3	233	231	10	-5	4	4	1308	1192	12	5	8	4	408	436	6	-4	14	4	556	572	8	
	-5	10	3	661	625	8	-4	16	3	200	175	10	-4	4	4	565	520	7	6	8	4	450	497	8	-3	14	4	474	440	8	
	-4	10	3	676	646	8	-3	16	3	236	245	10	-3	4	4	829	816	9	7	8	4	490	509	8	-2	14	4	447	449	8	
	-3	10	3	596	594	8	-2	16	3	249	230	9	-2	4	4	207	216	6	8	8	4	274	259	9	0	14	4	376	364	7	
	-2	10	3	549	532	7	-1	16	3	174	168	12	0	4	4	1077	1109	54	9	8	4	278	291	9	1	14	4	163	163	8	
	-1	10	3	434	433	7	0	16	3	198	185	11	1	4	4	197	187	6	-9	9	4	83	77	22	2	14	4	351	351	8	
	0	10	3	418	442	7	2	16	3	92	116	21	2	4	4	755	814	9	-8	9	4	731	694	9	3	14	4	432	437	7	
	1	10	3	526	538	8	-3	17	3	200	183	11	3	4	4	514	514	6	-7	9	4	443	415	8	4	14	4	434	446	8	
	2	10	3	579	610	8	-2	17	3	165	169	12	4	4	4	1205	1174	12	-6	9	4	445	446	8	5	14	4	132	155	16	
	3	10	3	649	662	8	-1	17	3	347	359	11	5	4	4	310	317	6	-5	9	4	303	278	7	6	14	4	224	239	10	
	4	10	3	611	638	8	0	17	3	161	162	12	6	4	4	743	725	8	-4	9	4	464	445	7	-5	15	4	277	275	9	
	5	10	3	312	321	8	1	17	3	187	178	11	8	4	4	197	210	9	-3	9	4	505	474	7	-4	15	4	173	161	12	
	6	10	3	424	433	8	2	17	3	144	108	13	9	4	4	77	12	20	-2	9	4	1293	1289	13	-4	15	4	230	245	10	
	7	10	3	343	338	8	3	17	3	345	328	14	10	4	4	470	511	9	-1	9	4	469	462	7	-3	15	4	244	244	9	
	8	10	3	245	241	10	4	17	3	489	515	18	-10	5	4	245	219	9	0	9	4	421	459	7	-2	15	4	222	250	10	
	-7	11	3	273	233	9	2	17	3	90	55	20	-9	5	4	475	461	8	2	9	4	1221	1278	13	0	15	4	342	365	7	
	-6	11	3	300	306	8	3	17	3	508	509	13	-8	5	4	270	282	8	3	9	4	476	491	7	1	15	4	222	243	9	
	-5	11	3	696	657	9	4	17	3	539	565	10	-7	5	4	258	258	8	5	9	4	430	447	7	2	15	4	230	237	9	
	-4	11	3	669	648	9	5	17	3	345	341	13	-6	5	4	222	204	8	6	9	4	282	275	7	3	15	4	249	250	10	
	-3	11	3	796	806	9	6	17	3	439	541	16	-5	5	4	962	911	11	7	9	4	431	445	8	4	15	4	141	154	15	
	-2	11	3	655	639	8	7	17	3	883	891	38	-4	5	4	947	883	10	6	9	4	404	422	9	-5	15	4	272	283	9	
	-1	11	3	397	388	7	8	17	3	523	673	36	-3	5	4	1591	1487	11	8	9	4	673	688	9	-4	16	4	418	416	12	
	0	11	3	68	74	15	9	17	3	47	47	15	-2	5	4	615	575	7	-3	9	4	85	76	22	-2	16	4	186	193	12	
	1	11	3	368	385	8	10	17	3	593	593	8	-1	5	4	780	736	9	-8	10	4	100	104	20	0	3	6	530	558	29	
	2	11	3	632	657	8	11	17	3	55	73	18	8	8	5	322	339	10	1	14	5	322	368	8	0	3	6	215	262	6	
	-1	16	4	176	190	15	-2	18	4	685	667	8	9	9	9	209	180	11	3	14	5	64	103	23	2	3	6	553	608	7	
	1	16	4	112	116	16	-1	18	4	5	769	774	-9	9	9	5	209	180	11	3	14	5	64	103	23	2	3	6	553	608	7

Table A8 (cont.)

Table A8 (cont.)	2	3	16	4	375	402	8	0	4	5	5	868	922	47	-8	9	9	5	342	301	8	4	14	5	452	475	8	3	3	6	1188	1247	12
	2	16	4	188	186	12	1	4	5	5	679	741	8	-7	9	9	5	242	234	9	5	14	5	341	333	8	4	3	3	3	305	325	7
	4	16	4	410	412	8	2	4	5	5	620	649	7	-6	9	9	5	506	485	8	6	14	5	270	267	9	5	3	3	3	365	404	7
	-2	17	4	152	182	14	3	4	5	5	74	96	15	-5	9	9	5	679	656	9	7	15	5	280	275	10	6	3	3	6	449	463	21
	-1	17	4	140	127	14	4	4	5	5	611	641	8	-4	9	9	5	64	38	21	8	15	5	268	275	9	8	3	3	6	605	627	8
	0	17	4	46	23	14	5	4	5	823	880	10	-3	9	9	5	703	673	8	9	15	5	410	382	8	10	3	3	6	423	443	8	
	1	17	4	113	121	17	6	4	5	209	208	8	-2	9	9	5	382	367	7	7	15	5	353	347	8	10	3	3	6	392	432	8	
	2	17	4	165	171	13	8	4	5	825	848	10	-1	9	9	5	411	385	7	8	15	5	469	473	19	10	4	4	6	433	419	8	
	3	17	4	308	322	9	9	4	5	123	131	14	0	9	9	5	733	738	24	8	15	5	365	367	8	-9	4	4	6	394	371	9	
	4	17	4	1147	1139	8	10	4	5	459	477	8	-1	9	9	5	359	376	7	7	15	5	377	397	9	-8	4	4	6	225	216	9	
	5	17	4	310	304	24	-10	4	5	281	302	10	2	9	9	5	654	665	8	8	15	5	279	267	9	-7	4	4	6	525	502	8	
	6	17	4	538	540	12	9	5	5	229	233	10	3	9	9	5	30	46	15	8	15	5	83	76	22	-5	4	4	6	608	576	7	
	7	17	4	512	502	25	-8	5	5	179	188	11	4	9	9	5	632	651	9	9	15	5	206	211	11	-5	4	4	6	343	338	7	
	8	17	4	824	834	18	-7	5	5	626	570	8	6	9	9	5	468	486	8	8	15	5	119	119	17	-4	4	4	6	1297	1205	13	
	9	17	4	249	250	11	-6	5	5	132	152	14	9	6	9	5	210	240	9	9	16	5	205	199	11	-3	4	4	6	397	359	6	
	10	17	4	288	331	38	-5	5	5	721	664	19	7	9	9	5	317	303	8	8	16	5	409	390	8	-2	4	4	6	1027	977	12	
	11	17	4	516	484	7	-8	10	9	117	121	13	9	9	9	5	187	192	11	11	16	5	145	140	11	-1	4	4	6	995	967	11	
	12	17	4	699	664	8	-7	10	9	699	664	8	-7	10	9	5	367	312	13	9	16	5	184	198	12	1	4	4	6	889	967	9	
	13	17	4	1287	1175	11	-6	10	9	1287	1175	11	-6	10	9	5	637	588	9	9	16	5	93	116	21	2	4	4	6	922	995	10	
	14	17	4	306	260	6	-5	10	9	306	260	6	-5	10	9	5	588	588	9	7	16	5	87	108	23	3	4	4	6	346	359	6	
	15	17	4	1543	1552	87	-4	10	9	1543	1552	87	-4	10	9	5	696	669	9	7	17	5	437	444	8	4	4	4	6	1187	1208	13	
	16	17	4	991	945	10	0	5	5	245	260	6	-3	10	9	5	429	410	9	9	17	5	112	105	17	5	4	4	6	329	346	7	
	17	17	4	1180	1126	13	1	5	5	1125	1168	17	-2	10	9	5	684	641	9	7	17	5	2015	2098	26	6	4	4	6	568	559	8	
	18	17	4	406	391	6	3	5	5	627	663	7	-1	10	9	5	484	499	7	7	17	5	63	43	12	8	4	4	6	220	202	9	
	19	17	4	772	759	8	4	5	5	470	498	11	0	10	9	5	40	23	13	7	17	5	280	263	7	9	4	4	6	344	376	8	
	20	17	4	717	656	17	6	5	5	139	125	11	2	10	9	5	449	504	7	8	17	5	352	352	5	-9	5	5	6	510	497	8	
	21	17	4	726	782	8	7	5	5	662	687	8	2	10	9	5	633	647	8	8	17	5	570	572	12	-8	5	5	6	157	168	12	
	22	17	4	388	395	6	8	5	5	158	150	11	3	10	9	5	695	686	8	8	17	5	349	382	12	-7	5	5	6	140	130	12	
	23	17	4	1532	1565	11	9	5	5	565	574	8	4	10	9	5	357	357	11	8	17	5	6	349	382	12	-6	5	5	6	536	493	8
	24	17	4	213	206	6	10	5	5	202	189	10	5	10	9	5	189	207	11	8	17	5	73	49	15	-4	5	5	6	691	678	8	
	25	17	4	1088	1117	10	-9	5	5	599	565	8	6	10	9	5	595	599	8	8	17	5	478	490	13	-3	5	5	6	669	620	8	
	26	17	4	900	958	10	-7	5	5	507	571	8	-8	10	9	5	308	316	13	9	17	5	137	150	14	-2	5	5	6	777	731	9	
	27	17	4	253	245	8	-6	5	5	584	545	8	-7	11	9	5	140	144	15	8	17	5	436	454	7	4	5	5	6	627	647	8	
	28	17	4	321	349	7	-5	5	5	547	514	8	-6	11	9	5	290	266	17	7	17	5	984	993	11	6	5	5	6	488	502	7	
	29	17	4	304	322	8	-4	5	5	549	514	8	-5	11	9	5	698	623	9	9	17	5	1352	1427	40	8	5	5	6	128	140	14	
	30	17	4	70	49	16	-3	5	5	469	471	7	-4	11	9	5	105	115	17	8	17	5	454	484	6	-9	5	5	6	156	162	12	
	31	17	4	431	414	7	-2	5	5	540	515	8	-3	11	9	5	189	164	10	8	17	5	935	1006	6	9	5	5	6	216	192	10	
	32	17	4	357	347	8	-1	5	5	722	718	9	-4	11	9	5	721	709	9	9	17	5	416	437	7	2	5	5	6	619	619	7	
	33	17	4	548	537	8	0	5	5	215	231	8	-2	11	9	5	146	129	11	7	17	5	436	454	7	4	5	5	6	597	628	8	
	34	17	4	611	611	8	-1	5	5	690	716	8	-1	11	9	5	293	299	7	7	17	5	984	993	11	6	5	5	6	627	647	8	
	35	17	4	658	620	8	1	5	5	489	505	7	0	11	9	5	128	128	12	7	17	5	474	483	7	7	5	5	6	488	502	7	
	36	17	4	181	169	8	2	5	5	504	519	7	1	11	9	5	279	289	7	8	17	5	1352	1427	40	8	5	5	6	128	140	14	
	37	17	4	611	606	8	3	5	5	519	519	7	2	11	9	5	118	125	14	9	17	5	454	484	6	-9	5	5	6	156	162	12	
	38	17	4	1501	1542	80	4	5	5	810	836	9	3	11	9	5	683	689	9	8	17	5	935	1006	6	9	5	5	6	216	192	10	
	39	17	4	437	437	7	6	5	5	543	545	8	4	11	9	5	176	174	11	8	17	5	416	437	7	-8	6	6	6	448	434	7	
	40	17	4	565	565	7	6	5	5	550	568	8	5	11	9	5	663	641	15	9	17	5	181	186	8	-6	6	6	6	668	624	8	
	41	17	4	171	175	7	7	5	5	121	119	15	6	11	9	5	116	117	15	8	17	5	567	590	8	-5	6	6	6	115	80	13	
	42	17	4	615	615	7	8	5	5	547	566	9	8	11	9	5	268	259	9	8	17	5	181	186	8	-4	6	6	6	755	730	9	
	43	17	4	171	175	7	-9	5	5	183	164	12	-7	12	9	5	134	145	13	9	17	5	828	870	9	-2	6						





Table A8 (cont.)

-2	9	6	200	211	9	4	15	6	154	142	13	9	4	5	7	329	326	8	-7	10	7	190	169	11	-2	1	8	446	459	7
-1	9	6	148	135	11	-2	16	6	399	408	11	-8	-8	5	7	280	267	9	-6	10	7	270	241	8	-1	1	8	633	706	8
0	9	6	322	319	17	0	16	6	186	176	8	-8	-8	5	7	644	594	8	-5	10	7	196	191	10	0	1	8	317	326	11
1	9	6	143	146	11	0	16	6	148	150	10	-6	-6	5	7	336	304	7	-4	10	7	590	541	8	1	1	8	665	708	8
2	9	6	183	183	7	0	16	6	176	172	12	-5	-5	5	7	682	609	9	-3	10	7	389	375	7	2	1	8	423	461	7
3	9	6	351	369	7	2	16	6	387	399	8	-5	-5	5	7	409	387	7	-1	10	7	357	366	7	3	1	8	1124	1173	13
4	9	6	166	168	11	2	16	6	426	433	8	-4	-4	5	7	84	79	17	-1	10	7	255	250	8	4	1	8	347	356	8
5	9	6	223	218	9	3	0	7	1014	1037	9	-3	-3	5	7	206	202	8	0	10	7	92	91	13	5	1	8	234	252	7
6	9	6	444	455	8	3	0	7	633	623	5	-2	-2	5	7	1004	978	11	1	10	7	225	261	8	6	1	8	316	330	7
7	9	6	142	140	13	5	0	7	1646	1633	27	-1	-1	5	7	595	565	7	2	10	7	335	365	7	8	1	8	476	478	8
8	9	6	258	266	9	5	0	7	610	608	8	0	0	5	7	1234	1258	31	3	10	7	364	378	7	9	1	8	554	561	8
-8	10	6	102	93	19	6	0	7	456	466	7	-1	-1	5	7	527	567	7	4	10	7	520	531	8	-9	2	8	365	367	8
-7	10	6	365	366	22	8	0	7	110	107	11	2	2	5	7	177	199	11	-8	10	7	172	181	12	-9	2	8	392	369	8
-6	10	6	62	67	22	8	0	7	123	121	11	3	3	5	7	934	999	11	-7	10	7	153	168	13	-6	2	8	667	631	8
-5	10	6	456	444	9	9	0	7	415	411	8	4	4	5	7	88	73	16	-5	10	7	167	149	12	-6	2	8	432	406	7
-4	10	6	210	206	9	-8	1	7	192	198	10	5	5	5	7	374	395	7	-4	10	7	82	77	22	-5	2	8	330	317	7
-3	10	6	345	356	9	-7	1	7	459	432	7	6	6	5	7	633	643	8	-6	11	7	539	465	8	-5	2	8	683	672	8
-2	10	6	213	203	8	-7	1	7	192	198	10	7	7	5	7	293	315	8	-4	11	7	178	163	11	-3	2	8	279	263	7
-1	10	6	585	581	7	-5	1	7	142	138	11	9	9	5	7	589	602	8	-3	11	7	436	406	7	-2	2	8	871	851	9
0	10	6	193	199	8	-4	1	7	980	972	10	-8	-8	5	7	242	282	10	-2	11	7	66	46	21	-1	2	8	764	789	9
1	10	6	544	576	8	-3	1	7	1617	1570	12	-6	-6	6	7	497	455	8	-1	11	7	183	177	10	0	2	8	729	796	8
2	10	6	322	348	7	-2	1	7	864	870	10	-7	-7	6	7	324	300	9	-1	11	7	142	130	10	2	2	8	793	853	10
3	10	6	190	191	10	-1	1	7	1090	1108	12	-6	-6	6	7	753	701	10	0	11	7	167	177	11	3	2	8	257	278	8
4	10	6	444	422	21	0	1	7	77	77	12	-5	-5	6	7	481	450	11	2	11	7	43	62	19	3	2	8	647	664	8
5	10	6	55	56	21	2	1	7	1050	1126	11	-3	-3	6	7	333	307	7	3	11	7	391	415	8	5	2	8	299	306	7
6	10	6	352	363	8	3	1	7	833	853	10	-2	-2	6	7	131	106	11	4	11	7	148	140	13	6	2	8	420	414	8
7	10	6	65	88	23	4	1	7	1542	1578	12	-1	-1	6	7	332	307	11	5	11	7	498	482	8	8	2	8	608	636	9
-6	11	6	113	114	17	3	1	7	653	691	8	-1	-1	6	7	747	724	8	6	11	7	122	86	15	8	2	8	356	375	8
-5	11	6	456	456	22	5	1	7	950	980	12	0	0	6	7	548	566	33	-1	12	7	143	143	14	9	2	8	346	365	8
-4	11	6	62	75	22	6	1	7	171	158	10	2	2	6	7	680	741	8	-6	12	7	180	166	12	-9	3	8	471	444	8
-3	11	6	395	367	7	8	1	7	440	434	7	3	3	6	7	147	139	10	-5	12	7	316	284	8	-8	3	8	298	265	8
-2	11	6	180	165	10	8	1	7	206	190	10	4	4	6	7	303	312	7	-3	12	7	458	423	8	-7	3	8	489	448	7
-1	11	6	288	283	7	-8	2	7	384	405	8	5	5	6	7	126	113	12	-3	12	7	293	284	8	-6	3	8	662	621	8
0	11	6	350	355	17	-8	2	7	290	281	8	6	6	6	7	423	443	7	-1	12	7	405	386	8	-5	3	8	392	395	7
1	11	6	268	282	18	-7	2	7	502	478	7	7	7	6	7	181	198	10	0	12	7	324	313	16	-4	3	8	1096	1061	11
2	11	6	185	202	10	-6	2	7	700	662	8	8	8	6	7	675	686	9	1	12	7	321	327	7	-3	3	8	180	182	9
3	11	6	151	161	12	-5	2	7	729	719	8	9	9	6	7	302	307	8	2	12	7	382	405	8	-1	3	8	606	605	8
4	11	6	359	367	22	-3	2	7	971	943	11	-8	-8	6	7	454	452	8	3	12	7	281	291	8	0	3	8	607	657	29
5	11	6	57	74	22	-3	2	7	1093	1048	13	-6	-6	7	7	345	319	7	4	12	7	413	431	8	1	3	8	569	593	7
6	11	6	439	457	8	-2	2	7	1085	1079	12	-5	-5	7	7	412	406	7	5	12	7	288	273	13	2	3	8	144	176	11
7	12	6	296	277	8	-1	2	7	732	702	8	-4	-4	7	7	364	338	7	-4	13	7	143	140	14	3	3	8	985	1046	11
-6	12	6	323	301	8	0	2	7	638	687	23	-3	-3	7	7	225	192	10	-2	13	7	159	171	13	4	3	8	126	164	13
-5	12	6	376	385	8	-1	2	7	667	702	8	-2	-2	7	7	151	144	7	-2	13	7	361	370	8	5	3	8	374	365	7
-4	12	6	164	152	12	3	2	7	1024	1053	12	0	0	7	7	290	272	7	0	13	7	109	115	17	3	3	8	602	626	8
-3	12	6	191	189	10	3	2	7	1027	1060	10	-1	-1	7	7	755	571	37	-1	13	7	88	85	20	7	3	8	444	442	8
-2	12	6	505	514	16	4	2	7	913	941	9	1	1	7	7	471	483	7	0	13	7	271	261	14	9	3	8	439	442	8
-1	12	6	43	44	16	6	2	7	686	715	8	2	2	7	7	152	164	10	2	13	7	123	106	14	9	4	8	392	391	7
0	12	6	479	503	7	8	2	7	646	657	7	3	3	7	7	200	215	9	-9	13	7	352	364	7	-8	4	8	376	343	7
1	12	6	196	199	10	9	2	7	487	474	9	4	4	7	7	269	283	7	-7	13	7	527	502	8	-7	4	8	269	239	8
2	12	6	157	155	12	-9	3	7	264	276	16	5	5	7	7	330	347	7	-6	14	7	115	99	16	-6	4	8	390	367	8
3	12	6	373	382	8	-8	3	7	158	151	12	6	6	7	7	380	401	8	-5	14	7	121	149	16	-5	4	8	435	408	7



Table AB (cont.)

-3	7	8	199	165	9	1	13	8	247	253	9	2	4	9	9	586	624	8	-2	10	9	476	458	7	-6	3	10	617	580	8
-2	7	8	589	549	7	2	13	8	532	558	14	3	4	9	9	482	501	11	-1	10	9	504	464	8	-5	3	10	328	310	7
-1	7	8	322	330	46	4	13	8	170	177	18	5	6	4	9	155	170	11	0	10	9	256	253	21	-4	3	10	323	300	7
0	7	8	870	885	46	4	13	8	476	496	8	6	4	9	9	486	496	8	1	10	9	424	476	8	-3	3	10	286	284	8
1	7	8	288	326	7	5	13	8	325	327	7	7	4	9	9	325	327	7	2	10	9	420	446	9	-2	3	10	422	405	7
2	7	8	513	538	7	4	13	8	434	449	8	8	4	9	9	434	449	8	3	10	9	738	775	9	-1	3	10	372	347	9
3	7	8	169	188	10	-4	14	8	465	472	8	8	5	9	9	465	472	8	4	10	9	475	477	8	0	3	10	339	343	9
4	7	8	469	492	7	-2	14	8	384	354	8	8	5	9	9	384	354	8	5	10	9	574	583	8	2	3	10	390	404	7
5	7	8	531	564	8	-1	14	8	606	591	8	8	5	9	9	606	591	8	6	10	9	294	306	9	3	3	10	261	288	8
6	7	8	494	540	8	0	14	8	459	420	8	8	5	9	9	459	420	8	3	10	9	404	390	8	4	4	10	295	292	8
7	7	8	186	214	11	1	14	8	637	614	9	8	5	9	9	148	174	12	5	11	9	637	554	8	5	3	10	287	314	8
8	7	8	280	290	9	2	14	8	521	502	8	8	5	9	9	379	353	7	-2	11	9	523	502	8	6	3	10	380	381	8
-8	7	8	76	71	22	3	14	8	379	353	7	7	-4	5	9	50	89	20	8	3	10	205	208	10	7	3	10	117	77	16
-7	7	8	328	311	8	-2	15	8	633	625	8	8	-5	9	9	512	477	7	0	11	9	68	69	16	-8	4	10	262	251	9
-6	7	8	401	398	8	-1	15	8	796	815	56	8	-3	9	9	633	625	56	1	11	9	189	206	11	-7	4	10	349	317	8
-5	7	8	424	391	8	0	15	8	580	619	8	8	5	9	9	580	619	8	2	11	9	488	504	8	-6	4	10	433	411	8
-4	7	8	624	610	8	1	15	8	459	487	7	7	4	11	9	459	487	7	3	11	9	511	547	8	-5	4	10	504	497	8
-3	7	8	319	316	7	2	15	8	350	388	8	8	3	11	9	359	367	7	4	11	9	394	382	8	-4	4	10	112	123	15
-2	7	8	380	365	7	1	15	8	459	487	7	7	3	11	9	459	487	7	5	11	9	326	295	9	-3	4	10	556	529	8
-1	7	8	495	497	8	2	15	8	437	479	5	5	5	9	9	426	422	8	3	12	9	426	421	8	-2	4	10	327	306	7
0	7	8	265	270	23	2	15	8	930	938	9	9	6	9	9	554	581	8	4	12	9	367	346	8	-1	4	10	419	438	10
1	7	8	452	498	7	3	15	8	130	131	5	5	6	9	9	368	361	8	5	11	9	426	421	8	0	4	10	291	315	8
2	7	8	340	363	7	4	15	8	499	499	20	20	8	5	9	41	81	10	3	12	9	213	309	8	2	4	10	59	48	21
3	7	8	294	311	7	5	15	8	110	101	7	7	8	6	9	113	173	13	4	12	9	313	309	8	3	4	10	510	533	8
4	7	8	572	595	8	6	15	8	178	192	8	8	-8	6	9	426	422	8	0	12	9	258	326	9	4	4	10	105	107	16
5	7	8	371	383	8	7	15	8	418	428	8	8	-7	6	9	554	581	8	1	12	9	367	346	8	5	4	10	479	489	8
6	7	8	397	395	8	8	15	8	63	34	16	16	-5	6	9	273	265	8	2	12	9	406	430	8	6	4	10	407	416	8
7	7	8	298	319	8	9	15	8	278	307	9	9	-4	6	9	39	56	18	3	12	9	353	362	8	7	4	10	300	318	9
8	7	8	64	76	23	9	15	8	89	105	20	20	-3	6	9	189	185	10	4	12	9	301	301	8	4	4	10	407	416	8
-7	7	8	378	341	8	-8	15	8	46	73	20	20	-3	6	9	412	368	7	5	12	9	280	285	10	6	4	10	256	238	10
-6	7	8	514	468	8	-7	15	8	154	150	11	11	-1	6	9	738	709	9	4	12	9	301	301	8	7	4	10	300	318	9
-5	7	8	506	481	8	-6	15	8	399	382	7	7	-1	6	9	1315	1318	72	5	12	9	280	285	10	4	4	10	170	165	12
-4	7	8	205	193	10	-5	15	8	596	589	8	8	0	6	9	665	719	9	-2	13	9	349	309	8	-7	5	10	445	432	8
-3	7	8	423	400	8	-4	15	8	350	335	7	7	1	6	9	354	366	7	-1	13	9	292	292	9	-5	5	10	200	185	10
-2	7	8	117	134	15	-3	15	8	104	107	14	14	2	6	9	197	188	9	0	13	9	98	78	28	-4	5	10	323	324	8
-1	7	8	560	520	8	-2	15	8	104	107	14	14	3	6	9	50	64	20	1	13	9	284	289	8	-3	5	10	454	442	7
0	7	8	522	538	35	-1	15	8	61	71	23	23	4	6	9	246	266	9	2	13	9	284	281	10	-2	5	10	138	138	13
1	7	8	500	523	7	0	15	8	114	88	12	12	5	6	9	631	649	8	3	13	9	313	300	9	-1	5	10	133	145	9
2	7	8	112	110	15	1	15	8	333	348	7	7	6	6	9	429	443	8	4	13	9	292	285	10	0	5	10	104	138	16
3	7	8	381	407	7	2	15	8	679	692	8	8	7	6	9	359	374	8	-2	14	9	292	273	9	1	5	10	421	449	7
4	7	8	188	173	11	3	15	8	578	589	8	8	8	6	9	466	443	8	-1	14	9	260	261	18	2	5	10	254	270	8
5	7	8	457	486	8	4	15	8	392	396	7	7	-7	7	9	264	271	10	0	14	9	318	318	12	4	5	10	297	320	8
6	7	8	462	468	8	5	15	8	135	134	13	13	-5	7	9	410	392	8	1	14	9	191	212	12	5	5	10	200	188	10
7	7	8	277	357	10	6	15	8	92	84	19	19	-3	7	9	363	333	7	0	14	9	270	278	9	6	5	10	418	427	8
-7	10	8	464	448	8	7	15	8	128	101	14	14	-3	7	9	118	111	14	2	14	9	132	140	9	5	5	10	174	165	12
-6	10	8	144	129	13	8	15	8	461	446	7	7	0	7	9	60	63	22	1	14	9	342	353	5	7	5	10	222	236	10
-5	10	8	81	68	21	-8	15	8	393	413	8	8	-2	7	9	951	979	50	2	12	9	208	228	10	2	10	12	222	236	10
-4	10	8	795	761	23	2	15	8	310	344	9	9	1	6	11	317	327	8	3	12	9	666	688	9	-1	11	12	238	226	10
-3	10	8	617	579	9	1	15	8	103	80	13	13	2	6	11	78	37	21	4	12	9	167	159	12	8	3	10	119	91	16
-2	10	8	121	126	15	3	15	8	75	44	19	19	3	6	11	135	161	14	5	12	9	311	301	8	1	11	12	235	221	10
-1	10	8	617	579	8	3	15	8	885	891	9	9	4	6	11	74	38	22	8	12	9	428	428	8	1	0	13	206	206	8
0	10	8	474	436	7	5	15	8	236	224	7	7	5	6	11	152	148	13	-6	14	9	294	294	7	2	0	13	133	438	6
-1	10	8	631	614	19	-1	15	8	128	142	11	11	-6	7	11	152	148	13	-5	14	9	2								

Table A8 (cont.)

1	6 10	568	610	8	7	0 11	43	25	14	-5	7 11	359	351	8	8	-4	3 12	470	444	8	4	0 13	491	488	7
2	6 10	431	453	7	8	-7	1 11	131	133	-3	7 11	392	365	8	8	-3	3 12	515	488	8	5	0 13	477	486	6
3	6 10	561	576	8	9	-6	1 11	326	300	-2	7 11	271	273	9	9	-2	3 12	483	465	8	-5	1 13	216	199	11
4	6 10	150	134	12	9	-4	1 11	233	233	-1	7 11	144	135	13	13	-1	3 12	495	489	8	-4	1 13	783	776	10
5	6 10	724	754	23	9	-4	1 11	984	948	0	7 11	729	715	9	9	0	3 12	126	107	21	-3	1 13	501	482	8
6	6 10	63	92	23	9	-3	1 11	108	82	0	7 11	198	202	7	7	1	3 12	464	468	8	-2	1 13	657	641	9
7	6 10	113	70	16	9	-2	1 11	625	612	1	7 11	667	716	14	14	2	3 12	474	484	8	0	1 13	217	217	10
-7	6 10	281	274	9	9	-1	1 11	205	207	2	7 11	130	142	14	14	4	3 12	472	444	8	0	1 13	75	70	16
-6	7 10	524	500	8	8	0	1 11	56	27	3	7 11	267	262	8	8	4	3 12	437	278	9	2	1 13	211	214	10
-5	7 10	432	408	8	8	1	1 11	177	195	5	7 11	352	353	8	8	5	3 12	272	297	9	3	1 13	616	629	9
-4	7 10	728	698	9	8	2	1 11	597	611	6	7 11	148	142	14	14	6	3 12	304	238	10	4	1 13	770	763	10
-3	7 10	532	471	8	8	3	1 11	942	944	5	7 11	349	353	8	8	-6	4 12	242	320	9	5	1 13	196	210	11
-2	7 10	609	589	8	8	4	1 11	248	294	-4	7 11	136	131	15	15	-5	4 12	306	212	9	-5	2 13	444	399	8
-1	7 10	511	490	8	8	5	1 11	302	294	-4	8 11	335	349	8	8	-4	4 12	252	212	9	-4	2 13	382	364	8
0	7 10	87	50	18	8	6	1 11	138	142	-1	8 11	286	278	8	8	-3	4 12	396	370	8	-3	2 13	516	478	8
1	7 10	464	484	8	8	7	1 11	200	190	-1	8 11	147	134	12	12	-2	4 12	271	264	8	-2	2 13	305	292	8
2	7 10	566	595	8	8	-7	2 11	116	111	0	8 11	624	642	39	39	-1	4 12	314	288	21	-1	2 13	372	362	16
3	7 10	463	471	8	8	-6	2 11	252	280	1	8 11	137	134	13	13	1	4 12	277	301	8	0	2 13	462	471	7
4	7 10	697	701	9	9	-5	2 11	272	239	2	8 11	259	275	9	9	2	4 12	258	266	9	2	2 13	356	371	7
5	7 10	391	408	8	8	-4	2 11	537	528	3	8 11	333	358	8	8	4	4 12	323	307	8	2	2 13	294	290	8
6	7 10	491	505	9	9	-3	2 11	290	295	4	8 11	142	137	14	14	5	4 12	236	231	10	3	2 13	484	486	9
7	7 10	258	272	9	9	-2	2 11	320	319	5	8 11	369	369	8	8	4	4 12	236	231	10	4	2 13	359	360	8
-6	8 10	410	389	8	8	-1	2 11	88	87	-5	9 11	223	210	11	11	-6	5 12	416	391	11	-5	3 13	545	518	10
-5	8 10	668	620	17	9	0	2 11	318	339	-4	9 11	723	694	9	9	-5	5 12	204	196	11	-4	3 13	83	75	22
-4	8 10	623	597	7	7	2	2 11	290	309	-3	9 11	55	426	8	8	-4	5 12	502	465	10	-3	3 13	435	421	8
-3	8 10	406	387	7	7	3	2 11	501	534	-2	9 11	438	426	8	8	-3	5 12	209	183	10	-2	3 13	466	444	8
-2	8 10	433	428	8	8	4	2 11	238	235	-1	9 11	250	247	9	9	-2	5 12	197	185	10	-1	3 13	58	57	16
-1	8 10	690	733	33	9	5	2 11	263	254	1	9 11	59	41	15	15	0	5 12	167	179	12	0	3 13	420	446	8
0	8 10	391	422	7	7	6	2 11	127	126	2	9 11	387	419	10	10	1	5 12	68	88	21	2	3 13	405	416	8
1	8 10	349	390	8	8	7	2 11	179	184	3	9 11	63	62	22	22	2	5 12	522	529	8	3	3 13	89	93	20
2	8 10	579	588	8	8	-7	3 11	408	380	4	9 11	662	684	10	11	3	5 12	196	187	10	4	3 13	506	507	8
3	8 10	72	114	23	9	-6	3 11	187	189	5	9 11	207	214	11	11	-4	5 12	455	456	8	5	3 13	261	253	9
4	8 10	626	612	9	9	-5	3 11	268	249	-4	10 11	495	465	24	24	6	5 12	471	380	9	-3	4 13	169	152	12
5	8 10	384	384	8	8	-4	3 11	375	363	-3	10 11	312	297	8	8	-5	6 12	224	216	10	-4	4 13	136	127	15
-6	9 10	250	250	10	8	-3	3 11	383	390	-2	10 11	363	349	8	8	-2	6 12	471	440	8	-3	4 13	234	249	10
-5	9 10	483	477	8	8	-2	3 11	724	708	0	10 11	312	297	8	8	0	6 12	224	216	10	-1	4 13	387	373	8
-4	9 10	553	521	8	8	-1	3 11	64	43	1	10 11	126	129	19	19	-4	6 12	176	159	12	0	4 13	632	638	16
-3	9 10	447	442	8	8	0	3 11	677	700	2	10 11	312	297	8	8	-5	6 12	224	216	10	-1	4 13	387	373	8
-2	9 10	225	201	10	10	1	3 11	627	382	7	10 11	126	129	19	19	-3	6 12	176	159	12	0	4 13	632	638	16
-1	9 10	570	562	9	9	3	3 11	362	356	7	10 11	270	293	9	9	-2	6 12	118	123	16	2	4 13	370	382	9
0	9 10	202	180	9	9	3	3 11	354	356	7	10 11	334	352	8	8	-1	6 12	394	369	8	2	4 13	236	247	9
1	9 10	527	549	8	8	5	3 11	384	399	8	10 11	454	472	15	15	0	6 12	49	26	15	3	4 13	144	168	13
2	9 10	199	217	10	10	6	3 11	170	184	12	10 11	56	79	23	23	1	6 12	338	382	8	4	4 13	142	142	13
3	9 10	405	432	8	8	7	3 11	383	393	8	10 11	120	95	16	16	0	6 12	49	26	15	5	4 13	125	116	15
4	9 10	507	525	8	8	-7	4 11	216	222	10	11 11	56	79	23	23	-3	6 12	189	174	10	-3	5 13	127	132	15
5	9 10	483	483	8	8	-6	4 11	431	423	8	11 11	45	45	22	22	5	6 12	432	437	8	-2	5 13	174	175	22
-6	10 10	262	251	15	15	-5	4 11	193	177	10	11 11	59	30	15	15	-4	6 12	280	276	9	-1	5 13	537	502	8
-5	10 10	146	142	12	12	-4	4 11	226	225	9	11 11	79	79	23	23	-3	7 12	462	443	8	0	5 13	316	296	13
-4	10 10	78	68	23	23	-3	4 11	183	164	11	11 11	170	172	12	12	-2	7 12	51	43	21	1	5 13	489	510	8
-3	10 10	185	192	12	12	-2	4 11	303	303	8	12 11	136	138	15	15	-1	7 12	403	383	8	2	5 13	163	162	13
-2	10 10	541	500	8	8	-1	4 11	423	402	8	12 11	87	55	17	17	0	7 12	158	175	12	1	5 13	183	183	13
-1	10 10	173	229	14	14	0	4 11	795	819	20	12 11	129	124	15	15	0	7 12	253	258	10	3	5 13	89	89	20
0	10 10	769	778	38	38	1	4 11	404	410	7	12 11	160	170	13	13	2	7 12	171	183	12	4	5 13	92	130	21
1	10 10	227	220	9	9	1	4 11	404	410	7	12 11	160	170	13	13	2	7 12	171	183	12	4	5 13	92	130	21

Table A8 (cont.)

Table A6 (Cont'd)	2	3	4	5	6	7	8	9	10	11	12	13	14	15	16	17	18	19	20	21	22	23	24	25	26	27	28	29	30
1	496	511	522	530	539	548	557	566	575	584	593	602	611	620	629	638	647	656	665	674	683	692	701	710	719	728	737	746	755
2	10	10	10	10	10	10	10	10	10	10	10	10	10	10	10	10	10	10	10	10	10	10	10	10	10	10	10	10	10
3	10	10	10	10	10	10	10	10	10	10	10	10	10	10	10	10	10	10	10	10	10	10	10	10	10	10	10	10	10
4	10	10	10	10	10	10	10	10	10	10	10	10	10	10	10	10	10	10	10	10	10	10	10	10	10	10	10	10	10
5	10	10	10	10	10	10	10	10	10	10	10	10	10	10	10	10	10	10	10	10	10	10	10	10	10	10	10	10	10
6	10	10	10	10	10	10	10	10	10	10	10	10	10	10	10	10	10	10	10	10	10	10	10	10	10	10	10	10	10
7	10	10	10	10	10	10	10	10	10	10	10	10	10	10	10	10	10	10	10	10	10	10	10	10	10	10	10	10	10
8	10	10	10	10	10	10	10	10	10	10	10	10	10	10	10	10	10	10	10	10	10	10	10	10	10	10	10	10	10
9	10	10	10	10	10	10	10	10	10	10	10	10	10	10	10	10	10	10	10	10	10	10	10	10	10	10	10	10	10
10	10	10	10	10	10	10	10	10	10	10	10	10	10	10	10	10	10	10	10	10	10	10	10	10	10	10	10	10	10
11	10	10	10	10	10	10	10	10	10	10	10	10	10	10	10	10	10	10	10	10	10	10	10	10	10	10	10	10	10
12	10	10	10	10	10	10	10	10	10	10	10	10	10	10	10	10	10	10	10	10	10	10	10	10	10	10	10	10	10
13	10	10	10	10	10	10	10	10	10	10	10	10	10	10	10	10	10	10	10	10	10	10	10	10	10	10	10	10	10
14	10	10	10	10	10	10	10	10	10	10	10	10	10	10	10	10	10	10	10	10	10	10	10	10	10	10	10	10	10
15	10	10	10	10	10	10	10	10	10	10	10	10	10	10	10	10	10	10	10	10	10	10	10	10	10	10	10	10	10
16	10	10	10	10	10	10	10	10	10	10	10	10	10	10	10	10	10	10	10	10	10	10	10	10	10	10	10	10	10
17	10	10	10	10	10	10	10	10	10	10	10	10	10	10	10	10	10	10	10	10	10	10	10	10	10	10	10	10	10
18	10	10	10	10	10	10	10	10	10	10	10	10	10	10	10	10	10	10	10	10	10	10	10	10	10	10	10	10	10
19	10	10	10	10	10	10	10	10	10	10	10	10	10	10	10	10	10	10	10	10	10	10	10	10	10	10	10	10	10
20	10	10	10	10	10	10	10	10	10	10	10	10	10	10	10	10	10	10	10	10	10	10	10	10	10	10	10	10	10
21	10	10	10	10	10	10	10	10	10	10	10	10	10	10	10	10	10	10	10	10	10	10	10	10	10	10	10	10	10
22	10	10	10	10	10	10	10	10	10	10	10	10	10	10	10	10	10	10	10	10	10	10	10	10	10	10	10	10	10
23	10	10	10	10	10	10	10	10	10	10	10	10	10	10	10	10	10	10	10	10	10	10	10	10	10	10	10	10	10
24	10	10	10	10	10	10	10	10	10	10	10	10	10	10	10	10	10	10	10	10	10	10	10	10	10	10	10	10	10
25	10	10	10	10	10	10	10	10	10	10	10	10	10	10	10	10	10	10	10	10	10	10	10	10	10	10	10	10	10
26	10	10	10	10	10	10	10	10	10	10	10	10	10	10	10	10	10	10	10	10	10	10	10	10	10	10	10	10	10
27	10	10	10	10	10	10	10	10	10	10	10	10	10	10	10	10	10	10	10	10	10	10	10	10	10	10	10	10	10
28	10	10	10	10	10	10	10	10	10	10	10	10	10	10	10	10	10	10	10	10	10	10	10	10	10	10	10	10	10
29	10	10	10	10	10	10	10	10	10	10	10	10	10	10	10	10	10	10	10	10	10	10	10	10	10	10	10	10	10
30	10	10	10	10	10	10	10	10	10	10	10	10	10	10	10	10	10	10	10	10	10	10	10	10	10	10	10	10	10

## References

1. (a) H. Perst in "Carbonium ions", G. Olah and P. von R. Schleyer, Eds., vol. V, Wiley-Interscience: New York, 1976, p. 1961.  
(b) G.A. Olah, A.M. White and D.H. O'Brien in "Carbonium Ions", G. Olah and P.von R. Schleyer, Eds., vol. IV, Wiley-Interscience: New York, 1973, p. 1697.
2. H. Perst in "Oxonium Ions in Organic Chemistry", Academic Press: New York, 1971.
3. C.U. Pittman, Jr., S.P. McManus and J.W. Larsen, *Chem. Rev.*, **72**, 357 (1972).
4. R.W. Taft, R.H Martin and F.W. Lampe, *J. Am. Chem. Soc.*, **87**, 2490 (1965).
5. F.H. Martin, F.W. Lampe and R.W. Taft, *J. Am. Chem. Soc.*, **88**, 1353 (1966).
6. M.S.B. Munsen and J.L. Franklin, *J. Phys. Chem.*, **68**, 3191 (1964).
7. B.G. Ramsey and R.W. Taft, *J. Am. Chem. Soc.*, **88**, 3058 (1966).
8. H. Paulsen, *Pure Appl. Chem.*, **41**, 69 (1975).
9. B. Capon, *Quart. Rev., Chem. Soc.*, **18**, 45 (1964).
10. L. Goodman, *Advan. Carbohydrate Chem.*, **22**, 109 (1967).
11. H. Paulsen, *Advan. Carbohydrate Chem. Biochem.*, **26**, 127 (1971).
12. C. Pederson, *Tetrahedron Lett.*, 511 (1967).
13. S. Spange, G. Heublein, H. Schultz, J. Lukaszcyk and Z. Jedlinsky, *J. Phys. Org. Chem.*, **3**, 195 (1990).

14. F.R. Jones and P.H. Plesch, *J. Chem. Soc., Dalton Trans.*, 927 (1979).
15. S. Hunig, *Angew. Chem., Int. Ed. Engl.*, **3**, 548 (1964).
16. S. Winstein and R. Boschan, *J. Am. Chem. Soc.*, **72**, 4669 (1950).
17. H. Paulsen, W.-P. Trautwein, F. Garrido-Espinosa and K. Heyns, *Chem. Ber.*, **100**, 2822 (1967).
18. S. Jacobsen, *Acta Chem. Scand.*, **B40**, 493 (1986).
19. S. Jacobsen, *Acta Chem. Scand.*, **B40**, 498 (1986).
20. J. Defaye, A. Gadelle, and C. Pedersen, *Carbohydrate Res.*, **205**, 191 (1990).
21. R. Miethchen, D. Peters, and C. Pedersen, *J. Fluorine Chem.*, **56**, 37 (1992).
22. (a) H. Paulsen and H. Behre, *Angew. Chem., Int. Ed. Engl.*, **8**, 886 (1969).  
(b) H. Paulsen and H. Behre, *Chem. Ber.*, **104**, 1281 (1971).
23. H. Paulsen and H. Meyborg, *Chem. Ber.*, **108**, 3176 (1975).
24. A. Pelter and M.E. Colclough, *Tetrahedron Lett.*, **27**, 1935 (1986).
25. T. Yamamoto, H. Suemune, and K. Sakai, *Tetrahedron*, **47**, 8523 (1991).
26. S. Machida, Y. Hashimoto, K. Saigo, J.-Y. Inoue and M. Hasegawa, *Tetrahedron*, **47**, 3737 (1991).
27. Y. Hayashi, K. Wariishi and T. Mukaiyama, *Chem. Lett.*, 1243 (1987).
28. T. Mukaiyama, Y. Hayashi and Y. Hashimoto, *Chem. Lett.*, 1627 (1986).
29. R. Szymanski, *Makromol. Chem.*, **192**, 2961 (1991).
30. (a) A. Wolinska and J. Lukaszczuk, *Acta Polym.*, **37**, 578 (1986).  
(b) Z. Jedlinski, A. Wolinska and J. Lukaszczuk, *Macromolecules*, **18**, 1648



- (1985).
31. (a) M. Gibas, *Makromol. Chem*, **188**, 675 (1987).  
(b) J. Lukaszczyk, *Makromol. Chem.*, **187**, 249 (1986).
32. (a) H.B. Burgi and J.D. Dunitz, *Acc. Chem. Res.*, **16**, 153 (1983).  
(b) H.B. Burgi, J.D. Dunitz and E.J. Shefter, *Acta Crystallogr. Sect. B: Struct. Crystallogr. Cryst. Chem.*, **B30**, 1517 (1974).
33. H.B. Burgi, J.D. Dunitz and E.J. Shefter, *J. Am. Chem. Soc.*, **95**, 5065 (1973).
34. (a) A.J. Kirby, *Adv. Phys. Org. Chem.*, **29**, 87 (1994).  
(b) A.J. Kirby, *Pure Appl. Chem.*, **59**, 1605 (1987).  
(c) M.R. Edwards, P.G. Jones and A.J. Kirby, *J. Am. Chem. Soc.*, **108**, 7067 (1986).  
(d) P.G. Jones and A.J. Kirby, *J. Am. Chem. Soc.*, **106**, 6207 (1984).  
(e) F.H. Allen and A.J. Kirby, *J. Am. Chem. Soc.*, **106**, 6197 (1984).  
(f) A.J. Kirby in "The Anomeric Effect and Related Stereoelectronic Effects at Oxygen", Springer-Verlag: New York, 1983.
35. M.R. Caira and J.F. de Wet., *Acta Crystallogr., Sect. B: Struct. Crystallogr. Cryst. Chem.*, **B37**, 709 (1981).
36. H. Paulsen and R. Dammeyer, *Chem. Ber.*, **106**, 2324 (1973).
37. H. Paulsen and R. Dammeyer, *Chem. Ber.*, **109**, 1837 (1976).
38. H. Paulsen and R. Dammeyer, *Chem. Ber.*, **109**, 605 (1976).
39. H. Paulsen and E. Schuttpelz, *Chem. Ber.*, **112**, 3214 (1979).

40. R.F. Childs, R.M. Orgias, C.J.L. Lock and M. Mahendran, *Can. J. Chem.*, **71**, 836 (1993).
41. U. Pindur, J. Muller, C. Flo and H. Witzel, *Chem. Soc. Rev.*, **16**, 75 (1987).
42. (a) H. Hart and D.A. Tomalia, *Tetrahedron Lett.*, 3383 (1966).  
(b) D.A. Tomalia and H. Hart, *Tetrahedron Lett.*, 3389 (1966).  
(c) H. Hart and D.A. Tomalia, *Tetrahedron Lett.*, 1347 (1967).
43. R.F. Childs, M.D. Kostyk, C.J.L. Lock and M. Mahendran, *Can. J. Chem.*, **69**, 2024 (1991).
44. G. Olah and A.M. White, *J. Am. Chem. Soc.*, **90**, 1884 (1968).
45. J. Lukaszczyk, *Pol. J. Chem.*, **55**, 2497 (1981).
46. C.U. Pittman, Jr., T.B. Patterson, Jr. and L.D. Kispert, *J. Org. Chem.*, **38**, 471 (1973).
47. H. Paulsen and E. Schuttpelz, *Org. Mag. Res.*, **12**, 616 (1979).
48. (a) R.A. Breslow, S. Garratt, L. Kaplan and D. LaFollette, *J. Am. Chem. Soc.*, **90**, 4051 (1968).  
(b) R.A. Breslow, L. Kaplan and D. LaFollette, *J. Am. Chem. Soc.*, **90**, 4056 (1968).  
(c) T.R. Forbus and J.C. Martin, *J. Am. Chem. Soc.*, **101**, 5057 (1979).  
(d) J.C. Martin, *Science*, **221**, 509 (1983).
49. (a) S.T. Graul and M.T. Bowers, *J. Am. Chem. Soc.*, **113**, 9696 (1991).

- (b) D.M. Cyr, L.A. Posey, G.A. Bishea, Chau-Chung Han and M.A. Johnson, *ibid*, 113, 9697 (1991).
- (c) J.L. Wilbur and J.I. Brauman, *ibid*, 113, 9699 (1991).
50. M. Hojo, T. Ichi and K. Shibato, *J. Org. Chem.*, 50, 1478 (1985).
51. (a) J. L. Riebsomer, J. Irvine and R. Andrews, *J. Am. Chem. Soc.*, 60, 1015 (1938).
- (b) J. L. Riebsomer, R. Baldwin, J. Buchanan and H. Burkett, *J. Am. Chem. Soc.*, 60, 2974 (1938).
52. P.H. Bentley and W. McRae, *J. Org. Chem.*, 35, 2082 (1970).
53. A.C. Cope and L. Field, *J. Org. Chem.*, 14, 856 (1949).
54. K.A. Saegebarth, *J. Org. Chem.*, 24, 1212 (1959).
55. (a) R.K. Harris in "Nuclear Magnetic Resonance Spectroscopy", Pitman Books Limited: London, 1983.
- (b) J. Sandstrom in "Dynamic NMR Spectroscopy", Academic Press: London, 1982.
- (c) L.M. Jackman and F.A. Cotton in "Dynamic Nuclear Magnetic Resonance Spectroscopy", Academic Press: New York, 1975.
- (d) K.G. Orrell, V. Sik and D. Stephenson, *Prog. Nucl. Magn. Reson. Spectrosc.*, 22, 141 (1990).
56. DNMR3 is available from the Quantum Chemistry Program Exchange, Indiana University. Program number 165.

57. EXCHANGE is available from R.E.D. McClung, Department of Chemistry, University of Alberta, Edmonton, Alberta, Canada, T6G 2G2.
58. (a) P.R. Wells in "Linear Free Energy Relationships", AP: New York, 1968.  
(b) N.B. Chapman and J. Shorter, Eds., "Advances in Linear Free Energy Relationships", Plenum Press: New York, 1972.  
(c) N.B. Chapman and J. Shorter, Eds., "Correlation Analysis in Chemistry, Recent Advances", Plenum Press: New York, 1978.
59. H.C. Brown and Y. Okamoto, *J. Am. Chem. Soc.*, **80**, 4979 (1958).
60. J.W. Baker and W.S. Nathan, *J. Chem. Soc.*, 1844 (1935).
61. (a) E. Berliner and F.J. Bondhus, *J. Am. Chem. Soc.*, **70**, 854 (1948).  
(b) H.C. Brown, J.D. Brady, M. Grayson, and W.H. Bonner, *J. Am. Chem. Soc.*, **79**, 1897 (1959).  
(c) P.D. Bartlett, *J. Chem. Educ.*, **30**, 22 (1953)
62. C.A. Vernon, *J. Chem. Soc.*, 423 (1954).
63. R.W. Taft and I.C. Lewis, *Tetrahedron*, **5**, 186, (1959).
64. W.A. Sweeney and W.M. Schubert, *J. Am. Chem. Soc.*, **76**, 4625 (1954).
65. M.J.S. Dewar in "Hyperconjugation", Ronald Press: New York, 1962.
66. V.J. Shiner, *J. Am. Chem. Soc.*, **76**, 1603 (1954).
67. A.D. Bain and J.A. Cramer, *J. Magn. Reson.*, **103**, 217 (1993).
68. J.K.M. Sanders and J.D. Merish, *Prog. Nucl. Magn. Reson. Spectrosc.*, **15**, 353 (1982).

69. J.K.M. Sanders and B.K. Hunter in "Modern NMR Spectroscopy. A Guide for Chemists", Oxford University: Oxford, 1988.
70. (a) S. Forsén and R.A. Hoffman, *J. Phys. Chem.*, **40**, 1189 (1964).  
(b) S. Forsén and R.A. Hoffman, *J. Phys. Chem.*, **39**, 2892 (1963).
71. A.D. Bain and J.A. Cramer, *in press*.
72. R.F. Childs, D.L. Mulholland and A. Nixon, *Can. J. Chem.*, **60**, 801 (1982).
73. S.E. Denmark, B.R. Henke and E. Weber, *J. Am. Chem. Soc.*, **109**, 2512 (1987).
74. (a) S. Shambayati, W.E. Crowe and S.L. Schreiber, *Angew. Chem., Int. Ed. Engl.*, **29**, 256 (1990).  
(b) M.T. Reetz, K. Harms and W. Reif, *Tetrahedron Lett.*, **29**, 5881 (1988).
75. J.D. Memory and N.K. Wilson in "NMR of Aromatic Compounds", Wiley-Interscience: New York, 1982.
76. (a) G.A. Olah and P.W. Westerman, *J. Org. Chem.*, **38**, 1986 (1973).  
(b) J. Brunn, R. Radeaglia, B. Lewanscheck, and S. Peust, *Z. Phys. Chem.*, **258**, 681 (1977).
77. A. Fratiello, R. Kubo, D. Liu, and G. Vidulich, *J. Chem. Soc., Perkin Trans. II*, 1415 (1975).
78. M. Allen and J.D. Roberts, *Can. J. Chem.*, **59**, 451 (1981).
79. H. Spiessacke and W.G. Schneider, *Tetrahedron Lett.*, 468 (1961)
80. (a) D.G. Farnum, *Adv. Phys. Org. Chem.*, **11**, 123 (1975).

- (b) D. Bethell in "Reactive Intermediates", vol. 1, M. Jones, Jr. and R.A. Moss, Eds., Wiley Interscience: New York, 1978.
- (c) G.K.S. Prakash and P.S. Iyer in "Reviews of Chemical Intermediates", vol. 9, Elsevier: Amsterdam, 1988.
81. (a) P.R. Wells, S. Ehrenson and R.W. Taft, *Prog. Phys. Org. Chem.*, **6**, 147 (1968).
- (b) S. Ehrenson, R.T.C. Brownlee and R.W. Taft, *Prog. Phys. Org. Chem.*, **10**, 117 (1973).
- (c) J. Shorter in "Similarity Models in Organic Chemistry, Biochemistry and Related Fields", Studies in Organic Chemistry, vol. 42., R.I. Zalewski, T.M. Krygowski and J. Shorter, Eds., Elsevier: Amsterdam, 1991, p. 77.
- (d) M. Godfrey, *ibid*, p. 149.
82. J. Shorter in "Correlation Analysis in Chemistry: Recent Advances", N.B. Chapman and J. Shorter, Eds., Plenum Press: New York, 1978.
83. (a) R.D. Topsom, *Prog. Phys. Org. Chem.*, **12**, 1 (1976).
- (b) M.J.S. Dewar and A.P. Marchand, *J. Am. Chem. Soc.*, **88**, 3318 (1966).
- (c) E.M. Schulman, K.A. Christensen, D.M. Grant and C. Walling, *J. Org. Chem.*, **39**, 2686 (1974).
84. (a) W.J. Hehre, R.W. Taft and R.D. Topsom, *Prog. Phys. Org. Chem.*, **12**, 159 (1976).
- (b) R.T.C. Brownlee, S. Ehrenson and R.W. Taft, *Prog. Phys. Org. Chem.*, **10**,

- 1 (1973).
85. W.F. Reynolds, P. Dais, D.W. MacIntyre, G.K. Hamer and I.R. Peat, *J. Magn. Reson.*, **43**, 81 (1981).
86. D.D.M. Wayner in "CRC Handbook of Organic Photochemistry", vol. 2, J.C. Scaiano, Ed., CRC Press, Inc.: Boca Raton, Florida, 1991.
87. O. Exner in "Advances in Linear Free Energy Relationships", N.B. Chapman and J. Shorter, Eds., Plenum Press: London, 1972.
88. Statistical Methods Manual, Operations Research Committee: Technical Section of the Canadian Pulp and Paper Association, 1962. Reprinted 1984.
89. (a) G.F. Fadhil, *Collect. Czech. Chem. Commun.*, **58**, 385 (1993).  
(b) D.J. Craik, R.T.C. Brownlee and M. Sadek, *J. Org. Chem.*, **47**, 657 (1982).  
(c) R.T.C. Brownlee and M. Sadek, *Aust. J. Chem.*, **34**, 1593 (1981).  
(d) J. Bromilow and R.T.C. Brownlee, *J. Org. Chem.*, **44**, 1261 (1979).  
(e) R.T.C Brownlee, *Tetrahedron Lett.*, 5187 (1972).
90. M. Szafran, B. Brycki, Z. Dega-Szafran and B. Nowak-Wydra, *J. Chem. Soc., Perkin Trans. II*, 1161 (1991).
91. D.W. Boykin and B. Nowak-Wydra, *Magn. Reson. Chem.*, **29**, 152 (1991).
92. C.N. Robinson, G.E. Stablein and C.D. Slater, *Tetrahedron*, **46**, 335 (1990).
93. C.N. Robinson, L.J. Wiseman, Jr. and C.D. Slater, *Tetrahedron*, **45**, 4103 (1989).
94. W. Adcock, W. Kitching, V. Alberts, G. Wickham, P. Barron and D. Doddrell,

- Org. Mag. Res.*, 10, 47 (1977).
95. R.F. Childs, M.D. Kostyk, C.J.L. Lock and M. Mahendran, *J. Am. Chem. Soc.*, 112, 8912 (1990).
96. (a) G.E.P. Box, W.G. Hunter and J.S. Hunter in "Statistics for Experimenters, An Introduction to Design, Data Analysis and Model Building", John Wiley and Sons: New York, 1978.
- (b) T.M. Krygowski, *Prog. Phys. Org. Chem.*, 17, 239 (1990).
97. PCMODEL is available from Dr. K. Gilbert, Serena Software, P.O. Box 3076, Bloomington, IN, U.S.A., 47402-3076.
98. AMPAC is available from the Quantum Chemistry Program Exchange, Bloomington, IN, U.S.A., 47405.
99. H.H. Jaffe and M. Orchin in "Theory and Applications of Ultraviolet Spectroscopy", John Wiley and Sons: New York, 1962.
100. H.B. Burgi and J.D. Dunitz, *Helv. Chim. Acta*, 54, 1255 (1971).
101. (a) A. Solladie-Cavallo and G. Solladie, *Org. Mag. Res.*, 10, 235 (1977).
- (b) A.R. Katritzky, R.F. Pinzelli and R.D. Topsom, *Tetrahedron*, 28, 3449 (1972).
- (c) A.G. Pinkus and H.C. Custard, Jr., *J. Phys. Chem.*, 74, 1042 (1970).
- (d) K.S. Dhami and J.B. Stothers, *Tetrahedron Lett.*, 631 (1964).
102. T.A. Halgren, *J. Am. Chem. Soc.*, 100, 6595 (1978).
103. (a) E.M. Arnett, C. Petro and P. von R. Schleyer, *J. Am. Chem. Soc.*, 101, 522



- (1979).
- (b) G.S. Hammond, *J. Am. Chem. Soc.*, **77**, 334 (1955).
- (c) J.E. Leffler, *Science*, **117**, 340 (1953).
104. G.A. Olah, M.D. Heagy and G.K.S. Prakash, *J. Org. Chem.*, **58**, 4851 (1993).
105. H.B. Schlegel in "New Theoretical Concepts for Understanding Organic Reactions", J. Bertran and I.G. Csizmadia, Eds., Kluwer Academic: Dordrecht, 1989.
106. I.H. Williams, A.B. Miller and G.M. Maggiora, *J. Am. Chem. Soc.*, **112**, 530 (1990).
107. E.M Arnett and C. Petro, *J. Am. Chem. Soc.*, **100**, 5408 (1978).
108. P. Vogel in "Carbocation Chemistry", Elsevier: New York, 1985.
109. X. Creary, *Chem. Rev.*, **91**, 1625 (1991).
110. M.N. Paddon-Row, K.N. Houk, T.T. Tidwell, *Tetrahedron Lett.*, **23**, 383 (1982).
111. Walker and Stuart, *Acta Crystallogr.*, **A39**, 158 (1983).
112. J.M. Stewart and S.R. Hall, The XTAL System of Crystallographic Programs Tech. Rept. TR-1364, University of Maryland, College Park, U.S.A. (1983).
113. SHELXTL PLUS 4.2, Siemens Crystallographic Research Systems, Siemens Analytical X-ray Instruments, Inc., (May, 1990).